

**Measurement of Nitrogenous Species
And Solar Intensity During the 1997
Southern California Ozone Study**

**Final Report
Contract No. 96-540**

**California Air Resources Board
Monitoring and Laboratory Division
2020 L Street
Sacramento, CA 95814**

Prepared by:

Dennis R. Fitz
William P.L. Carter
Center for Environmental Research and Technology
College of Engineering

Ernesto Tuazon
Air Pollution Research Center

University of California
Riverside, CA 92521
(909) 781-5791
(909) 781-5790 fax

Revised March 1, 2000

Disclaimer

The statements and conclusions in this report are those of the contractor and not necessarily those of the California Air Resources Board. The mention of commercial products, their source or test use in connection with the materials reported herein is not to be construed as either an actual or implied endorsement of such products.

Acknowledgments

This report was submitted in fulfillment of ARB Contract 96-540, "Measurement of Nitrogenous Species and Solar Intensity During the 1997 Southern California Ozone Study." Work was completed as of June 1998.

We wish to thank the many staff members of CE-CERT who worked so hard to conduct this study. These include Mike Boeck, Kurt Bumiller, John Collins, Andrew Glideswell, Dongmin Luo, Mac McClanahan, Irina Malkina, Tim Nelson, and Jeff Shu. We appreciated the cooperation from ARCO (Gimma Borestain), Los Angeles Department of Water and Power (Michael Coia and Denise Whaley), Mt. Wilson Observatory (Bob Cadman), San Diego Air Pollution Control District (Mahmood Housain), the South Coast Air Quality Management District (Mike Agnew, Rene Bermudez, Rudy Eden, Curt Miller, Sandy Ryan), Union Pacific Railroad (Barry Watkins), the University of California, Los Angeles, the U.S. Navy (Lee Eddington, Rogert Helvey, Jay Rosenthal), and the Ventura County Air Pollution Control District (Dennis Mikels). We thank the Air Resources Board TSD, the U.S. Navy (Jerry Finlinson), and Southern California Edison for supplying measurement equipment without charge. The PAN, TCE, and PPN measurements were conducted under subcontract with DGA & Associates (Daniel Grosjean and Eric Grosjean), whose diligent work resulted in a high-quality and complete data set. Finally, we thank the many ARB staff members who provided guidance and assistance in conducting this study (Bart Croes, Leon Dolislager, Ash Lashgari, Jim Pederson, and Tony VanCuren).

Table of Contents

Disclaimer	i
Acknowledgments	ii
Abstract	iii
Glossary	viii
Executive Summary	1
1.0 Introduction and Objectives	4
2.0 Approach	5
2.1 Measurement Sites and Parameters	5
2.2 Measurement Methods	5
2.2.1 Nitrogenous Species	5
2.2.2 Solar Intensity	8
2.2.3 Other SCOS97-NARSTO Support Measurements	11
2.3 Data Management Overview	14
3.0 Results	16
3.1 Nitrogenous Species	16
3.1.1 NO _y Instrument Laboratory Evaluation	16
3.1.2 NO _y and NO _y - NA Measurements	36
3.1.3 Tunable Diode Laser Absorption Spectrometer	65
3.1.4 Diffusion Denuder Sampling	73
3.1.5 PAN, PPN, and TCE Measurements	85
3.1.6 Long Path-length Fourier Transform Infrared Spectrometry	92
3.2 Radiation Measurements	95
3.2.1 Non Wavelength Selective	95
3.2.2 Wavelength Selective Instruments	104
3.2.3 NO ₂ Actinometry	105
3.2.4 UV Aethalometer (Black Carbon)	108
3.2.5 Light Scattering	109
3.3 Other Support Activities	116
3.3.1 Ozone Monitoring	116
3.3.2 Meteorological Measurements at Mira Loma and Diamond Bar	128
3.3.3 Quality Assurance Auditing	129
3.3.4 NO _y Analyzer Audit Comparisons	131
3.3.5 PAN Audits	132
4.0 Conclusions	134
5.0 Recommendations	135
6.0 Future Research Needs	136
7.0 References	137

List of Figures

Figure 3-1	Time Series Plots of NO and NO ₂ During the Smog Chamber Evaluation.....	27
Figure 3-2	Time Series Plots of NO _y , NO, and NO ₂ During Smog Chamber Evaluation.....	28
Figure 3-3	Time Series Plots of NO _y - NA, NO and NO ₂ During the Smog Chamber Evaluation.....	29
Figure 3-4	Time Series Plots of NA During the Smog Chamber Evaluation.....	30
Figure 3-5	Time Series Plots of NA During the Smog Chamber Evaluation.....	31
Figure 3-6	Time Series Plot of UCD and SD NO _y Analyzer Response as a Function of Temperature, First Test.....	33
Figure 3-7	Response of UCD and SD NO _y Analyzers as a Function of Temperature, First Test.....	34
Figure 3-8	Time Series Plot of UCD and SD NO _y Analyzer Response as a Function of Temperature, Second Test.....	35
Figure 3-9	Response of UCD and SD NO _y Analyzers as a Function of Temperature, Second Test.....	35
Figure 3-10	Summary of NO _y Measurements Performed in Azusa, CA, for SCOS97- NARSTO IOP Periods.....	40
Figure 3-11	Summary of NO _y Measurements Performed in Banning, CA, for SCOS97-NARSTO IOP Periods.....	44
Figure 3-12	Summary of NO _y Measurements Performed in Diamond Bar, CA, for SCOS97-NARSTO IOP Periods.....	47
Figure 3-13	Summary of NO _y Measurements Performed in Los Angeles (North Main), CA, for the SCOS97-NARSTO IOP Periods.....	48
Figure 3-14	Summary of NO _y Measurements Performed in Mira Loma, CA, for SCOS97-NARSTO IOP Periods.....	51
Figure 3-15	Summary of NO _y Measurements Performed at San Nicolas (Bldg. 279), CA, for SCOS97-NARSTO IOP Periods.....	53
Figure 3-16	Summary of NO _y Measurements Performed in Simi Valley, CA, for SCOS97-NARSTO IOP Periods.....	56
Figure 3-17	Summary of NO _y Measurements Performed at Soledad Mountain, CA, for SCOS97-NARSTO IOP Periods.....	59
Figure 3-18	Summary of Measurements Performed at UC Riverside Agricultural Operations for SCOS97-NARSTO IOP Periods.....	62
Figure 3-19	HNO ₃ Concentrations Determined by TDLAS and NO _y Analyzer at Azusa during SCOS97-NARSTO IOP Periods.....	66
Figure 3-20	NO ₂ Concentrations Determined by TDLAS and SCAQMD NO- NO _x Analyzer at Azusa During SCOS97-NARSTO IOP Periods.....	69
Figure 3-21	Plot of TDLAS Nitric Acid Concentrations Compared with Those from NO _y Analyzer (ppb).....	72
Figure 3-22	Plot of TDLAS NO ₂ Concentrations Compared with Those from the NO _x Analyzer (ppb).....	73
Figure 3-23	Collocated Denuder Ammonia Measurements.....	74
Figure 3-24	Collocated Diffusion Denuder Nitric Acid Measurement.....	76
Figure 3-25	Ammonia Concentrations in Azusa by Diffusion Denuder Method.....	77
Figure 3-26	Ammonia Concentrations in Riverside by Diffusion Deoder Method.....	78
Figure 3-27	Ammonia Concentrations in Mira Loma by Diffusion Denuder Method.....	79
Figure 3-28	Nitric Acid Concentrations in Azusa by Diffusion Denuder Method.....	80
Figure 3-29	Nitric Acid Concentrations in Riverside by Diffusion Denuder Method.....	81
Figure 3-30	Nitric Acid Concentrations in Mira Loma by Diffusion Denuder Method.....	82
Figure 3-31	Comparison of Denuder Ammonia Measurements with FTIR at Mira Loma.....	83
Figure 3-32	Comparison of TDLAS and Denuder Nitric Acid at Azusa.....	84

Figure 3-33	PAN, PPN, and TCE Concentrations in Azusa for SCOS97-NARSTO IOP Periods	86
Figure 3-34	PAN, PPN, and TCE Concentrations in Simi Valley for SCOS97-NARSTO IOP Periods	89
Figure 3-35	FTIR Measurements of Ammonia at Mira Loma	94
Figure 3-36	Comparison of FourEppley TUVB Sensors	97
Figure 3-37	Total Solar Radiation, UV Solar, and Diffuse Solar Radiation at Mt. Wilson for SCOS97-NARSTO IOP Periods	99
Figure 3-38	Total Solar Radiation, UV Solar, and Diffuse Solar Radiation at CE-CERT in Riverside, CA, for SCOS97-NARSTO IOP Periods	102
Figure 3-39	A Typical Shaded and Unshaded Solar Spectral Intensity Determined by the LICOR on August 28, 1997	105
Figure 3-40	Values of k , Determined on the CE-CERT Roof for SCOS97-NARSTO IOP Periods	106
Figure 3-41	Concentration of Black Carbon on the CE-CERT Roof for SCOS97-NARSTO IOP Periods	110
Figure 3-42	Coefficient of Light Scattering (b_{sp}) at CE-CERT for the SCOS97-NARSTO IOP Periods	114
Figure 3-43	Ozone Concentrations at San Nicolas Island during SCOS97-NARSTO IOP Periods	115
Figure 3-44	Ozone Concentrations at ARCO Tower Penthouse during SCOS97-NARSTO IOP Periods	116
Figure 3-45	Ozone Concentrations at Mt Wilson during SCOS97-NARSTO IOP Periods	126
Figure 3-46	Ozone Concentrations at Tehachapi during the SCOS97-NARSTO IOP Periods	128
Figure 3-47	Comparison of CE-CERT and Pelican PSP Total Solar Radiometers	130
Figure 3-48	Comparison of CE-CERT and Pelican UV Radiometers	131

List of Tables

Table E-1	Measurement Sites and Data Collection.....	1
Table 2-1	Measurement Sites and Data Collection.....	7
Table 2-2	CE-CERT QC Code Descriptions.....	15
Table 3-1	Summary of Laboratory Acceptance Testing of Thermo Environmental Model 42CY NO _y Analyzers.....	20
Table 3-2	Species and Standards.....	21
Table 3-3	Smog Chamber Evaluation Results	23
Table 3-4	Bias and Precision with Final SCOS Calibration Applied	25
Table 3-5	Bias and Precision after Normalization	25
Table 3-6	Summary of Zero Checks, Span Checks, and Calibration of NO _y Analyzers.....	37
Table 3-7	Denuder Sampling Days and Locations.....	74
Table 3-8	Spectra Measurement Dates and Times	93
Table 3-9	Sensor Calibration Factors.....	98
Table 3-10	Summary of NO _y Audit Comparisons.....	132
Table 3-11	Summary of PAN Audits.....	133

Glossary

ARB or CARB	California Air Resources Board
AVES	AeroVironment Environmental Services
b_{sp}	Coefficient of particle scattering
BC	“Black” or “elemental” carbon
CE-CERT	College of Engineering-Center for Environmental Research and Technology, University of California, Riverside
DAS	Data acquisition system
DGA	Daniel Grosjean and Associates
FTIR	Fourier transform infrared
GC	Gas chromatograph
IC	Ion chromatograph
IOP	Intensive Operation Period
IR	Infrared
k_1	Photolysis rate of nitrogen dioxide
L	Liter
$\mu\text{g}/\text{m}^3$	Micrograms per meter cubed
msl	mean sea level (altitude)
NA	Nitric acid
NPN	n-propyl nitrate
NO_x	Oxides of nitrogen
NO_y	Reactive nitrogenous species
PAN	Peroxyacetyl nitrate
PPN	Peroxypropionyl nitrate
ppb	Part per billion
ppt	Part per trillion
RH	Relative humidity
RMS	Root mean square
RSD	Relative standard deviation
SCAQMD	South Coast Air Quality Management District
SCOS97-NARSTO	1997 Southern California Ozone Study – North American Research Strategy for Tropospheric Ozone
SoCAB	South Coast Air Basin
STI	Sonoma Technology Inc.
TCE	Tetrachloroethylene

TDLAS.....Tunable diode laser absorption spectrometer

UV.....Ultraviolet

WD.....Wind direction

WS.....Wind speed

Executive Summary

A wide variety of aerometric data was obtained at fifteen sites during the SCOS97-NARSTO study. Table E-1 summarizes the locations, parameters, instruments, and data collection methods that were employed. These data have all been incorporated into the SCOS97-NARSTO database maintained by the California Air Resources Board. The bulk of the measurements were to quantify concentrations of nitrogenous species and measure solar radiation characteristics.

Table E-1. Measurement Sites and Data Collection.

Location	Site Code	Instrument	Parameters	Data Logger	Data Averaging Period	Comments
ARCO Tower	ARCO	Dasibi 1003 AH	O ₃	1 channel	1hr	
Azusa	AZSA	T42CY-2Converter	HNO ₃ ,NO _y	SCAQMD	1hr	
Azusa		TDLAS	HNO ₃ ,NO ₂	PC	1hr	Intensive periods only
Azusa		Double Denuder for HNO ₃ , NH ₃	HNO ₃ ,NH ₃	NA	3-4 hr	Intensive periods only
Azusa		PAN Analyzer	PAN,PPN,MCF	Chart	1hr	Intensive periods only reported
Banning	BANN	T42CY-2Converter	HNO ₃ ,NO _y	SCAQMD	1hr	
Banning		Qualimetrics T&RH Sensor	T and RH	SCAQMD	1hr	
CE-CERT	RICE	Actinometer, NO ₂	kl	Campbell, manual	1hr	Intensive periods only
CE-CERT		Brewer Radiometer	Spectral Intensity	U of Georgia	NA	
CE-CERT		Eppley UV	UV Radiation	Campbell	3 Min	
CE-CERT		Eppley PSP	Total radiation	Campbell	3 Min	
CE-CERT		Eppley PSP	Total radiation	Campbell	3 Min	
CE-CERT		Eppley 828	Total radiation	Campbell	3 Min	
CE-CERT		Eppley 828, shaded	Total radiation	Campbell	3 Min	
CE-CERT		Licor Radiometer	Spectral Intensity	PC	1hr	Intensive periods only
CE-CERT		Magee Actinometer	bap (EC)	PC	3 Min	
CE-CERT		Yankee Radiometer	Spectral Intensity	PC	3 Min	
CE-CERT		RM Young Humidity Sensor	T,RH	Campbell	3 Min	
CE-CERT		MRI 1597 Nephelometer	bsp	Chart, PSU PC	1hr/6min	Periods depends on data source
CE-CERT		Vaisala RS80 Radiosonde	T,P,WS,WD,RH	PC	15 sec	Last radiation intensive only
Diamond Bar	DIAM	T42S-2con	HNO ₃ ,NO _y	Campbell	1hr	
Diamond Bar		Qualimetrics T&RH Sensor	T and RH	Campbell	1hr	
Los Angeles	LANM	T42/CE-CERT 2 con	HNO ₃ ,NO _y	SCAQMD	1hr	
Mira Loma	CHIM	T42CY-2Converter	HNO ₃ ,NO _y	Campbell	1hr	
Mira Loma		Qualimetrics T&RH Sensor	T and RH	Campbell	1hr	
Mira Loma		Double Denuder for HNO ₃ , NH ₃	HNO ₃ ,NH ₃	NA	4 hr	Intensive period only
Mira Loma		RM Young Anemometer	WS,WD	WS,WS	1hr	
Mira Loma		SAPRC longpath FTIR	HNO ₃ /NH ₃	PC	7 min	Intensive periods only
Mt. Wilson	WILS	ASI Tape Sampler	COH	Campbell	3 Min	
Mt. Wilson		Brewer Radiometer	Spectral Intensity	PC	NA	
Mt. Wilson		Dasibi O ₃	O ₃	Campbell	3 Min	
Mt. Wilson		Eppley UV	UV Radiation	Campbell	3 Min	
Mt. Wilson		Eppley 828, Shaded	Total radiation	Campbell	3 Min	
Mt. Wilson		Eppley 828	Total radiation	Campbell	3 Min	
Mt. Wilson		Eppley PSP	Total radiation	Campbell	3 Min	
Mt. Wilson		Yankee Radiometer	Spectral Intensity	PC	3 Min	
Mt. Wilson		Qualimetrics T&RH Sensor	T and RH	Campbell	3 Min	
Mt. Wilson		Optec NGN Nephelometer	bsp	Campbell	3 Min	
Pomona	POMN	Vaisala RS80 Radiosonde	T,P,WS,WD,RH	PC	15 sec	Intensive periods only
San Nicolas Is	SNIC	T42S-1 Converter	NO,NO _y	Campbell	1hr	
San Nicolas Is		Dasibi 1003 AH	O ₃	Campbell	1hr	
Simi Valley	SVAL	T42CY-2Converter	HNO ₃ ,NO _y	VCAPCD	1hr	
Soledad Min.	SOLM	T42CY-2 Converter	HNO ₃ ,NO _y	SDAPCD	1hr	
UCLA	UCLA	Vaisala RS80 Radiosonde	T,P,WS,WD,RH	PC	15 sec	
UCR-AG Ops	UCDC	T42CY-2Converter	HNO ₃ ,NO _y	SCAQMD	1hr	
UCR-AG Ops		Double Denuder for HNO ₃ , NH ₃	HNO ₃ ,NH ₃	NA	3-4 hr	
UCR-AG Ops		Qualimetrics T&RH Sensor	T and RH	SCAQMD	1hr	
UCR-Pierce	RIPR	Qualimetrics T&RH Sensor	T and RH	Chart	NA	Dr. Prather has data

An objective was to quantify nitrogen oxide concentrations as accurately as possible. To this end, a significant effort was made to measure total reactive nitrogen oxides (NO_y) and nitric acid (NA). NO_y is an operational definition that includes all nitrogenous species that are readily oxidized by the converter of commercial chemiluminescent NO- NO_x analyzers. To measure NO_y in ambient air it is necessary to place the converter that reduces nitrogenous species to NO

outside to avoid adsorption/desorption that may occur in sample lines, especially after they pass from ambient to a temperature-controlled environment. No inlet filter is used for NO_y to avoid nitric acid produced from the volatilization of particulate ammonium nitrate. The analyzers were equipped with dual converters that went to a single detector; a switching valve was used to alternate between the two modes. Prior to one of the converters, nitric acid was removed by a combination of a nylon filter and a NaCl-coated fabric denuder. One channel measures NO_y , the other NO_y without nitric acid, $\text{NO}_y\text{-NA}$. The difference between the two, therefore, gives the concentration of nitric acid, NA.

Thermo Environmental model 42 chemiluminescent analyzers were used for all NO_y , NO , and NA measurements. Six new model 42CY dual external converter instruments were tested in the laboratory to verify that performance specifications could be obtained (two additional new instruments were also evaluated but operated by others). A model 42C and a model 42S retrofitted with a second converter, with one externally mounted while a second model 42S was used with a single external converter. All instruments were evaluated in the laboratory for their responses to known concentrations of NO , NO_2 , HNO_3 , HONO , and n-propyl nitrate. After adjusting several of the converter temperatures, all were found to have equivalent responses relative to NO . They were then installed and calibrated at their designated sites.

Sites for determining NO_y and NA were located in Azusa, Banning, Diamond Bar, Los Angeles (downtown), Mira Loma, Soledad Mountain, Riverside, San Nicolas Island, and Simi Valley. The single converter instrument was used at San Nicolas Island. Site checks were conducted every two to three weeks throughout the SCOS97-NARSTO measurement window at which time the zero and span were checked, as were the converter efficiency for NO_2 and n-propyl nitrate. With the exception of Diamond Bar, where the instrument malfunctioned for a period of time, a high percentage of data recovery was obtained. The analyzer at Los Angeles also malfunctioned, but was immediately replaced with a spare. Two problems identified by the site checks were that the $\text{NO}_y\text{-NA}$ channel filter could overload at the sites of higher air pollutant concentrations and the NO_y response to zero air was often elevated, again at the sites with higher concentrations.

After the study, all of the $\text{NO}_y\text{-NA}$ and NO_y instruments were returned to the laboratory to simultaneously sample synthetically generated photochemical smog in an environmental chamber. The response of all of the instruments to NO and NO_2 in this "as is" condition had a bias of -6% from the reference analyzer. The among-analyzer precision was 7%. The other significant finding was that the responses of the NO_y channels, while all the same prior to irradiation (when only NO and NO_2 starting reagents were present), diverged considerably with continuing irradiation. This indicates that the converter efficiencies were now dissimilar for a nitrogenous species produced during the irradiation. Since the addition of NaCl-coated denuders to the sample lines made the response similar, it is suspected that nitric acid was the cause of the varied response.

To complement the NO_y and NA measurements, a number of other measurements of nitrogenous species were made at selected sites. At Azusa and Simi Valley, peroxyacetyl nitrate (PAN), peroxypropyl nitrate (PPN), and tetrachloroethylene (TCE) were measured with a gas chromatograph equipped with an electron capture detector. At Azusa, nitric acid and nitrogen dioxide were measured during Intensive Operating Periods (IOPs) with a tunable diode laser absorption spectrometer (TDLAS). The nitric acid data from the TDLAS and chemiluminescent analyzer were poorly correlated. At Mira Loma, ammonia was measured with a long-path Fourier transform infrared spectrometer (FTIR). Diffusion denuder samples were also collected at Azusa and either Riverside or Mira Loma three times per day over three-hour intervals to quantify nitric acid and ammonia. The nitric acid denuder data were poorly correlated with the TDLAS, although the ammonia denuder data were highly correlated with the FTIR.

Audits of CE-CERT operated NO_x/NA instruments consisted of calibration checks performed by local air quality management districts. NO/NO_x and NO_x/NA analyzers operated by other SCOS97-NARSTO participants were in turn audited by CE-CERT. All analyzers were within $\pm 8\%$ of each other with a standard deviation of 6%. The CE-CERT operated instruments were found to have a bias of -6% due to a change in concentration of the NO reference standard. The data were corrected for this bias. Synthetically generated PAN was placed in a Teflon bag to compare the responses between the PAN chromatographic analyzers operated at Azusa with the Luminol-based instruments operated at the Cajon Pass and Calabasas. The response of the Calabasas instrument was found to be three times lower than the other two.

Sunlight intensity was monitored on both the CE-CERT roof and from a shelter located at the top of Mt. Wilson. At both sites, Eppley broadband radiometers (both shaded and unshaded) were used in addition to UV radiometers. Light scattering was also characterized at both sites with integrating nephelometers (MRI model 1597 at CE-CERT and Optec NGN-2 at Mt. Wilson) while light absorption was measured with a Magee Scientific UV aethalometer at CE-CERT and a Research Appliance Co. AISI sampler at Mt. Wilson. Both sites were also equipped with two types of spectral radiometers. One was a Brewer model MKIV and the other, which also measured diffuse radiation via a shadow band, was a Yankee model UVMRF. These instruments were operated remotely: the Brewer by the University of Georgia and the Yankee by Colorado State University. These organizations will provide those spectral data. During two radiation intensives and for as many of the IOP days as possible, we made manual measurements at hourly intervals on the CE-CERT roof. Spectral intensity was measured with a LICOR model LI-1800. The NO_2 photolysis rate, k_1 , was measured by flowing the dilute gas through a quartz tube and monitoring the amount of NO produced using a chemiluminescent NO_x analyzer. During these periods we also manually shaded the Eppley radiometers periodically and used a VHS camcorder to document visibility and cloud cover.

1.0 Introduction and Objectives

Despite many years of emission reductions, Southern California is still classified by the U.S. Environmental Protection Agency (EPA) as a "serious" non-attainment area for ozone. To formulate additional cost-effective emission control strategies, a better understanding of the meteorological and chemical processes contributing to high ozone concentrations was needed. While the South Coast Air Basin (SoCAB) has been the subject of several intensive studies to understand the origin and formation of ozone, a new study was needed for several reasons. These include the effects of reformulated gasoline on the emissions inventory and the application of new emissions control technologies since the last major study, the Southern California Air Quality Study (SCAQS) in 1987.

The 1997 Southern California Ozone Study – North American Research Strategy for Tropospheric Ozone (SCOS97-NARSTO) was conducted to provide a new and expanded understanding of the distribution of ozone in Southern California and the mechanisms of ozone formation. This study emphasized the collection of data on the vertical concentration of ozone and meteorological parameters. A planning document (Fujita et al., 1996) was prepared and was refined by a series of committees specializing in various technical areas. The centerpiece of the study was a planned fifteen forecast days for high ozone, during which extensive measurements of meteorology and pollutant concentrations were to be made.

Ozone is produced in a complex photochemical reaction involving hydrocarbons and nitrogen oxides. To understand these photochemical processes for model evaluation, it is important to obtain accurate data on concentrations of these species. One objective of this project was to collect nitrogen oxide concentration data at nine locations in Southern California during the SCOS97-NARSTO. The oxides are emitted from combustion sources primarily as nitric oxide with a small fraction of nitrogen dioxide. In the atmosphere, these are oxidized to a number of products such as nitrogen dioxide, nitric acid, nitrous acid, nitrate radicals, and organic nitrates (such as peroxyacetyl nitrate, PAN). The sum of these reactive species is referred to as NO_y . Accurate measurements of these species is needed for evaluating and using photochemical airshed models. Routine nitrogen oxide monitors used in the SoCAB do not provide adequate data and a network of specialized instruments was needed. Such measurements are particularly important in southern California, where the concentrations are consistently higher than the rest of the United States.

Many Southern California air basins are also in non-attainment of the National Ambient Air Quality Standards for PM_{10} , particulate matter less than 10 micrometers aerodynamic diameter. Since components of PM_{10} are produced by the same photochemical processes that lead to ozone formation, it is appropriate that SCOS97-NARSTO also focus on the mechanism of particulate matter generation by these processes. Nitric acid is the final product in the photochemical oxidation of NO. While nitric acid is a gaseous compound, it reacts readily and reversibly with gaseous ammonia to produce solid ammonium nitrate, which in the atmosphere is found primarily in the fine fraction of particulate matter (e.g., <2.5 micrometers aerodynamic diameter). The equilibrium concentration of solid ammonium nitrate and its gaseous precursors is dependent on temperature and the ratio of nitric acid to ammonia. Therefore, to understand the potential for ammonium nitrate production it is necessary to characterize both nitric acid and ammonia concentrations. One critical source of ammonia in the SoCAB is dairy operations west of Riverside. As air containing photochemically generated nitric acid moves easterly with the on-shore flow in the afternoon, it passes through the feedlot area, and particulate ammonium nitrate is formed. Another objective of the project was to measure the concentration of ammonia in the Riverside area to characterize these particulate formation processes.

Ambient solar light intensity and spectrum are key input parameters to the atmospheric chemistry of photochemical airshed models. This varies as a function of atmospheric haze, humidity, and zenith angle. Despite this, the past generation of air quality models, such as the UAM, have parameters representing all the other factors. In recognition of this deficiency in the present models, the California Air Resources Board (ARB) funded the development of improved solar radiation models for application to urban and regional air quality modeling. Intensive radiation measurements were made to provide data needed to evaluate the improved solar radiation models that are being developed.

2.0 Approach

2.1 Measurement Site Parameters

Table 2-1 summarizes the measurement sites, instruments used, parameters measured and the averaging interval for instruments operated under this contract.

2.2 Measurement Methods

2.2.1 Nitrogenous Species

While a network providing detailed measurements of all major nitrogenous species was highly desirable, our approach was formulated to gain the maximum benefit from the resources available. This included a large network where total NO_y was measured using commercial chemiluminescent analyzers with externally mounted converters. A subset of these were equipped with a second converter which sampled air from which nitric acid (NA) was removed, allowing this species to be quantified by difference. For comparison, at one NO_y/NA site, a tunable diode laser absorption spectrometer (TDLAS) was used to measure nitric acid directly. This instrument was also used to measure NO_2 concentrations without interferences due to NO_y components other than NO and NO_2 . At three of the NO_y/NA sites, NaCl -coated diffusion denuders were used to independently measure nitric acid for comparison. Peroxyacetyl nitrate (PAN) and peroxypropionyl nitrate (PPN) were measured at two sites using a gas chromatograph equipped with an electron capture detector. A long path-length Fourier transform infrared spectrometer (FTIR) was used at one site to measure ammonia concentrations. Ammonia was also quantified at this and two other sites using phosphoric acid-coated diffusion denuders.

Chemiluminescent Oxides of Nitrogen Analyzer

This instrument uses the chemiluminescent reactions of NO with O_3 to quantify concentrations of NO . In one cycle of the instrument ambient NO is quantified (NO channel), while in a second ambient air is passed through a heated catalytic converter to reduce odd reactive nitrogen species (NO_y) to NO . A single detector is used and the airstreams are controlled with a solenoid valve. Two features of this model are that the converter is placed in the ambient air (with the rest of the instrument located in a temperature-controlled shelter) and the solenoid is downstream of the converter. This arrangement minimizes the loss of nitric acid in the sampling lines, thus allowing all NO_y components to be quantified. We added a second converter attached to the usual NO sampling line. Air in this line is selectively scrubbed of nitric acid prior to the converter using a combination of a sodium chloride-coated fabric denuder followed by a nylon filter. The difference in the measurements between the two channels, therefore, is presumably due to nitric acid.

Table 2-1. Measurement Sites and Data Collection.

Location	Site	Instrument	Parameters	Data	Data Averaging	Comments
ARCO Tower	ARCO	Dasibi 1003 AH	O3	1 channel	1hr	
Azusa	AZSA	T42CY-2 Converter	HNO3, NOy	SCAQMD	1hr	
Azusa		TDLAS	HNO3, NO2	PC	1hr	Intensive periods only
Azusa		Double Denuder for HNO3, NH3	HNO3, NH3	NA	3-4 hr	Intensive periods only
Azusa		PAN Analyzer	PAN, PPN, MCF	Chart	1hr	Intensive periods only reported
Banning	BANN	T42CY-2 Converter	HNO3, NOy	SCAQMD	1hr	
Banning		Qualimetrics T&RH Sensor	T and RH	SCAQMD	1hr	
CE-CERT	RICE	Actinometer, NO2	KI	Campbell, manual	1hr	Intensive periods only
CE-CERT		Brewer Radiometer	Spectral Intensity	U of Georgia	NA	
CE-CERT		Eppler UV	UV Radiation	Campbell	3 Min	
CE-CERT		Eppler PSP	Total radiation	Campbell	3 Min	
CE-CERT		Eppler PSP	Total radiation	Campbell	3 Min	
CE-CERT		Eppler 828	Total radiation	Campbell	3 Min	
CE-CERT		Eppler 828, shaded	Total radiation	Campbell	3 Min	
CE-CERT		Licor Radiometer	Spectral Intensity	PC	1hr	Intensive periods only
CE-CERT		Magee Aethelometer	bap (EC)	PC	3 Min	
CE-CERT		Yankee Radiometer	Spectral Intensity	PC	3 Min	
CE-CERT		RM Young Humidity Sensor	T, RH	Campbell	3 Min	
CE-CERT		MRI 1597 Nephelometer	bsp	Chart, PSU PC	1hr/6min	Periods depends on data source
CE-CERT		Vaisala RS80 Radiosonde	T, P, WS, WD, RH	PC	15 sec	Last radiation intensive only
Diamond Bar	DIAM	T42S-2 con	HNO3, NOy	Campbell	1hr	
Diamond Bar		Qualimetrics T&RH Sensor	T and RH	Campbell	1hr	
Los Angeles	LANM	T42/CE-CERT 2 con	HNO3, NOy	SCAQMD	1hr	
Mira Loma	CHIM	T42CY-2 Converter	HNO3, NOy	Campbell	1hr	
Mira Loma		Qualimetrics T&RH Sensor	T and RH	Campbell	1hr	
Mira Loma		Double Denuder for HNO3, NH3	HNO3, NH3	NA	4 hr	Intensive period only
Mira Loma		RM Young Anemometer	WS, WD	WS, WS	1hr	
Mira Loma		SAPRC longpath FTIR	HNO3/NH3	PC	7 min	Intensive periods only
Mt. Wilson	WILS	ASI Tape Sampler	COH	Campbell	3 Min	
Mt. Wilson		Brewer Radiometer	Spectral Intensity	PC	NA	
Mt. Wilson		Dasibi O3	O3	Campbell	3 Min	
Mt. Wilson		Eppler UV	UV Radiation	Campbell	3 Min	
Mt. Wilson		Eppler 828, Shaded	Total radiation	Campbell	3 Min	
Mt. Wilson		Eppler 828	Total radiation	Campbell	3 Min	
Mt. Wilson		Eppler PSP	Total radiation	Campbell	3 Min	
Mt. Wilson		Yankee Radiometer	Spectral Intensity	PC	3 Min	
Mt. Wilson		Qualimetrics T&RH Sensor	T and RH	Campbell	3 Min	
Mt. Wilson		Optec NGN Nephelometer	bsp	Campbell	3 Min	
Pomona	POMN	Vaisala RS80 Radiosonde	T, P, WS, WD, RH	PC	15 sec	Intensive periods only
San Nicolas Is	SNIC	T42S-1 Converter	NO, NOy	Campbell	1hr	
San Nicolas Is		Dasibi 1003 AH	O3	Campbell	1hr	
Simi Valley	SVAL	T42CY-2 Converter	HNO3, NOy	VCAPCD	1hr	
Soledad Min.	SOLM	T42CY-2 Converter	HNO3, NOy	SDAPCD	1hr	
UCLA	UCLA	Vaisala RS80 Radiosonde	T, P, WS, WD, RH	PC	15 sec	
UCR-AG Ops	UCLC	T42CY-2 Converter	HNO3, NOy	SCAQMD	1hr	
UCR-AG Ops		Double Denuder for HNO3, NH3	HNO3, NH3	NA	3-4 hr	
UCR-AG Ops		Qualimetrics T&RH Sensor	T and RH	SCAQMD	1hr	
UCR-Pierce	RIPR	Qualimetrics T&RH Sensor	T and RH	Chart	NA	Dr. Prather has data

Luminol PAN, NO, NO_y, NO₂ Analyzer

This instrument was evaluated to determine whether the Unisearch Associates Inc. LPA-4 luminol chemiluminescent analyzer could measure PAN and NO₂ with sufficient accuracy, precision, and data capture to meet the measurement goals of SCOS97-NARSTO. As stated in the Field Study Plan, the goal was a detection limit of less than 1 ppbv with no measurable interferences. While not specified in the Plan, to collect useful data the capture goal should be approximately 90%.

The LPA-4 utilizes the detection of the chemiluminescent when NO₂ or peroxyacetyl nitrate reacts with a solution containing luminol. With the addition of sodium sulfite to the luminol solution to prevent ozone interferences, no other common air pollutants were found by the manufacturer to respond to this detector. As an NO₂ monitor, the PAN concentration must be independently determined to correct for its interference. This is done by using a gas chromatograph to separate PAN from NO₂ and organic nitrates, thermal conversion of PAN to NO₂, followed by chemiluminescent detection. The instrument can, therefore, provide interference-free NO₂ and PAN concentrations in ambient air.

GC-ECD PAN Analyzer

An SRI model 8610 gas chromatograph (GC) equipped with a Valco model 140BN electron capture detector (ECD) and a carbowax-coated Chromosorb P packed column was used to quantify peroxyacetyl nitrate (PAN), peroxypropionyl nitrate (PPN) and tetrachloroethylene (TCE) concentrations at the Azusa and Simi Valley monitoring sites. Ambient samples were injected every 30 minutes for the entire SCOS97-NARSTO period; data were retrieved for the entire study period but chromatographs were analyzed only for the IOP days. Methyl chloroform was not quantified because it eluted on the steep tail of the oxygen peak, and the concentration determination was, therefore, highly uncertain.

PAN and PPN were synthesized for calibration purposes in the liquid phase by nitrating the corresponding percarboxylic acid. The liquid was placed in an impinger purged with purified air to produce the species in the gas phase. The concentration was determined by the response to a chemiluminescent NO-NO_x analyzer in the NO_x mode. The TCE was calibrated with compressed gas standard obtained from Professor Rei Rasmussen at the Oregon Graduate Institute of Science and Technology.

Tunable Diode Laser Absorption Spectrometer

A Unisearch Associates Inc. model TAM-150 tunable diode laser absorption spectrometer was used to independently measure nitric acid and nitrogen dioxide concentrations at the Azusa site. This instrument uses lasers and a low-pressure analysis cell to quantify fine absorption features in the near infrared. These features are sufficiently fine that there is negligible chance that other compounds will interfere; the measurements is, therefore, very specific with few interferences. For many compounds, the sensitivity is less than 1 ppb. This instrument has been used in a number of air pollution studies to measure trace air contaminants (Anlauf et al., 1991; Mackay and Schiff et al., 1987).

This analyzer was calibrated by generating nitric acid and nitrogen dioxide using permeation tubes in separate holders, but both housed in an oven maintained at 60±0.1°C. Nitrogen was used to continuously flush the tube holders. During calibrations, the effluent from the tubes was diluted with purified air. The concentration of nitric acid in the diluted air stream was independently measured using the chemiluminescent NO_y/NO_y-NA analyzer located at the site. It was possible to use the NO_y channel alone to do this since the permeation source produced only

pure nitric acid. The nitric acid concentration was independently verified by sampling the calibration with a pair of NaCl-coated fabric denuders and analyzing the extracted denuders for nitrate.

Long Path-length Infrared Spectrometer

To characterize the concentration of ammonia at Mira Loma, a long-path Fourier transform infrared spectrometer was used. The kilometer-path-length infrared spectroscopic system consisted of a set of 25-meter basepath, open multiple-reflection optics which was interfaced to a Mattson Instruments Inc. Sirius 100 Fourier transform infrared (FTIR) spectrometer. This spectrometer has a maximum resolution capability of 0.1 cm^{-1} and is equipped with a PC-based data system. Except for a modification in the in-focus end of the optical assembly, it was the same FTIR system that was employed during a 1995 field comparison study of nitric acid methods conducted in Claremont, CA (Fitz and Tuazon, 1997). The present improvement in the optics (Tuazon and Fitz, to be published) consisted of additional corner reflectors, as described by White (1976). These provided a significant increase in stability of the optical system's beam output that is being directed to the infrared detector.

Concentrations of ammonia were determined from the absorbance of 1103.4 cm^{-1} , a band for which few atmospheric interferents have been observed. Each spectrum was averaged over five to ten minutes, allowing at least ten measurements per hour. The detection limit was approximately 1 ppb.

Diffusion Denuder

Samples were collected in Azusa, Mira Loma and Riverside using fabric denuders developed previously in this laboratory (Fitz and Tuazon, 1997). The denuders were coated with sodium chloride for removing nitric acid and coated with phosphoric acid to remove ammonia. A pair of denuders was used in each sampler to assess denuder collection efficiency. Samples were collected at a flow rate of 9 L/min during each IOP at approximately three-hour intervals. After sampling, the denuders were extracted. The extracts from ammonia denuders were analyzed for ammonium by the indole-phenol blue technique, while those from the nitric acid denuder were analyzed for nitrate by ion chromatography.

2.2.2 Solar Intensity

Southern California Edison previously operated a network of sensors to characterize solar radiation in the SoCAB. Since these data are no longer collected, it was necessary to re-establish a monitoring program. The light available for photochemical modeling is a sum of both the direct and diffuse radiation. The direct radiation is attenuated by particles, either by scattering or absorption. The diffuse radiation is increased by scattering and surface albedo. The scattering intensity depends on particle characteristics such as concentration, size and composition. A variety of parameters must therefore be measured to determine the appropriate intensity levels for the models.

Radiometers were used to determine total intensity for the entire spectrum and the UV component. Three types of spectral radiometers were used to measure intensity as a function of wavelength, each having several advantages and disadvantages. These data will be used as inputs into photochemical models so that applicable photolysis rates might be more accurately calculated. The most important photolysis rate for photochemical modeling is that for NO_2 . This was measured directly at one site. Integrating nephelometers were used to measure light scattering while light absorption was determined from the attenuation of light through particle collection filters.

As a reference, one site was located on top of Mt. Wilson, which is usually above the inversion and, therefore, subject to lower particulate pollutant concentrations than the lower elevations in the SoCAB. Riverside was chosen as the site in the polluted layer since particulate concentration, and therefore light scattering and absorption, are among the highest in the SoCAB. The manual methods to measure spectral intensity and NO₂ photolysis rates were used here.

UV and Total Radiometry

- **Eppley model PSP and 8-48 Total Solar Radiometers**

These pyranometers measure the amount of radiant energy collected by a planar black body absorber cover with a glass hemisphere. As such, they measure total light intensity at all wavelengths, including infrared. The two models are similar, but the PSP is a more accurate instrument.

The PSP was designed for the measurement of sun and sky radiation, totally or in defined broad wavelength bands. It comprises a circular multi-junction wire-wound Eppley thermopile that has the ability to withstand severe mechanical vibration and shock. Its receiver is coated with Parson's black lacquer (non-wavelength selective absorption). This instrument is supplied with a pair of removable precision ground and polished hemispheres of Schott optical glass. Both hemispheres are made of clear WG295 glass, which is uniformly transparent to energy between 0.285 to 2.8 micrometers.

The model 8-48 has a detector consisting of a differential thermopile with the hot-junction receives blackened and the cold-junction receivers whitened. The receiver is of radial wire-wound plated construction with the black segments coated with a flat black coating and the white with barium sulfate. Built-in temperature compensation with thermistor circuitry is incorporated to free the instrument from effects of ambient temperature. A precision ground optical glass hemisphere of Scott glass WG295 uniformly transmits energy from 0.285 to 2.8 micrometers.

During selected intensive operating days, the model PSP sensors at CE-CERT were manually shaded once per hour to determine diffuse radiation. The model 8-48 sensors were set up in pairs, one of each pair being shaded with a shadow band at all times.

- **Eppley Ultraviolet Photometer**

This instrument measures total ultraviolet radiation. It uses a planar diffuser to collect all incoming light. After passing through a filter that passes only ultraviolet light, the light is measured with a photometer. A specially designed Teflon diffuser reduces the radiant flux to acceptable levels and also provides close adherence to the Lambert cosine law. An encapsulated narrow bandpass (interference) filter limits the spectral response of the photocell to the wavelength interval 0.295 to 0.385 micrometers, with negligible secondary transmission. During selected intensive operating days the sensor was manually shaded once per hour to determine diffuse radiation. During portions of the study a second instrument of the same model was operated next to the primary instrument but permanently shaded.

Spectral Radiometry

- **Brewer model MKIV Spectrophotometer**

This instrument analyzes the solar UV spectrum to measure the amount of ozone, sulfur dioxide, and nitrogen dioxide in the earth's atmosphere. It does this by tracking the sun so that solar radiation is directed into the entrance of a diffraction grating. It also can take the spectrum of solar radiation integrated over a hemisphere. The two modes range from 280 to 320 nm (O₃ and SO₂) or 420-510 nm (NO₂) with a resolution of 0.1 nm. This instrument provides the best available measurement of the solar spectrum in the UV range that is currently available. The instrument was operated remotely by Colorado State University, Fort Collins.

- **Yankee Environmental Systems UV-MFRSR Spectral Radiometer**

The Yankee Environmental Systems UV Multifilter Rotating Shadowband Radiometer (UV-MFRSR) uses 7 independent interference filter photodiode detector combinations to make total horizontal solar irradiance measurements at 300, 305.5, 311.4, 317.6, 325.4, 332.4, and 368 nm (nominal 2 nm full width at half maximum bandwidth) through a single Lambertian detector. A computer-controlled, automatic rotating shadow band permits the near simultaneous determination of total horizontal, direct normal and diffuse radiation at each filter passband.

- **LICOR model LI-1800 Spectral Radiometer**

This instrument can take the spectrum of the sun using a spherical diffuser. It is used to obtain a cosine function of the light intensity. It has a broader spectral range than the Brewer (300-850 nm), while its resolution is considerably less (4 nm), and is considered to be less accurate in the short wavelength region. It does not track the sun. It was operated manually only during selected intensive operating days. The sensor was used to collect a spectrum of total solar radiation followed immediately by a spectrum of diffuse radiation approximately once per hour. The diffuse spectrum was obtained by manually shading the spectroradiometer sensor with a small disk.

NO₂ Actinometry

This actinometer measured the NO₂ photolysis rate. It used a stream of nitrogen dioxide in nitrogen flowing through a quartz tube. The amount of NO₂ photolyzed was measured with a chemiluminescent oxides of nitrogen analyzer. The photolysis rate was calculated from the inlet/outlet concentrations, the tube geometry, the flow rate, and the effective quantum yield (Zafonte et al., 1977). It was operated manually only during selected intensive operating days.

Magee Scientific model AE-16U Aethalometry

The AE-16U aethalometer collects the aerosol continuously on a quartz fiber filter, and determines the increment of optically-absorbing material collected per unit volume of sampled air. Since "elemental" or "black" carbon (BC) is the dominant optically absorbing material in the submicron size range, the measurement is interpreted as a mass of BC according to calibrations performed by intercomparison with chemical analysis techniques. The optical measurement is radiometric, and no external calibration materials are required: Filter tape is the only material used. The aethalometer measures an increment of less than 1 nanogram of BC on its filter. At a flow rate of 10 L/min and a time-base of 10 minutes, the corresponds to a resolution of 10 ng m⁻³ of BC.

Nephelometry

Integrating nephelometers were used to measure the particle light scattering coefficient. These measurements were needed to calculate the k_1 for running airshed models. A MRI model 1597 was used at CE-CERT in Riverside, and an Optec model NGN2 was used at Mt. Wilson. These instruments have a light source and measure the amount of light scatter to a photomultiplier tube for the MRI instrument and a photodiode array for the Optec instrument. The NGN2 is a newer design that uses an open optical chamber rather than a sealed optical chamber through which air must be moved.

2.2.3 Other SCOS97-NARSTO Measurements and Activities

The following instruments, although not part of the original proposal, were added to the project to provide data to better meet the SCOS97-NARSTO objectives.

Photometric Ozone Analyzers

Dasibi 100AH ozone analyzers were operated at Mt. Wilson, San Nicolas Island, and the ARCO Tower in downtown Los Angeles. Ozone and meteorological measurements were also made at Tehachapi under funding from a related ARB-sponsored SCOS97-NARSTO project. These instruments are equivalent to the EPA reference method.

Meteorological Measurements

RM Young Meteorological propeller and vane wind sensors were operated at Mira Loma. Qualimetrics temperature and RH sensors were installed in Banning, Mira Loma, Mt. Wilson, Diamond Bar, UCR Ag Ops, and UCR Pierce Hall. These instruments used a thermocouple for temperature measurements and a lithium chloride electrochemical cell to determine RH.

During IOPs, Vaisala model RS80 rawinsondes were launched four times per day at UCLA and at the SCAQMD's Pomona Air Quality Monitoring Station. These measured wind speed, direction, temperature, relative humidity, and altitude. Data were recorded to approximately 20,000 feet.

Quality Assurance Audits

Quality Assurance Audits of NO_y and ozone analyzers were performed with a Columbia Scientific model 1700 dilution calibrator/ozone source. The ozone reference was a CE-CERT Dasibi 1003AH transfer standard. The NO reference was a cylinder of certified NO in nitrogen. Audits were performed on all aircraft, while audit checks (single point) were performed at Barstow and Twentynine Palms.

Comparisons were made between the CE-CERT-operated Eppley PSP and UV radiometers with those on the STI and Caltech aircraft. The references for the CE-CERT radiometers were factory calibrations performed in May, 1997. These instruments are expected to have stable outputs; the operator manual suggests that yearly factory calibrations be performed.

Audit comparisons were performed to evaluate the accuracy of the PAN measured by ECD and Azusa with the PAN measured with Luminol LPA-4 instruments operated by AVES at Calabasas and Cajon Pass. A 100 L bag with a nominal 50 ppb of PAN was prepared in the CE-CERT laboratory by injecting a known amount of PAN in solution prepared using the method of Holdren and Spicer (1984). This bag was analyzed for PAN at the CE-CERT laboratory and transported to the sites. During transport, the vehicle's air conditioning was turned on to its highest setting, and the vents were directed toward the bag. The PAN concentration was checked at the CE-CERT laboratory after returning.

Retrofit of AeroVironment NO_x Analyzers to NO_y Analyzers

AeroVironment Environmental Services (AVES) was contracted by the ARB to operate NO-NO_x analyzers at sites located in the Cajon Pass and Calabasas. Thermo Environmental model 42C analyzers were installed in their standard configuration. To collect data equivalent to CE-CERT-operated instruments and to account for all NO_y species, the converters at these sites were removed from these two instruments and placed in a shelter on the roof of the air quality monitoring trailer. AVES collected and reported the data from these instruments as originally contracted. At the end of the study, the instruments were reconfigured to their standard design.

Presentation of NO_y Quality Assurance Workshops

The measurement of NO_y and the use of these analyzers to measure nitric acid by difference was a new experience for the SCOS97-NARSTO participants. To review the quality of the data and provide feedback on potential problems, two NO_y workshops were presented by CE-CERT.

Collection of Tracer Tubes

During the release of tracer gas for IOPs, tracer tubes were set out and collected at the Downtown Los Angeles site on North Main Street. Sampled tubes were returned to Tracer Environmental Sciences and Technologies for analysis.

Preparation of Sites for the SCOS97-NARSTO Aerosol Study

Existing portable shelters at UC Riverside Agricultural Operations area were prepared to host the participants of the aerosol study. Tasks included securing approval, cleaning the shelters, and installing additional power. A trailer was prepared for use at the Mira Loma site. This involved installation of additional power circuits and arranging transportation to and from the site.

Preparation of a Site for Radical Measurements

To accommodate the equipment from Portland State University, it was necessary to install a circuit and meter for 400 amps of three-phase electrical power at the back of the CE-CERT building located at 1200 Columbia Avenue in Riverside. A phone line also was installed. To provide CO measurements for these researchers, a Thermo Environmental Instruments model 48 IR correlation analyzer normally used for our smog chamber experiments was set up to sample ambient air except for brief periods when it was necessary to characterize the chamber's CO concentration at the beginning of the experiment. Workspace was made available in our laboratory, as was Internet access.

2.3 Data Management Overview

Source data received for this project includes written logbook and data sheet entries, data logger text files, instrument output text files, strip charts, analytical laboratory results, and reduced data sets. The list below identifies data sources.

- Nitrogen Species Related Measurements

NO_y analyzers: NO_y, NO_y-

CE-CERT sites: CE-CERT data logger files

SCAQMD sites: fixed format text files, received via FTP daily

SDAPCD site: e-mail report format text files, received via WWW interface and e-mail

VCAPCD site: report format text files, received periodically via e-mail

TDLAS: HNO₃, NO₂

Reduced data sets, faxed daily by operator

FTIR: NH₃

Reduced data set, delivered by UCR/SAPRC in spreadsheet format at end of study

Diffusion denuders: HNO₃, NH₃

Written data sheets and laboratory results

GC-ECD: PAN, PPN, TCE

Reduced data set, delivered by DGA in spreadsheet format at end of study

- Radiation Related Measurements

UV and Total Solar Radiometry: UVR, DIFUV, TSR, DIFSR

CE-CERT data logger files

NO₂ actinometry: k₁
Written logbook entries

LICOR Spectroradiometry: direct and diffuse spectrums in UV-Visible range
Instrument output files

Aethalometry

Instrument output files and CE-CERT data logger files

Nephelometry: b_{sp}

MRI 1597: strip-charts and Portland State University data logger files

NGN-2: instrument output files and CE-CERT data logger files

- Other Supporting Measurements

UV photometry: ozone
CE-CERT data logger files

Meteorology: WS, WD, TMP, RH
CE-CERT data logger files

In all cases the data sets were converted to Excel spreadsheets for calibration adjustments, calculation of computed values, plotting, validation, and flagging. The NO_y data sets from SCAQMD and SDAPCD were received on a nearly daily basis. The NO_y data from the CE-CERT and VCAPCD sites were received approximately every 1 to 3 weeks. The NO_y data sets were reviewed as soon as they were received in order to verify proper operation of the NO_y analyzers. Time series plots of NO_y, NO_y⁻, NO_x, NO and O₃ were printed each day for each site, and reviewed for anomalies. Operational problems with the analyzers were noted and corrected, but the data were not flagged during this preliminary review.

At the end of the study, all data sets received comprehensive review. For continuous data we examined logbook entries, calibration data, time series plots, and scatter plots. For the UV and total solar radiation data, this included determination for each data point whether it was in full sun, full shade or partial shade. For HNO₃ and NH₃ denuder samples, we reviewed data sheets, blank values, back-denuder to front-denuder ratios, and comparisons with continuous FTIR and TDLAS data. SCOS97-NARSTO QC codes were applied to all data sets during this final review, the primary codes indicating valid, suspect, invalid, or missing. When the data were judged suspect or invalid, reviewers assigned an additional CE-CERT QC code indicating the nature of the problem. Table 2-2 shows the CE-CERT QC codes, the corresponding SCOS97-NARSTO database QC code, and a description of the reason for the code. The CE-CERT QC codes were included in the delivered data sets. Once data were screened, data validation level was set to level L1a.

Table 2-2. CE-CERT QC Code Descriptions

CE-CERT QC Code	SCOS97-NARSTO QC Code*	Description
BAD	IV	Data unacceptable for use
BT	SS	Wind speed below threshold for wind direction sensor
CAL	CL	Instrument calibration taking place
CLG	IV	NO _y filter clogged
CNV	IV	NO _y converter malfunction
F	VD	Full shade for radiometers
FLT	SS	Filter problem

MI	MI	Data missing
MIS	IV	Data missing
not done		Not yet screened and flagged
NT	SS	Wind speed near threshold of wind direction sensor
OFF	IV	Instrument offline
OK	VD	Data OK
OVT	SS	Shelter temperature too high
OVR	IV	Data off scale
P	IV	Partial shade for radiometers
PWR	IV	Station power out
SCL	IV	Scaling error causing erroneous data
SUS	SS	Data suspect (general)
SUSA	SS	Radiometer in mountain shadow AM or PM
SUSB	SS	RAC sampler response drifting
SUSC	SS	Radiation data suspect due to clouds
SUSD	SS	Radiometer has dip caused by horizon ring
SUSE	SS	Data suspect; rises or falls dramatically from prev. readings
SUSI	SS	Inconsistent with expected values
SUSL	SS	Consistently low response
SUSN	VD	Noisy aethalometer, marked valid
SUSP	SS	Sudden sharp spike in data
SUSR	SS	Data suspect; not representative of expected trends
SUSS	SS	Data suspect; extremely scattered in small time increments
UNT	SS	Shelter under temperature

* Meaning of SCOS97-NARSTO QC codes: VD=valid, SS=suspect, IV=invalid, MI=missing, CL=QC sample

After the data sets were calibrated, screened, and flagged, they were reformatted into the SCOS97-NARSTO database format prescribed by the ARB. This database format is described in Excel workbook SCOSINFO.xls, available from the ARB ftp server themis.arb.ca.gov in directory/pub/data/scos97/documents/. Various lookup tables within this workbook define all database field names, field formats, site names, measured variables, measurement units, measurement methods, QC codes, and investigators, as well as defining file naming conventions. A typical data record contains the following fields:

- Data source (investigator organization)
- Site
- Sample start date
- Sample start time
- Sample duration
- Parameter name (i.e. species name)
- Measurement device (specific instrument model)
- Result (one measured value)
- Precision (for specific value in Result field)
- Below detection limit flag
- SCOS97-NARSTO QC code
- Validation level

Once data were converted to SCOS97-NARSTO format they were submitted to the ARB via ftp.

3.0 Results

This project generated a significant volume of ambient measurement data. All data have been submitted to the SCOS97-NARSTO data base manger; hard copy of the data collected will not

be submitted in this report due to this large volume. In this section we describe our results with respect to the following (not all will apply to any specific measurement):

- Laboratory evaluations.
- Summary of field operations.
- Quality assurance.
- Summary of data.
- Summary of the measurements obtained.
- Discussions of the data with respect to internal consistency.

3.1 Nitrogenous Species

3.1.1 NO_y Instrument Laboratory Evaluation

An LPA-4 was set up for laboratory evaluation. A number of problems were encountered when the instrument was used to sample synthetically generated PAN. During these tests, the liquid pumping system of the instrument failed, and it was necessary to send it back to the factory. The inability to measure PAN was traced to a bad column that had not been adequately tested at the factory due to the need to perform our laboratory evaluation on the short time schedule that was necessary to deploy instruments for the SCOS97-NARSTO field study. Since there was not sufficient time to retest the LPA-4 and the instrument did not appear to be reliable, a decision was made to purchase Thermo Environmental model 42CYs, instruments that are based on well-developed technology.

Thermo Environmental 42CY Acceptance Testing

Due to the late ordering and delivery of the Thermo Environmental model 42CY analyzers and the need to install them in time to meet SCOS97-NARSTO timelines, it was necessary to modify the acceptance protocol. Since calibrations were performed at installation, linearity was established at that time. Zero and span checks were performed on a routine basis on-site, zero and span drift could be monitored under actual monitoring conditions. While we performed as complete as acceptance testing as possible while still meeting the SCOS97-NARSTO time schedule, the emphasis on laboratory evaluation shifted to the performance of the converter for NO_y species, several of which could not be easily generated outside the laboratory.

Before acceptance testing, instruments were turned on, allowed to stabilize for 12 or more hours, and then zero-checked. A compressed gas source of ultra zero grade air, which had been further purified by passing through a Purafil cartridge, was used. Analyzers were then evaluated using EPA-developed methods to test for linearity, zero drift, span drift, and detection limit (US EPA, 1984; Federal Register, 1975) to determine whether instruments operated within the specifications supplied by the manufacturer.

I. Linearity Test

Multi-point calibrations were performed using a dilution calibrator supplied with zero air from an Aadco purification system and a certified NO in nitrogen compressed gas source. Six calibration points were used to cover the range from zero concentration to 120ppb in even increments. Least squares regressions of the results were performed. Linearity was validated if all points were within 1% of the least squares regression line or if the regression coefficient is greater than 0.99.

II. Zero Drift

The manufacturer specified the zero drift as "negligible." During laboratory evaluations, it was found that the zero response depended on the previous usage of the instrument, with nitric acid and ambient air causing a significant hysteresis. Acceptable zero drift was therefore defined as less than 1 ppb over a 24-hour period. Zero checks were made two or more times over a minimum of 24 hours. The difference in response divided by the time interval was used to calculate the zero drift rate.

III. Span Drift

Span checks at a nominal 125 ppb were made two or more times over a minimum of 24 hours. The difference in the values divided by the time was designated as span drift and compared with the manufacturer specification of $\pm 1\%$ of scale for acceptance. It should be noted that dilution calibrators used to generate the span gas are generally only repeatable to $\pm 1\%$. Results were acceptable if they differed by less than 4% of scale.

IV. Lower Detectable Limit

The lower detectable limit is defined as twice the noise, which was determined from taking the standard deviation of zero reading responses. This is defined as the instrument noise. The manufacturer specifications are 25 pptV noise and a lower detectable limit of 50 pptV at the 120 second averaging time.

Converter Testing

A variety of oxidized nitrogenous species have been shown to be quantitatively converted to NO by the molybdenum catalysts typically used in chemiluminescent oxides of nitrogen analyzers. These include NO₂, HNO₃, HONO, and peroxyacetyl nitrate (PAN) (Winer et al., 1974). These species were quantified when the analyzer inlet was routed through the converter; they are operationally defined as NO_y. Other nitrogen oxides such as nitrous oxide, alkyl nitro compounds, and reduced nitrogen such as ammonia have been reported to show very little conversion. The objective of these tests was to determine the converter efficiency for the nitrogenous species that are expected to contribute to NO_y. The basic approach was to sample from a synthetic source of these species and determine the concentration of NO_y measured, compared with that expected. Since the amount expected cannot be easily quantified directly for nitric acid, nitrous acid, PAN, or n-propyl nitrate, one or more approaches were used to determine concentrations of these gases:

- The concentration of the tested species was measured with a NO_y analyzer that had been calibrated with a certified NO source. A second converter, which had been shown to be effective (although knowing the degree of effectiveness is not necessary) was then added in series to determine whether any additional conversion occurs. If not, then the concentration of the test gas can be determined directly by the response of the NO_y analyzer.
- The concentration of the tested species was measured with an NO_y analyzer and the converter temperature incrementally raised until no further gain in response occurs. One then assumes that complete conversion is occurring.
- The responses of two or more NO_y analyzers (or the same analyzer but different channels if a dual converter system is used) give the same response to the test gas.

In practice, we relied on a combination of the second two methods for each species, after using the first method on a single analyzer that was used to compare with the others. NO_y analyzers were tested to various NO_y species; an acceptable response was 90% of that expected or 95% converter efficiency. Gases evaluated for converter efficiency were generated as follows:

- NO₂

NO₂ was generated by the gas phase titration with ozone using a commercial dilution calibration instrument equipped with an ozone generator and plumbed for performing gas phase titration. Prior to dilution, NO in nitrogen was allowed to mix with air that had passed through an ultraviolet light-based ozone generator. NO_y was sampled with the light off and then with the light adjusted to titrate approximately 70% of the NO. The change in response to the change in NO₂ concentration is therefore a measure of converter efficiency.

- Nitric Acid

Nitric acid vapor was generated by flowing clean, dry air past a permeation tube containing liquid nitric acid. The concentration was estimated by measuring the permeation and gas flow rates and verified with an NO_y analyzer as described above.

- Nitrous Acid

Nitrous acid was generated by the sublimation of ammonium nitrite (Vecera and Dasgupta, 1991). This has been demonstrated to be a clean and constant nitrous acid source. Ammonium nitrite placed in a copper tube was held at constant temperature in a refrigerator. A constant amount of dry nitrogen was passed through the tube and then diluted with zero air. The concentration was determined with a combination of the three methods as described above.

- PAN

PAN was prepared in solution by reacting peracetic acid with nitric acid (Holdren and Spicer, 1984) in a hydrocarbon solvent. The amount and purity in the solution was quantified by IR in a 0.25mm liquid cell. An aliquot of the solvent was injected into a 100 liter Teflon chamber and allowed to vaporize. The PAN concentration was estimated from the IR absorbance and verified with a NO_y analyzer as described above.

- n-Propyl Nitrate

This compound is known to be stable in compressed gas cylinders and is more difficult to reduce to NO than nitric acid (Hartsell, 1997). Diluting a compressed source of n-propyl nitrate may therefore provide a convenient and effective method of determining the efficiency of an NO_y converter. A commercially prepared and analyzed source of n-propyl nitrate in nitrogen was diluted with zero air. The concentration of the source was verified with a NO_y analyzer as described above.

NO_2 was generated in the 80 ppb range, PAN was prepared three times (80-130 ppb), and NPN was generated in the 50 ppb range. HONO and HNO_3 were generated in the 5-15 ppb range.

Results

Table 3-1 summarizes the final results from the laboratory testing at the time the instruments were taken from the lab for installation. Not included are results that led to repairs or raising the converter temperatures or replacing the converters. Serial numbers beginning with 38 are model 42, those starting with 52 are 42S, and those with 58 are model 42CY. In most cases, if the converter was not efficient for NO_2 , it was not efficient for the other NO_y species. Due to the limitations in time and equipment, testing of the NO_y components was not done in a specific order. For example, if a converter was found to be ineffective for NPN prior to NO_2 testing, we would first raise the converter temperature or replace the converter before testing other species. Thus, we could not determine whether a converter was efficient for one species but not for another. Approximately half of the converters required some temperature increase, and two required replacement.

Table 3-1. Summary of Laboratory Acceptance Testing of Thermo Environmental Model 42CY NO_y Analyzers.

NO _y Channel										NO or NO _y -NA Channel																
Serial #	Zero Drift ppb/24hr	Span Drift %/24 hr	Linearity R ²	Converter Temp C	NO ₂ -based Con Eff. %	NPN, ppb	NPN, corr	HNO ₃ , ppb	HONO, ppb	PAN, ppb	PAN, corr	Zero Drift ppb/24 hr	Span Drift %/24 hr	Linearity R ²	Converter Temp C	NO ₂ -based Con Eff. %	NPN, ppb	NPN, corr	HNO ₃ , ppb	HONO, ppb	PAN, ppb	PAN, corr	Location Used	Comments		
38576		0.2	4		325	100	26.7	40.3	50.6	5.5	11.0					100	25.9	39.5	51.9	5.7	11.7			DTLA	1	
38576					38576							0.5	4.2			336				10.9	9.9	97/A	97**		RI	
42CTL-58372-317					336	97.6				10.2	10.1	104/A	104**													
42CTL-58313-317					327	10.1	10.2	111/A	111**							327				9.1	9.2	108/A	108**	Mira Loma	2	
42CTL-58312-317					325					9.5	105/A	105**														
42S-52354-292					350		31.1		10.9	12.2	111/A	111**									9.7	101/A	101**			
42S-52354-292						100	30.4		6.7															Diam. Bar		
42S-52354-292	0.2					99	42.5	47.1	4.8	132/C	132	0.0				99	44.4	46.2	4.4		133/C	133		RI		
42S-52353-292					325	98.4			10.1	10.7	115/A	115**												R2		
42CTL-58438-314					330				6.4	8.0	29/A					331				7.3	8	15/A		Simi Vly	3	
42CTL-58438-314R						95.3										337	99.1								4 RI	
42CTL-58438-314	0	1.4	1.0000		337	100	44.4	47.6	5.6	26.0	79.9	86.6	0.4	1.1	1.0000		100	44.5	47.5	5.5	25.2	79.4/B	84.7		R2	
42CTL-58439-314					338	98.2	30.0		6.7	10.5						345	97.6	29.5		7.4	10.3			Sid Mtn.	5	
58439						99.6	43.5			23.6	82.5/B	87.1				99.4	43.0				23.2	80.3/B	84.9		RI	
58439	0	0.5	0.9999		347		45.1	47.3	5.0	7.0		0.0	0.8	0.9999		43.5	47.6	5.3	7	p 119				R2		
58440	0	0.8	1.0000		322	98.9	31.0	33.3*	7.6	11.5		0.0	0.6	1.0000	342	99.5	30.9	33.2*	7.5	11.6			Riverside	6		
58441	0.2				328	101.3			4.11			0.2			351	98.5			3.3					Azusa		
58441					350	100	38.1			47/B	54.1					100	15.1				32.4/B	37.3			RI	
58441		0.4	1.0000			99.8	41.3	47.5	4.78							351	96.9	41.3	47.5						R2	
58507	0.1	1.8	1.0000		327	98.3	47.9	49.4	6.2	1.8	122/C	126	0.2	1.8	1.0000	335	97.1	48.0	49.5	6.0	1.8	124/C	128			
58313	0	2.4	1.0000			99.0	63.4	47.1	7.2	2.5	132/C	100	0.2	3.2	1.0000	100	63.6	46.7	7.0	2.7	130/C	99.1				

Comments and Notes

- (1) Calibrates low.
 - (2) Raised NO_y-NA converter temp from 313, p.7.
 - (3) Calibration and converter problem.
 - (4) New NO_y-NA converter.
 - (5) Corrected HONO problems, raised P.
 - (6) HONO ball 5.3, not 11.7.
- A = PAN bag test on 6/9/97.
 B = PAN bag test on 6/23/97.
 C = PAN bag test on 7/1/97.
 RX = retest #.

corr = corrected for NO span factor.

* Calculated concentration = 34.0 ppb.

** Not corrected for span factor.

With the exception of SN58312, which was the first installed, all of the instruments purchased under ARB contract met the acceptance criteria. All of the final NPN tests showed high converter efficiency and gave results near the expected calculated concentrations. The PAN test on the instrument used for Azusa (SN58441) gave low and differing results on each channel. Since the converters otherwise checked with high efficiency for the other NO_y species, we suspect that there may have been a sampling line connection problem that occurred during the test.

Smog Chamber Evaluation

After the study was completed, instruments were received from the field and tested. Analyzers were set up to sample synthetic smog created in our 40m^3 indoor Teflon chamber during the course of a six-hour irradiation. At the same time we monitored NO_y with a Teco 42, PAN with a GC-ECD, ozone with a Dasibi 1003AH, and NO_2 and HNO_3 with a TDLAS. Chamber experiments used our standard VOC surrogates- NO_x mixtures, which have been well characterized chemically by measurements and mechanistic modeling.

The first goal of smog chamber evaluation was to characterize the performance of the analyzers as received from the field for NO , NO_x , NO_y , NO_y - (NO_y scrubbed of HNO_3), and nitric acid (NA). The analyzers were not recalibrated. For each analyzer, the calibration factors last used in the field were applied before data analysis.

The second goal was to characterize the performance of the analyzers for NA after eliminating as much bias as possible. Towards this goal, data from the NO , NO_x , NO_y , NO_y - channels of each analyzer were normalized during the dark phase of the bag experiment to correct for span and offset factors. This eliminated spurious NA caused by differences in the NO_y and NO_y - span and offset factors for a given analyzer, and eliminated differences in NA among analyzers caused by differences in span and offset factors among analyzers.

Table 3-2 lists the species examined toward these goals and the designated standard for each.

For both goals, the specific objectives for each species were to determine:

1. The bias of each analyzer with respect to the designated standard.
2. The single analyzer precision for each analyzer.
3. The precision among analyzers.

Table 3-2. Species and Standards.

Species	Standard
NO	Teco42 in NO mode
NO_2	Teco42 NO_x mode – Teco42 NO mode
NO_x	Teco42 in NO_x mode
NO_y	Teco42 in NO_x mode
NO_y -	Teco42 NO_x mode – TDLAS NA
NA	TDLAS NA

Two types of bias were calculated:

1. The slope of the linear regression of measured concentration vs. the designated standard.
2. The offset of the linear regression of measured concentration vs. the designated standard.

Single analyzer precision was calculated as the standard deviation of the residuals about the regression line. Among analyzer precision was calculated as a pooled estimate. For each five-minute measurement observation, the standard deviation among the six or eight test analyzers was calculated. These standard deviations were pooled over the entire concentration range of the test.

- **NO_y Instrument Preparation**

All instruments were used in the same condition they were in when removed from the field. Denuders and filters to remove HNO₃ were not renewed for the first run (they were renewed after the first run). Instruments that were found to require significant repairs not reflected in the final on-site calibration were not included as their performance would not be representative of their performance during SCOS97-NARSTO. Analyzers were started up and allowed to stabilize without the sample pump on to verify proper operational parameters. Instruments were not individually calibrated.

- **Tunable Diode Laser Absorption Spectrometer Preparation**

The TDLAS was operated in the NO₂ and HNO₃ mode. Data were collected by the internal computer and stored as one-minute averages. Permeation tubes were used to supply a steady-state concentration of each gas for calibration purposes. The output of the tubes was diluted with zero air to concentrations ranging from 10-50 ppb. The concentrations were determined with a selected NO_x analyzer. This analyzer was calibrated by using a Columbia Scientific model 1700 gas dilution calibrator by blending NO in nitrogen of certified concentration with ultra zero grade air.

- **Chamber Run Conditions**

We used a mode of operation called the full surrogate. This VOC surrogate consists of a mixture of eight species. Total NO_x was less than 200 ppb (target was 104 ppb NO; 45 ppb NO₂) so that all analyzers will remain within their operating range. These NO_x concentrations are used for our standard full-surrogate chamber runs to determine hydrocarbon reactivity to form ozone. These are representative of areas in the SoCAB subject to the highest pollutant concentrations. Such NO_x concentrations are higher than those found in other urban areas of the United States, so the results from the chamber experiments reported here may not be applicable to other areas. We selected VOC concentrations, which were expected to give an ozone peak after 3-4 hours.

- **Chamber Run Procedures**

The chamber was operated in the single-chamber mode (36 m³) and filled with ultra-zero air humidified if required to 20% RH (the first two runs were performed dry). While still in the dark, NO_y analyzer pumps were turned on and readings manually logged from the display at five-minute intervals. Data were logged in the same instrument order throughout the experiment. Data were logged for at least one half hour prior to NO being injected into the chamber (still in the dark) and data logged for another one half hour after injection. NO₂ was injected into the chamber (still in the dark) and data logged for one half hour. The lights were then turned on and data logged every five minutes for the following six hours or until the ozone concentration peaked.

- Data Analysis and Results

Table 3-3 identifies the analyzers compared in the study and shows the final SCOS97-NARSTO calibration values applied. Analyzers received from STI and Barstow were not provided with calibration factors. We applied a slope of 1.0 and an offset of 0 ppb to these analyzers.

Results are provided first using the calibration factors above, and second after normalizing all results to the reference analyzer. Results for all three chamber runs were very similar. No significant changes in the slopes relative to the reference analyzer were observed after filter and denuder renewal that occurred after the first run. The mean slope for NO_y was 0.95 before or after the changeout. For NO_y^- the slope was 0.95 before the changeout and 0.94 after. The standard deviation of the mean was 0.07 for all four cases.

Table 3-3. Smog Chamber Evaluation Results.

S/N	Site/Species	SCOS97 Slope	SCOS97 Offset	Used for Chamber Tests (Yes/No)
38576	LANM NO_x , NO	Ref.	Ref.	No: Instrument failed, was converted to NO_x analyzer and used as reference
52554	DIAM NO_y , NO_y^-			No: Analyzer failed
52583	SNI NO , NO_x			No: Analyzer failed
57247	STI Aircraft #2 NO_y , NO	1.00 1.00	0.0 0.0	Yes
57248	STI Aircraft #1 NO_y , NO	1.00 1.00	0.0 0.0	Yes
58507	BARST NO_y , NO_y^-			No: Analyzer failed
58312	BANN NO_y , NO_y^-	1.07 1.08	1.3 1.4	Yes
58313	CHIM NO_y , NO_y^-			No: Analyzer failed
58372	29 Palms NO_y , NO_y^-	1.00 1.00	0.0 0.0	Yes
58438	SVAL NO_y , NO_y^-	0.96 0.98	1.5 0.7	Yes
58439	SOLM NO_y , NO_y^-	1.29 1.30	1.5 1.5	Yes
58440	UCDC NO_y , NO_y^-	1.30 1.24	1.1 0.0	Yes
58441	AZSA NO_y , NO_y^-	1.23 1.25	0.6 0.3	Yes

The calculations of precision and bias are based on the results from the second chamber run. The measured VOC concentrations (ppmv) for this run were as follows:

<i>n</i> -Butane:	0.137
<i>n</i> -Octane:	0.073
Ethene:	0.024
Propene:	0.019
<i>i</i> -2-Butene:	0.020
Toluene:	0.062
<i>m</i> -Xylene:	0.063
Formaldehyde:	0.061 (estimated from injection)

Table 3-4 shows precision and bias using the final SCOS97-NARSTO calibration values. The slopes, intercepts and standard errors for NO, NO₂, NO_y, and NO_y- are calculated from the regression of these responses against the reference analyzer, using only the dark period data, when only NO and/or NO₂ are present. As discussed in subsequent paragraphs, it is not meaningful to calculate these values when photochemical products are present. Precision and bias for NA are calculated using data from the entire chamber run. This value is the standard deviation of the six (NO_y-, NA) or eight (NO_y) analyzer responses for each five-minute observation, pooled over all observations in the run. The coefficient of variation (CV) for this value was calculated relative to the mean concentration over the entire run.

Using final SCOS97-NARSTO calibration values, the single analyzer precision is 0.8 ppb for the directly measured species, which represents about 0.5% of concentrations used. The mean bias is about

-6%, and the among-analyzer precision is 7 or 8%. The among-analyzer precision calculated from the standard deviation of the slopes agrees with the among analyzer precision calculated from pooled standard deviations of individual five-minute observations. For NA vs. TDLAS and for NO₂ vs. TDLAS, the single analyzer precision is about 2.5 ppb. This is contributed to by scatter in the TDLAS as much as by scatter in the NO_y analyzers. The NO_y analyzer NA response is biased high by about a factor of 5, and zero offsets range from -2.0 to +6.7. The among-analyzer precision is about 20%. Though not shown in the table, the NO_y analyzer NO₂ response is also biased very high during the photochemically active portion of the chamber run. These bias issues will be discussed after first presenting the normalized results.

Table 3-5 shows the precision and bias after normalizing the NO_x, NO, NO_y, and NO_y- responses to the reference analyzer. Since the results have been normalized, the bias is now zero for these species, and the precision is about the same as before. NO₂ and NA were not directly normalized. Instead they are calculated by difference from the normalized quantities. NO₂ is calculated as NO_y-NO, and NA is calculated as NO_y - NO_y-. Normalization of NO_y and NO produces good results for NO₂ during the dark period. Bias for NO₂ ranges from -1.5 to +1.6%, depending on which analyzer is used as reference. Precision has been improved for NA. The standard deviation of the slopes is 11%, and the pooled standard deviation is 5.0 ppb, which is about 15% of mean levels. (These precisions are improved to 5% and 3.4 ppb respectively if Azusa is removed from the calculations). However, even though NO_y and NO_y- have been normalized, the NA by difference remains biased high by a factor of 5.

Table 3-4. Bias and Precision with Final SCOS97-NARSTO Calibrations Applied.

Ser. NO.	Site	Slope	Int. (ppb)	Std. Err. (ppb)	Slope	Int. (ppb)	Std. Err. (ppb)	Slope	Int. (ppb)	Std. Err. (ppb)
Single Analyzer precision and bias		NO v. NO Ref.			NO ₂ v. NO ₂ Ref.			NO ₂ v. TDLAS NO ₂		
57247	STI#2	0.871	1.3	0.8	0.910	1.3	0.8	0.889	1.5	2.3
57248	STI#1	0.922	1.0	0.6	0.863	-0.9	1.7	0.841	-0.4	2.4
Single Analyzer precision and bias		NO _y v. NO _x Ref.			NO _y v. NO _x Ref.			NA v. TDLAS HNO ₃		
57247	STI#2	0.881	2.2	1.2	0.983	0.3	0.9	5.19	0.9	2.5
57248	STI#1	0.896	1.6	0.6						
58312	BANN	0.977	0.5	0.9						
58372	BARST	1.056	2.2	0.9						
58438	SVAL	0.907	0.7	0.6						
58439	SOLM	0.960	-0.2	0.9	0.970	-0.3	0.8	5.22	-1.6	2.2
58440	UCDC	0.935	0.9	0.6	0.884	1.7	0.5	4.47	6.7	3.6
58441	AZSA	0.865	5.5	0.6	0.844	6.5	0.9	3.36	2.0	2.3
Single Analyzer pooled precision:		0.9			0.7			2.6		
Multi Analyzer mean:		0.935	1.675	14.0	0.941	1.900	10.0	4.763	1.600	7.0
stdev:		0.062	1.758		0.074	2.420		0.842	3.282	
CV:		6.7%			7.8%			17.7%		
precision among analyzers:										
cv among analyzers				7.9%			6.9%			21.1%

Table 3-5. Bias and Precision after Normalization.

Ser. NO.	Site	Slope	Int. (ppb)	Std. Err. (ppb)	Slope	Int. (ppb)	Std. Err. (ppb)	Slope	Int. (ppb)	Std. Err. (ppb)
Single Analyzer precision and bias		NO v. NO Ref.			NO ₂ v. NO ₂ Ref.			NO ₂ v. TDLAS NO ₂		
57247	STI#2	1.000	0.0	0.9	1.016	-0.3	0.9	0.991	0.0	2.6
57248	STI#1	1.000	0.0	0.7	1.007	-0.1	0.6	0.985	0.4	2.4
Single Analyzer precision and bias		NO _y v. NO _x Ref.			NO _y v. NO _x Ref.			NA v. TDLAS HNO ₃		
57247	STI#2	1.000	-0.2	1.3	1.000	0	0.9	5.29	1.6	2.6
57248	STI#1	1.000	0.1	0.7						
58312	BANN	1.000	0.0	0.9						
58372	BARST	1.000	-0.1	0.8						
58438	SVAL	1.000	0.0	0.6						
58439	SOLM	1.000	-0.1	0.9	1.000	0	0.8	5.39	-0.1	2.3
58440	UCDC	1.000	0.0	0.6	1.000	0	0.6	5.01	-1.2	3.0
58441	AZSA	1.000	0.1	0.7	1.000	0.1	1.1	3.99	-0.7	2.3
Single Analyzer pooled precision:		0.9			0.7			2.5		
Multi Analyzer mean:		1.000	-0.025	4.8	1.000	0.017	1.0	w/ and w/o AZSA		5.0; 3.4
stdev:		0.000	0.104		0.000	0.041		5.0; 5.2	0.250	
CV:		0.0%			0.0%			0.55; 0.24	1.244	
precision among analyzers:								11%; 4.6%		
cv among analyzers				2.6%			0.7%			15%; 10%

Figures 3-1 through 3-5 show time series plots of the normalized concentrations for various species during the course of the third chamber run (with humidified air). This run was used since the TDLAS was recalibrated immediately before the run started and therefore is expected to have more accurate measurements than in the previous two experiments. The starting VOC concentrations were as follows:

n-Butane:	0.330
n-Octane:	0.104
Ethene:	0.059
Propene:	0.046
t-2-Butene:	0.049
Toluene:	0.089
m-Xylene:	0.090
Formaldehyde:	0.062 (estimated from injection)

Figure 3-1 shows a time series plot of NO, NO₂ by TDLAS, and NO₂ by difference. Also shown are the modeled concentrations using an updated version (Carter, 1998) of the SAPRC-97 (Carter et al., 1997) mechanism. As soon as the lights are turned on, at 11:38 hours, the NO begins to drop rapidly and NO₂ begins to rise. Note that all three NO analyzers agree with themselves throughout the course of the run and follow the modeled concentrations. The TDLAS NO₂ and the NO₂ calculated by difference (NO_x - NO for the reference analyzer, and NO_y - NO or the single converter NO_y analyzers) agree with each other at first. However, as the NO₂ reaches its peak, the NO₂ by difference exceeds the TDLAS NO₂. The TDLAS NO₂ peaks sharply, then falls steadily to zero by the time of ozone maximum at the end of the irradiation period. The agreement between the TDLAS and the modeled NO₂ is good until the end of the irradiation period (15:28 hours) when the TDLAS values rise for no apparent reason (this effect was not observed in the previous runs in which all data collection was stopped at the end of the irradiation period). The NO₂ by difference continues to register higher concentrations and did not change when the irradiation stopped. The variations in the NO₂ concentrations from the three chemiluminescent instruments increase with the irradiation time. The LANM analyzer concentrations dropped abruptly shortly after the irradiation started. Indicating possible enhanced nitric acid removal since this run was with humidified air. This plot shows that the NO₂ by difference measured by either the NO_x analyzer (LANM) or the NO_y analyzers (STI#2, STI#1) is not NO₂. Instead, it is some other component of NO_y. The bias ranges from none at the beginning of the run to infinite by the end of the run. It is likely that this component is nitric acid. One indication of this is that the NO₂ values from the NO_x analyzer are lower than either NO_y analyzer, suggesting greater NO_y losses in the NO_x analyzer.

Figure 3-2 shows a time series plot of NO_y concentrations along with NO, TDLAS NO₂, and modeled NO₂. Note that all of the NO_y analyzers and the NO_x analyzer agree with one another until NO₂ approaches its peak. After that, the NO_x and NO_y responses fall gradually over the course of the run, but at a variety of different rates. The responses of the different analyzers diverge as the run continues, with the NO_x analyzer having a lower response than any of the NO_y analyzers.

Figure 3-1. Time Series Plots of NO and NO₂ During the Smog Chamber Evaluation.

4/9/98

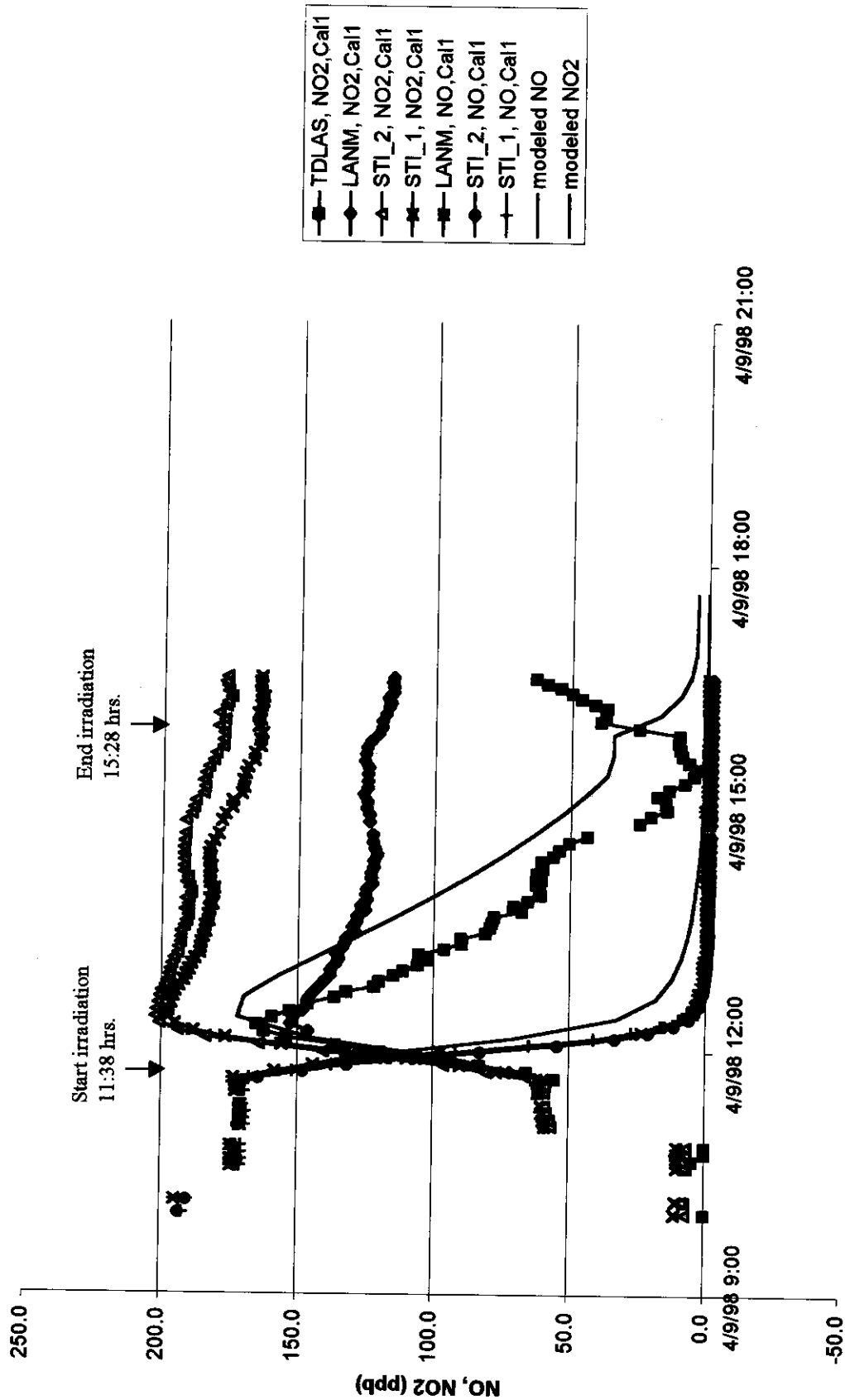


Figure 3-2. Time Series Plots of NO_y, NO and NO₂ During the Smog Chamber Evaluation.

4/9/98

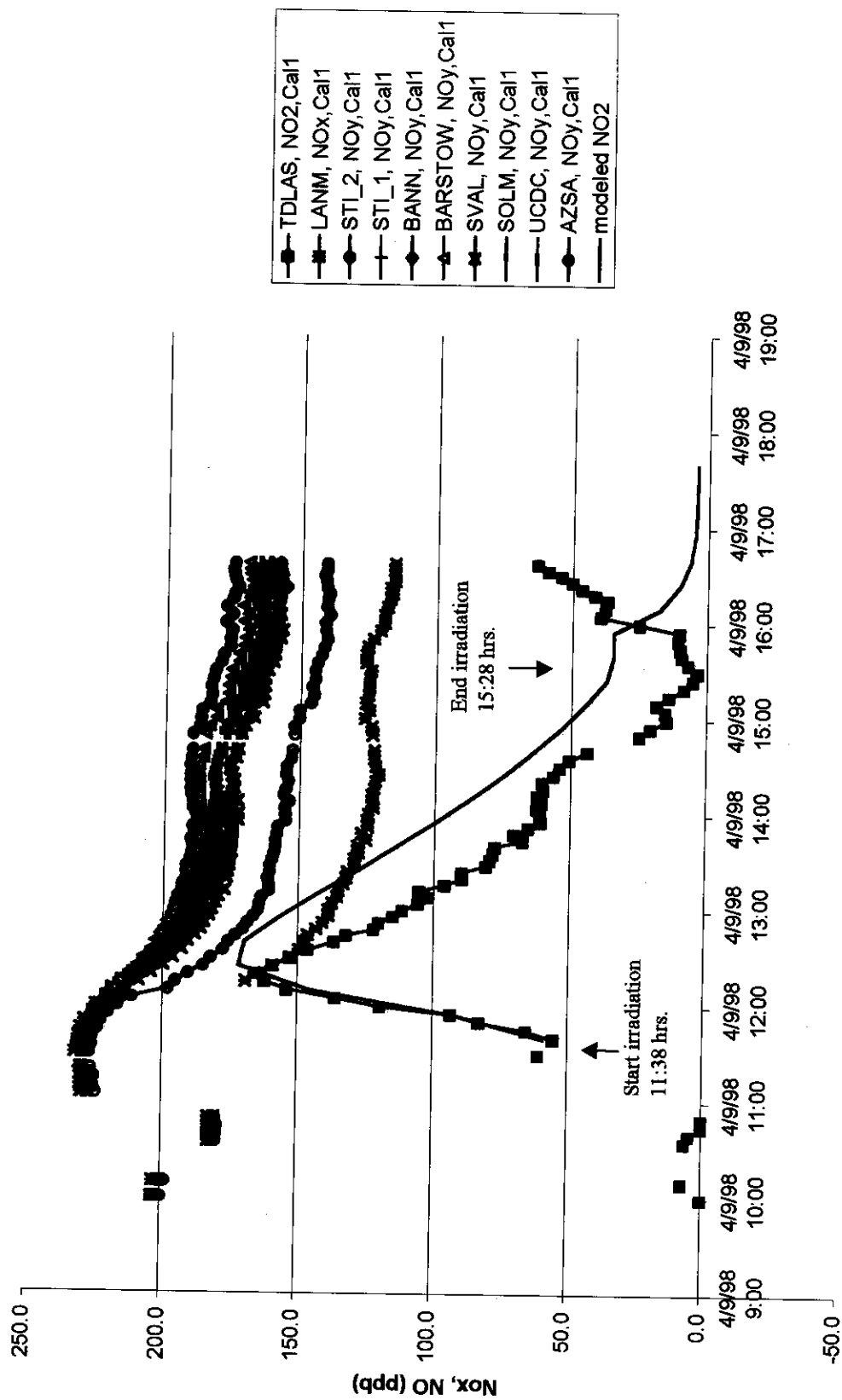


Figure 3-3. Time Series Plots of NO_x-NA, NO and NO₂ During the Smog Chamber Evaluation.

4/9/98

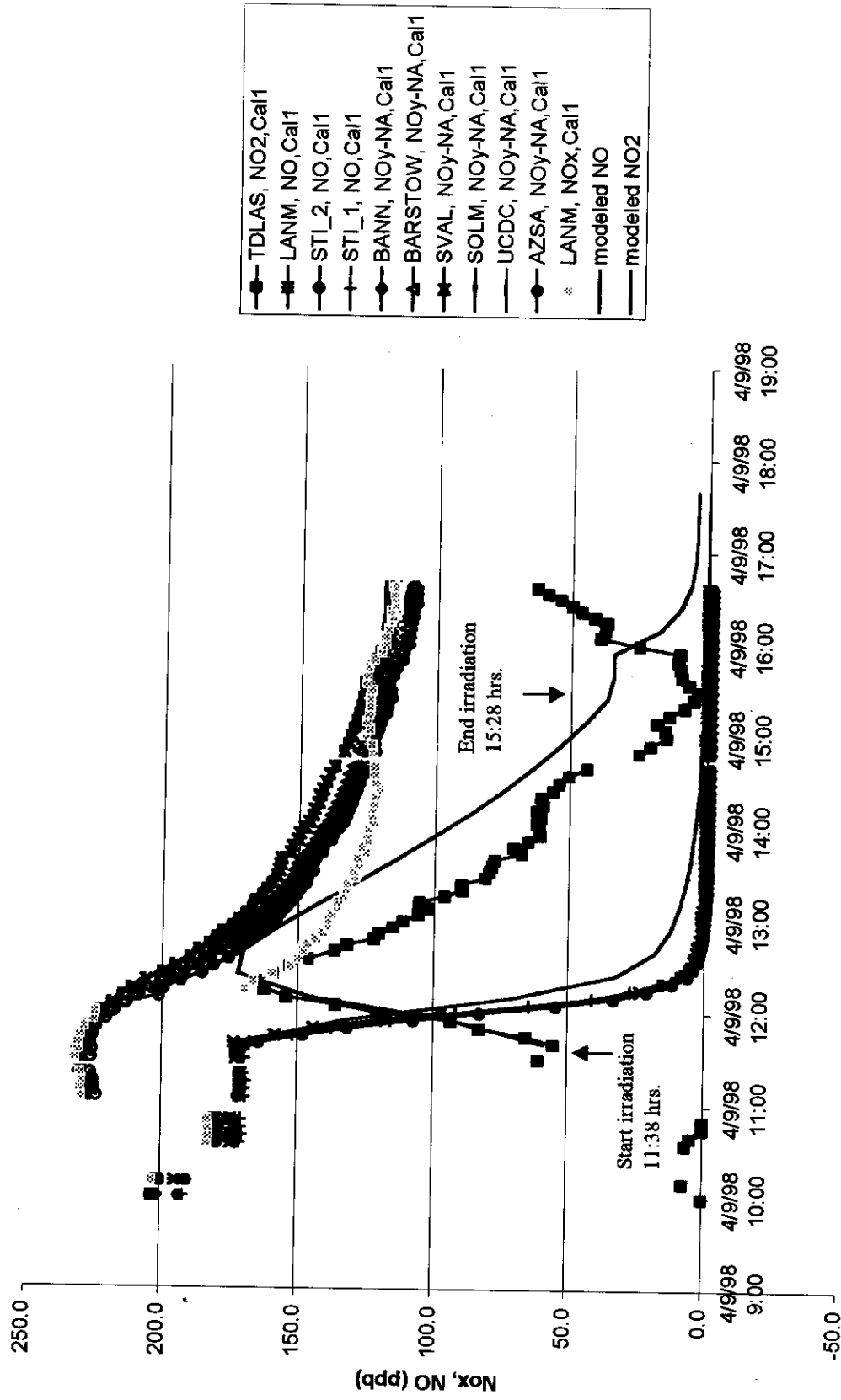


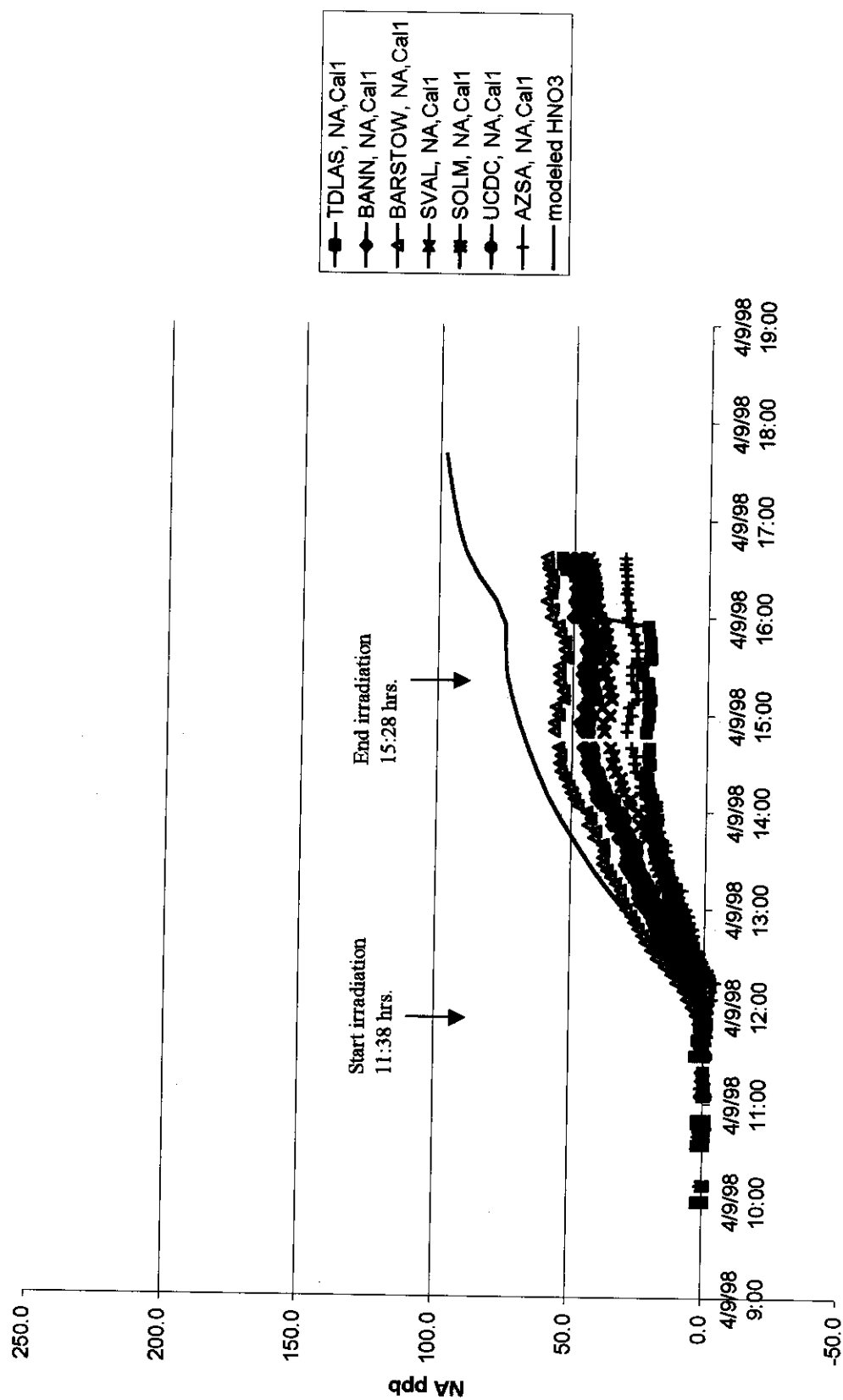
Figure 3-4. Time Series Plots of NA During the Smog Chamber Evaluation.**4/9/98**

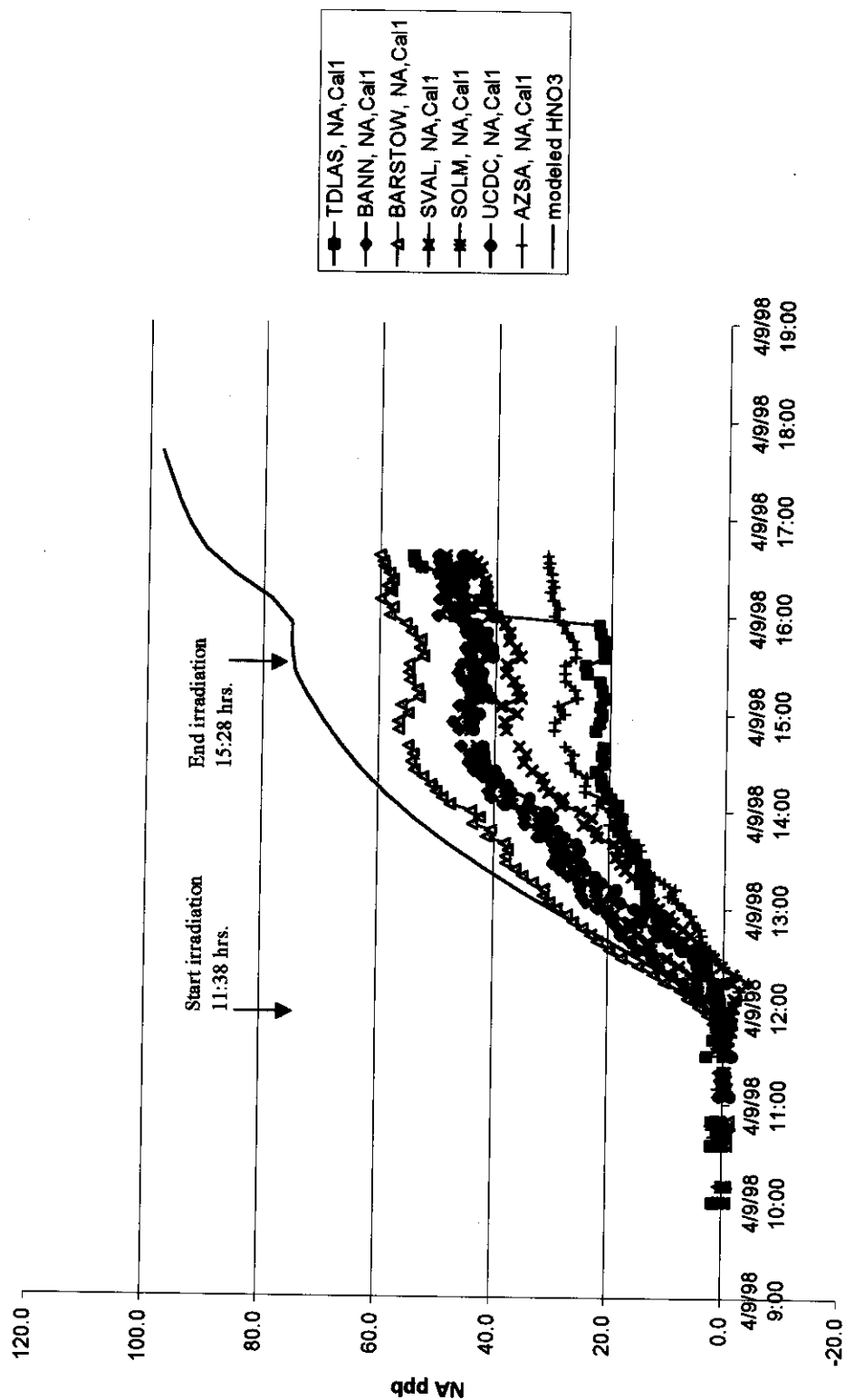
Figure 3-5. Time Series Plots of NA During the Smog Chamber Evaluation.**4/9/98**

Figure 3-3 shows that the component causing the divergence in response is removed by the NaCl filter. In this figure the NO_y - responses of the six dual converter analyzers, including Azusa, are grouped very closely. The divergence in NO_y response coupled with the consistency in NO_y - response leads to a divergence in response for the difference, NA.

Figure 3-4 shows NA by difference along with HNO_3 measured by the TDLAS and the modeled concentrations. First, note that the TDLAS HNO_3 concentrations are the lowest during the irradiation period. The modeled HNO_3 is the highest since the model does not include wall losses. At the end of the irradiation period, the TDLAS nitric acid, like the NO_2 concentrations, rose sharply to a value similar to that obtained from the chemiluminescent analyzers. Note that an increase (although not as large) is also predicted from the model. At first look, the among analyzer variability, excluding Azusa, appears reasonable. But this is attributable to the scale. Figure 3-5 shows the same plot at larger scale and a large variability of the nitric acid measurements. Note that in the dark the TDLAS concentration values were similar to those from the chemiluminescent method. The less responsive analyzers seem to lag the more responsive analyzers and are offset from each other rather than proportional to each other. This causes very large percent differences between analyzers at concentrations of interest for ambient study. The lag, as well as the overall response slope, is probably a function of converter interactions with NA and similar compounds. It is not likely to remain a stable feature of the system.

Temperature Stability Study

Although they are purported to have compensation software, the Thermo Environmental model 42CY NO_y analyzers were suspected of having a response that was dependent on temperature and pressure. Unlike the instruments used at the ground sites, the aircraft-based instruments would be subject to rapid changes in temperature and pressure. While the instrument will respond quickly to pressure changes, temperature changes are expected to take much longer because the mass of the instrument will function as a large buffer to changes in its surrounding temperature. In order to assess the uncertainty caused by temperature changes, the instruments were evaluated in the laboratory.

The NO_y analyzers used in the UCD and San Diego aircraft were placed in a small storage room under a stairwell. Both analyzers showed, in "as received" condition, that temperature and pressure correction features were on. The room was equipped with two 1500 watt electric space heaters. A handheld temperature monitor was used to manually record temperatures inside the room, with the sensor immediately in back of the analyzers and the readout display maintained outside the room. A dilution calibrator maintained outside the room was used to generate a consistent nominal 100 ppb source of NO. Quarter-inch outside diameter PFA Teflon tubing was used to provide the sample to both NO_y analyzers via PFA Teflon tubing using two "T"s, one of which was vented to the atmosphere. The vent was checked before and after the evaluation with a rotameter to ensure adequate flow. The NO and NO_y response of each analyzer was recorded manually using a digital volt meter.

The temperature response study was conducted twice. Figures 3-6 through 3-9 present the results. Figure 3-6 shows a time series plot of the first test. Starting at room temperature, the heat was turned on while sampling zero air. Although the SD analyzer showed some erratic noise, there was no change in the observed concentrations. The instruments were then allowed to sample

NO while the temperature was maintained at 52°C, after which the heaters were turned off. The instrument response from both increased in a similar manner as they cooled. Turning the heaters back on caused the response to start decreasing. The resolution of the figure does not show the time lag in instrument response as the temperature is changed. Ten to fifteen minutes were necessary before an instrumental response was observed, although environmental temperature of the instrument changed 5-10°C.

Figure 3-6. Time Series Plot of UCD and SD NO_y Analyzer Response as a Function of Temperature, First Test.

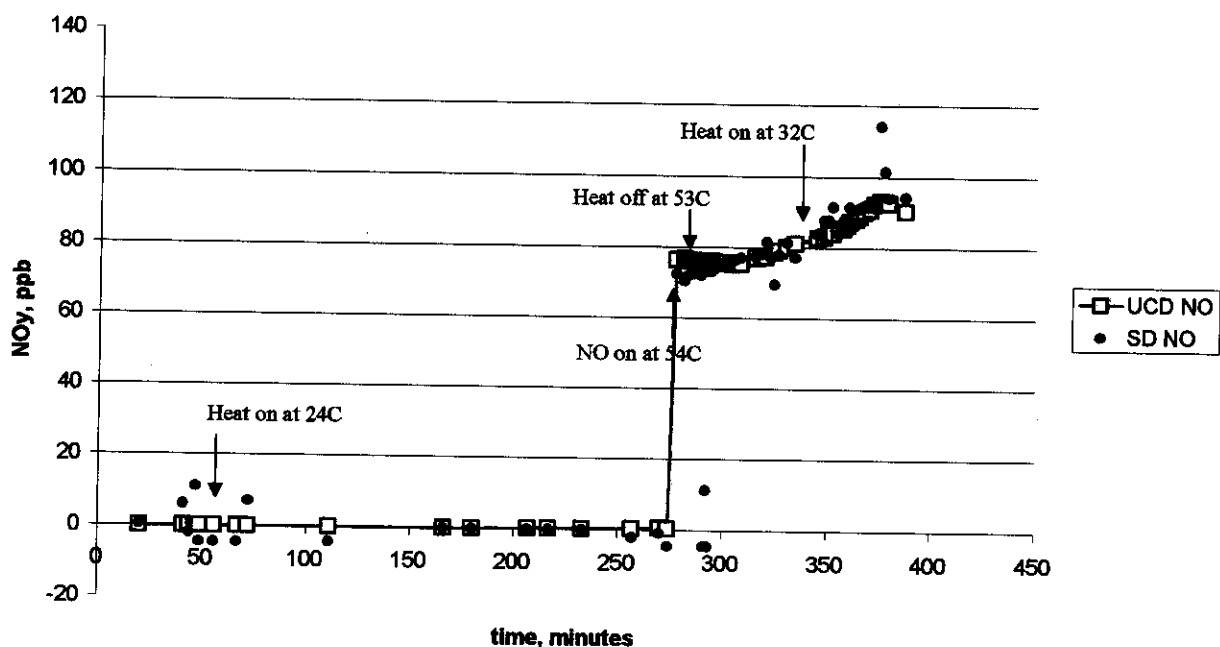


Figure 3-7 is a plot of response to NO and zero air as a function of temperature for the first test. Both instruments show a similar response. The experiment was repeated by starting with the room at 52°C and obtaining zero air and NO response. This was followed by turning the heat off and letting the room cool, and then turning the heat back on. Figure 3-8 shows a time series plot. The results are similar to those obtained in the previous experiment for the cooling mode: The NO response increases as the temperature decreases. During heating, the reverse was observed. Figure 3-9 shows the response as a function of temperature, again with results similar to those obtained during the first test.

Figure 3-7. Response of UCD and SD NO_y Analyzers as a Function of Temperature, First Test.

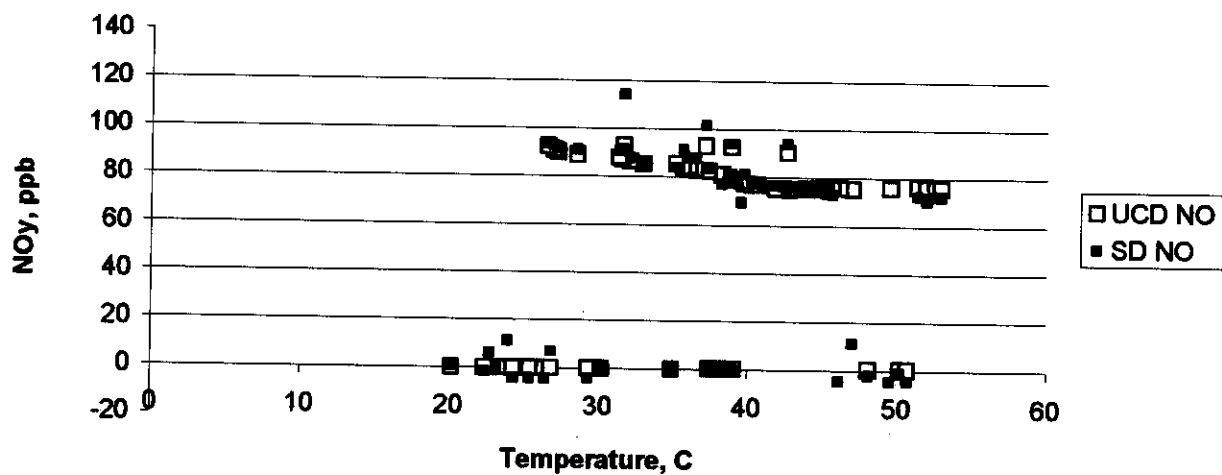


Figure 3-8. Time Series Plot of UCD and SD NO_y Analyzer Response as a Function of Temperature, Second Test.

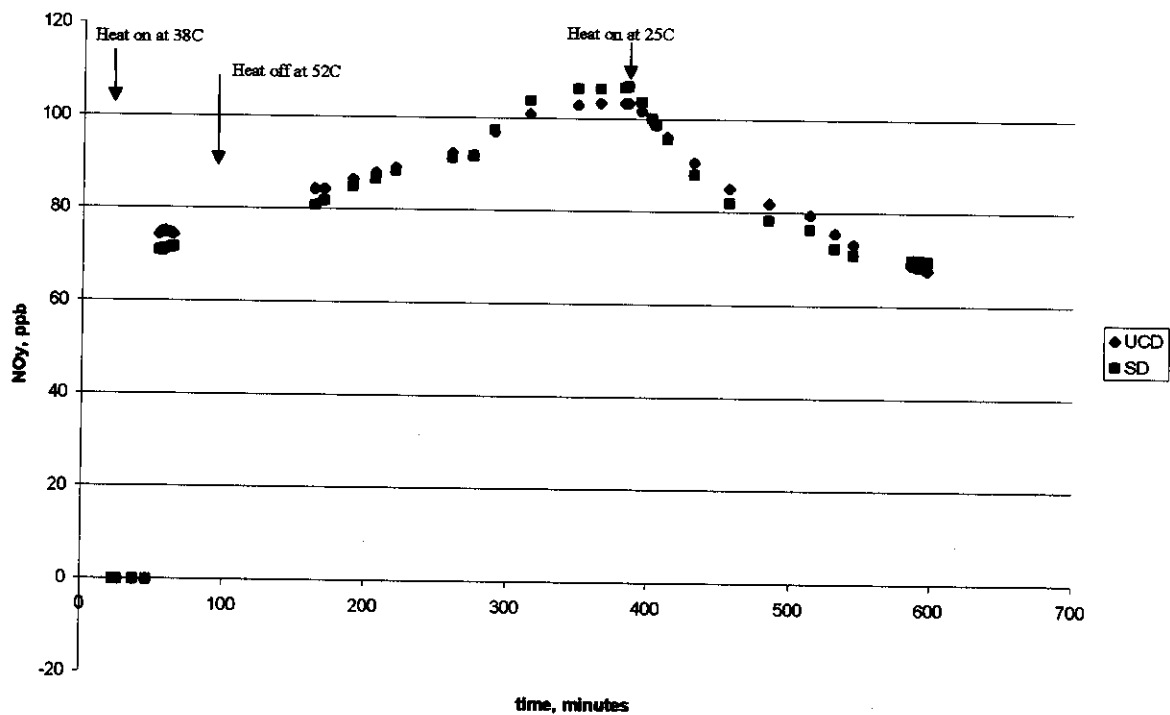
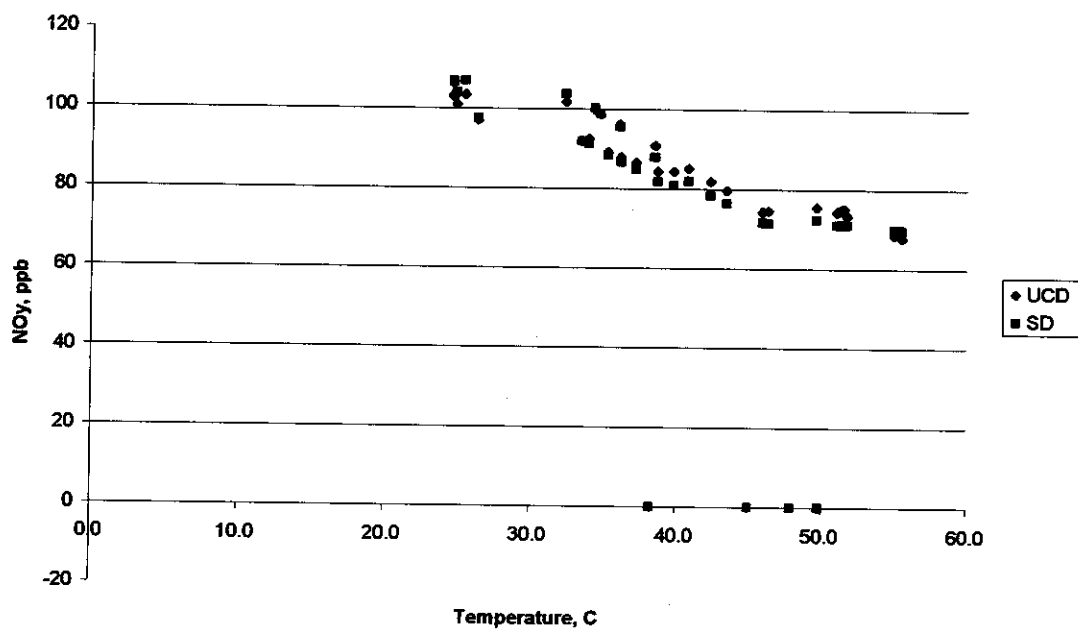


Figure 3-9. Response of UCD and SSD NO_y Analyzers as a Function of Temperature, Second Test.



These experiments showed that despite the temperature correction function, the Thermo Environmental NO_y analyzers showed a significant response to changes in temperature. We do not recommend correcting the aircraft data, however, because of the long time lag between a change in environmental temperature and a change in instrument response unless the temperature of the aircraft remains stable for the ten to fifteen minutes required for the instrument to reach thermal equilibrium.

3.1.2 NO_y and NO_y -NA Measurements

The sites were made operational in June and early July as instruments were received from the vendors and evaluated in the laboratory. Instruments were given a multi-point calibrations soon after installation. No adjustments were made to make the direct outputs match the calibration. The outputs were logged as was, and calibration factors applied in post-processing. This approach, adopted by CE-CERT Quality Assurance, has been found useful to track the overall drift of the instrument and allows traceable corrections to the data. Zero, span and converter efficiency checks were performed at intervals of approximately two weeks. These were performed with the same calibration equipment each time to ensure comparability between instruments. In a further effort to ensure comparability, site checks were all performed by a single technician with the occasional oversight by senior CE-CERT staff.

At sites shared with local air quality monitoring stations, data were logged using the permanent on-site data acquisition systems. These data were checked daily against the site NO_x analyzer to ensure that the NO_y tracked the NO_x and was equal or higher in concentration. Table 3-6 summarizes the results of the calibration and checks. The instruments were generally stable for the entire SCOS97-NARSTO operational period. The exceptions were when analyzers failed at downtown Los Angeles and Diamond Bar and at Soledad Mountain after October 14, when water apparently entered the sampling line caused NO_y and NO_x factors to rise significantly. For this reason, the calculation of the standard deviations at Soledad Mountain were done separately for October 14 and 23.

Daily plots of NO_y and NO_y - were reviewed as data were received. If available, NO_x , NO , and O_3 were included on these plots for the analyzers operated at the AQMD and APCD sites (AZSA, BANN, LANM, SOLM, SVAL, and UCDC). The plots were examined for expected diurnal trends, relationship between NO_y and NO_y -, and relationship between NO_y analyzer response with NO_x , NO , and O_3 data. Data for time periods that the instrument was off-line, and for time periods having converter failures were marked missing or invalid as appropriate.

Before Filter Change										After Filter Change										Comments		
Date	NOY Zero	NOY-NA	NOY ppb	NOY-NA ppb	NOY factor	NOY-NA factor	NOY Zero ppb	NOY-NA Zero ppb	NOY ppb	NOY-NA ppb	NOY factor	NOY-NA factor	NOY GPT, ppb	NOY-NA GPT, ppb	NOY GPT % eff.	NOY-NA GPT % eff.	NOY NPN ppb	NOY-NA NPN, ppb	NOY NPR % eff.		NOY-NA % eff.	NOY Ave factor
RIVERSIDE (SN 58440)																						
1-Jul		NA	NA	NA			0.6	0	103.1	101.7	1.14	1.13	99.2	96.9	94.0%	92.5%	31.4	31.1	80.0%	79.0%	1.14	1.13
21-Jul		109.5	113.5	1.16	1.12	1.12	0.5	0.1	99.6	105.5	1.28	1.20	99.8	103.9	100.3%	97.6%					1.22	1.16
28-Jul		102.5	101.2	1.25	1.25	1.25	0.7	-0.1	94.2	97.9	1.36	1.29	93.7	96.8	99.2%	98.2%					1.30	1.27
15-Aug		101.1	98.2	1.28	1.28	1.28	1.7	0	94.2	97.8	1.37	1.30	92.2	95.9	98.6%	98.9%					1.32	1.29
29-Aug		98.7	93.4	1.30	1.30	1.30	0.8	0	92.2	97.3	1.39	1.30	91.3	96.4	98.4%	98.5%	32.9	32.0	87.0%	86.0%	1.34	1.23
16-Sep		98.1	82	1.31	1.55	1.55	1.2	0	96.6	95.4	1.33	1.33	93.7	94.3	95.2%	98.2%	32.9	32.0	87.0%	86.0%	1.32	1.44
8-Oct		98.1	65.2	1.32	1.93	2.2	-0.5	0.4	91.2	94.8	1.42	1.33	90.3	94.8	98.4%	100.0%	32.9	33	92.0%	89.0%	1.37	1.63
24-Oct		88.2	90.4	1.44	1.41	1.41	0.3	0.4					87.8	90.9	99.3%	100.9%	31.3	32.5	1.0%	1.0%	1.44	1.41
Average				1.27	1.22	1.22	1.10	0			1.33	1.27			97.7%	97.9%			65.0%	63.4%	1.30	1.24
Std. Dev.				0.06	0.09	0.09	0.64	0.08			0.08	0.07			2.2%	2.5%					0.08	0.08
SOLEAD MOUNTAIN (SN 58439) converter 58313																						
10-Jul							2.4	0	118.7	116.7	1.09	1.09	118.1	117.1	99.2%	100.5%	39.1	37.6	85.0%	82.0%	1.09	1.09
23-Jul		119.1	117.6	1.08	1.08	1.08	1.3	0.4	119.3	117.7	1.07	1.08	119.5	117.7	100.3%	100.0%					1.08	1.08
21-Aug		124	118.6	1.05	1.08	1.08	3.1	0.7	119.9	118.7	1.09	1.07	119.4	117.7	99.3%	98.7%					1.07	1.08
17-Sep		113.6	111.6	1.15	1.15	1.15	3.5	0.9	112.3	109.8	1.17	1.16	110.9	108	98.0%	97.4%	41.3	39.9	96.0%	93.0%	1.16	1.15
Average				1.08	1.10	1.10	2.38	0.5			1.10	1.10			99.2%	99.1%					1.10	1.10
Std. Dev.				0.05	0.04	0.04	1.9	0.39			0.04	0.04			0.9%	1.4%					0.05	0.04
14-Oct							1.9	2	97	96.5	1.33	1.34	96	96	98.3%	98.2%					1.33	1.34
23-Oct							1	1	102	101	1.26	1.27	101	101	98.4%	100.0%	34.0	34.0	85.0%	86.0%	1.26	1.27
Average							1.45	1.5			1.29	1.30			98.4%	98.6%			88.8%	87.2%	1.29	1.30
Std. Dev.							0.64	0.71			0.06	0.05			0.1%	0.6%					0.06	0.05
SAN NICOLAS ISLAND																						
3-Jul							2.6	0.1	89.1	86.1	1.16	1.17	88.9		99.6%						1.16	1.17
29-Jul							-0.27	0.1	47.2	47.4	1.22	1.23	47.4		100.7%						1.22	1.23
9-Sep							-0.3	0	42.5	41.7	1.36	1.39	42.8		99.3%						1.36	1.39
21-Oct							-0.1	0	43.9	43.7	1.32	1.34	43.7		1.00%						1.32	1.34
Average							-0.22	0.05			1.27	1.28			0.01%						1.27	1.28
Std. Dev.							0.11	0.06			0.09	0.10									0.09	0.10
SIMI VALLEY (SN 58438)																						
7-Jul							1.25	0.31	123.4	123.2	1.04	1.03	124.1	123.8	100.9%	100.8%	42.2	41.7	88.0%	87.0%	1.04	1.03
24-Jul		131	129.7	0.97	0.97	0.97	0.2	-0.6	128.2	127.9	0.99	0.99	127.9	126.3	99.6%	98.0%					0.98	0.98
30-Jul		127.6	127.4	0.98	0.98	0.98	-0.5	-0.3	127.7	126.4	0.99	1.00	126.8	125.8	99.9%	99.3%					0.99	1.00
20-Aug		133	131	0.95	0.97	0.97	-0.7	-0.3	130.6	131	0.97	0.97	128.8	129.8	97.8%	98.6%					0.96	0.97
2-Sep		130.6	130.7	0.97	0.97	0.97	-0.4	-0.5	130.6	130.7	0.97	0.97	129.1	129.2	98.2%	98.2%	45.4	43.7	88.0%	85.0%	0.97	0.97
13-Sep		133.8	127.4	0.97	1.00	1.00	3.5	0.9	134.8	131.7	0.97	0.97	133.1	134.7	97.9%	98.3%	48.5	46.5	90.0%	86.0%	0.90	0.97
10-Oct		144.4	122.4	0.89	1.02	1.02	1.2	-1.7	139.1	136	0.92	0.92	138.2	134.7	99.0%	98.5%					0.91	0.95
31-Oct		138.7	126.8	0.92	0.89	0.89	0.6	-1.6	142.7	138.1	0.88	0.91	137.7	136.1	94.4%	97.7%	48.6	47.9	87.0%	87.0%	0.91	0.95
Average				0.96	0.99	0.99	1.5	0.7			0.97	0.97			98.6%	98.5%			88.2%	85.6%	0.96	0.98
Std. Dev.				0.04	0.02	0.02	1.5	1.4			0.04	0.03			1.1%	1.0%					0.04	0.03

Notes:
 Factors are based on a single NO span cylinder using a single Columbia model 1700 calibrator referenced to the NIST.
 Factors are based on DAs unless otherwise noted.
 Converter efficiency is based on the following eqn: $(NOY-NOY2)/(-369*(NOY-NOY2)) / (631*(NOY-NOY2)) * 100$ where subscripts z, s, & g are for zero, span, and gpt values respectively; 369 & 631 is the NO/NO2 gpt split ratio
 NPN efficiency is based on stated tank concentration, values reported are normalized by the span check to calculate efficiency.

Calibration factors were determined by reviewing the calibration and zero/span checks. In most cases the change in the factor over the monitoring period appeared random, with no trend or rapid changes. During such periods, mean factors were determined and used since they average the day-to-day variability in both the analyzer and the calibration source. During span checks, the analyzer response was checked before and after changing the NO_y - channel inlet filter. In eight cases, the response of the NO_y - channel was substantially reduced by the old filter, and returned to previous values after installation of a fresh inlet filter. In these cases the instruments correctly sensed the problem and the low-pressure alarm was activated as noted in the comments in the table (LP alarm). When these changes were large, we tried fitting an interpolated span factor to the data period leading up to the filter change. However, as discussed below, this was not successful. Instead, we based span factors on span checks conducted immediately after the filter change, and we marked data in the period leading up to the filter change as suspect.

After application of correct span factors, we replotted the diurnal time series for each site for each day, and we plotted scatterplots of NO_y vs. NO_x data where possible. Outliers in the scatterplots were investigated or removed or marked suspect. The time series show that NO_y and NO_y - generally agree with each other fairly closely, with relatively small differences attributed to NA or instrument artifacts. At some sites and times, clogging of the NO_y filter led to reduced response for the NO_y - channel as shown by the span checks and time series plots. We tried fitting a linear trend to the span factor for the NO_y - channel for the period leading up to the filter change. However, based on examination of the time series plots, the linear fit overcorrected some time periods and undercorrected other periods. We therefore based our span factors on fresh filter span checks only, and we marked the NO_y - channel data suspect during these periods.

We only flagged NO_y or NO_y - data as suspect if there was a clear problem with the NO_y or NO_y - data. Flags for NA by difference were set to the worse of the two contributing measurement flags, NO_y or NO_y -. We reviewed the NA data, but we did not change the flags based on the behavior of the NA data. We observed that "normal" operation of the NO_y analyzer includes drifts and time lags between the two channels that often led to unreasonable NA data such as negative values of nitric acid. The NA concentrations are generally small differences between two larger numbers, and are noisy. Further, the errors are not random, but tend to follow diurnal patterns. There are two reasons for diurnal patterns in the NA errors. First, NO_y follows a strong diurnal pattern with a large morning peak. Small discrepancies in span factors are magnified during the morning NO_y peak. Second, there appear to be time lags in the response to NA and similar compounds. Nitric acid and other species follow a strong diurnal profile driven by the daily photochemical cycle. The measurement times of interest, such as an afternoon peak in nitric acid, are also the times that the concentrations are changing most rapidly. The hourly NA data are strongly affected by these rapid changes, though the daily average may be reasonable.

Results

Figures 3-10 through 3-18 summarize the hourly-averaged data obtained from the NO_y instruments operated by CE-CERT during the SCOS97-NARSTO IOP periods. The most striking feature is that at every location where the dual converter NO_y/HNO_3 system was used, the NO_y and the NO_y -NA were very nearly the same. Taking the difference of two similar values to obtain nitric acid concentration will therefore result in considerable uncertainty. Given that the converters for NO_y appeared to have a higher zero offset apparently due to holdup of nitric acid or particulate nitrate (most noticeable at the locations of higher concentrations), the bias for nitric acid would generally be on the high side when the concentrations were low and biased low when the concentrations were high. There are, nevertheless, periods when nitric acid concentrations determined by this difference method are negative.

Figure 3-10. Summary of NO_y Measurements Performed in Azusa, CA, for SCOS97-NARSTO IOP Periods.

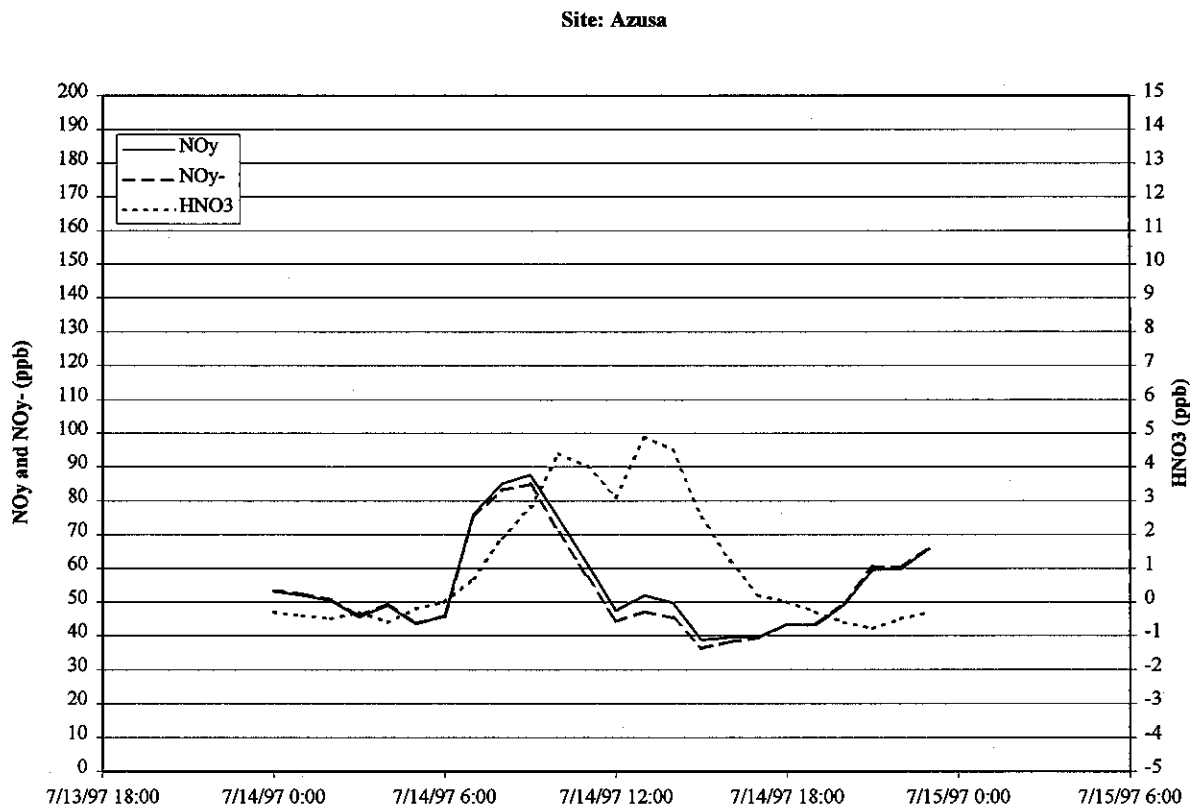
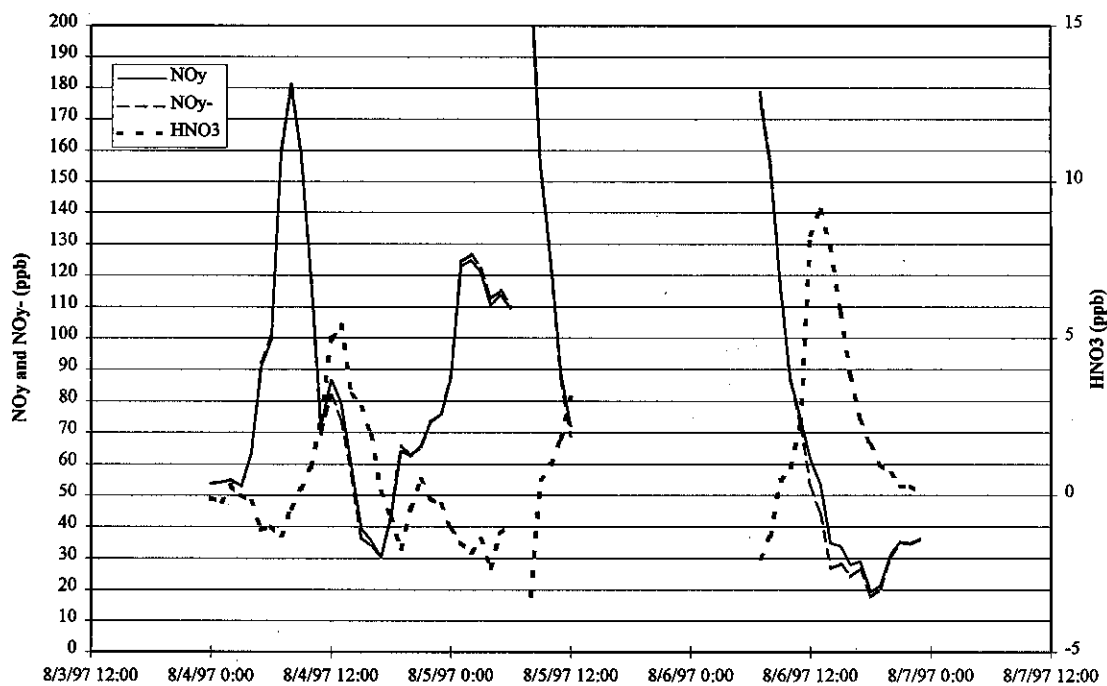


Figure 3-10, continued.

Site: Azusa



Site: Azusa

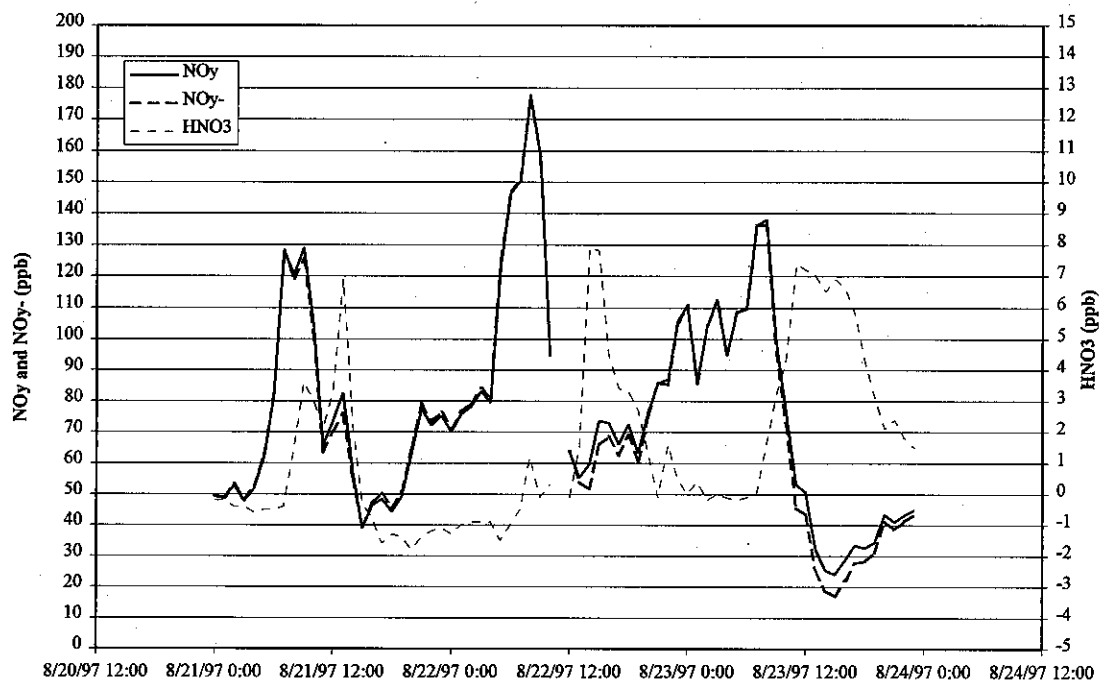
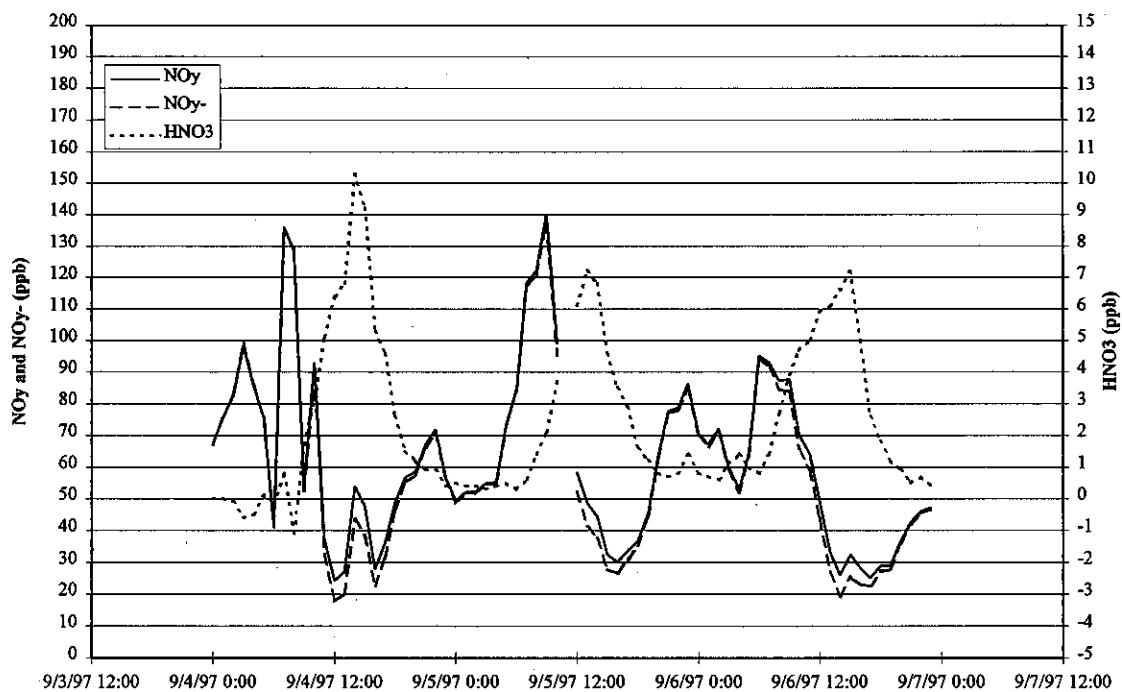


Figure 3-10, continued.

Site: Azusa



Site: Azusa

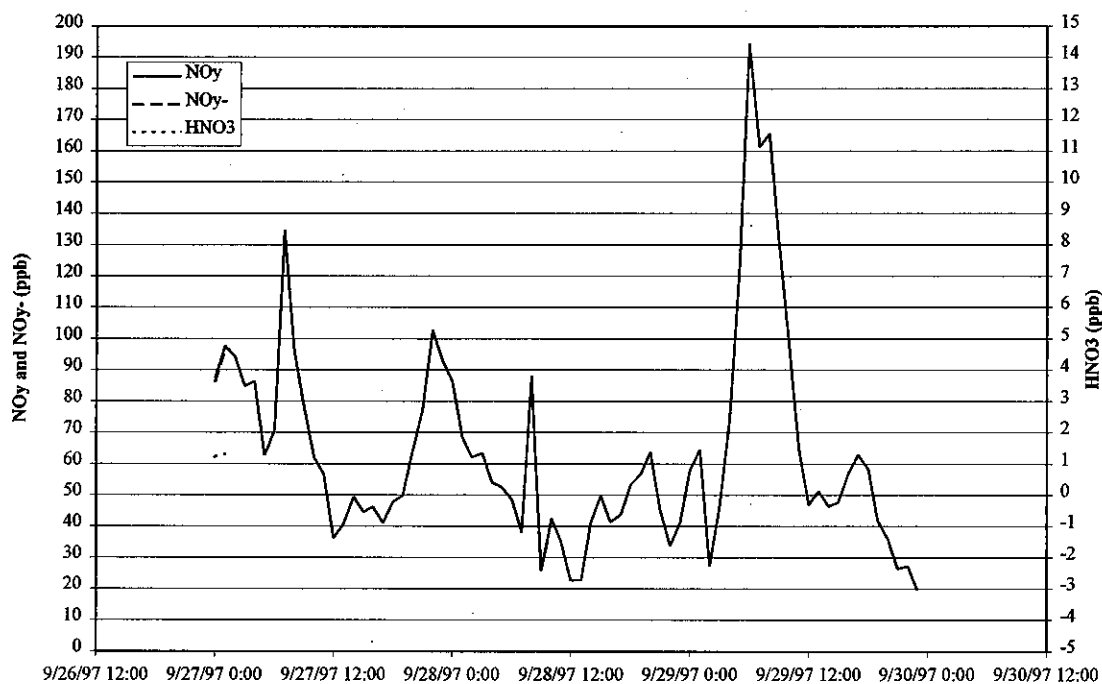


Figure 3-10, continued.

Site: Azusa

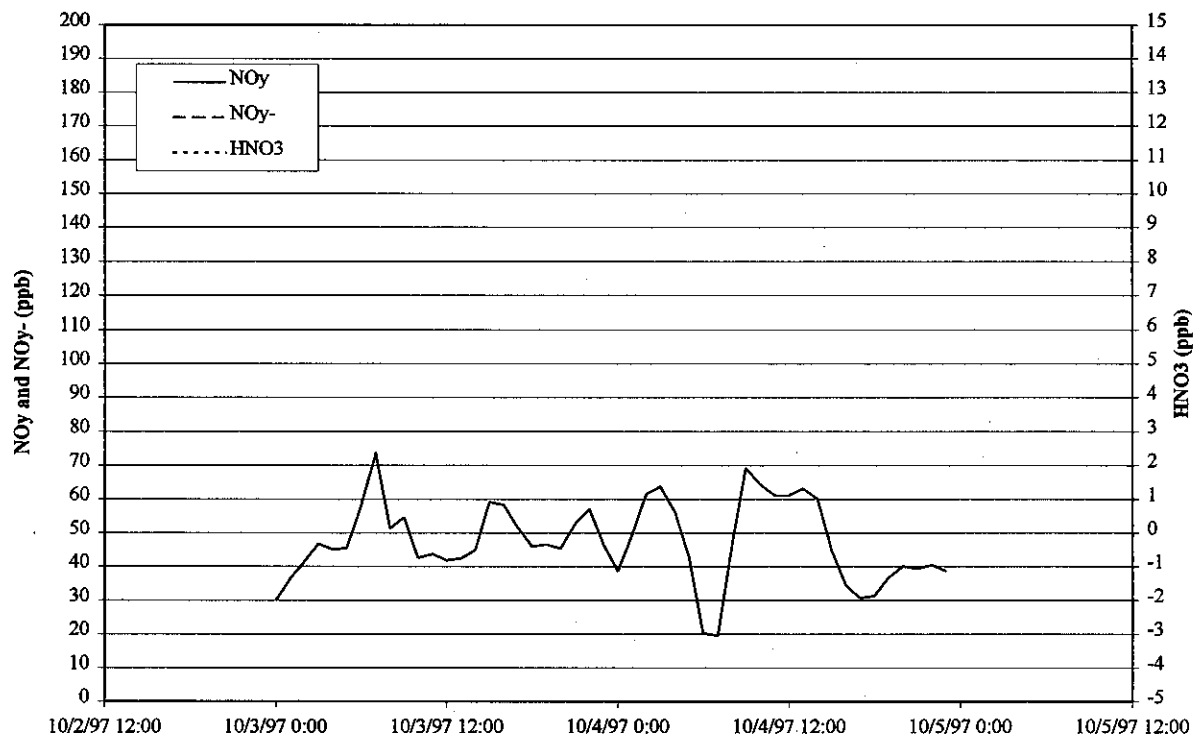


Figure 3-11. Summary of NO_y Measurements Performed in Banning, CA, for SCOS97-NARSTO IOP Periods.

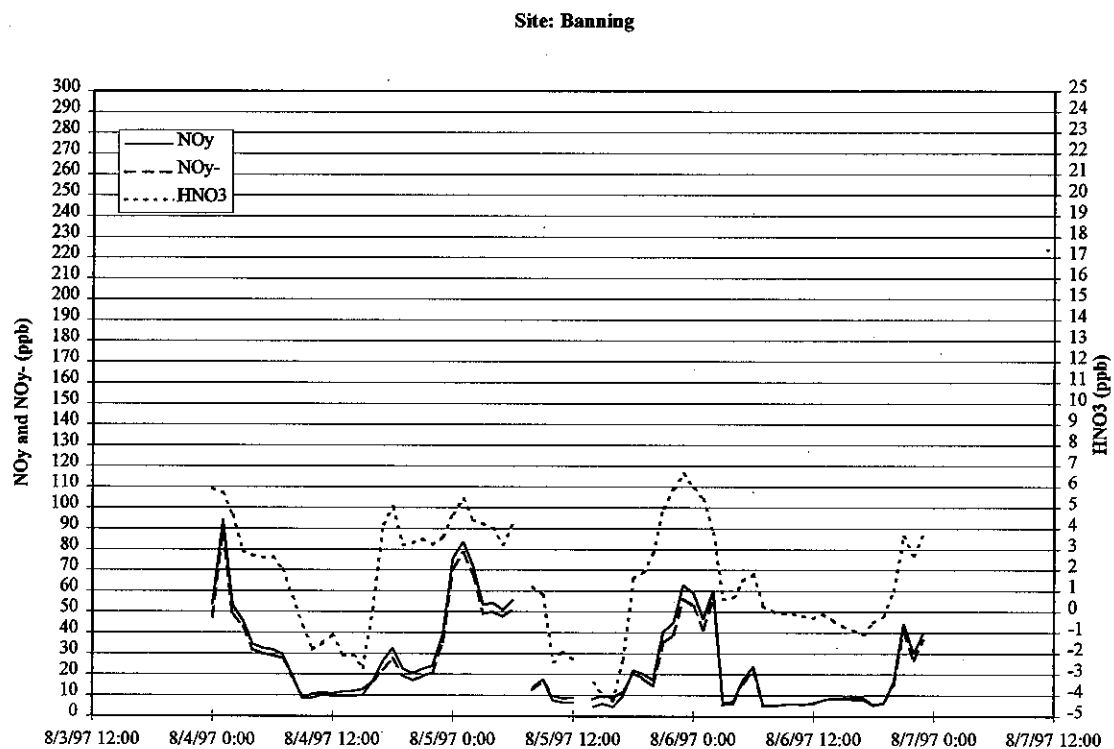
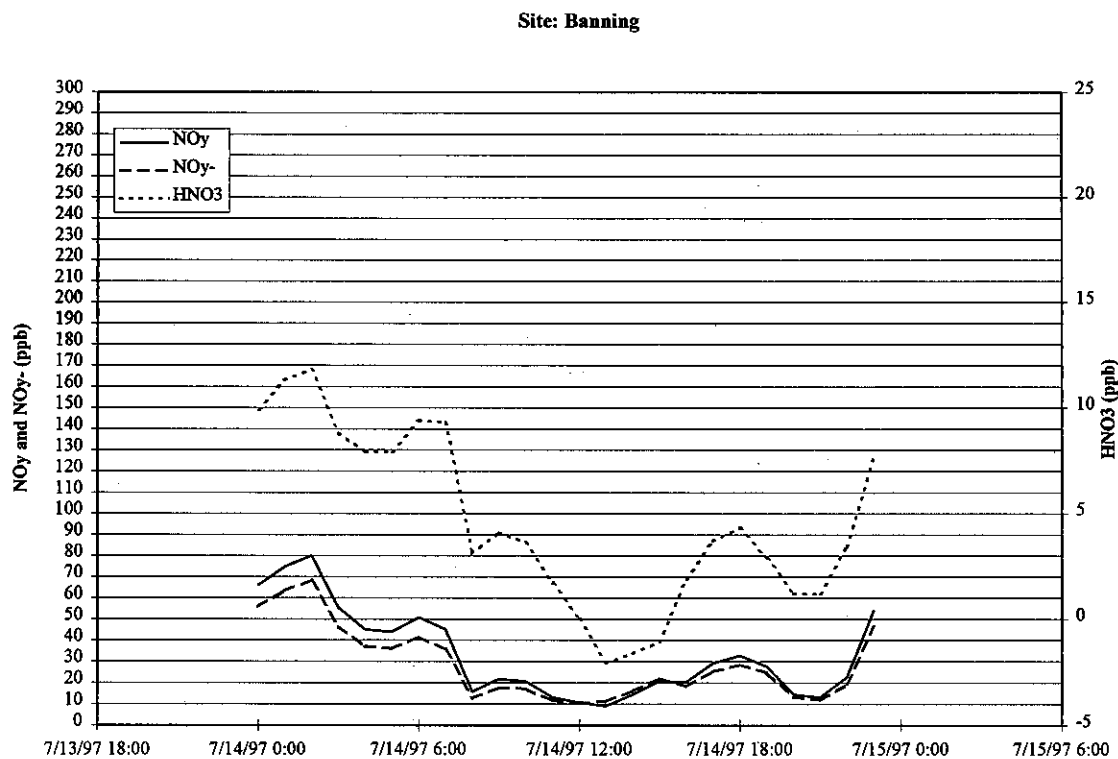
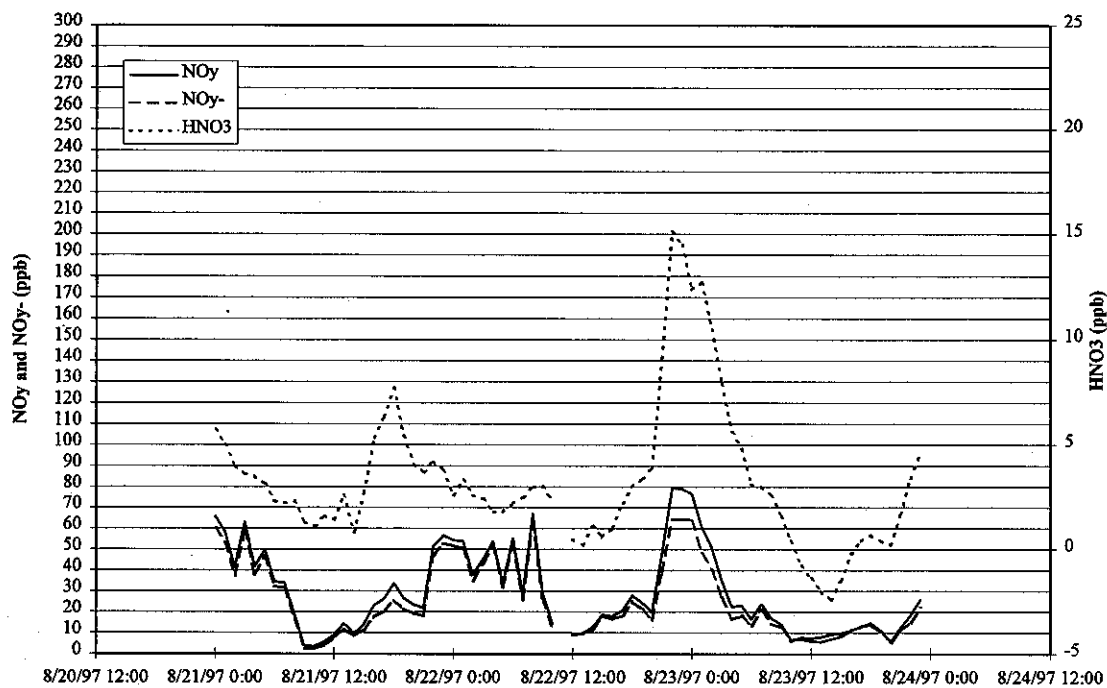


Figure 3-11, continued.

Site: Banning



Site: Banning

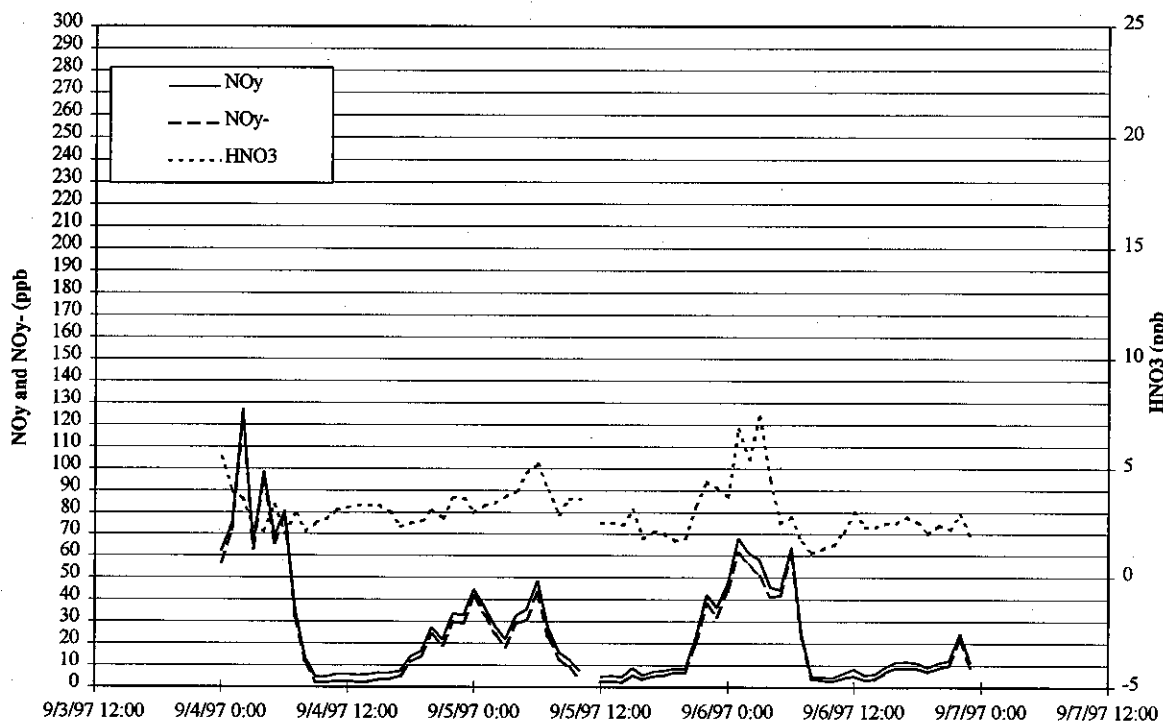
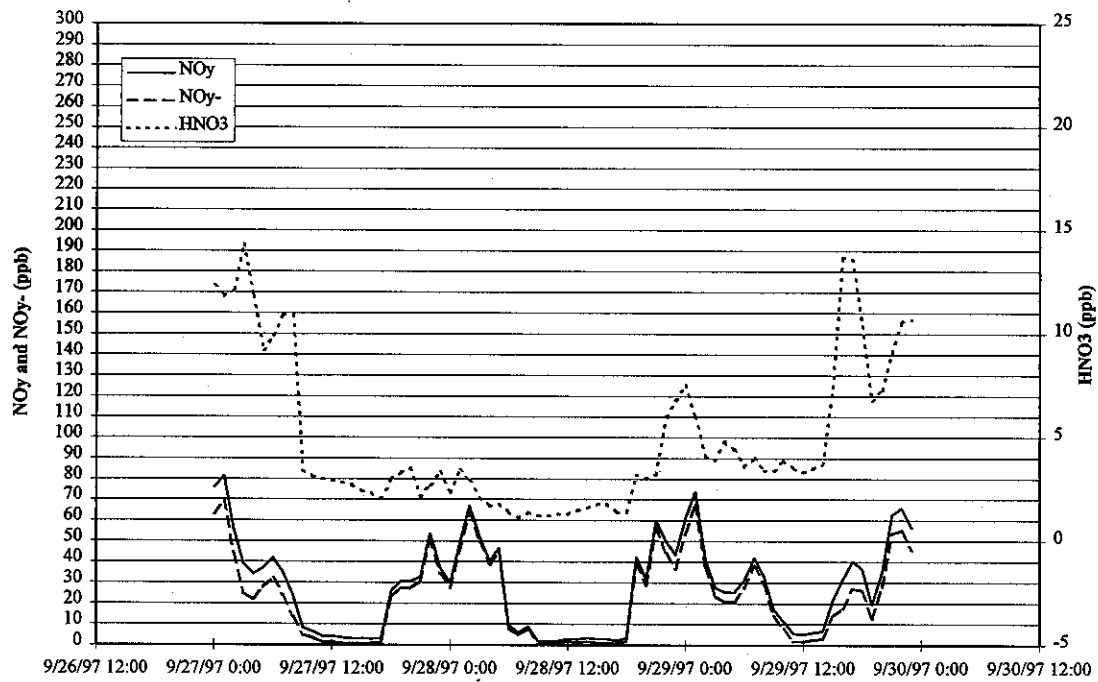


Figure 3-11, continued.

Site: Banning



Site: Banning

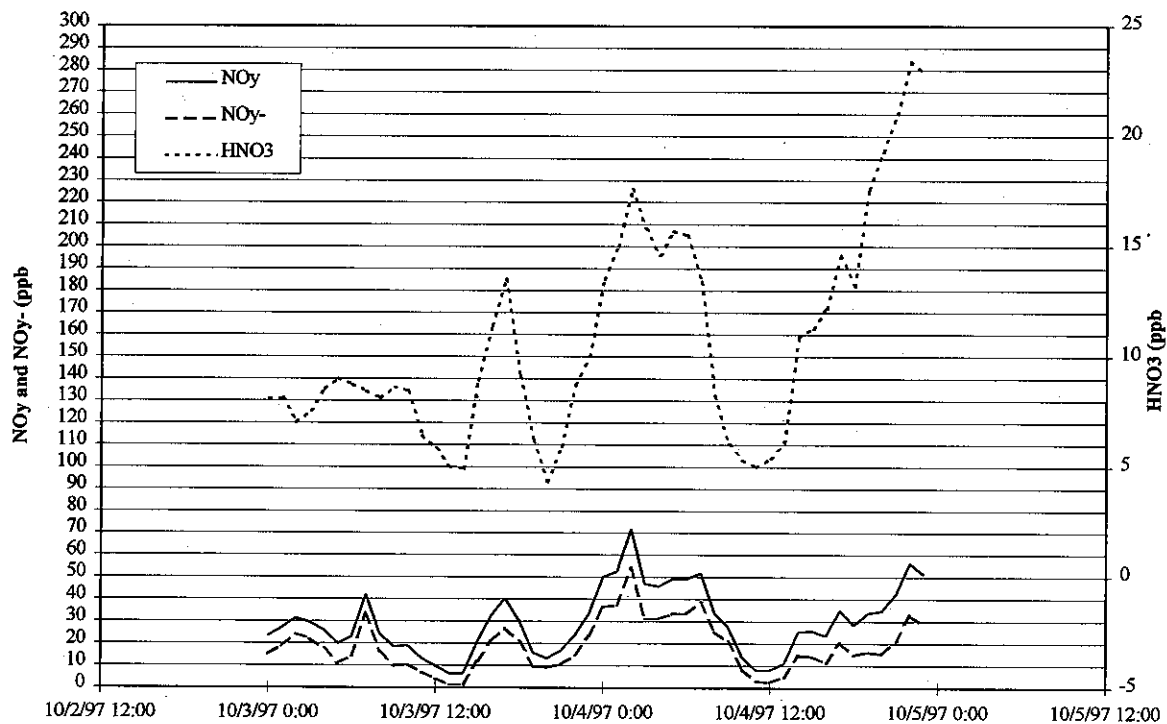


Figure 3-12. Summary of NO_y Measurements Performed in Diamond Bar, CA, for SCOS97-NARSTO IOP Periods.

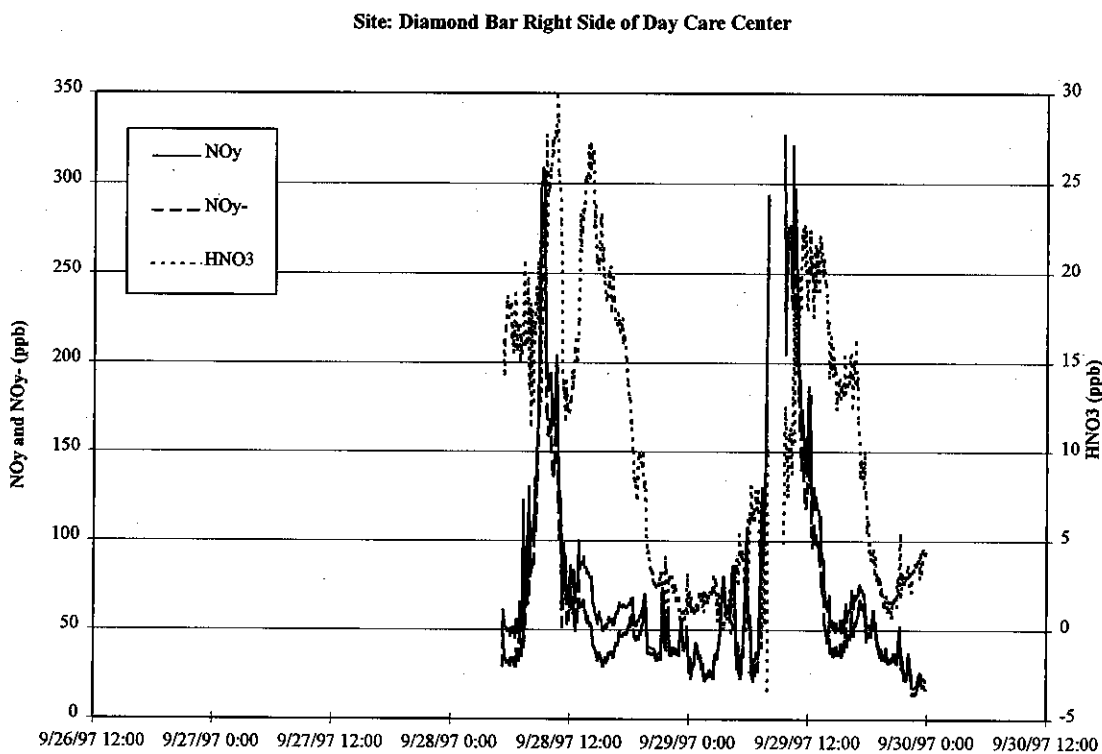
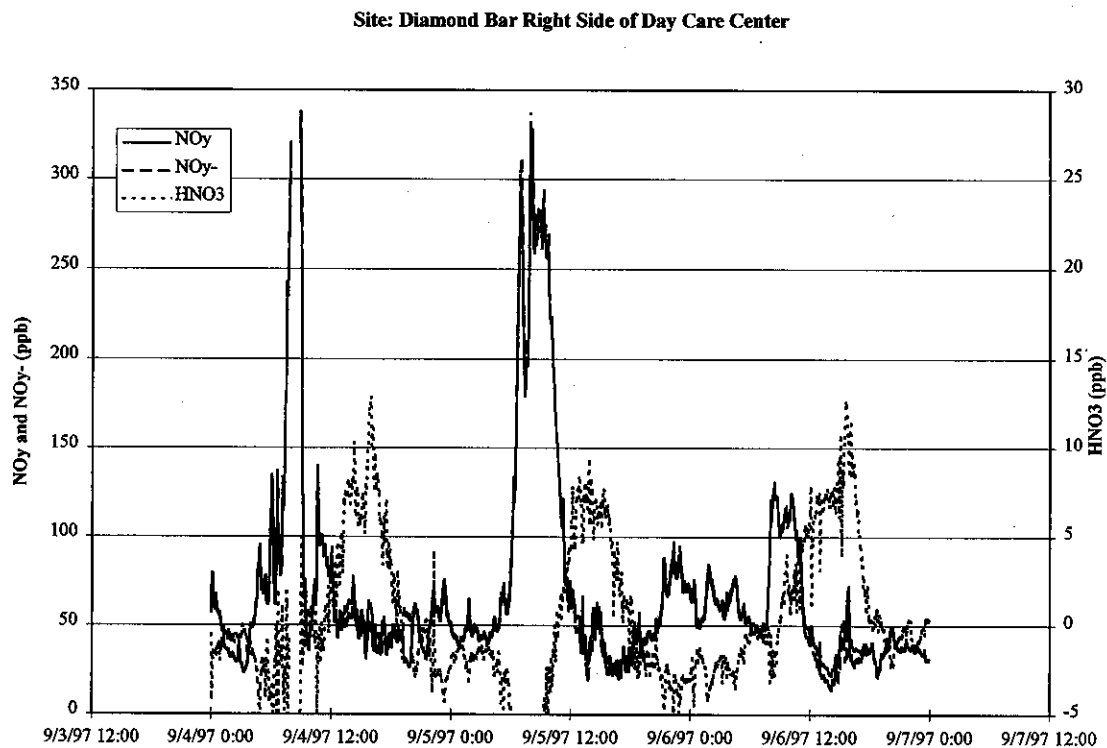


Figure 3-13. Summary of NO_y Measurements Performed in Los Angeles (North Main), CA, for SCOS97-NARSTO IOP Periods.

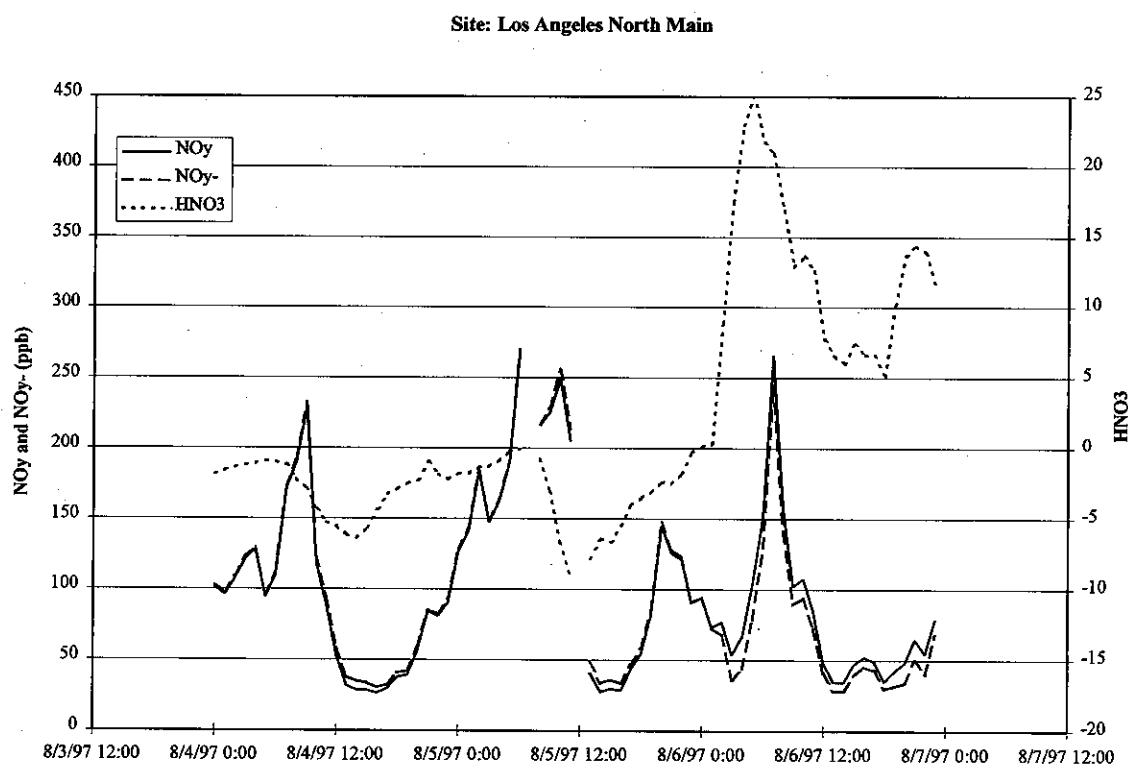
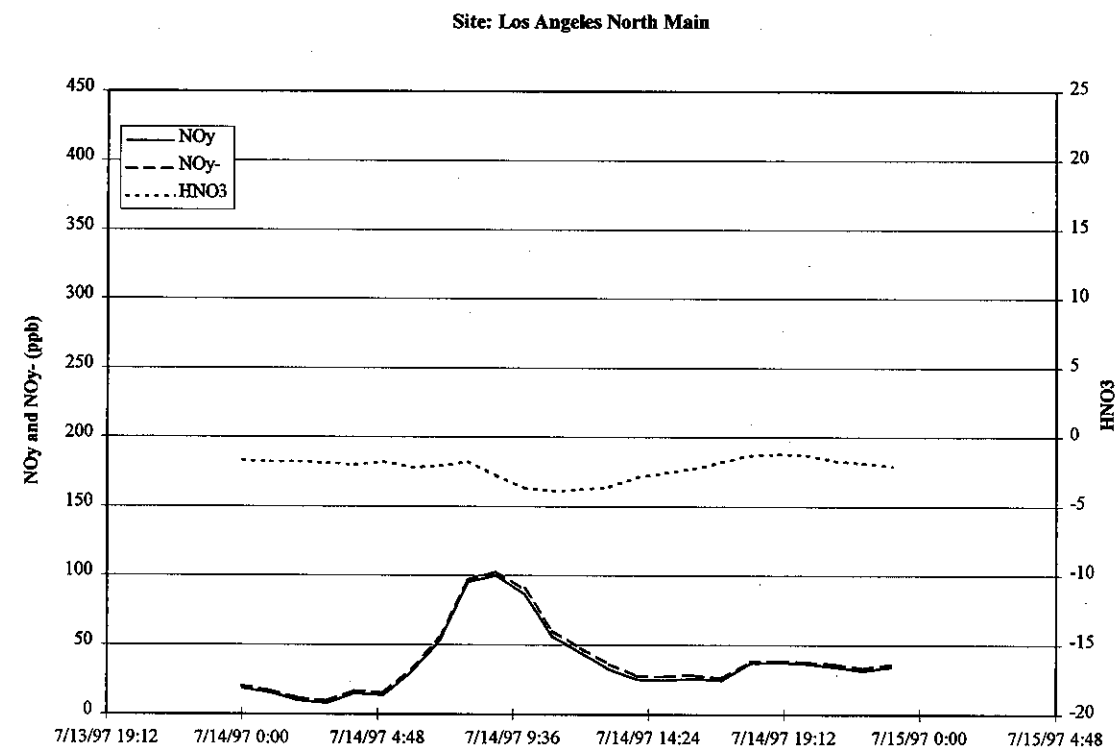
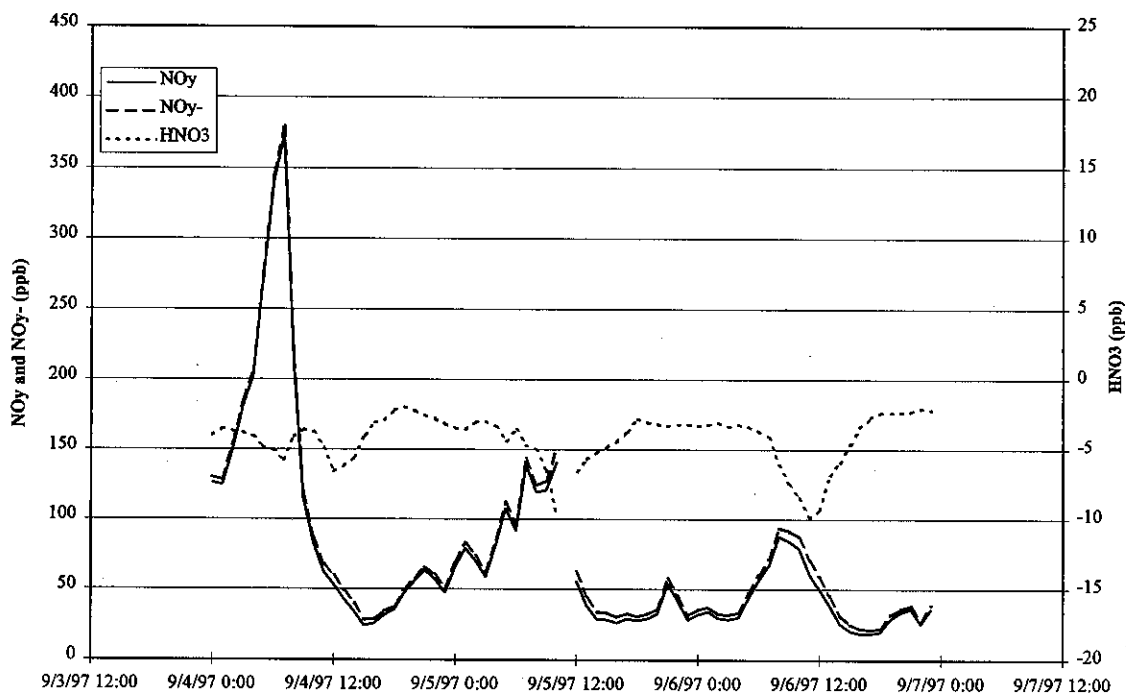


Figure 3-13, continued.

Site: Los Angeles North Main



Site: Los Angeles North Main

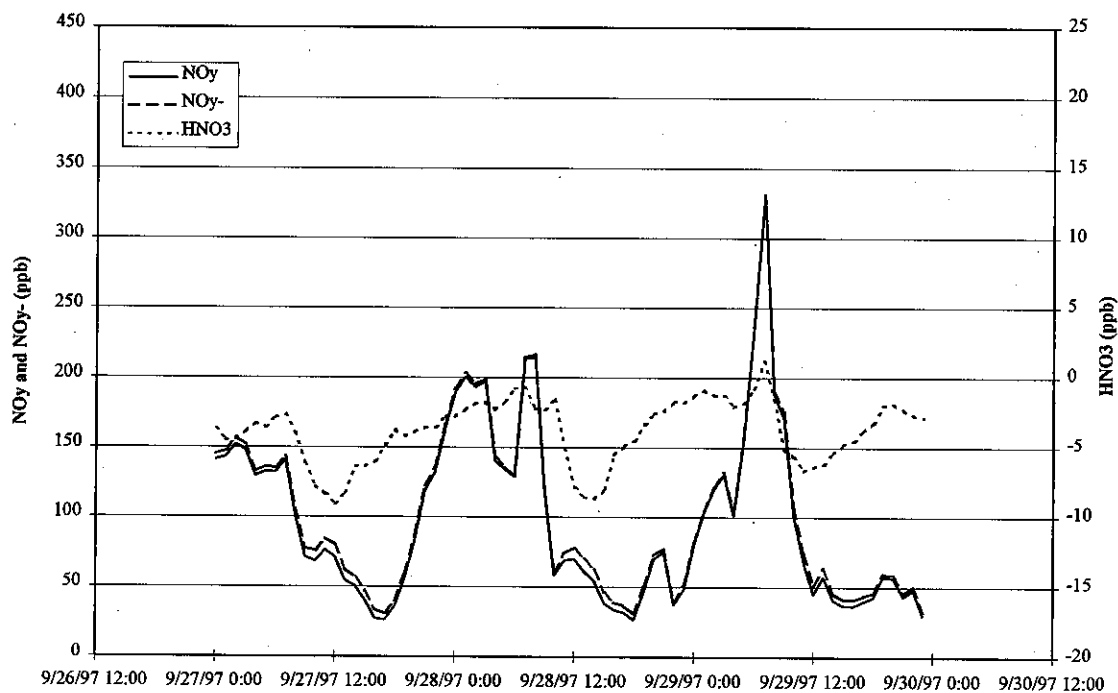


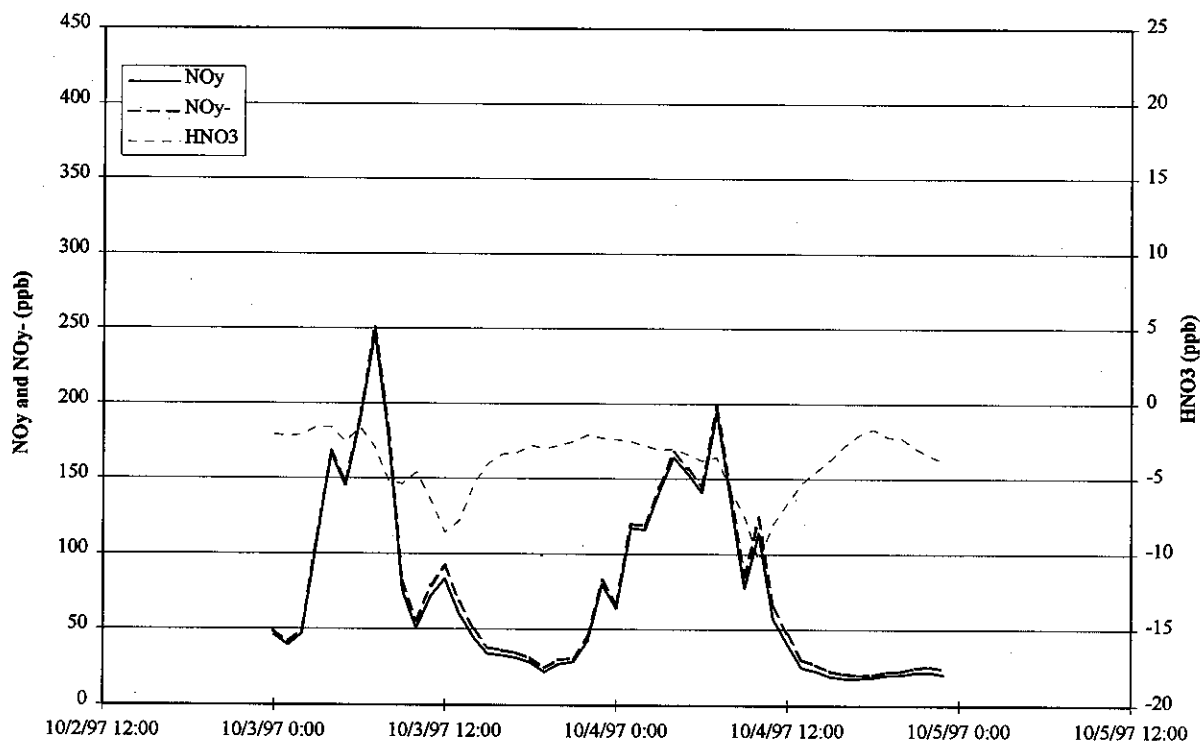
Figure 3-13, continued.**Site: Los Angeles North Main**

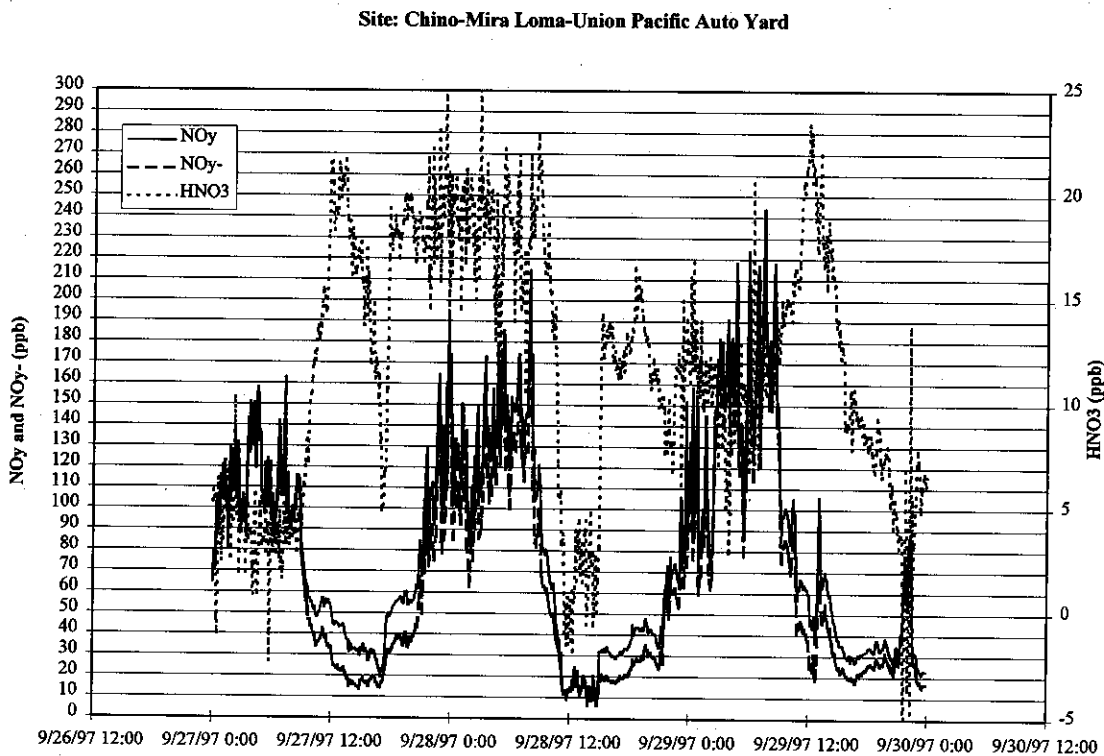
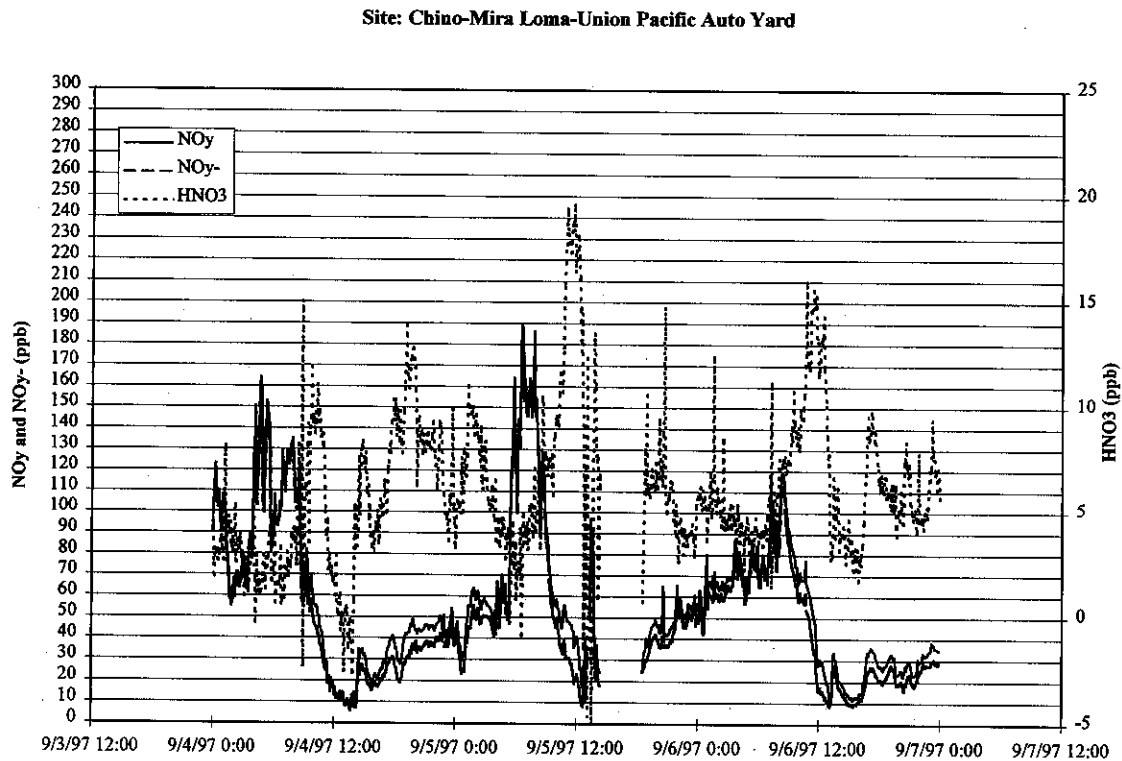
Figure 3-14. Summary of NO_y Measurements Performed in Mira Loma, CA, for SCOS97-NARSTO IOP Periods.

Figure 3-14, continued.

Site: Chino-Mira Loma-Union Pacific Auto Yard

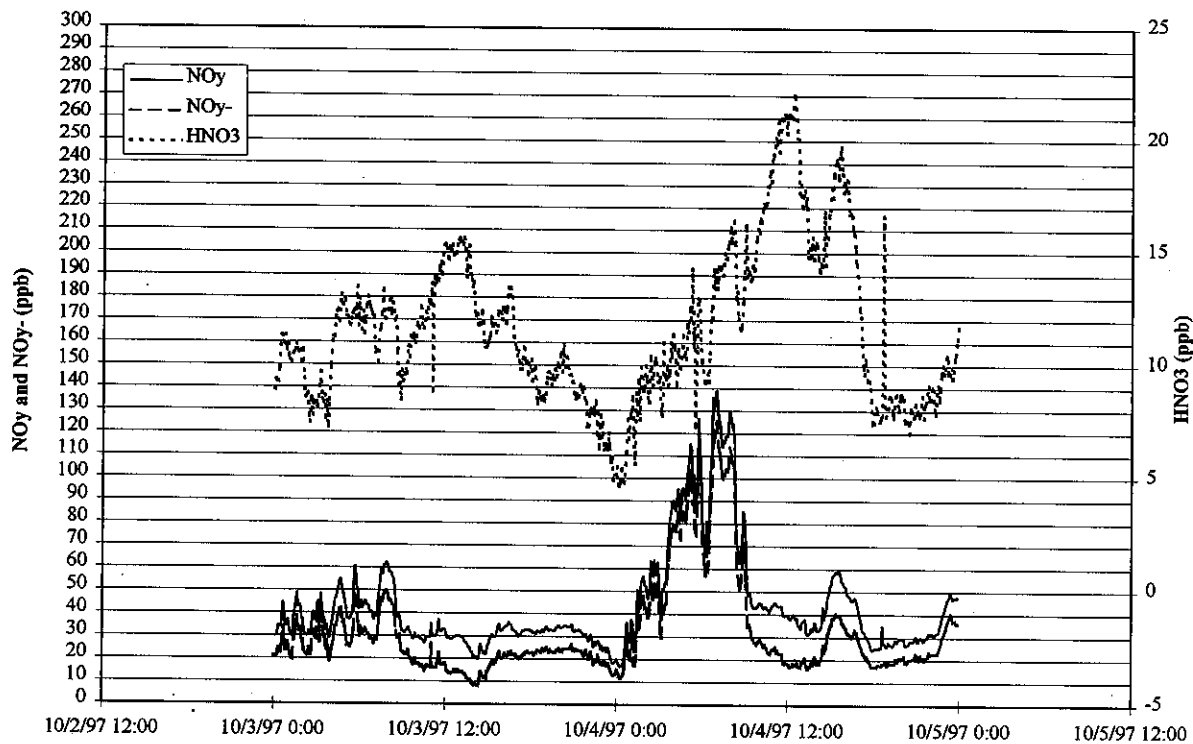
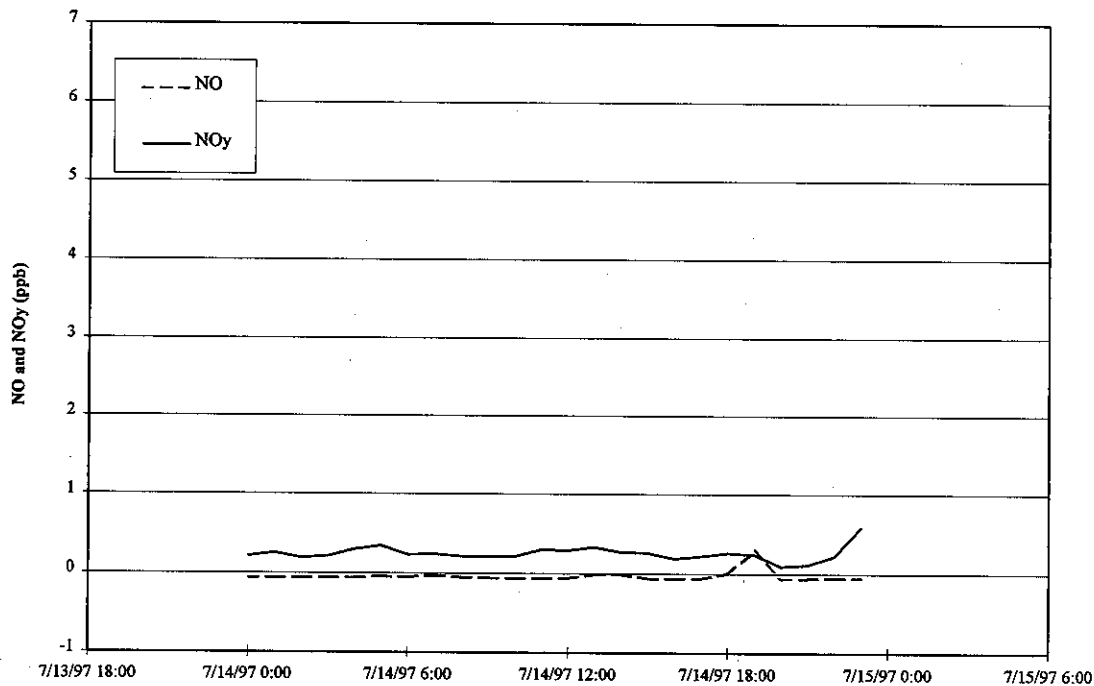


Figure 3-15. Summary of NO_y Measurements Performed at San Nicolas (Bldg. 279), CA, for SCOS97-NARSTO IOP Periods.

Site: San Nicolas Island NE Bldg 279



Site: San Nicolas Island NE Bldg 279

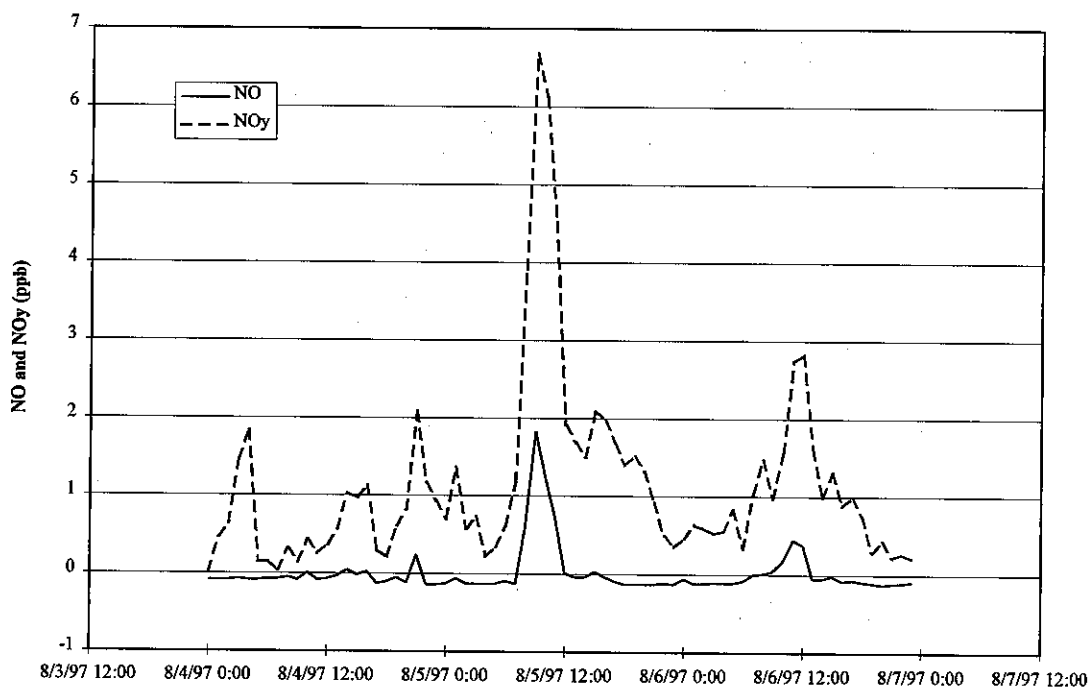
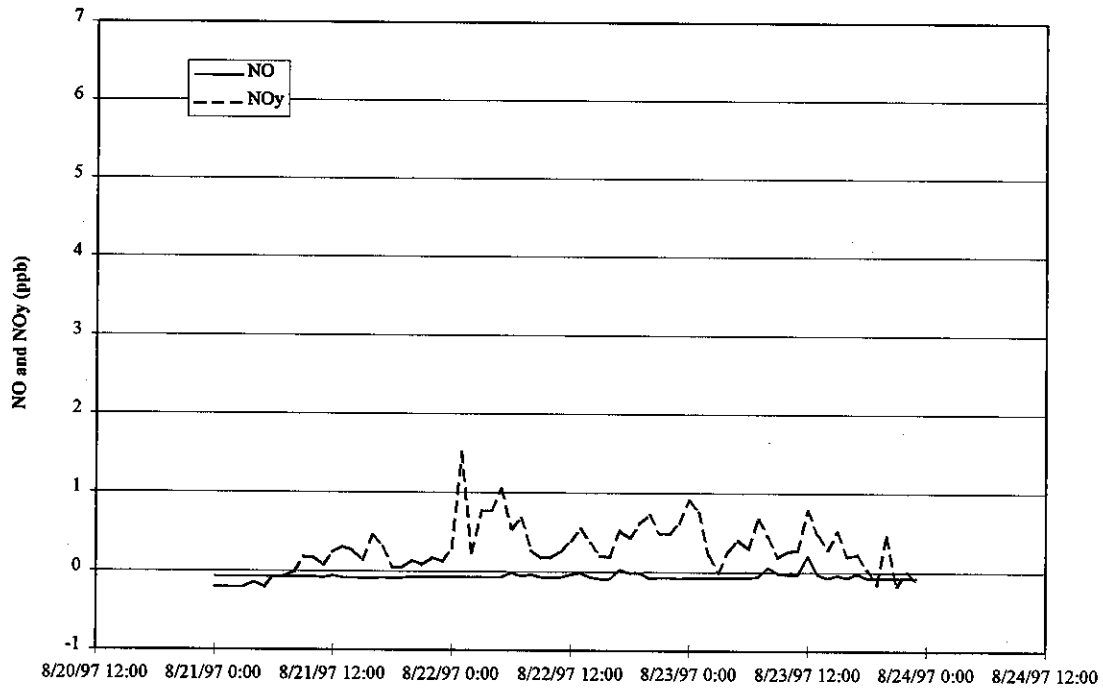


Figure 3-15, continued.

Site: San Nicolas Island NE Bldg 279



Site: San Nicolas Island NE Bldg 279

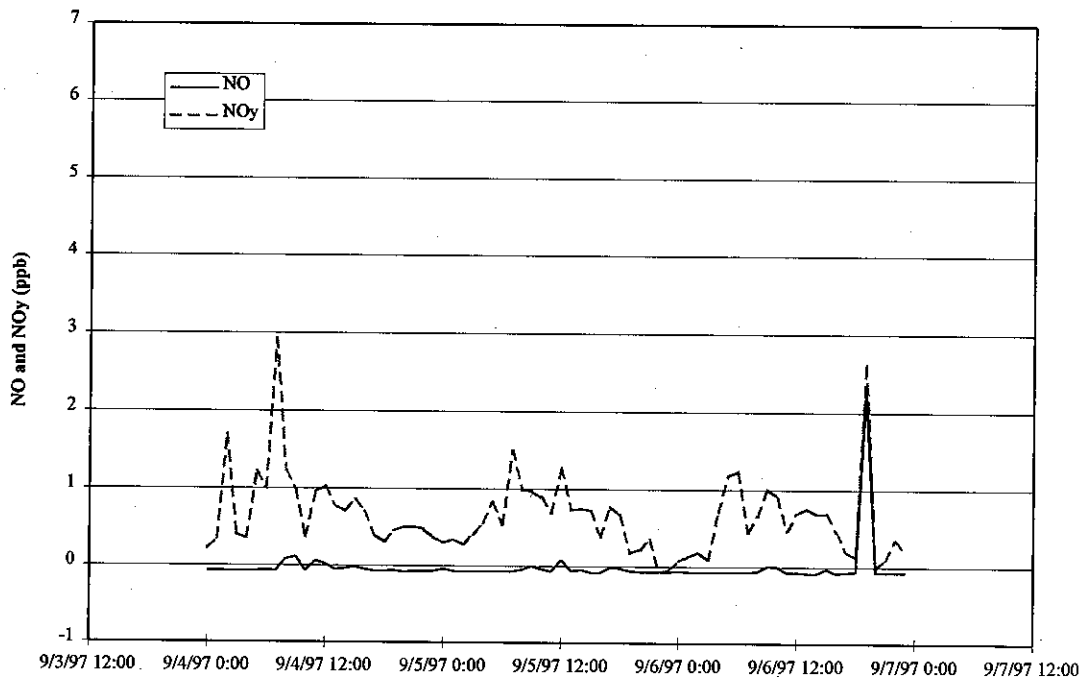
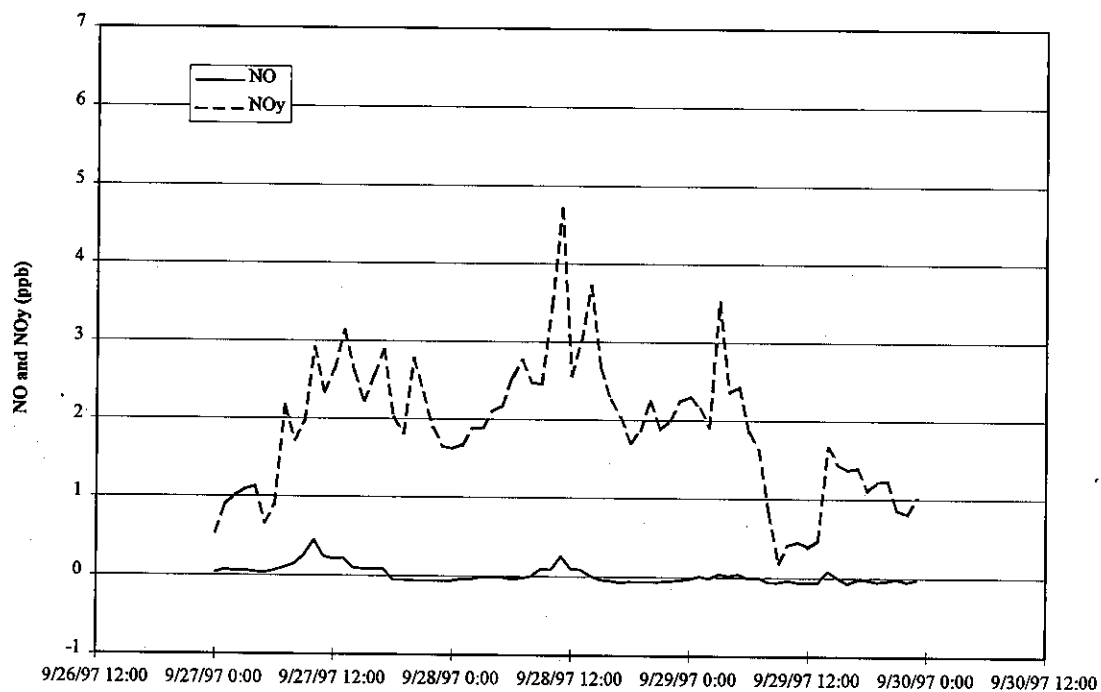


Figure 3-15, continued.

Site: San Nicolas Island NE Bldg 279



Site: San Nicolas Island NE Bldg 279

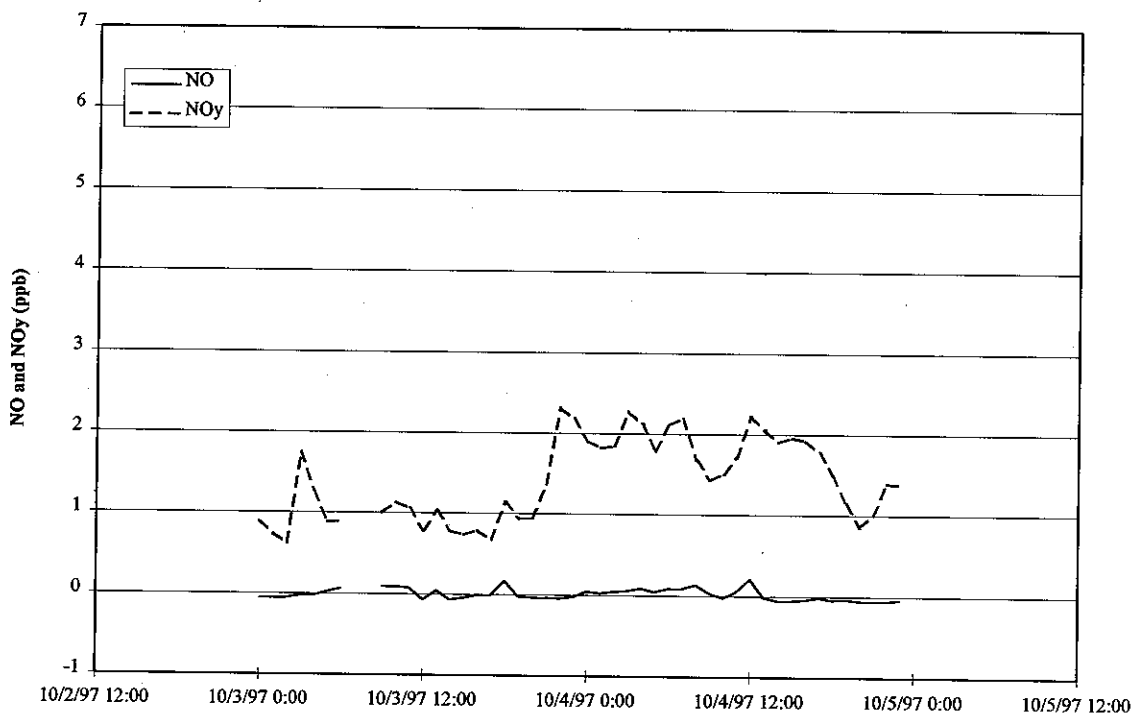


Figure 3-16. Summary of NO_y Measurements Performed in Simi Valley, CA, for SCOS97-NARSTO IOP Periods.

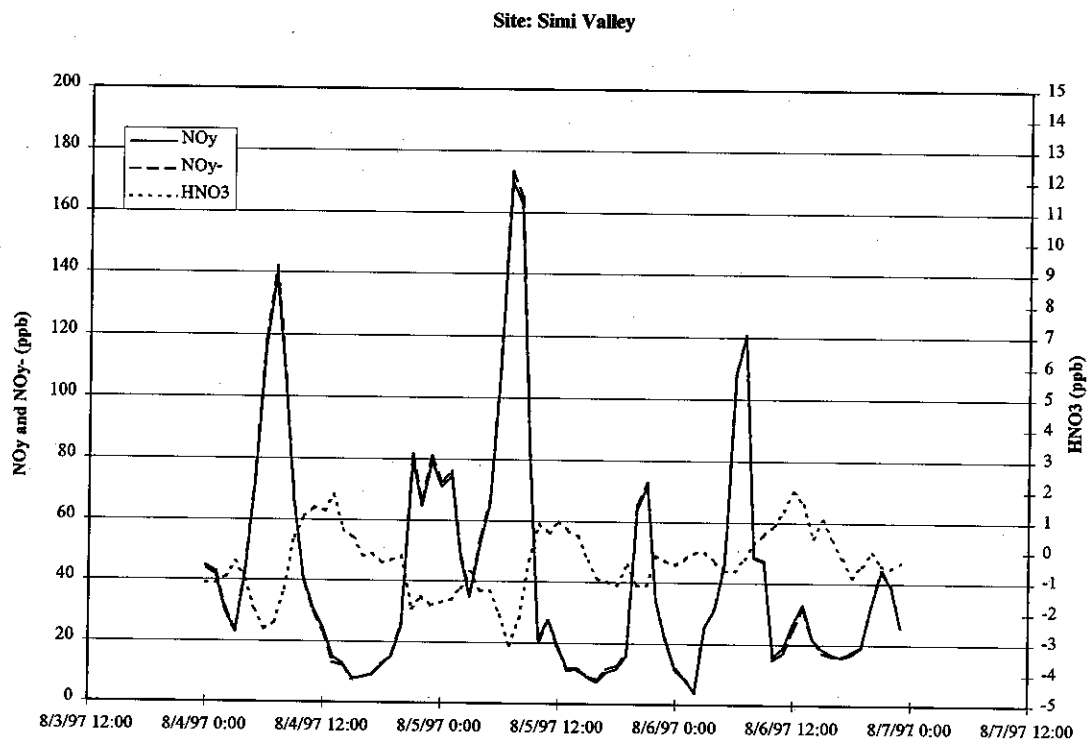
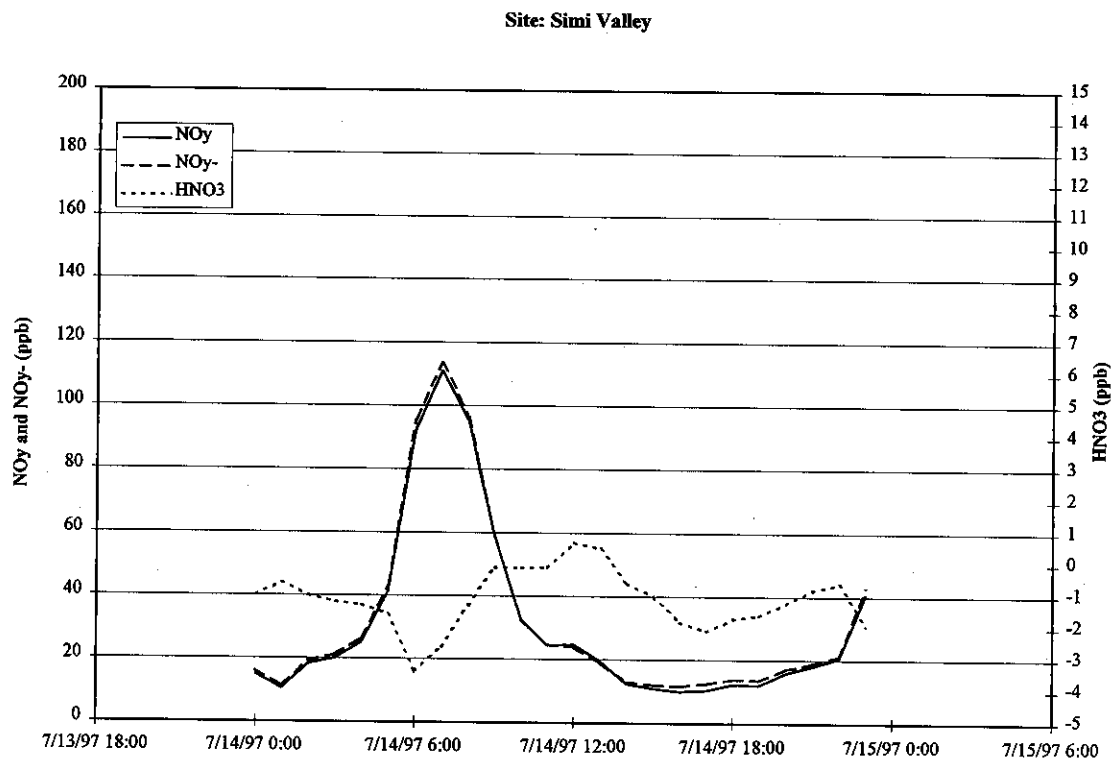
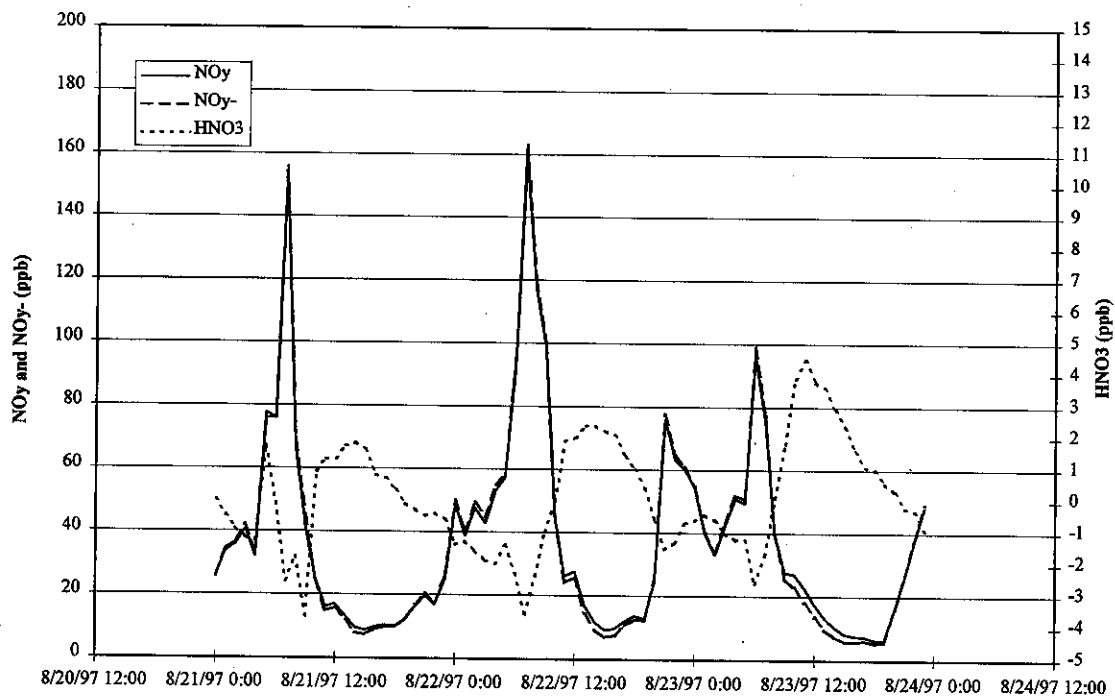


Figure 3-16, continued.

Site: Simi Valley



Site: Simi Valley

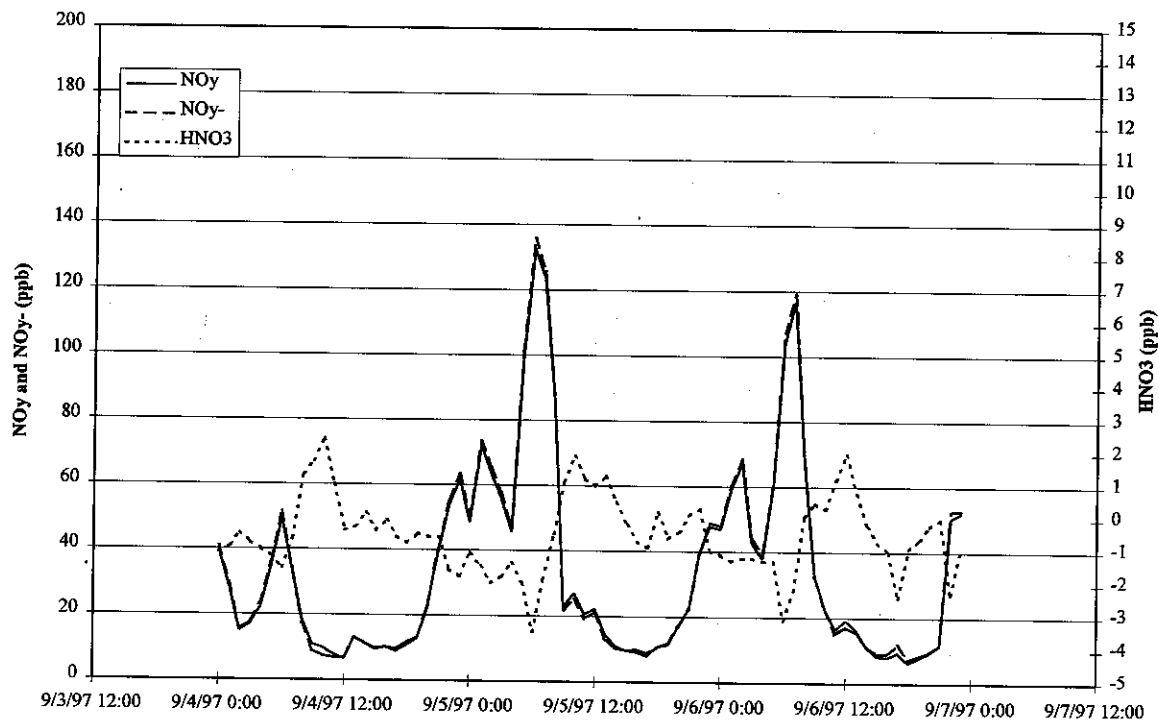
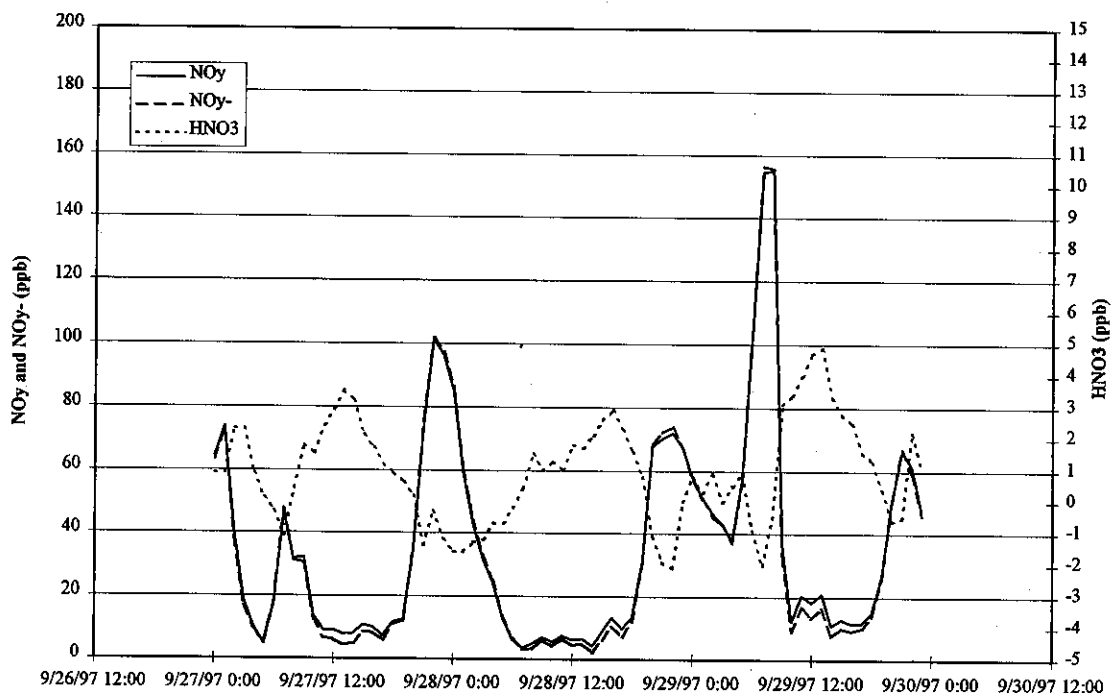


Figure 3-16, continued.

Site: Simi Valley



Site: Simi Valley

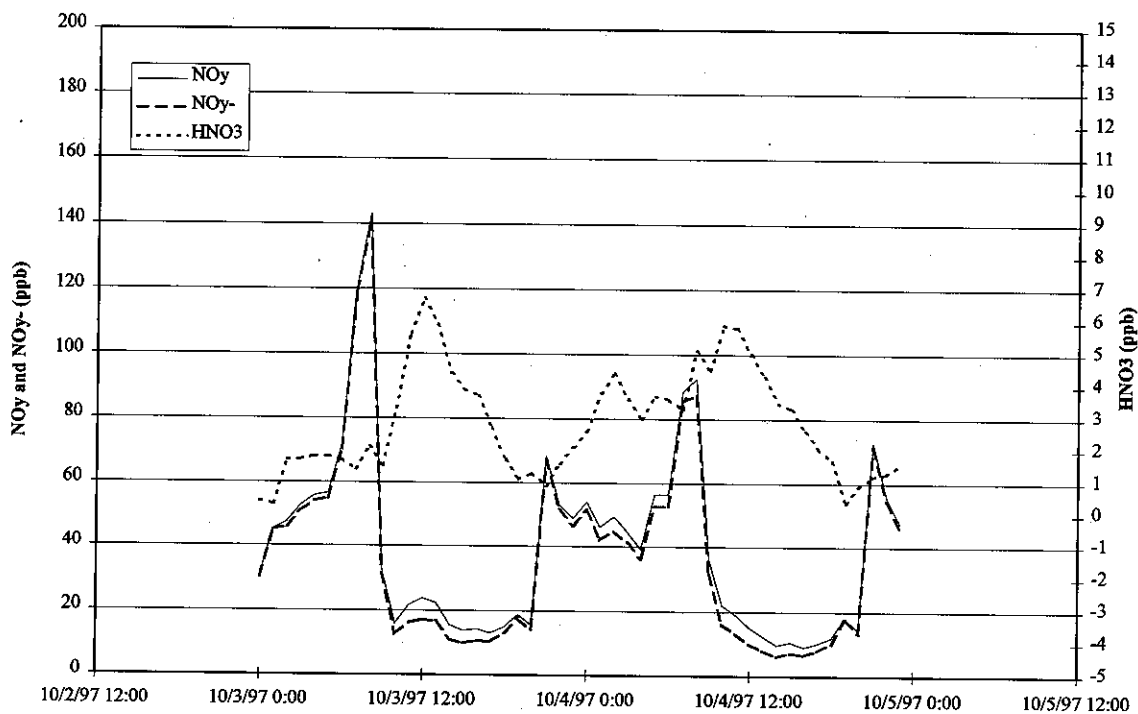


Figure 3-17. Summary of NO_y Measurements Performed at Soledad Mountain, CA, for SCOS97-NARSTO IOP Periods.

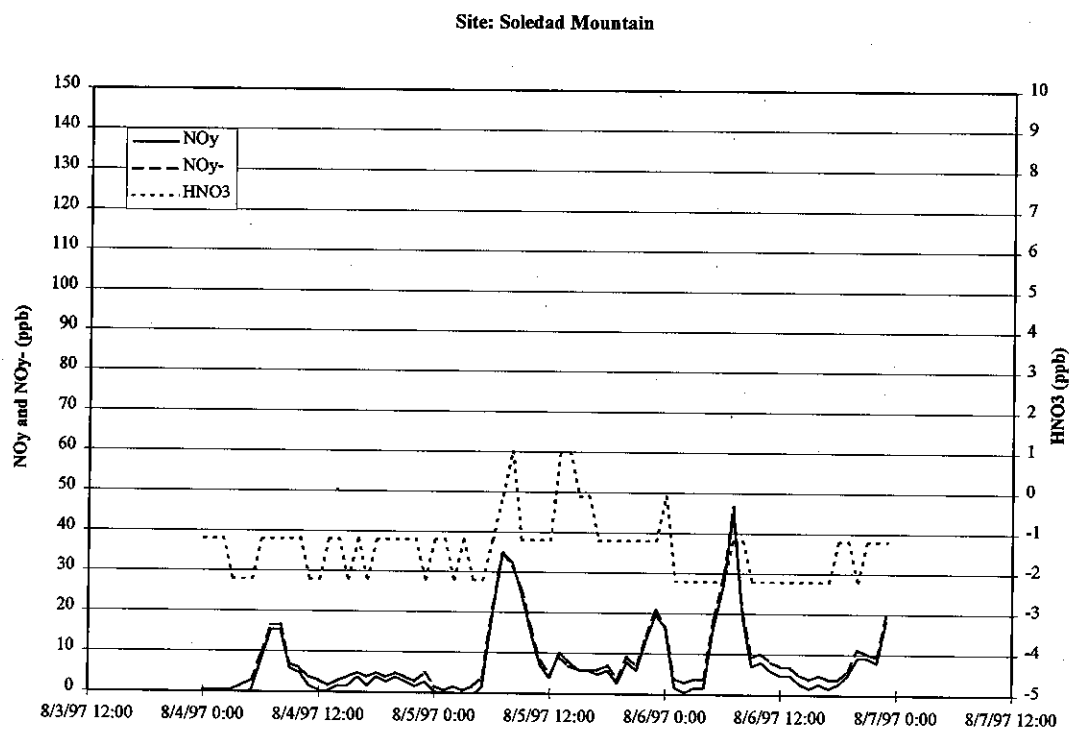
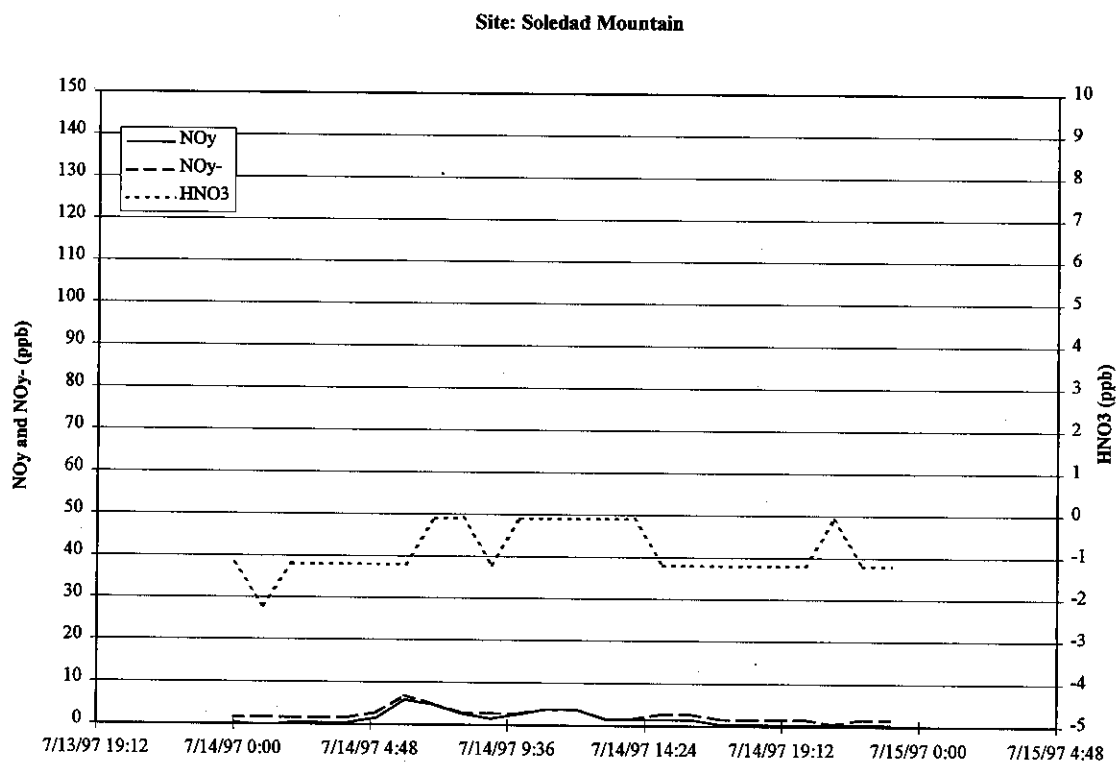
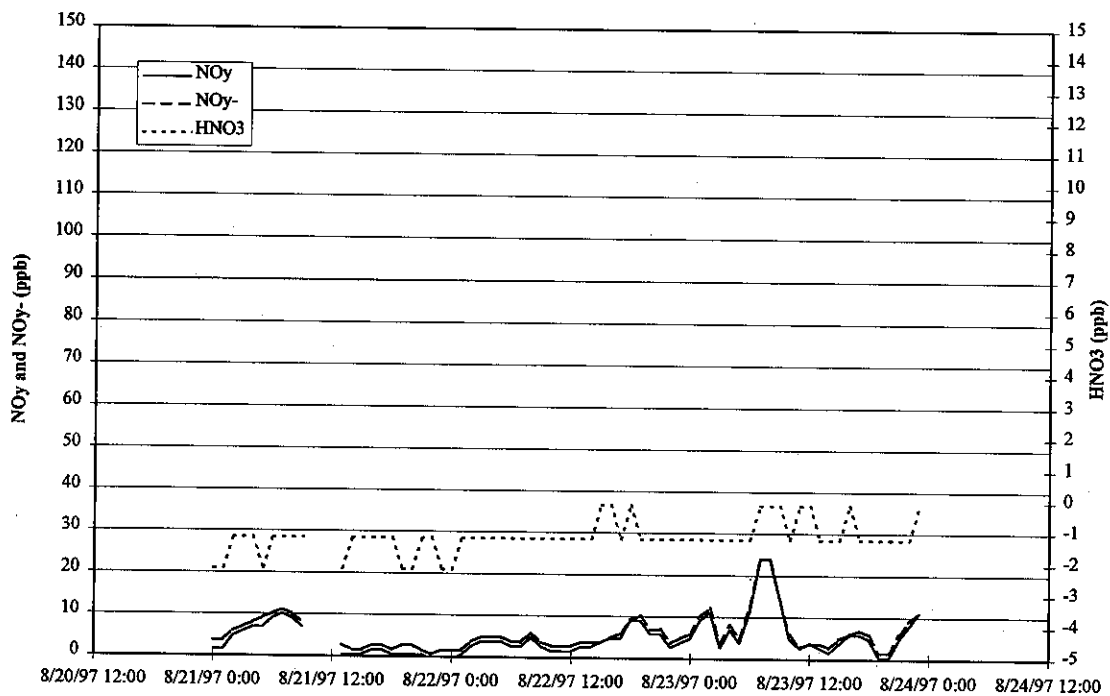


Figure 3-17, continued.

Site: Soledad Mountain



Site: Soledad Mountain

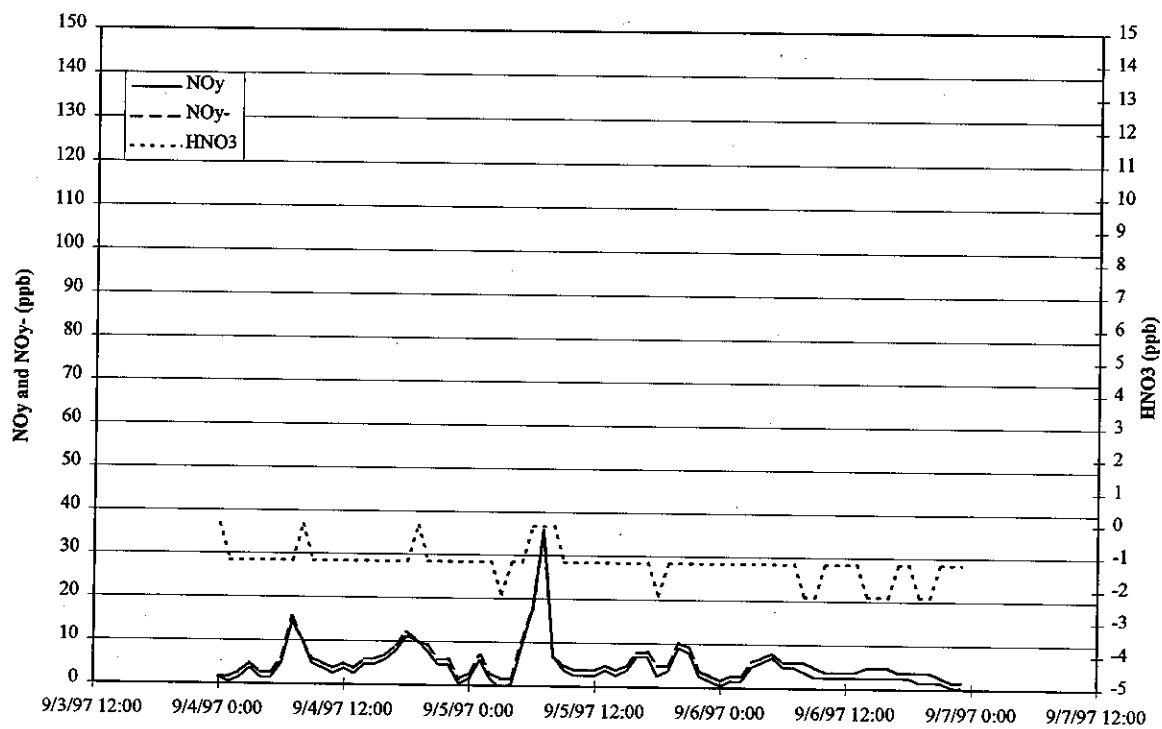


Figure 3-17, continued.

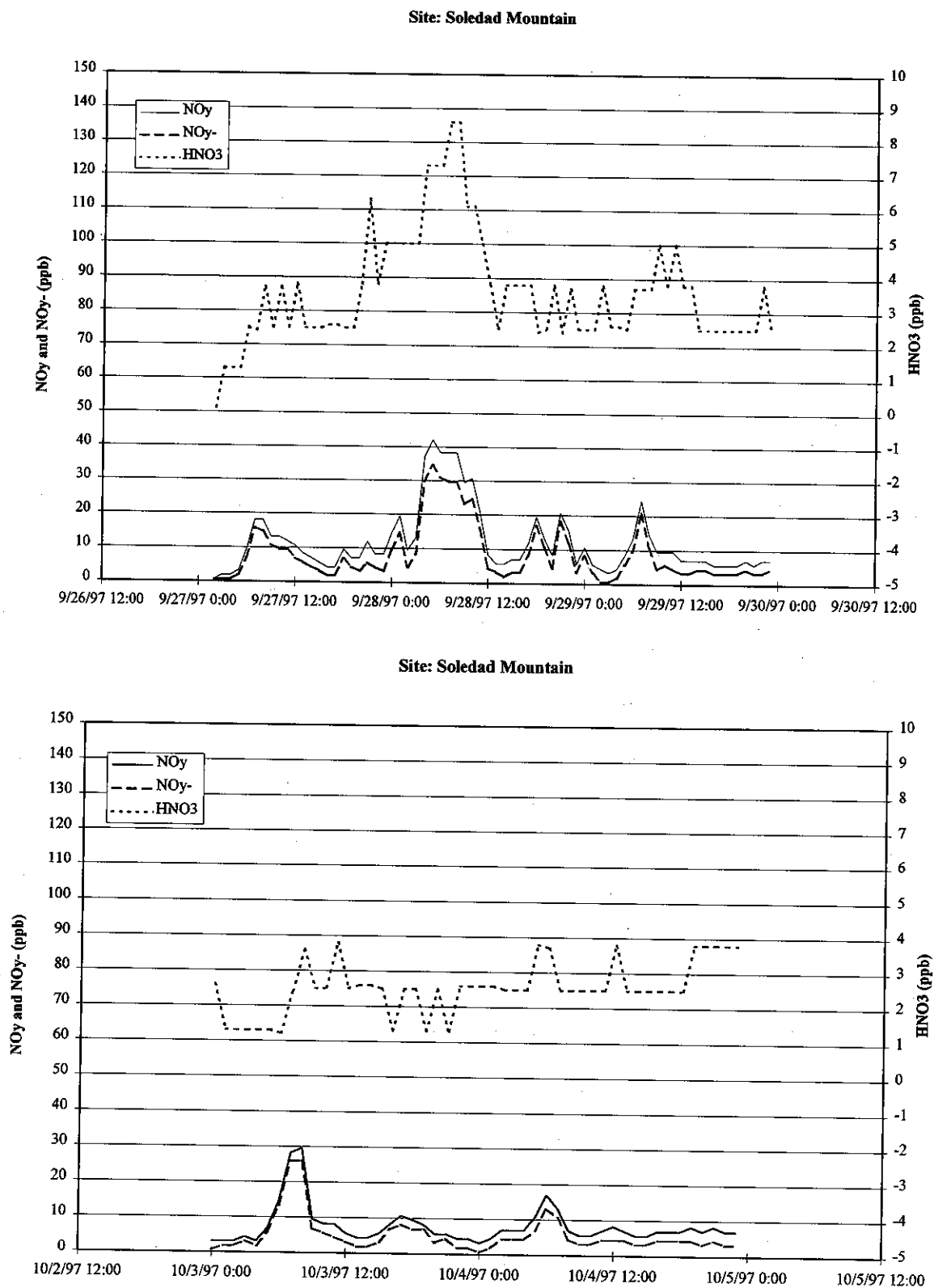


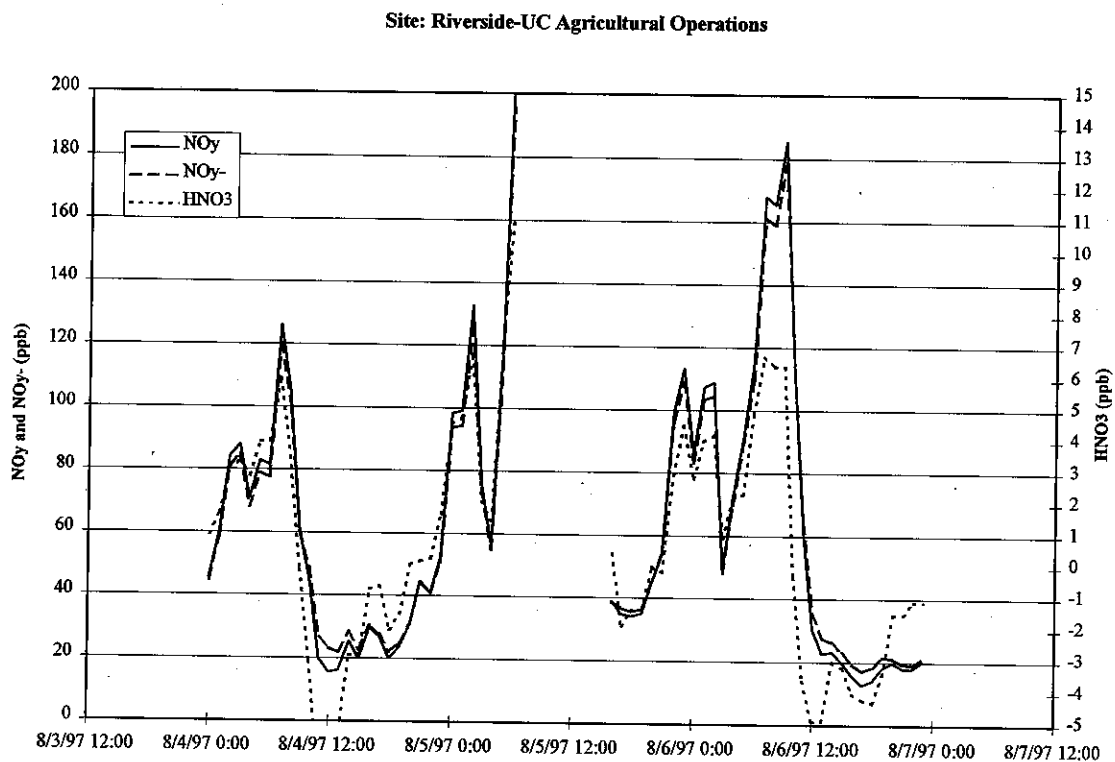
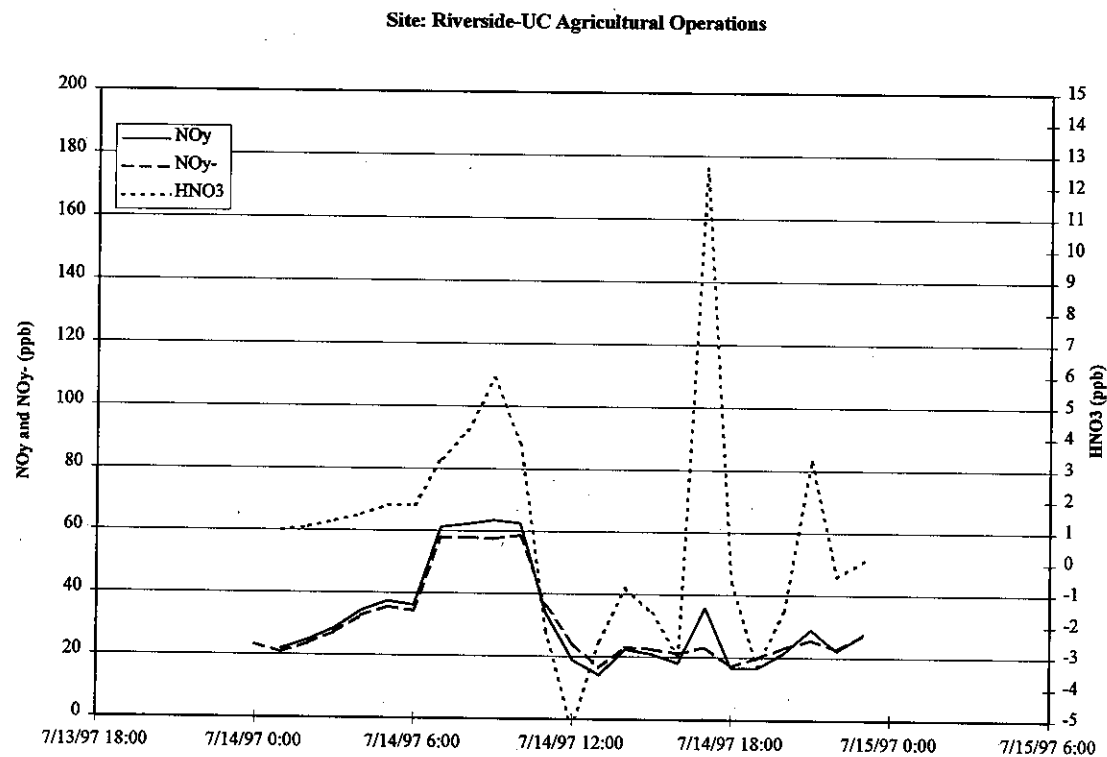
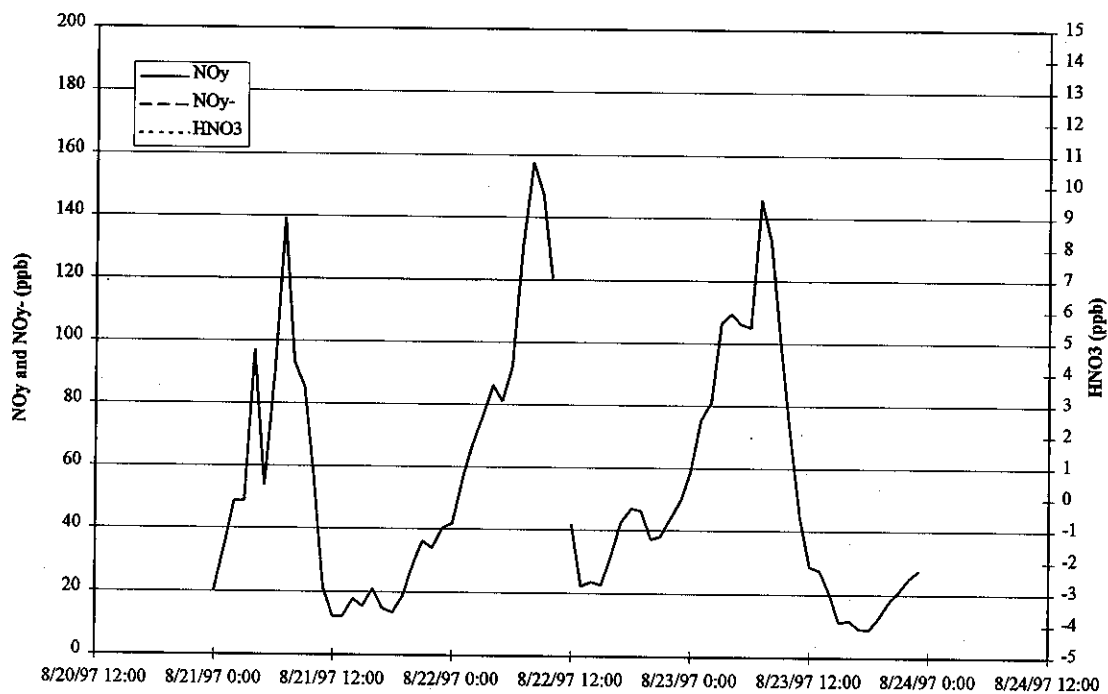
Figure 3-18. Summary of NO_y Measurements Performed at UC Riverside Agricultural Operations for SCOS97-NARSTO IOP Periods.

Figure 3-18, continued.

Site: Riverside-UC Agricultural Operations



Site: Riverside-UC Agricultural Operations

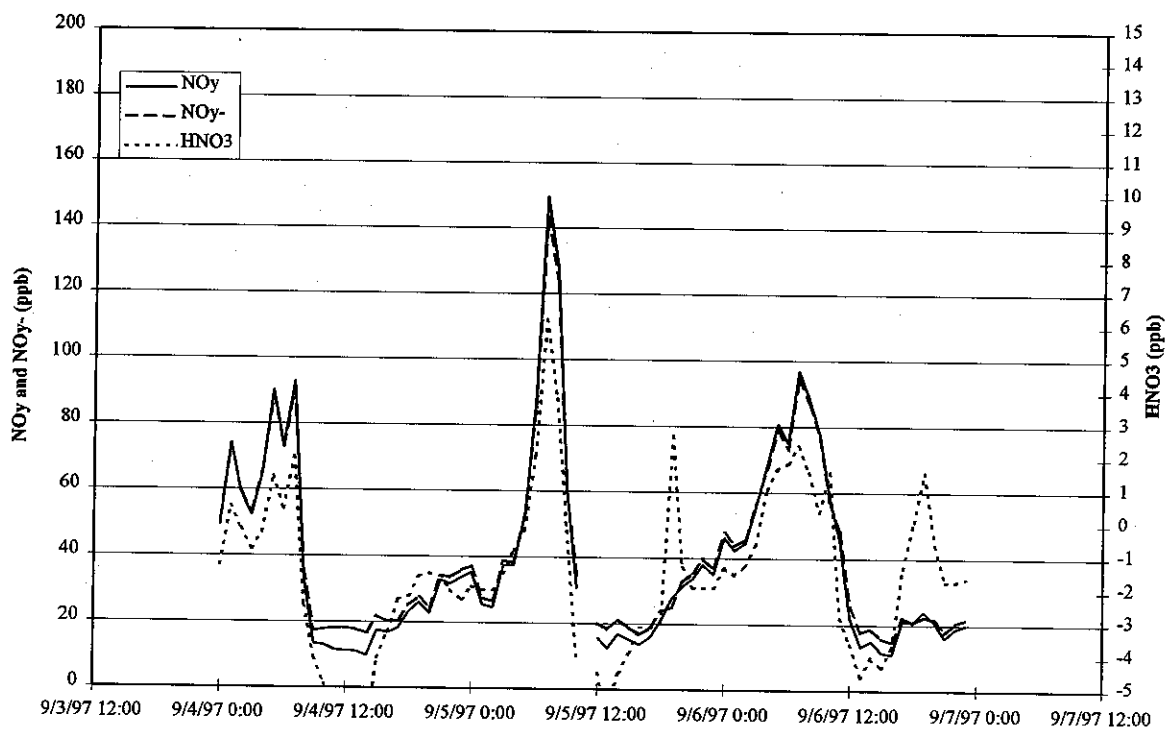
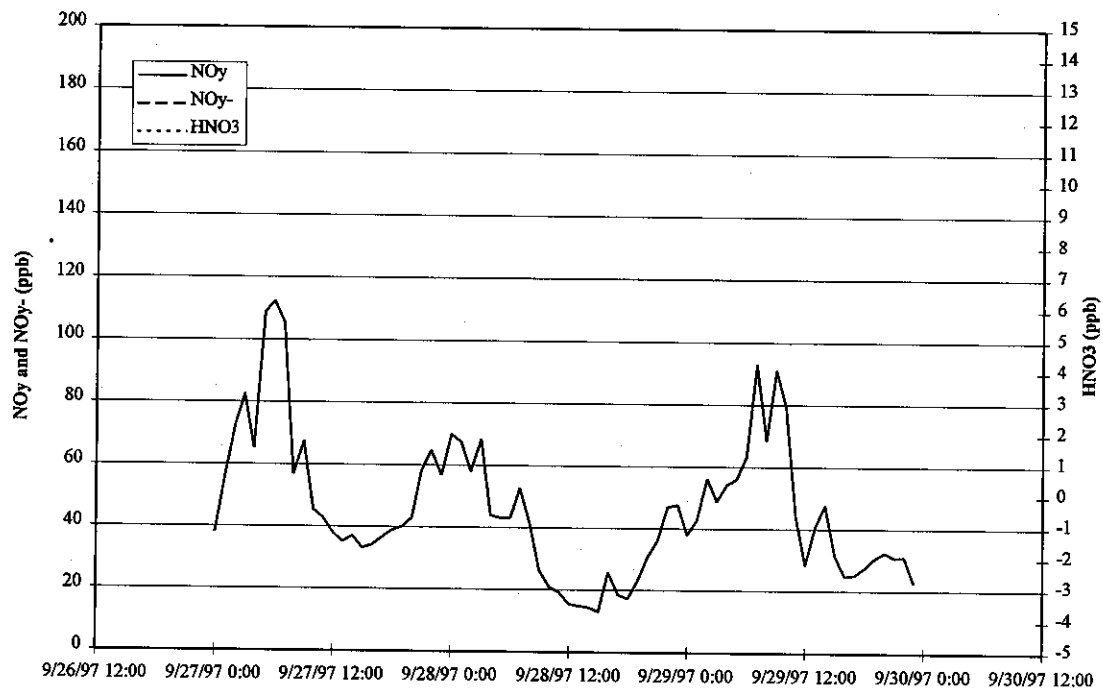
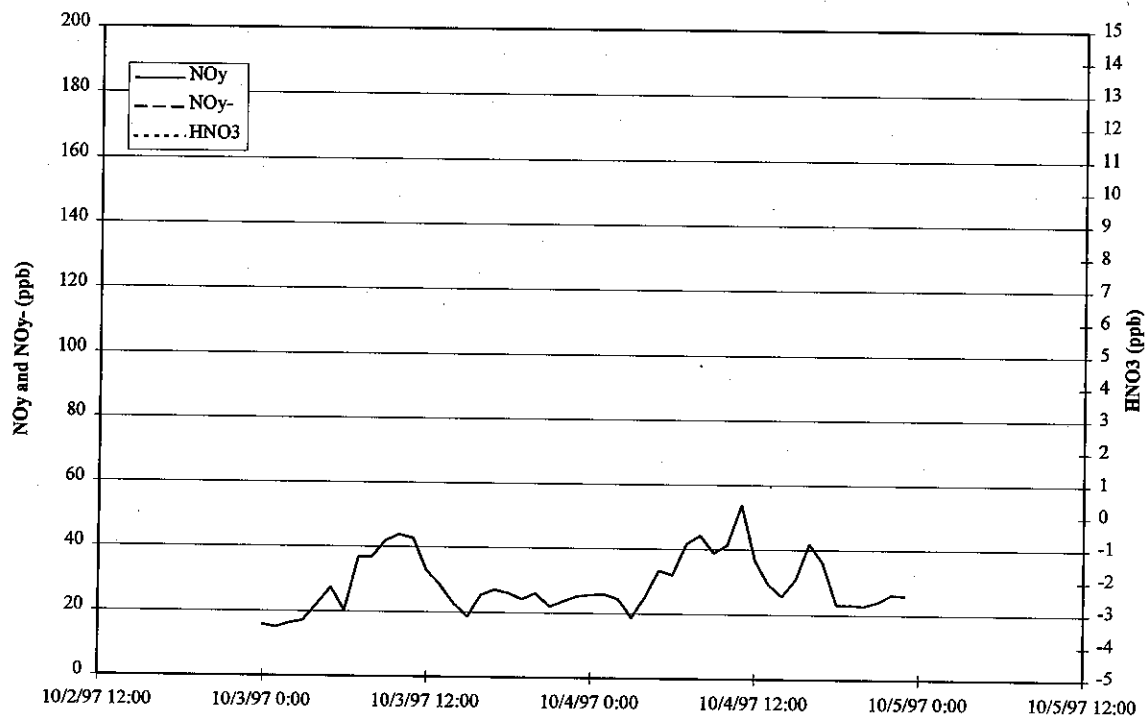


Figure 3-18, continued.

Site: Riverside-UC Agricultural Operations



Site: Riverside-UC Agricultural Operations



The data for Azusa, shown in Figure 3-10, show nitric acid concentrations peaking at approximately 10 ppb around midday. These concentrations are generally lower than those measured by the TDLAS. This is to be expected if nitric acid is being retained by the converter. Figure 3-11 for the Banning site shows that the nitric acid concentration appeared to peak about midnight. It is not clear whether this was an artifact of the measurement method or whether it represents transport of nitric acid created farther upwind. This site was generally high for nitric acid concentrations, with a peak value of 15 ppb observed. Figure 3-12 for Diamond Bar shows the highest NO_y concentrations observed, reaching 350 ppb. The concentration varied significantly, perhaps because of the close proximity to the 57 Freeway. Nitric acid concentrations peaked around midday, reaching nearly 30 ppb on September 28, the highest concentration observed with the NO_y analyzers. Figure 3-13 summarizes the concentrations for the Los Angeles site located on North Main Street. While high concentrations of nitric acid were observed during the morning of August 6, for much of the time the nitric acid concentrations were negative. This site used a Thermo Environmental model 42C, which has less sensitivity than the model 42S or 42CY. This site also utilized a Monitor Labs NO_x converter and not the Thermo Environmental device. The NO_y data for the Mira Loma site are summarized in Figure 3-14. The NO_y generally peaked in the early morning, while the nitric acid concentrations appeared to be persistently high. The nitric acid may be biased high due to the high NO_y concentrations often observed when the analyzer's zero was checked. High concentrations of ammonia were also routinely observed at this site; therefore, the nitric acid measured by the NO_y analyzer may be an artifact of the analyzer. Figure 3-15 shows the NO_y and NO for San Nicolas Island. As expected for a background site, the concentrations are low, although there were several periods when the concentrations spiked, indicating transport from a source area. Virtually none (with the exception of the periods of high NO_y concentrations on August 5 and September 6) of the NO_y was found to be NO , also consistent with a background site. The concentrations for the Simi Valley site are summarized in Figure 3-16. High NO_y spikes were observed primarily in the morning; these could be due to a local source. Low concentrations were generally observed later in the day, with some days showing significant concentrations of nitric acid and others with values near zero. Figure 3-17 shows the data for Soledad Mountain. The NO_y concentrations were generally the lowest observed in the network except for San Nicolas Island. The resolution of the nitric acid concentrations, ± 1 ppb, was clearly limited by the data acquisition system used at that site. Significant nitric acid concentrations were observed only for the series of IOPs starting on September 28. The concentrations for the site at the University of California, Riverside, are summarized in Figure 3-18. This site showed major spikes of NO_y and nitric acid occurring in the early morning. Airshed modeling of these episodes is needed to determine whether the spikes are the result of transport. The peak nitric acid of 13 ppb was observed in the afternoon of July 14.

3.1.3 Tunable Diode Laser Absorption Spectrometer

The instrument was operated for both SCOS97-NARSTO IOP days and Aerosol Intensive days. On the day prior to these intensives, the instrument was placed in the sampling mode and the absorption features for HNO_3 and NO_2 were checked and calibrated.

Figure 3-19 shows the nitric acid concentrations at Azusa determined by both the TDLAS and the Thermo Environmental NO_y analyzer. The peak nitric acid concentrations occurred in the early afternoon. Except for the IOPs in October, the peaks from the TDLAS were all higher than those from the NO_y analyzer. During the IOPs in early August, the air conditioner at the site malfunctioned, and the temperature in the shelter was over 40°C in the afternoon. The data, therefore, are suspect for both instruments.

Figure 3-19. HNO_3 Concentrations Determined by TDLAS and NO_y Analyzer at Azusa During SCOS97-NARSTO IOP Periods.

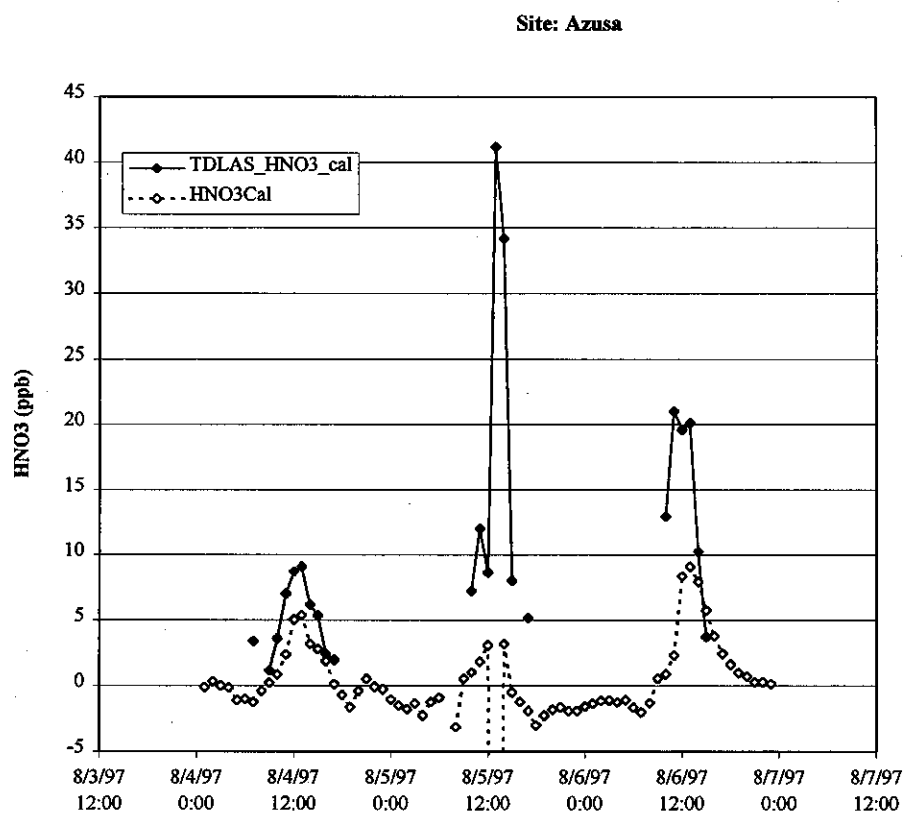


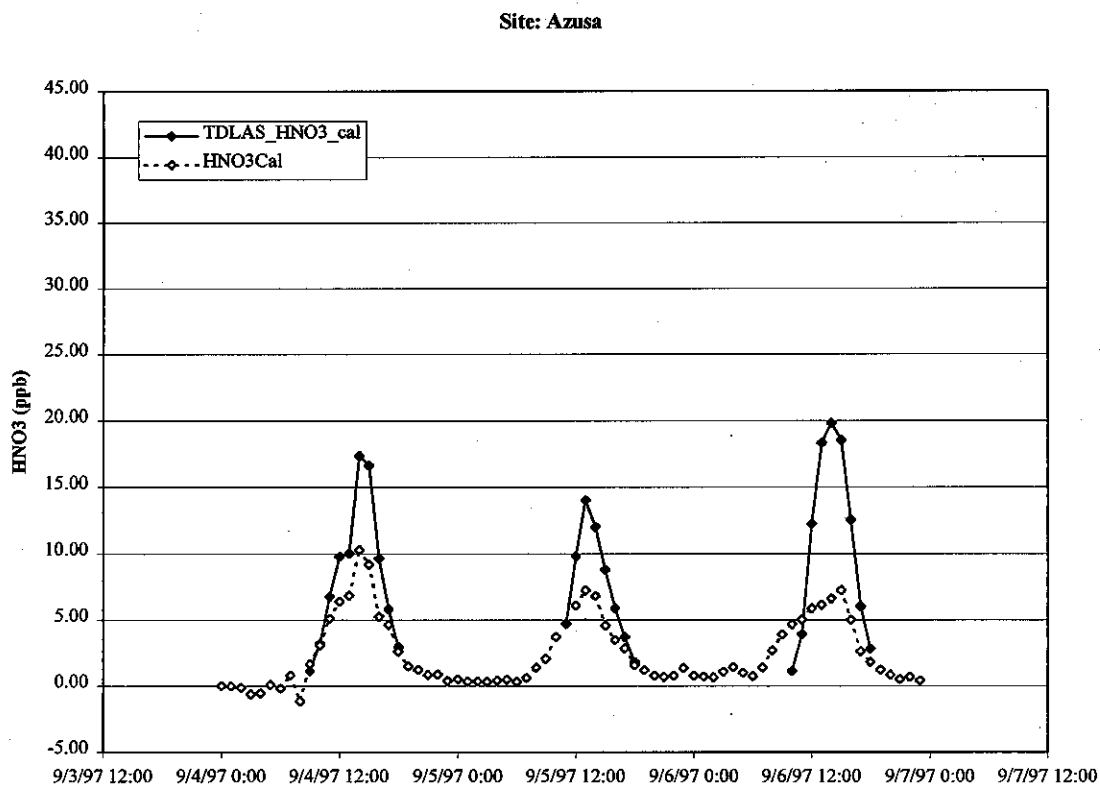
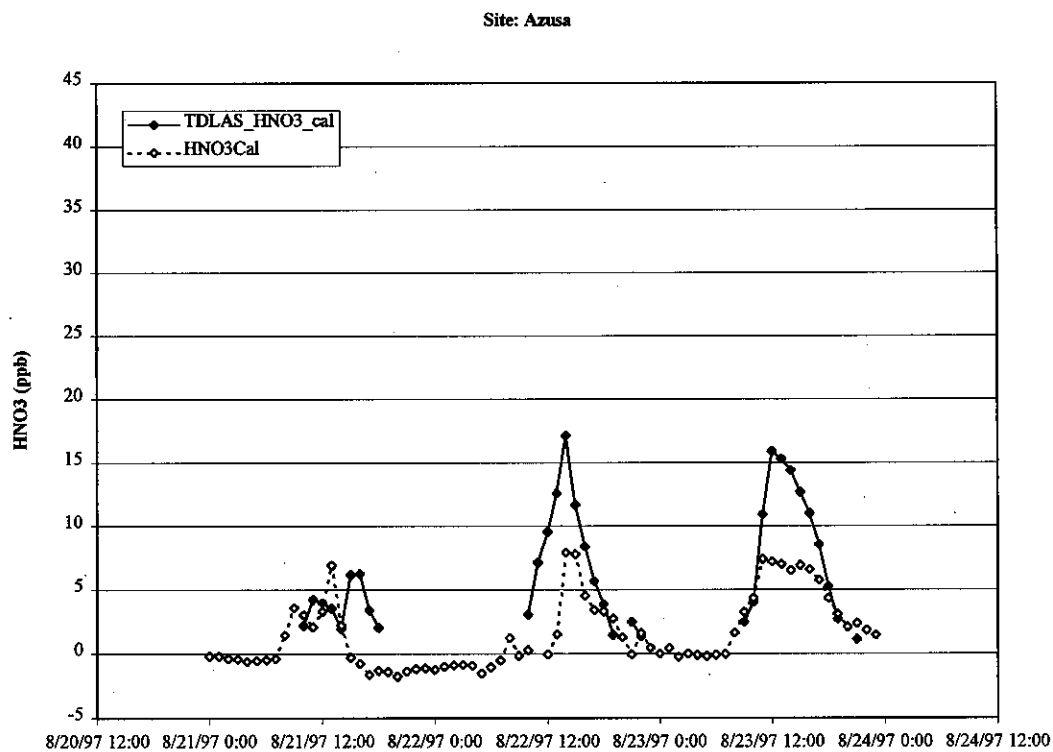
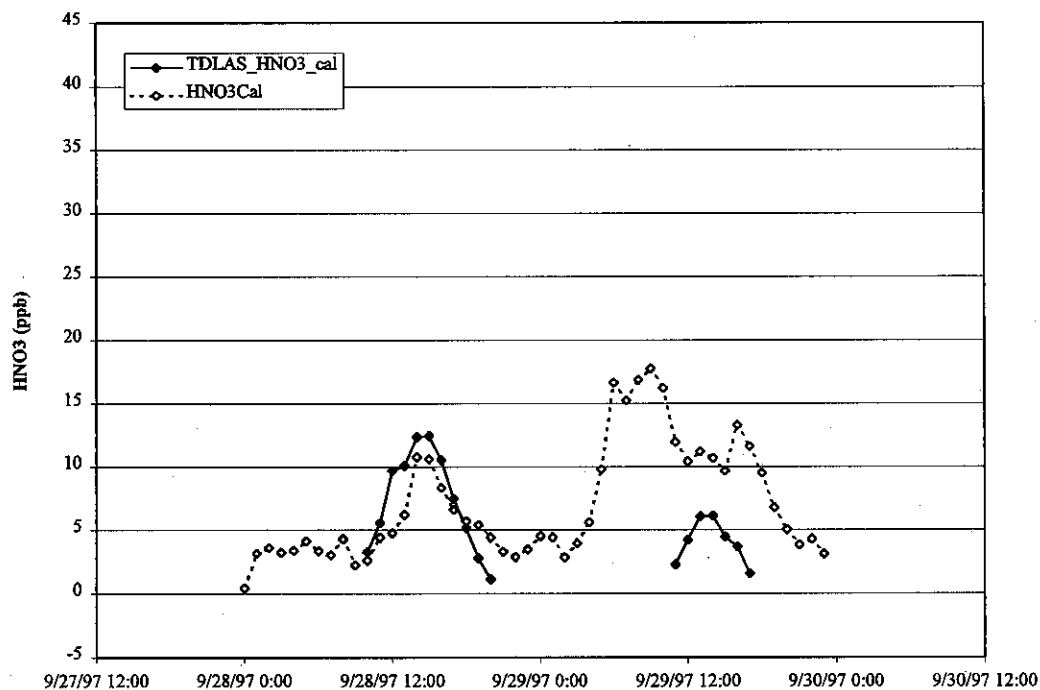
Figure 3-19, continued.

Figure 3-19, continued.

Site: Azusa



Site: Azusa

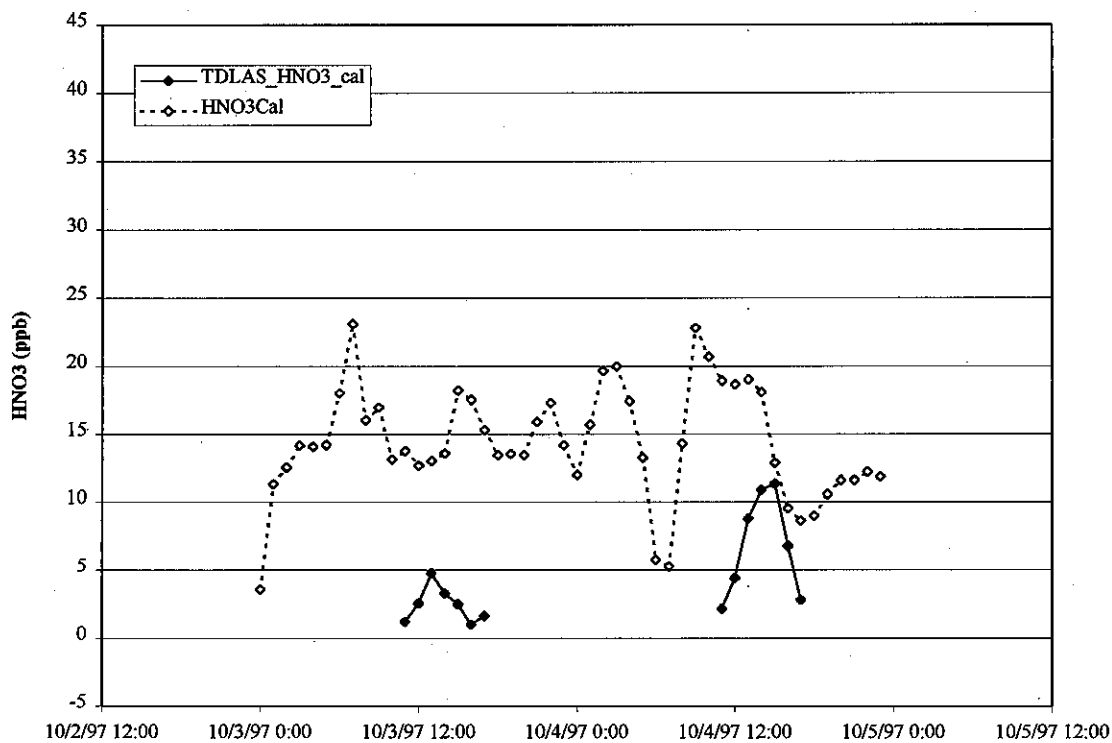


Figure 3-20 shows the NO_2 concentrations at Azusa determined by both the TDLAS and the chemiluminescent $\text{NO}-\text{NO}_x$ analyzer operated by the SCAQMD. The previous caution about the excessive heating during the early August IOPs applies. Except for this early August IOP, the TDLAS NO_2 is generally lower than that determined from the difference of NO_x and NO .

Figure 3-20. NO_2 Concentrations Determined by TDLAS and SCAQMD $\text{NO}-\text{NO}_x$ Analyzer at Azusa during SCOS97-NARSTO IOP Periods.

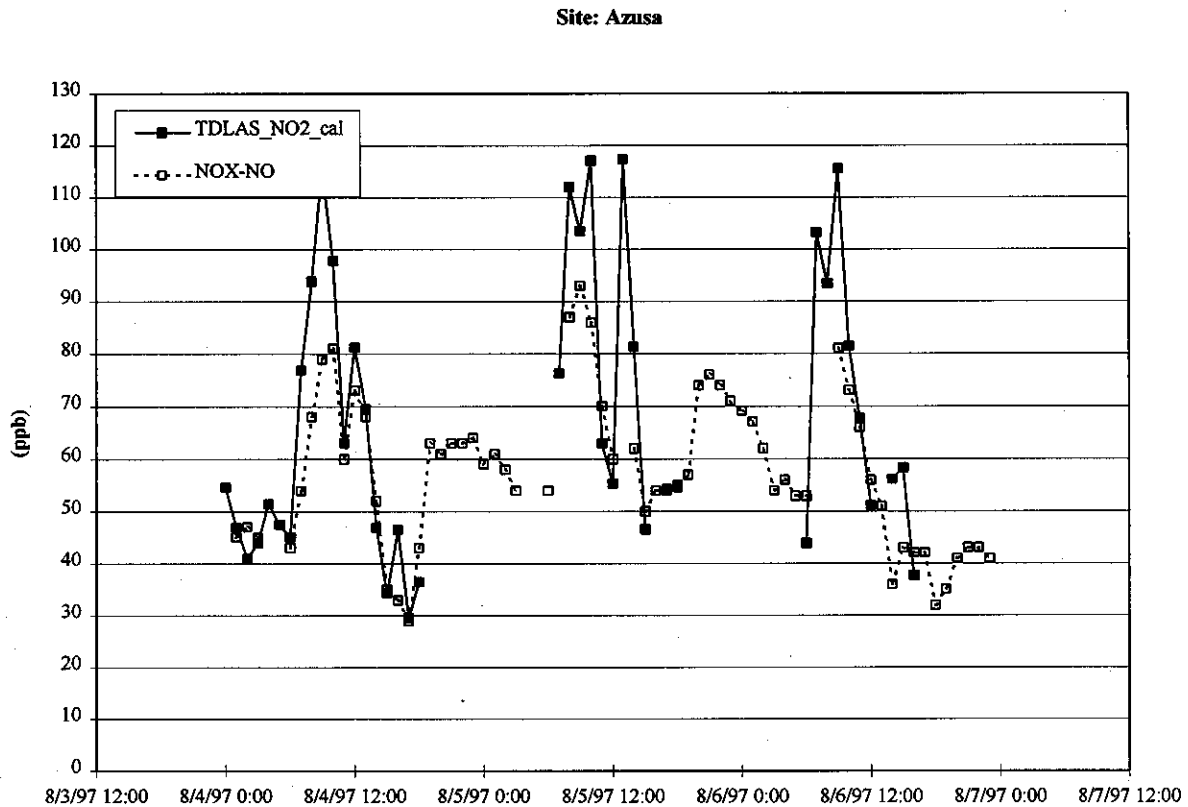
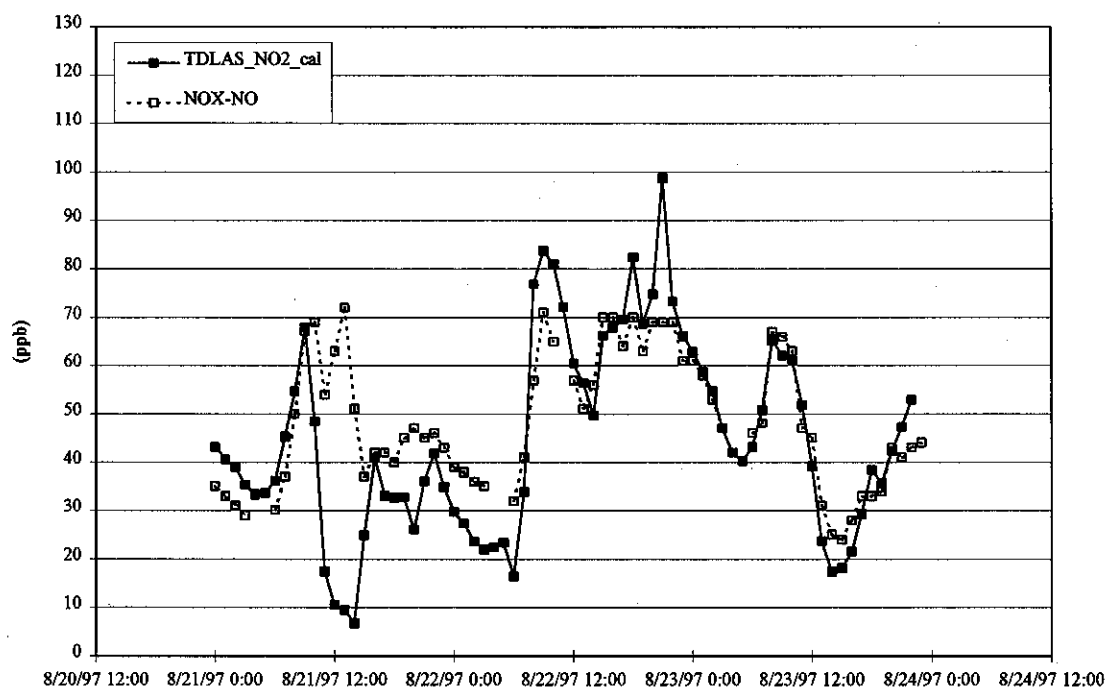


Figure 3-20, continued.

Site: Azusa



Site: Azusa

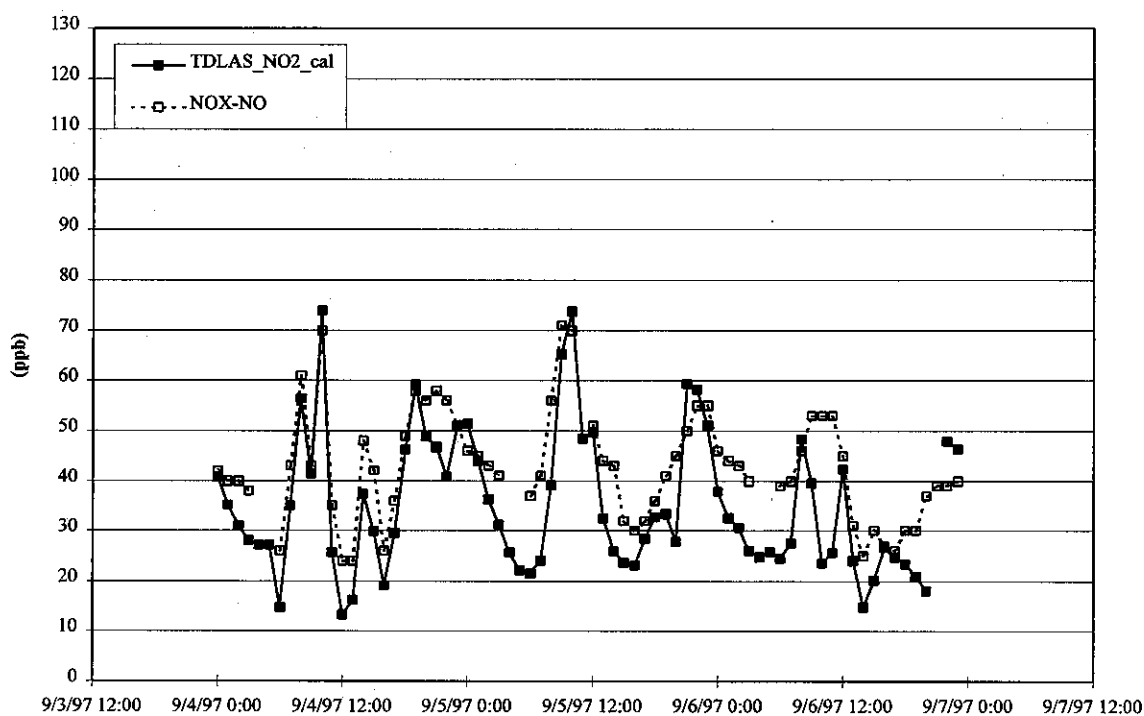
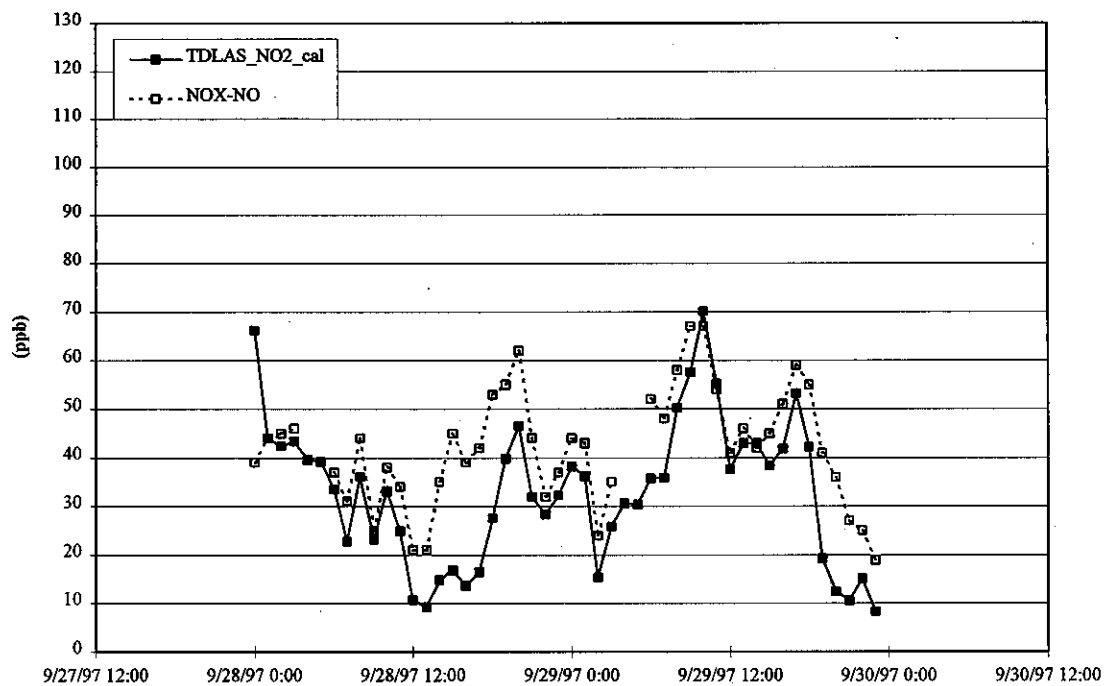
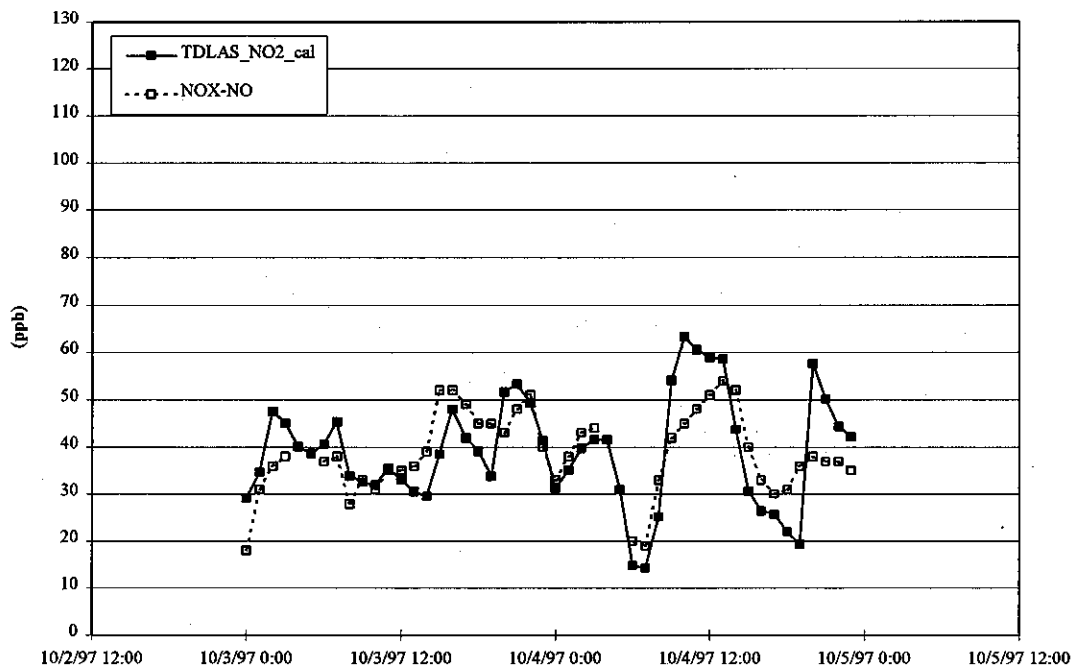


Figure 3-20, continued.

Site: Azusa



Site: Azusa



Comparison with Other Methods

Figure 3-21 plots the nitric acid concentrations determined from the TDLAS vs. those determined from the dual converter NO_y analyzer for all periods for which data are available. While there is general agreement showing the TDLAS reading higher, the correlation is poor, mostly due to about a dozen points where the TDLAS is much higher than the dual converter system.

Figure 3-22 plots the NO_2 concentrations determined from the TDLAS vs. those determined from the NO_x analyzer operated by the SCAQMD for all periods for which data are available. The correlation here is much better, and there are few outliers. There is, however, a substantial intercept that may reflect the NO_x analyzer responding to species other than NO and NO_2 .

Figure 3-21. Plot of TDLAS Nitric Acid Concentrations Compared with Those from NO_y Analyzer (ppb).

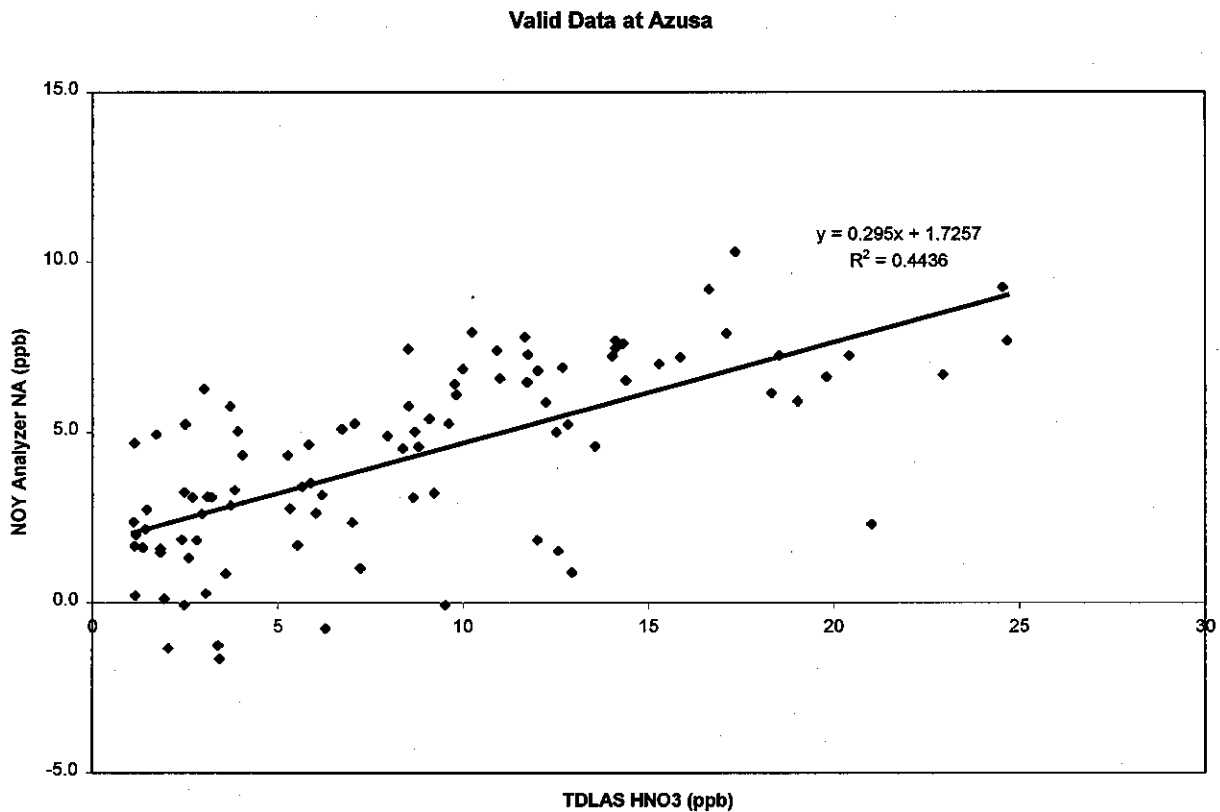
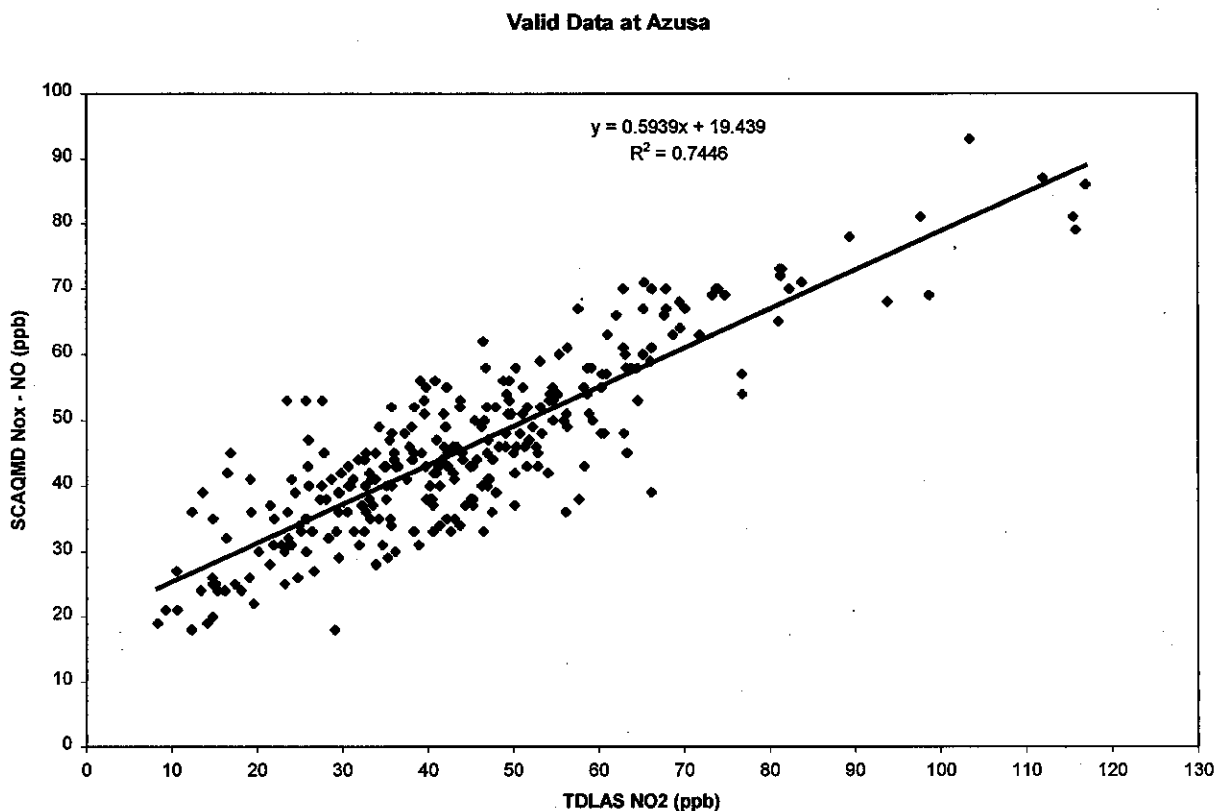


Figure 3-22. Plot of TDLAS NO₂ Concentrations Compared with Those from the NO_x Analyzers (ppb).



3.1.4 Diffusion Denuder Sampling

Diffusion denuders for nitric acid and ammonia were set up initially at the Riverside Agricultural Operations site and at the SCAQMD air monitoring site in Azusa. Pairs of denuder substrates (the second one was used to evaluate break-through) were mounted in Savillex multi-stage 47 mm filter holders. Flows were controlled with a needle valve and monitored with a flowmeter downstream of the denuders. Two banks of samplers were used so one could be set up while the other sampled. Each bank had one denuder holder for collecting nitric acid and another for ammonia. Timers were used to automatically switch sample collection. Flow checks were made at the beginning and end of the sampling periods with a single separate rotameter. This was done to provide a consistent flow measurement to ensure that the filter holders were not leaking. Blanks were collected using denuders that were loaded into the filter holder, attached to the sampling lines that were not activated, and allowed to stay there for a sampling period. Except for flow, they were treated exactly as the denuders used for sampling.

The initial sampling intervals (in PDT) were as follows:

0700-1000
 1000-1300
 1300-1600
 1600-1900

The samplers at Azusa were operated for both SCOS97-NARSTO IOPs and Aerosol Intensives. After the Aerosol Intensive on August 28, 1997, the sampler at Azusa was moved to the Aerosol Intensive sampling site in Mira Loma on the Union Pacific facility at the corner of Etiwanda and Galena. After this move, all the samples (Riverside, Mira Loma, and Azusa) were collected on the Aerosol Intensive sampling schedule (PDT):

0620-1000
 1020-1400
 1420-1800

After the IOP on September 29, the Mira Loma Sampler was moved back to Azusa.

Samples were collected and analyzed for the days listed in Table 3-7. Collocated samples were collected for selected periods only at the Riverside location. The phosphoric acid-coated denuders were extracted in water in a laminar fume hood and analyzed by a manual indole phenol blue method. The NaCl-coated denuders were extracted in deionized water and analyzed with an automated ion chromatograph (IC). All of the data were corrected for blank values.

Table 3-7. Denuder Sampling Days and Locations.

Date	Riverside	Azusa	Mira Loma
7/14	X	X	
8/4	X	X	
8/5	X	X	
8/6	X	X	
8/20		X	
8/22	X	X	
8/23	X	X	
8/27		X	
8/28		X	
9/4	X		X
9/5	X		X
9/6	X		X
9/27			lost period
9/28	X		X
9/29	X		X
10/3	X	X	
10/4	X	X	

Several samples were invalidated because flow measurements in the log sheets showed a high likelihood that the filter holders had leaked. Since phosphate ion was an analyte in the IC analyses, analysis of the data showed that for several sampling periods the phosphoric acid-coated denuders were mistakenly logged as NaCl-coated. Since the most likely scenario was that the denuder substrates were switched, data for both denuders for those sampling periods were invalidated. Finally, there were several sampling periods in which the nitrate or ammonia on the first denuder was about ten times lower than on the second, indicating that they were switched during handling somewhere between unloading in the field and analysis in the laboratory. Data from these sets were retained after switching back the values into the proper orientation. For all

samples, the collection efficiency of the denuders was calculated from the amounts on the front and back denuders. These were relatively constant, averaging 92% for ammonia and 85% for nitric acid. To obtain the concentration reported, the concentration determined on the front denuder was then divided by the efficiency.

Figures 3-23 and 3-24 plot the results of collocated sampling performed in Riverside. The ammonia plot was constructed by removing one outlier from the first IOP day. The likely cause was the site operator not following procedures for checking for leaking substrate holders. During the next IOP in early August, a number of collocated samples were invalidated due to leaking filter holders. After this time the operator was retrained in collection protocol. The scatter for the nitric acid is considerably lower than for the ammonia measurements despite the much lower concentrations. This may be due to contamination during substrate handling caused by ammonia emitted from humans during denuder handling.

Figure 3-23. Collocated Denuder Ammonia Measurements.

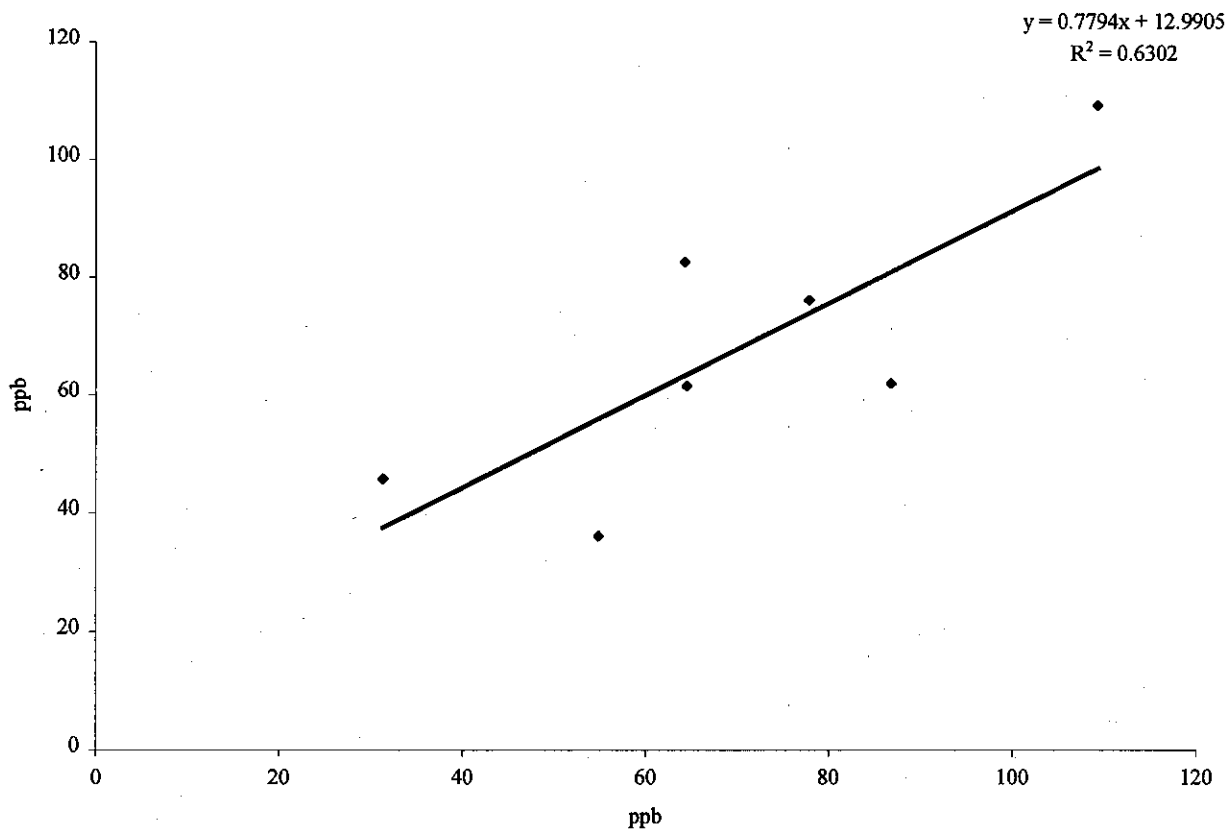
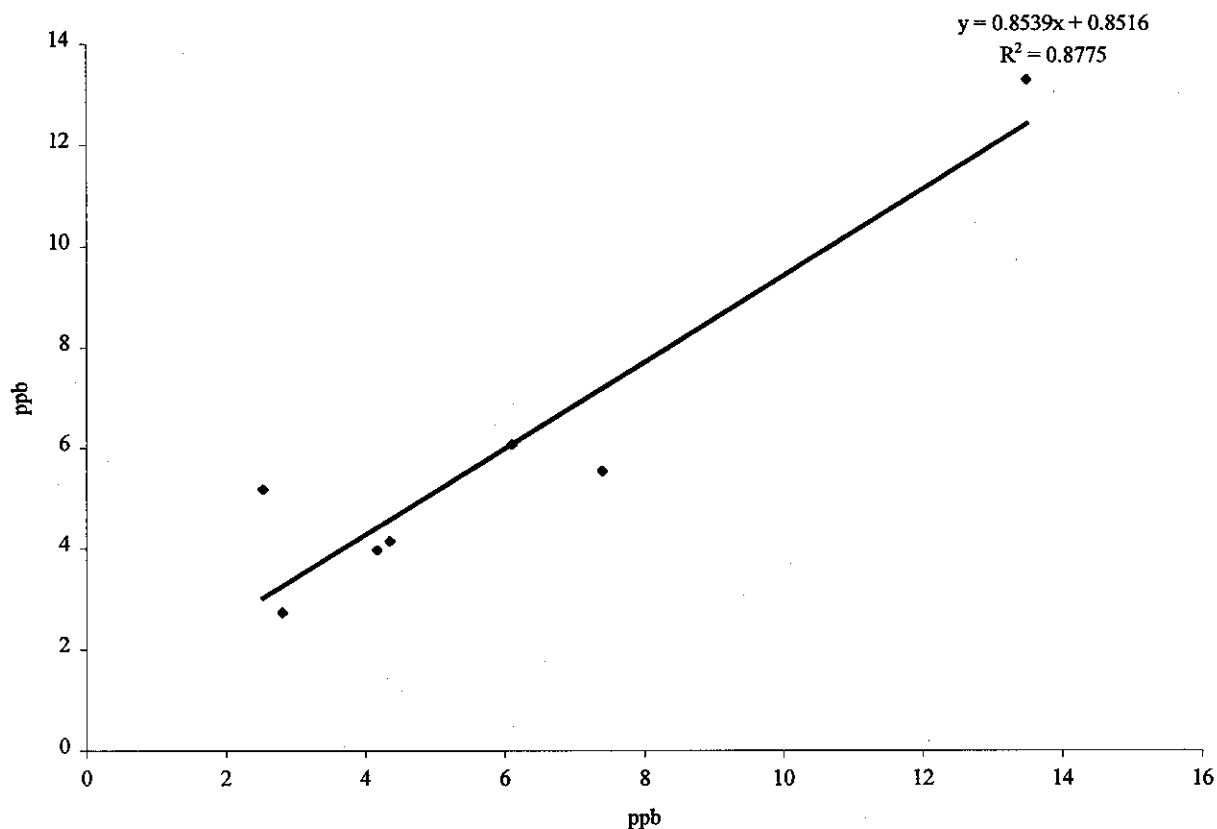


Figure 3-24. Collocated Diffusion Denuder Nitric Acid Measurement.

Figures 3-25 to 3-27 summarize the ammonia concentrations measured via the denuder method at all three sites. It is clear that ammonia is highest in Mira Loma and lowest (by nearly an order of magnitude) in Azusa. Riverside appears to show one period of substantial ammonia, which was not observed at Mira Loma.

Figures 3-28 through 3-30 summarize the nitric acid concentrations measured via the denuder method at all three sites. Reflecting the opposite of the trend for ammonia as expected, nitric acid is highest in Azusa and lowest in Mira Loma. The IOP period in early August had the highest overall concentrations.

Figure 3-25. Ammonia Concentrations in Azusa by Diffusion Denuder Method.

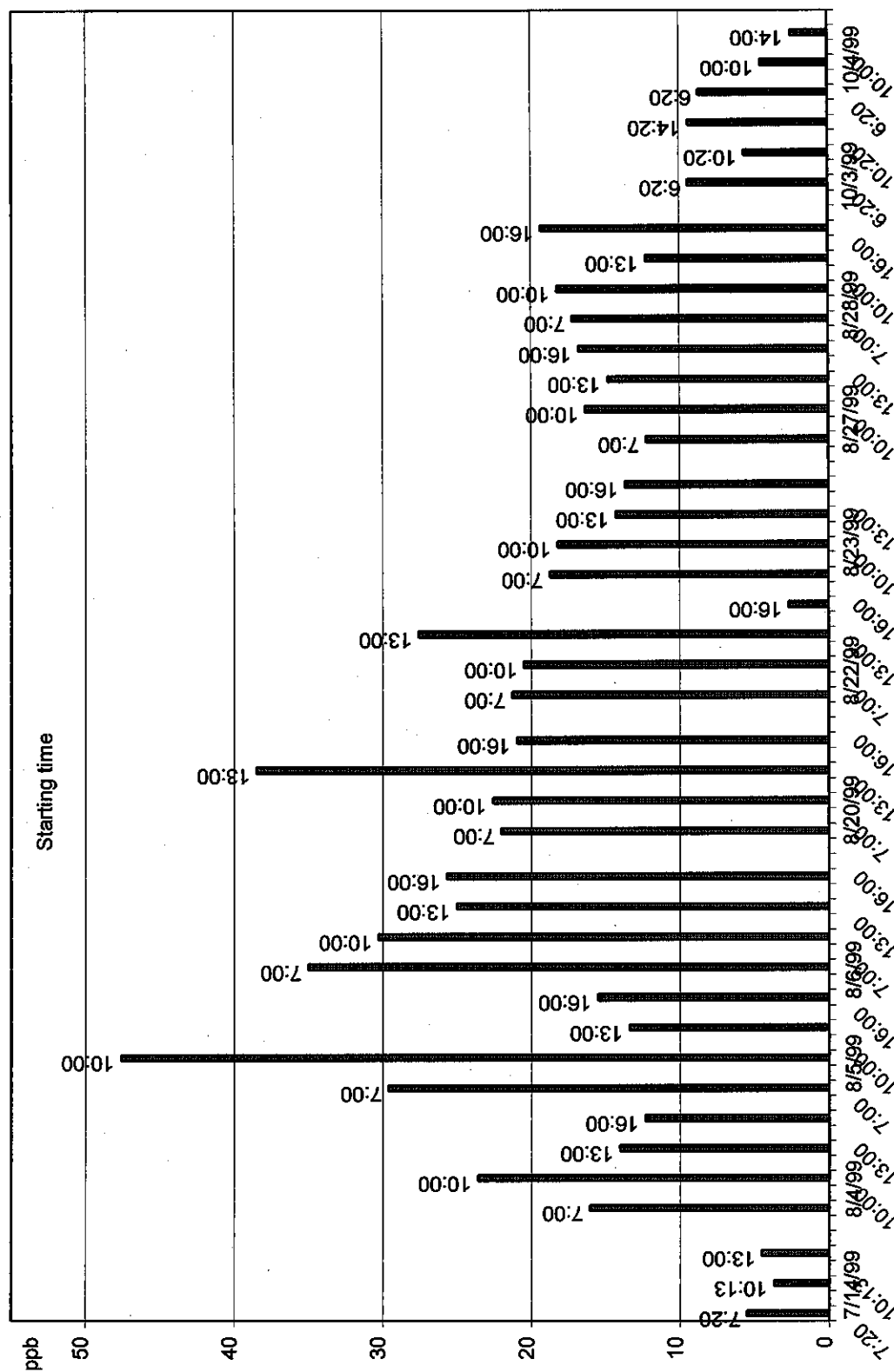
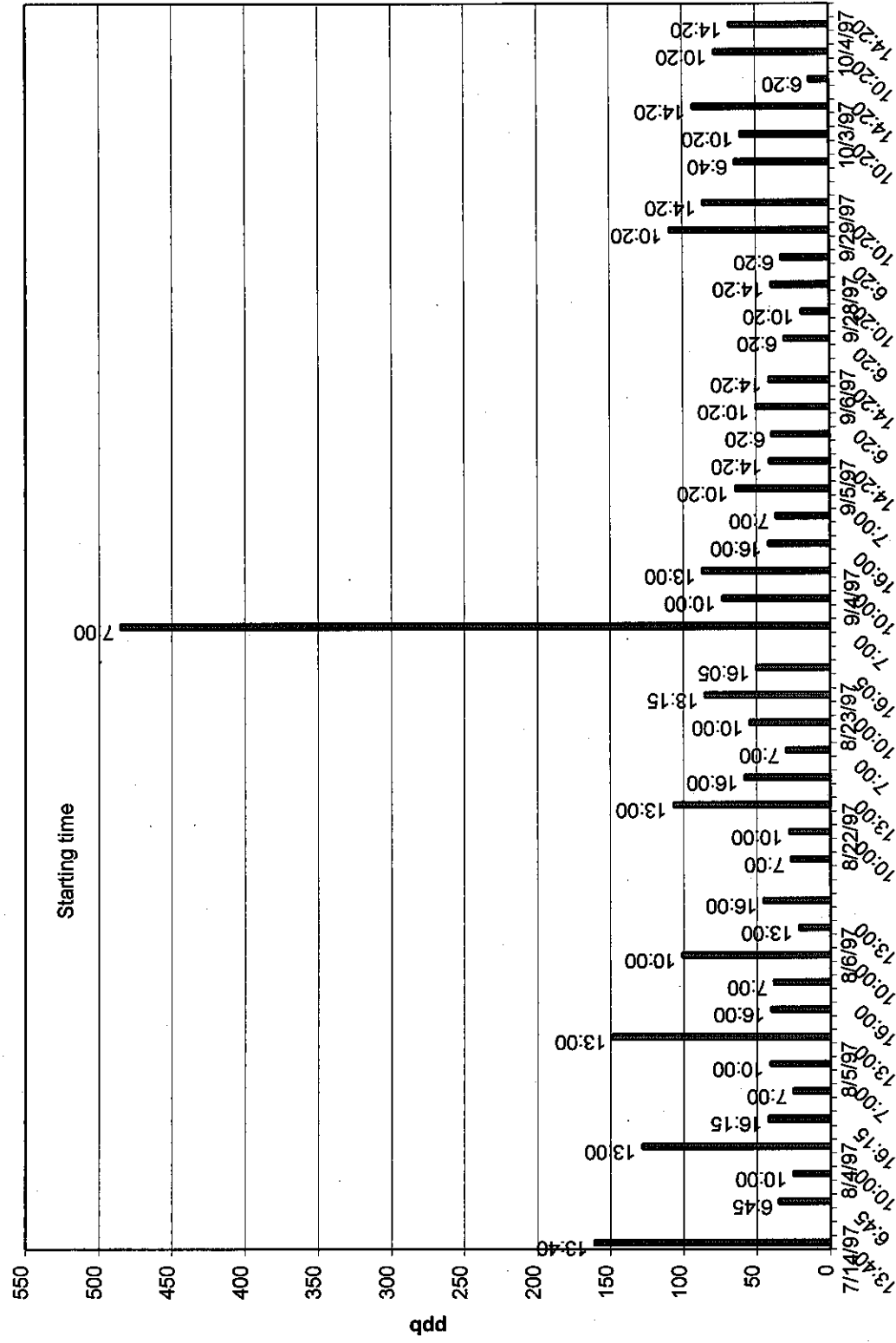
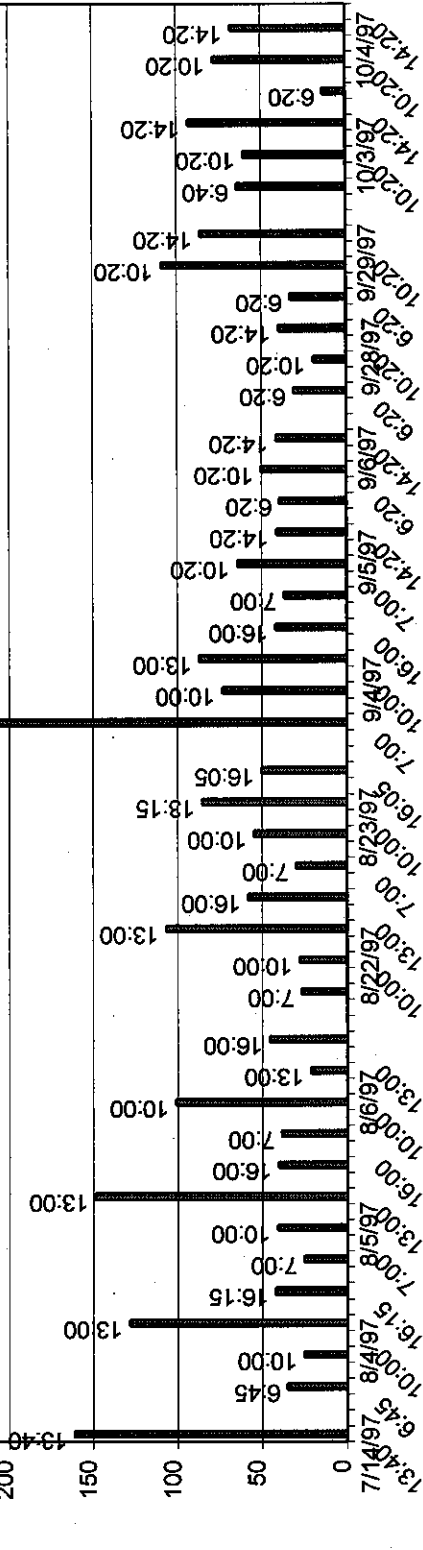


Figure 3-26. Ammonia Concentrations in Riverside by the Diffusion Denuder Method.**Figure 3-27. Ammonia Concentrations in Mira Loma by the Diffusion Denuder Method.**

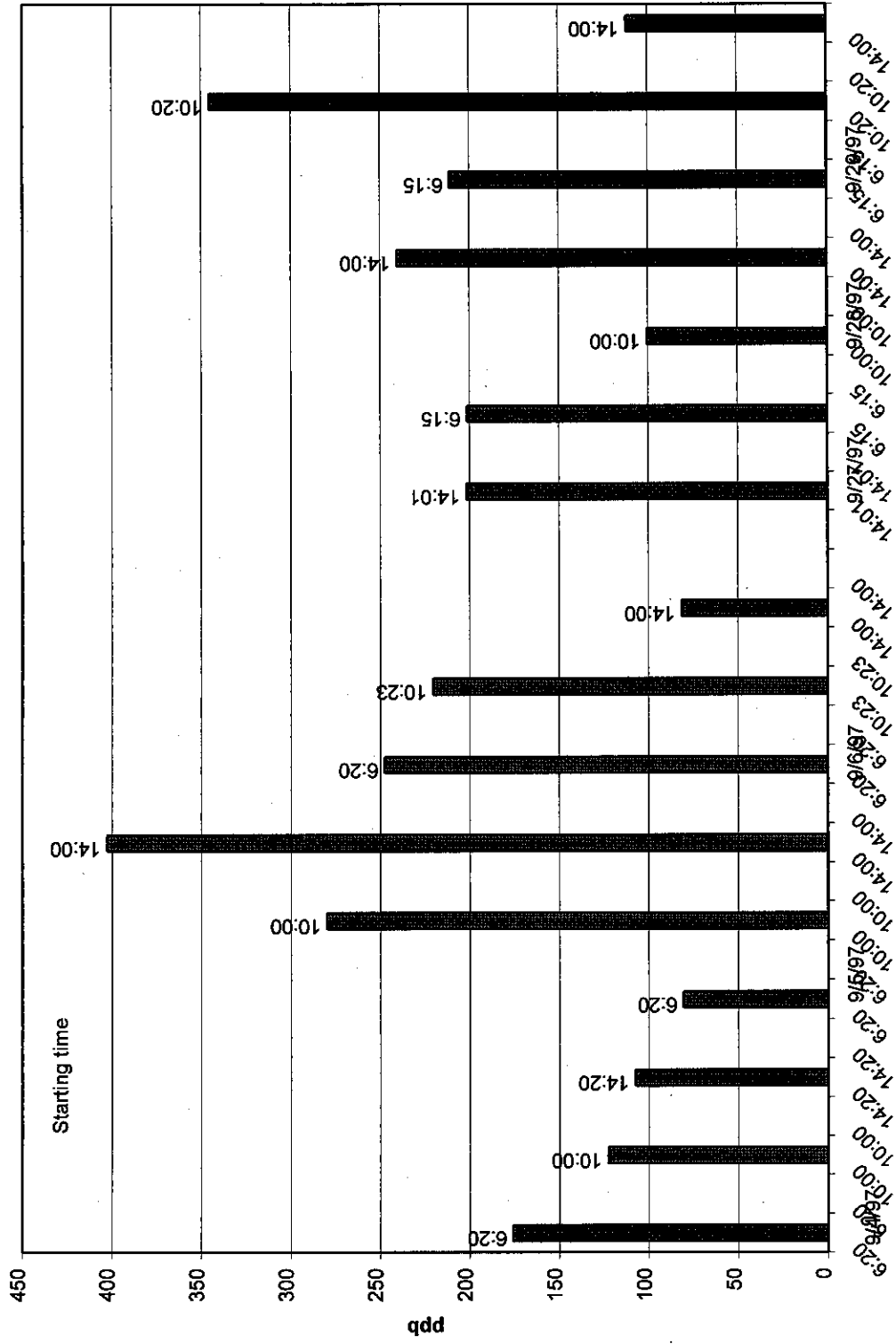


Figure 3-28. Nitric Acid Concentrations in Azusa by the Diffusion Denuder Method.

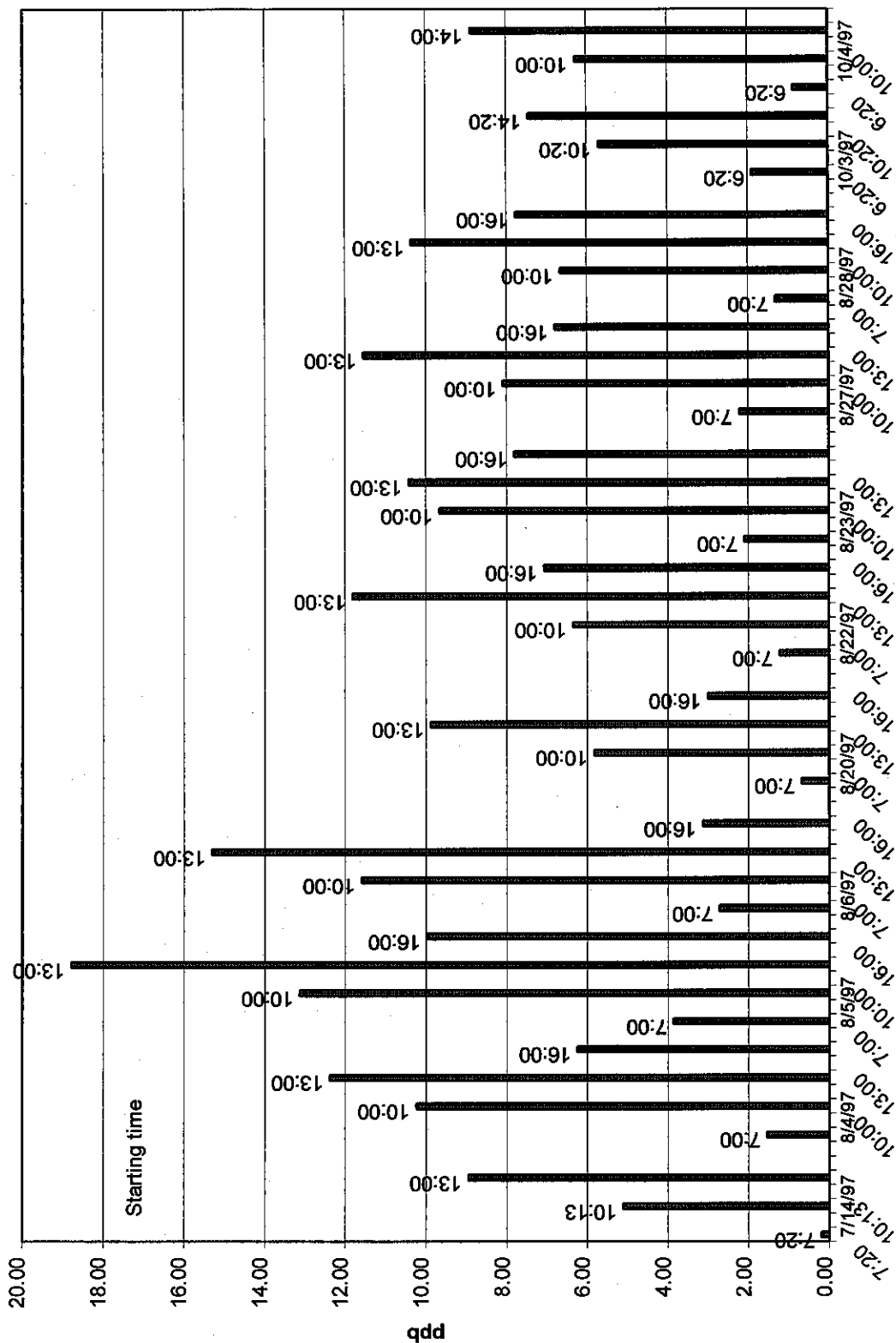


Figure 3-29. Nitric Acid Concentrations in Riverside by the Diffusion Denuder Method.

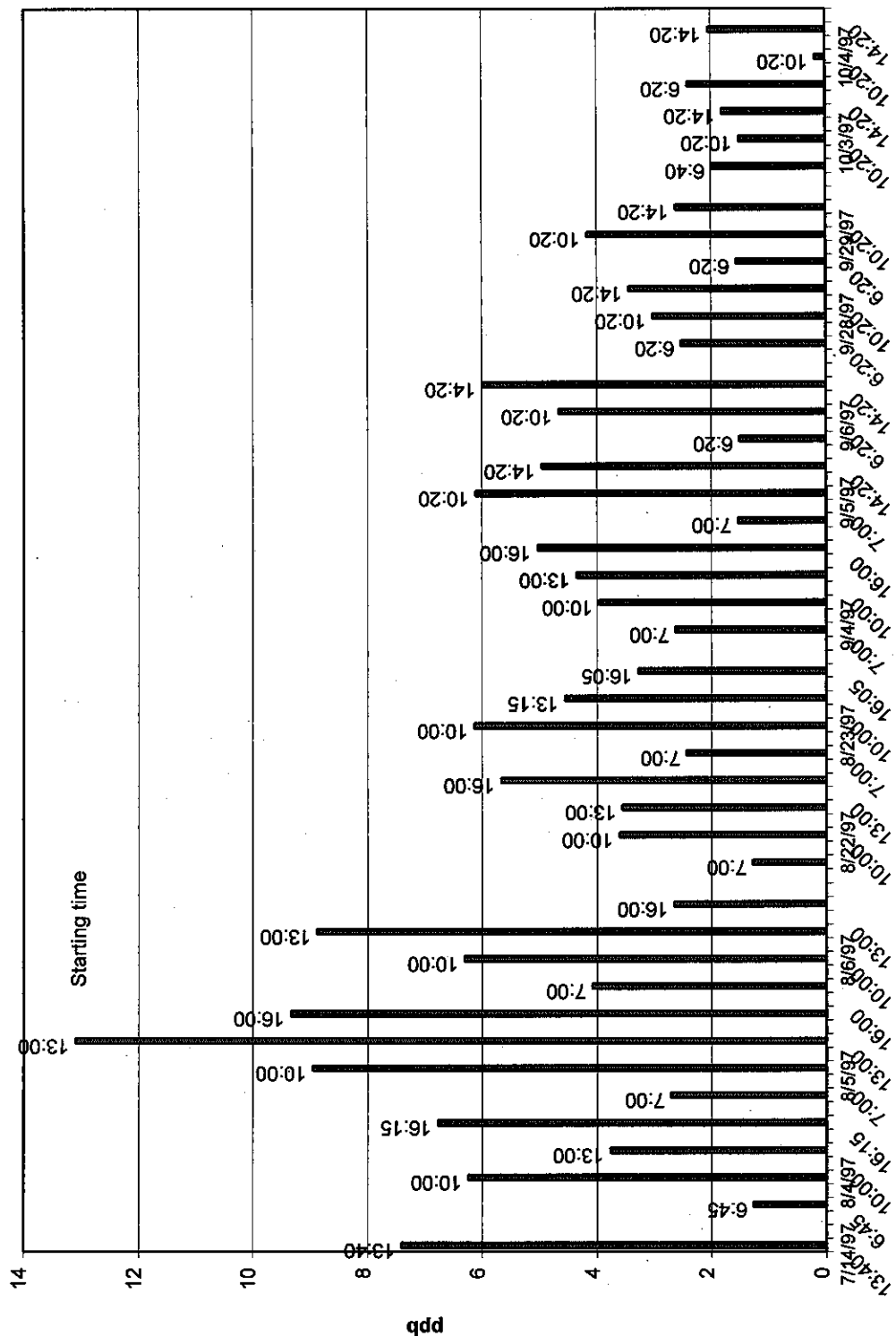
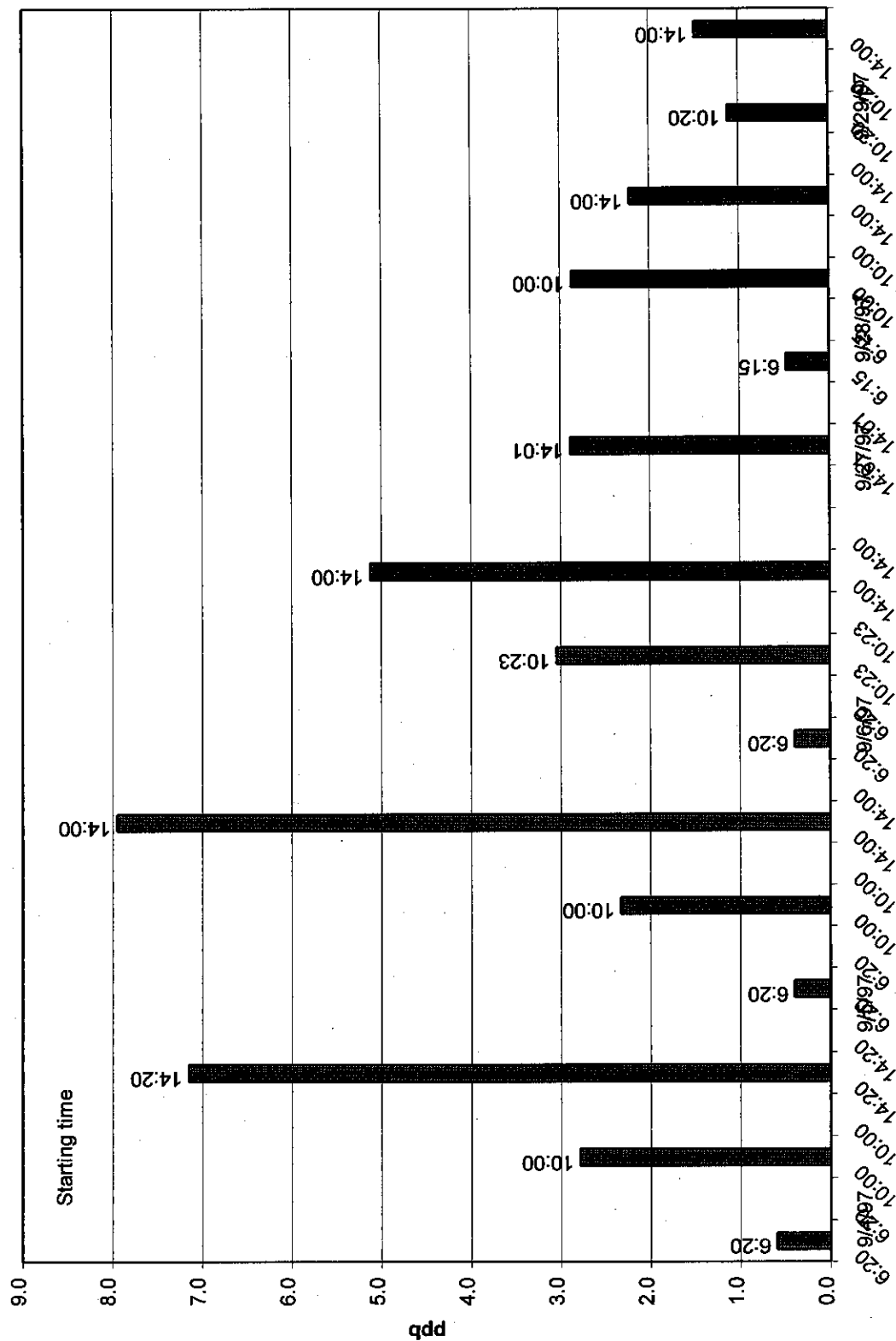


Figure 3-30. Nitric Acid Concentrations in Mira Loma by the Diffusion Denuder Method.



Comparison with Other Methods

Figure 3-31 compares the ammonia denuder data collected at Mira Loma with the collocated long-path IR. Due to the high concentration of ammonia at this site, the blank values were significant. Some of the data were corrected for blank values for the passive sampling that occurred while the sampler was loaded, waiting for the timer to turn the sampler on. This was the only site where it was necessary to use the timer (at Riverside and Azusa CE-CERT staff were available to manually operate the sampler). In some cases blanks were collected during this period, and these blank values were applied directly to the collocated sampling denuder. For others, however, blanks were not collected. (There was no intention of collecting blanks for each sample, but for a 10% subset.) For the latter cases samples were corrected by a mean value. If the sample was not subjected to passive sampling, the denuder values were corrected by the mean blank of the back denuder, which would be more representative of the contamination due to handling.

Figure 3-31. Comparison of Denuder Ammonia Measurements with FTIR at Mira Loma.

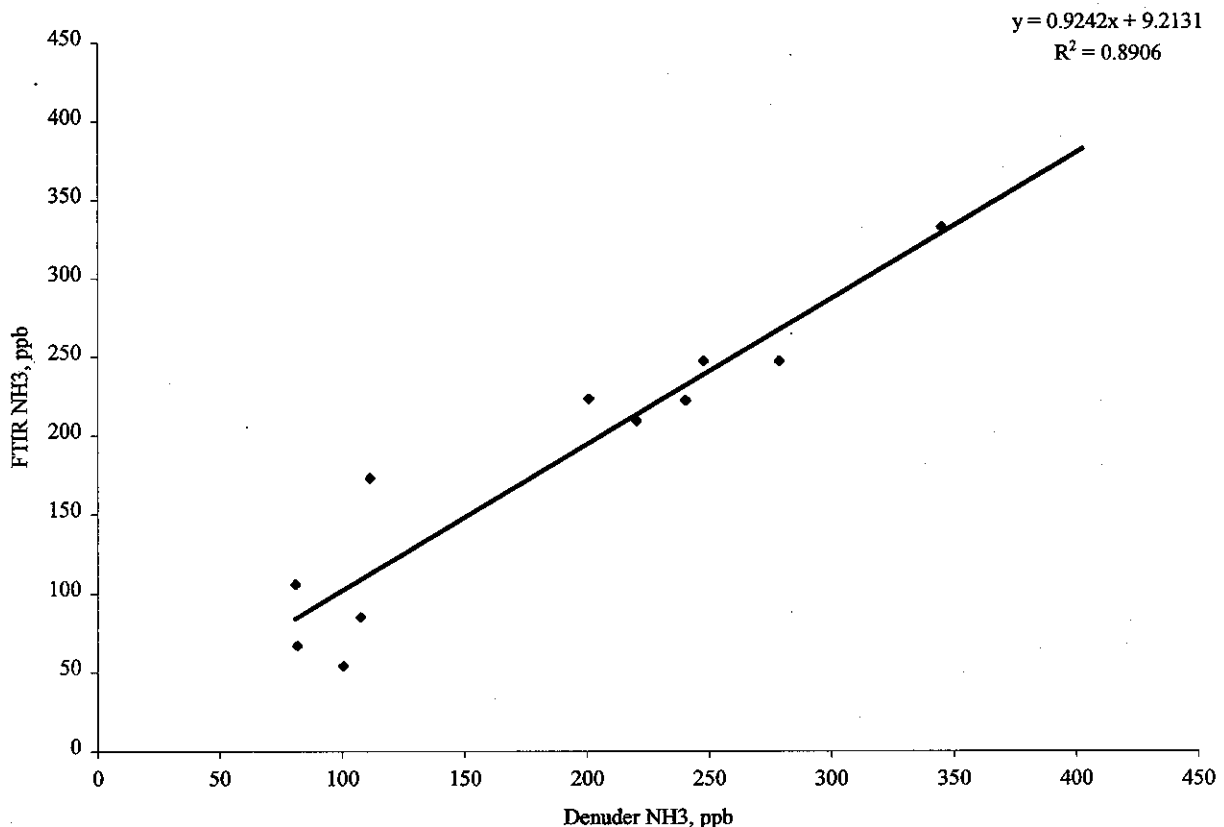
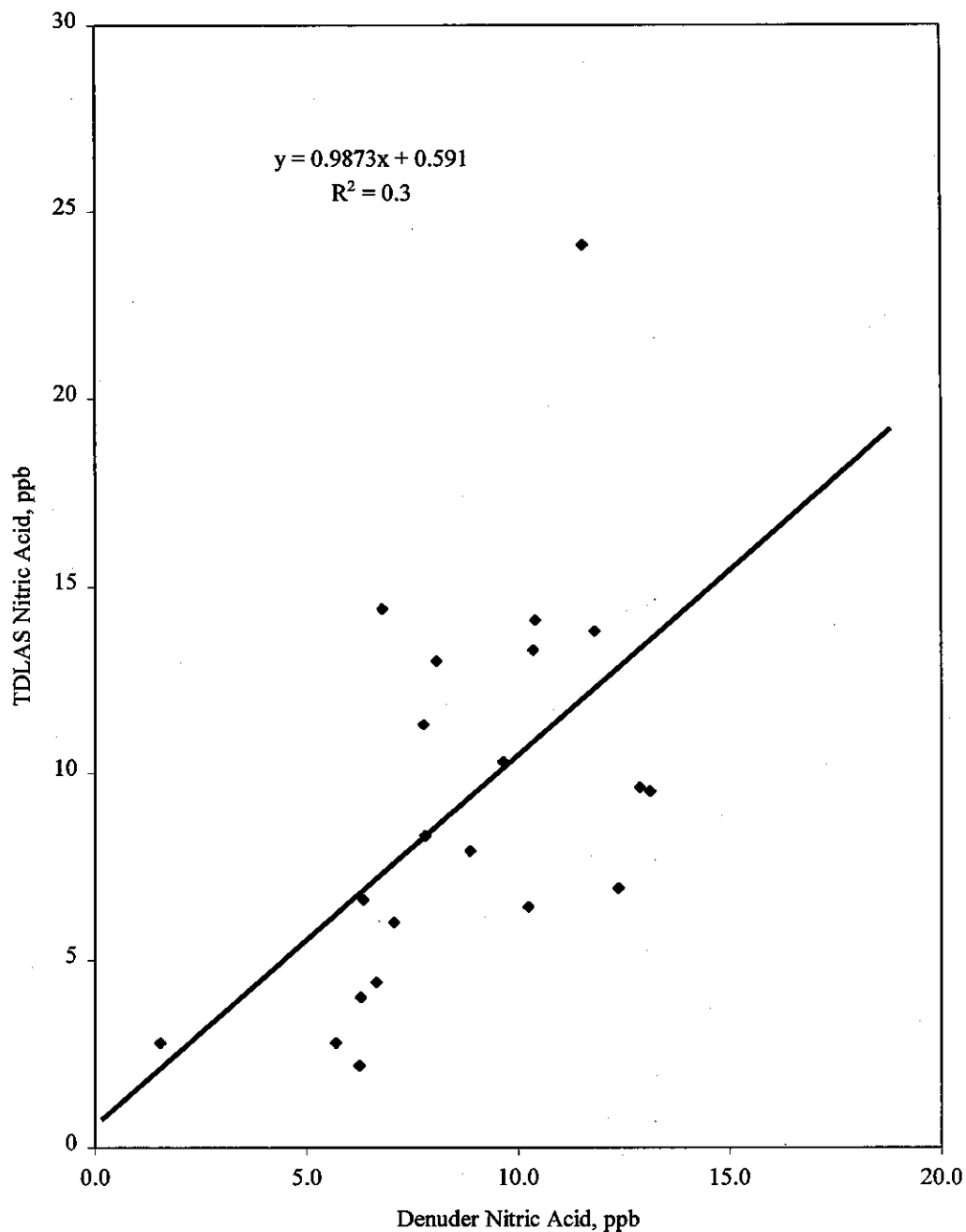


Figure 3-32 compares the nitric acid denuder data collected at Azusa with the collocated TDLAS. There is a significant amount of scatter, which is typical of other field comparison studies (Spicer et al., 1982; Hering et al., 1988; Anlauf et al., 1991). It should be noted that there are few values less than 6 ppb. This is because the first sampling period started between 06:20 and 07:00 and ended at 10:00 hours. Since there was little nitric acid before 09:00, the nitric acid determined by the TDLAS was usually below detection until then. With much of the TDLAS data missing, it was often not feasible to calculate an average for the denuder sampling period. Sampling periods starting at 09:00 and ending at 19:00 hours would have been more useful in making this

comparison. Given the poor correlation and slope near unity, we cannot determine whether there is a bias between the two methods.

Figure 3-32. Comparison of TDLAS and Denuder Nitric Acid at Azusa.



3.1.5 Peroxyacetyl Nitrate (PAN), Peroxypropionyl Nitrate (PPN), and Tetrachloroethylene (TCE) Measurements

These measurements were made by DGA under contract to CE-CERT. The DGA final report contains the experimental details and is attached as Appendix A. Detection limits for PAN, PPN, and TCE were 28, 42, and 30 ppt, respectively at Azusa and 38, 49, and 35 ppt at Simi Valley. Although not quantified, a methyl chloroform peak was observed in nearly all chromatograms studied. Prior to deployment, multi-point calibrations were made in the laboratory using a 3.5 m³ Teflon chamber, while 125 L bag PAN standards were prepared in the laboratory and transported to the measurement sites for span checks. Span checks were made at intervals of approximately two weeks, for a total of eight for the SCOS97-NARSTO measurement window. In addition to span checks, the instruments were checked more frequently for proper operation.

Measurements at Azusa were delayed until 12:00 hours on July 14, 1997, due to the power on the site being upgraded. The air conditioner at this site failed on August 5 for about one week. To correct data, calibration factors were determined as a function of temperature and applied based on the recorded shelter temperature.

Quality Assurance Results

For the 125L transfer bags, good agreement (within 7%) was found between PAN and PPN quantification using the DGA and Simi Valley chemiluminescent NO-NO_x analyzers.

The span checks for PAN showed that the response factor had a relative standard deviation (RSD) of 7% at Azusa and 6% at Simi Valley. For TCE it was 13% at Azusa and 9% at Simi Valley. The retention times were found to be stable for all three compounds at both sites, with an average RSD of 3%. During span checks the repeatability of the PAN injections were $\pm 1\%$ while the TCE injections were within $\pm 3\%$. Span checks with and without the on-site sampling line verified that there were no losses in the lines.

The overall uncertainty was estimated to be $\pm 15\%$ for PAN and PPN and 25% for TCE.

Results

Figures 3-33 and 3-34 are time series plots of the hourly-averaged concentrations measured at Azusa and Simi Valley, respectively, for all of the IOP days. PAN was detected in nearly every analysis and showed the expected diurnal profiles that parallel ozone concentrations. The highest PAN concentration measured, 4.1 ppb, was at Azusa and was significantly lower than those reported in previous studies (Grosjean et al., 1996). PPN was highly correlated with PAN with an R of 0.94 at Azusa and 0.92 at Simi Valley. PPN concentrations were also lower than in previous studies although the ratios were similar. TCE levels were higher in Azusa by an average factor of 2.5. TCE was not correlated with PAN or PPN at either site, the R values being less than 0.2.

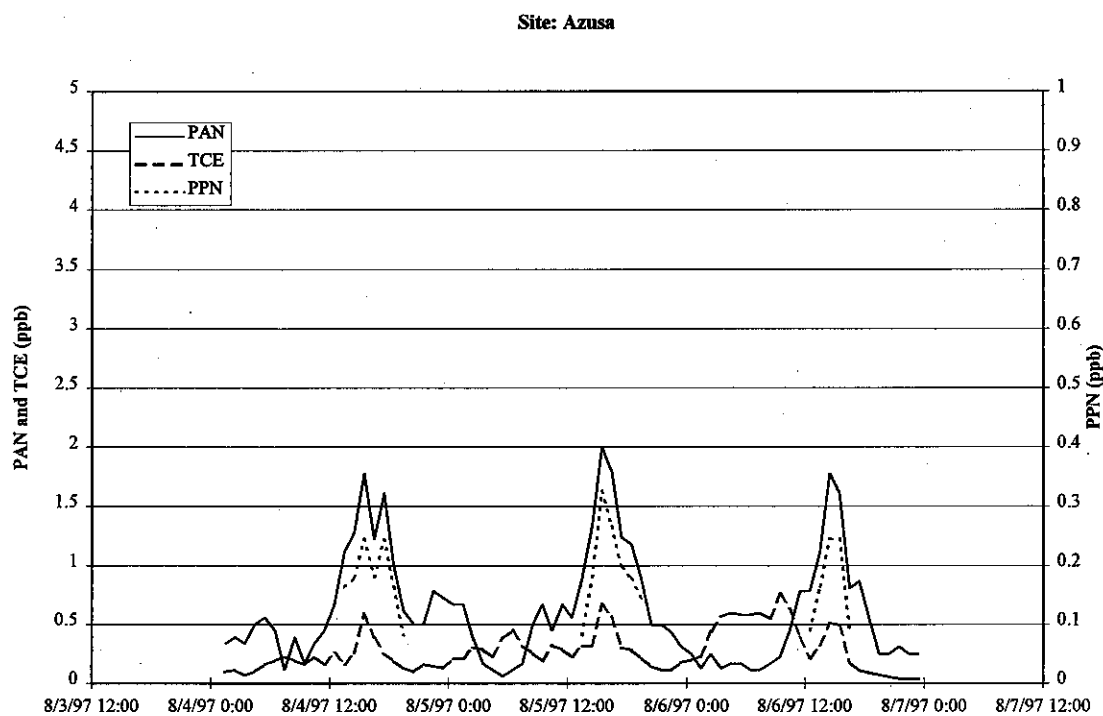
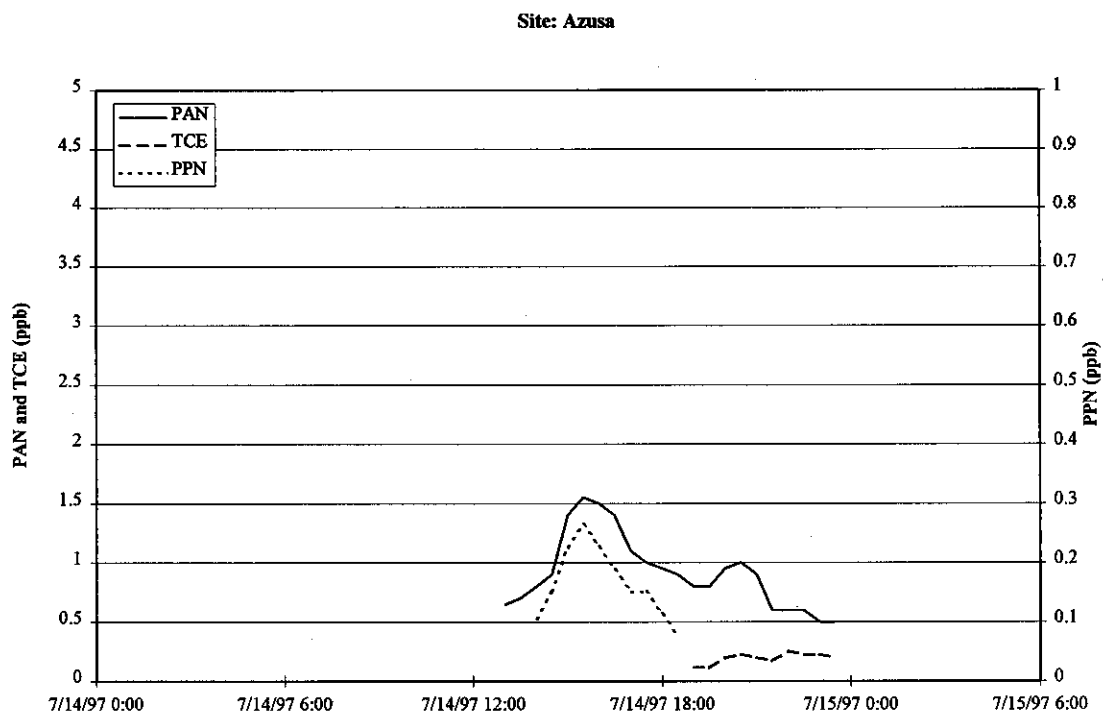
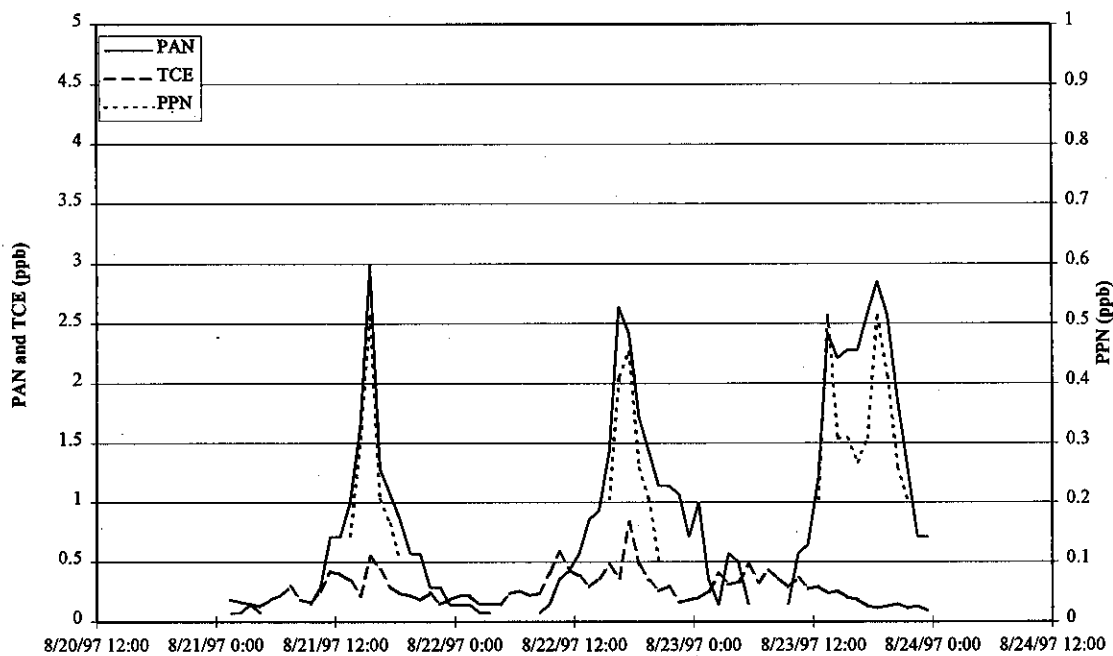
Figure 3-33. PAN, PPN, and TCE Concentrations in Azusa for SCOS97-NARSTO IOP Periods.

Figure 3-33, continued.

Site: Azusa



Site: Azusa

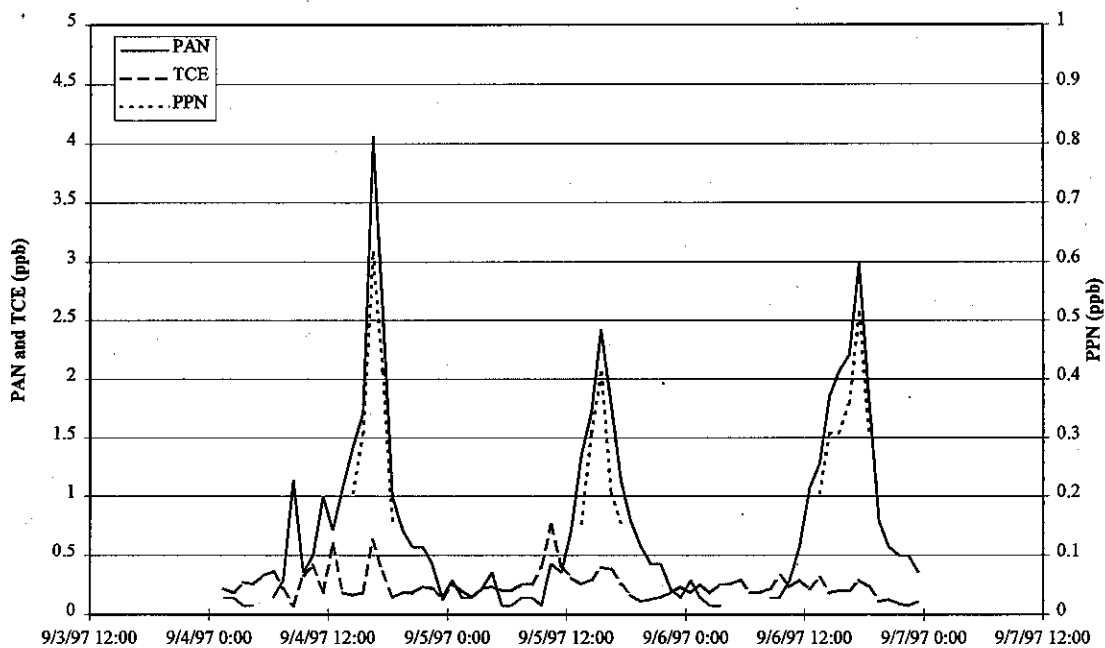
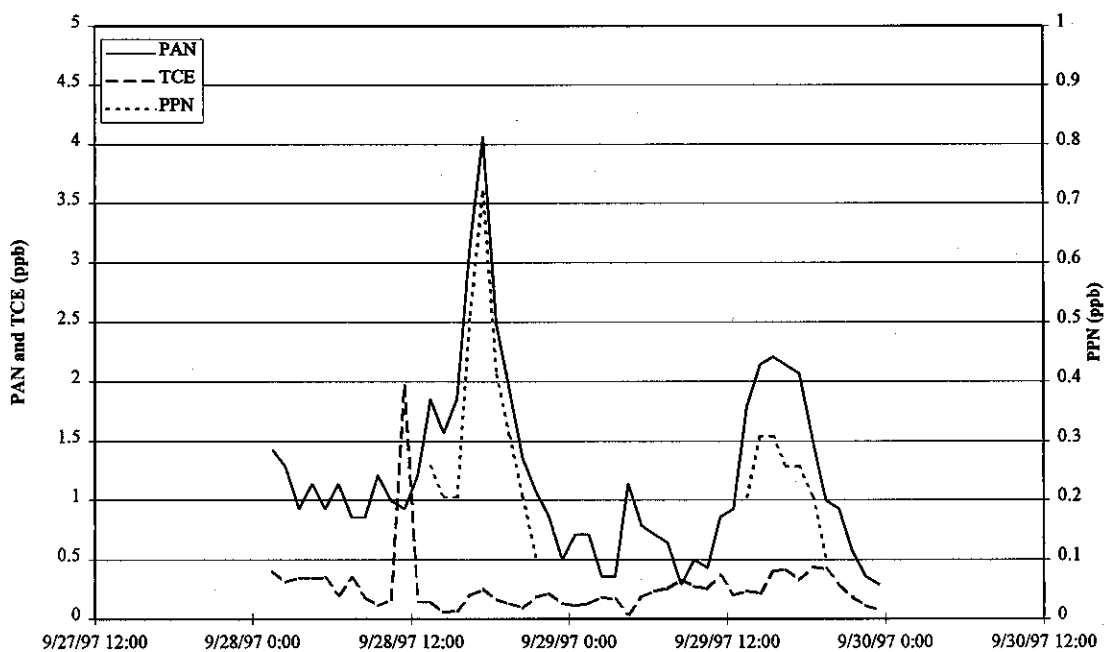


Figure 3-33, continued.

Site: Azusa



Site: Azusa

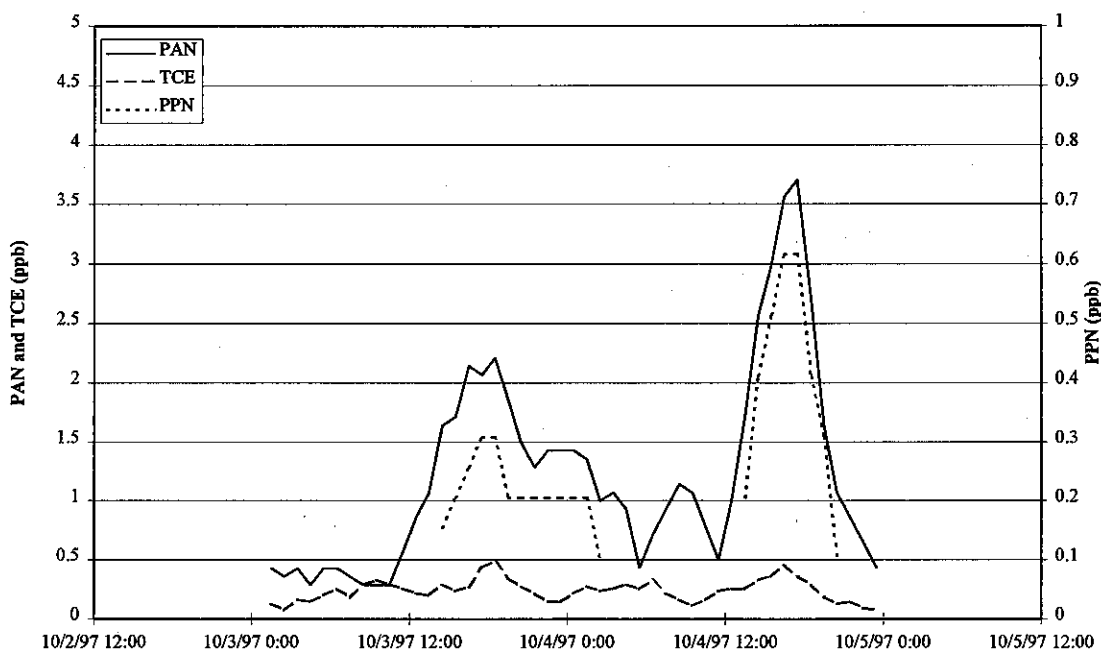


Figure 3-34. PAN, PPN, and TCE Concentrations in Simi Valley for SCOS97-NARSTO IOP Periods.

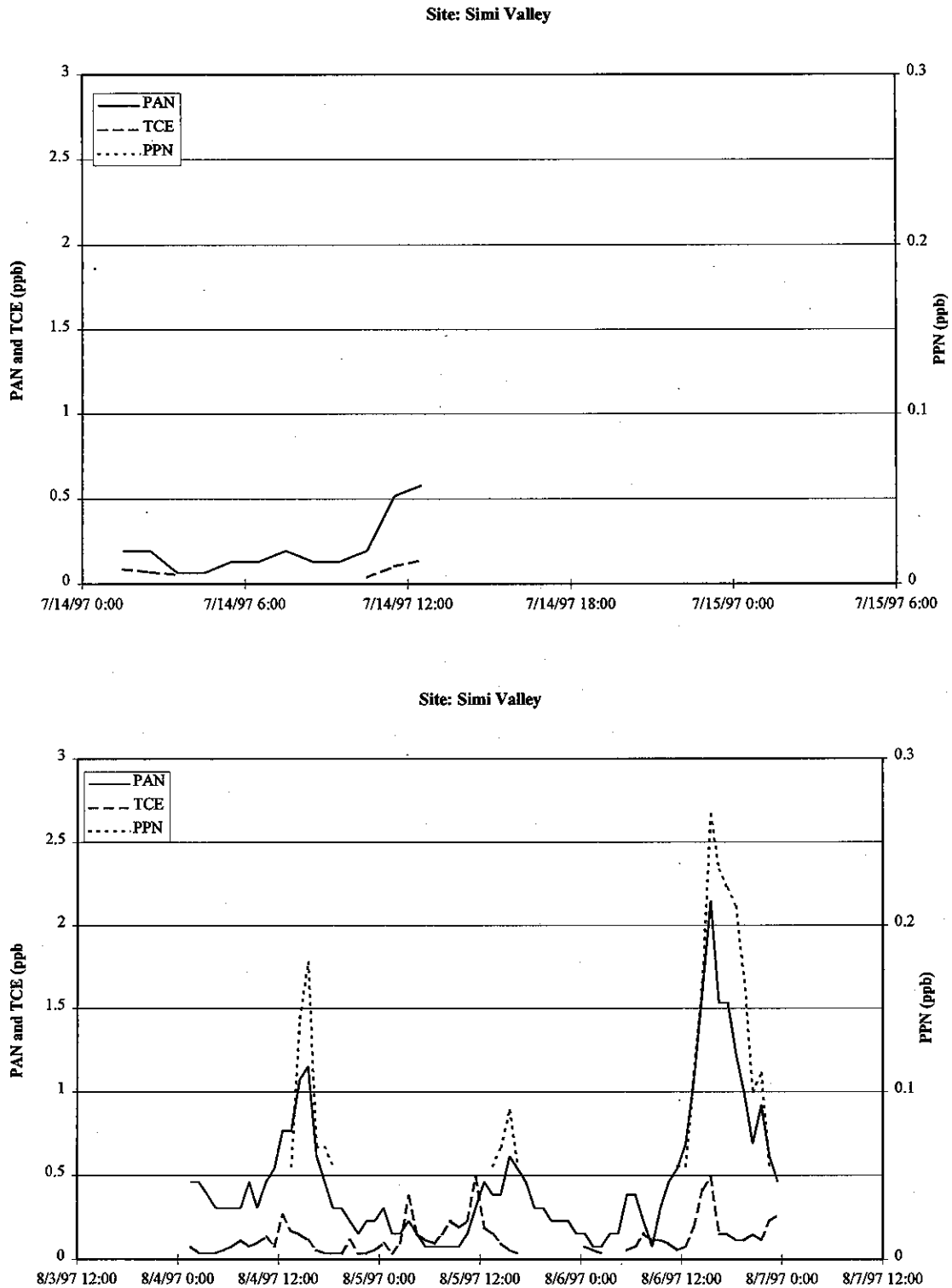
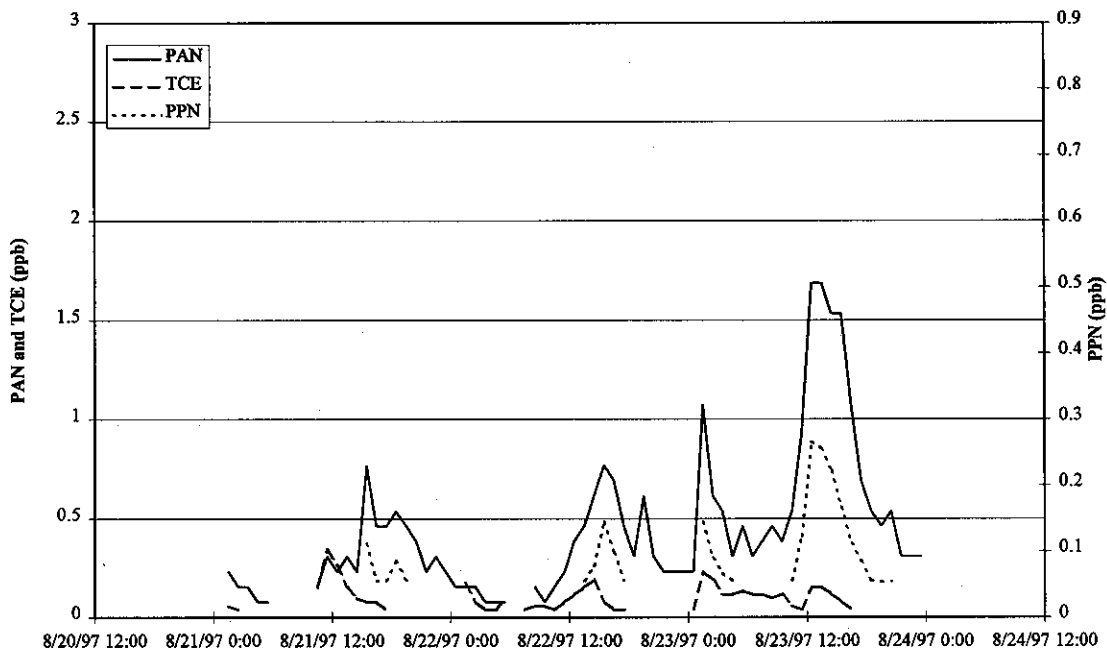


Figure 3-34, continued.

Site: Simi Valley



Site: Simi Valley

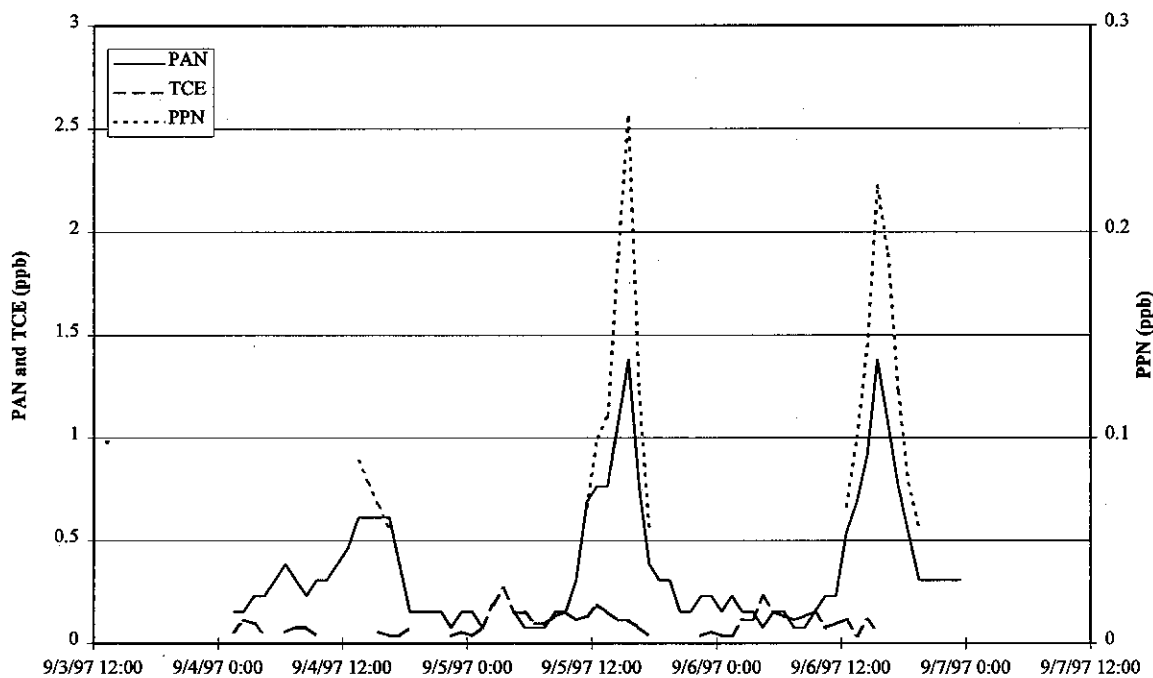
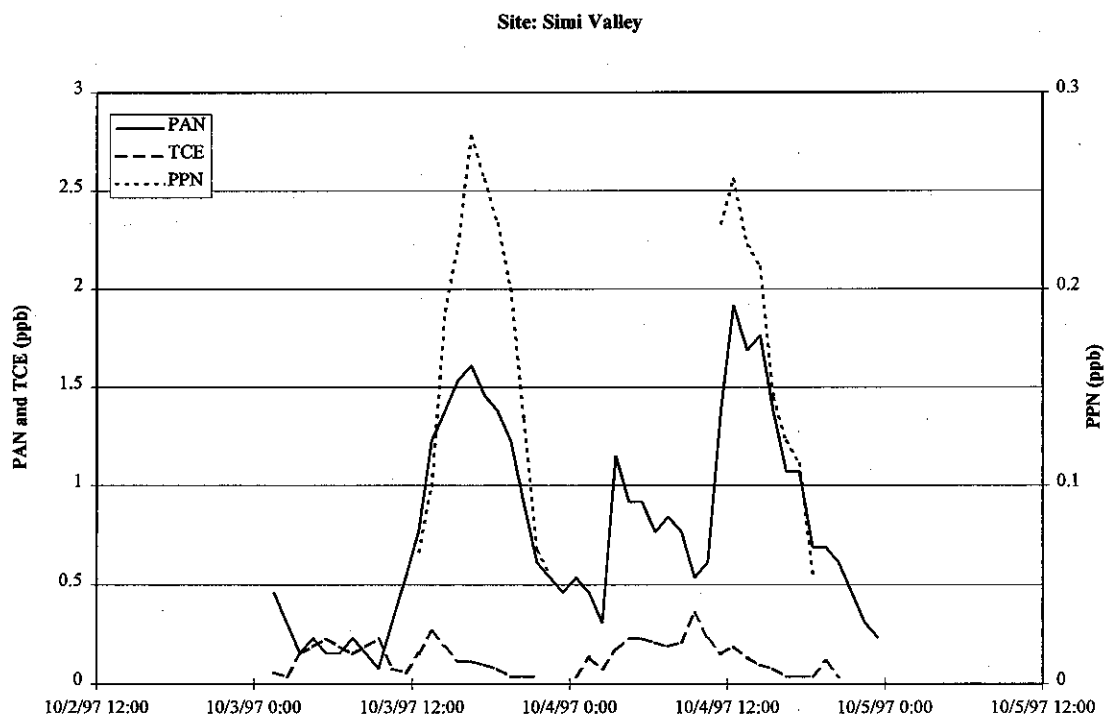
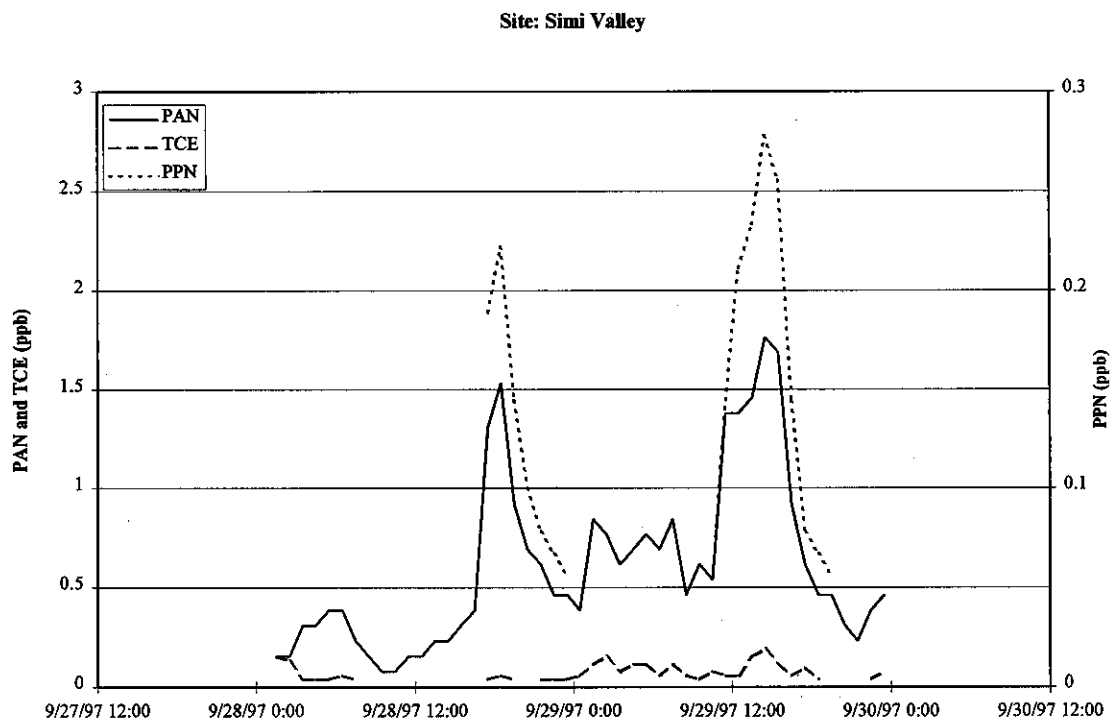


Figure 3-34, continued.



3.1.6 Long Path-length Transformation Infrared Spectrometry (FTIR)

The FTIR spectrometer was housed in an air-conditioned shed. The mirror assemblies, which were located outdoors, were shaded from direct sunlight by protective shields. The infrared beam originating from the spectrometer and the return beam from the multiple-reflection optics passed through holes on the shed's wall. The spectrometer bench and the mirror's support frames all rested on concrete pads, and the optical system's support bases were further weighted down with cinder blocks for added stability. The optical axis of the present 25 m basepath FTIR system was 1.2-1.5 m above ground. The FTIR facility was located inside the Union Pacific compound in Mira Loma, along the southern half of the east fence.

The instrument was fully optimized on September 10, 1997, 17:11 PDT. From that time on the NH_3 detection limit was 1 ppb, while prior to that it was approximately 4 ppb. The instrument performance was adequate for the high NH_3 levels that prevailed at the Mira Loma site throughout the monitoring period.

Each archived record is a spectrum in the range 700-3200 cm^{-1} range (file size = 299 kb). Program routines were written to extract separate spectral segments containing the analytical absorption "lines" at 1103.4 cm^{-1} and 868.0 cm^{-1} , convert them to absorbance scale, and tabulate the peak-to-baseline values. Each processed segment was stored, and another routine was employed to rapidly scan each segment visually for correctness of the baselines drawn. No background spectra were necessary for a ratio, since both analytical lines were devoid of interference. The average peak-to-baseline absorption coefficients (base 10) obtained from several calibrations (including those from past field studies) and employed in the present calculations were 19.3 $\text{atm}^{-1} \text{cm}^{-1}$ and 10.3 $\text{atm}^{-1} \text{cm}^{-1}$ for the 1103.4 cm^{-1} and 868.0 cm^{-1} peaks, respectively, with uncertainties of $\pm 6\%$ for both values. The concentration values were derived from the 1103.4 cm^{-1} line, except for those corresponding to 0.7 absorbance units where measurements from the 868.0 cm^{-1} line were employed to avoid deviation (non-linearity) from the Beer-Lambert equation.

From the Beer-Lambert equation $c = A/(l)$, an equation was derived expressing the error e of the concentration c in terms of the uncertainties in the absorbance A , absorption coefficient, and path-length l . The error in the established 1000-meter path-length is less than 0.5% and, therefore, its contribution to e is negligible. As noted above, the uncertainty in the absorption coefficient is $\pm 6\%$. The uncertainties in the peak-to-baseline readings come mainly from the noise in the spectra and are similar for spectra in time blocks where a common operational optimization of the instrument applies. The concentration corresponding to 2x RMS noise has been used to approximate the error arising from the uncertainty in the absorbance reading. Representative RMS noise values were determined from randomly selected spectra in the different time blocks. The error expressions derived are:

$$\text{For September 4 to September 6, 1997} \quad e^2 = 26.8 + 0.0036c^2$$

$$\text{For September 10, 1997: 0404-1656 PDT} \quad e^2 = 15.1 + 0.0036c^2$$

For September 10, 1997: 1711 PDT to
Sep 12, 1997 (inclusive) and
Sep 28- Sep 30, 1997

$$e^2 = 6.7 + 0.0036c^2$$

where the first term of e^2 reflects the error due to noise (as it affects A readings) and the second term is due to the error in . The absolute values of e have been reported in the data tabulation as Abs_precis.

Results

Spectra were recorded every 5 minutes with a resolution of 0.13 cm^{-1} (full width at half-maximum), a total path-length of 1000 m, and an averaging time of 4 minutes. The observed NH_3 concentrations ranged from 11 ppbV to 776 ppbV. The dates and approximate time blocks of the available NH_3 data are given in Table 3-8. The total FTIR measurements have been submitted to the ARB.

Table 3-8. Spectra Measurement Dates and Times.

Date	Time Block	Comments
4-Sep097	**0000-1400**	No data, power interruption the night before caused instrument problems and overall delay.
	1400-2400	
5-Sep-97	0000-1400	
	1400-1900**	No data due to power failure.
	1900-2400	
6-Sep-97	0000-2400	
10-Sep-97	**0000-0400**	Unusable data due to extremely poor spectra; instrument was left running normally at 21:30 PDT of previous night; IR beam obstruction suspected; spectra returned to normal after this period.
	0400-2400	
11-Sep-97	0000-2400	
12-Sep-97	000-2400	
13-Sep-97	0000-2400	
28-Sep-97	0000-2400	
30-Sep-97	0000-2200	

Figure 3-35 is a time series plot for all the valid ammonia measurements from the FTIR. These data show a large amount of variability in ammonia concentrations as would be expected several kilometers west of a large source.

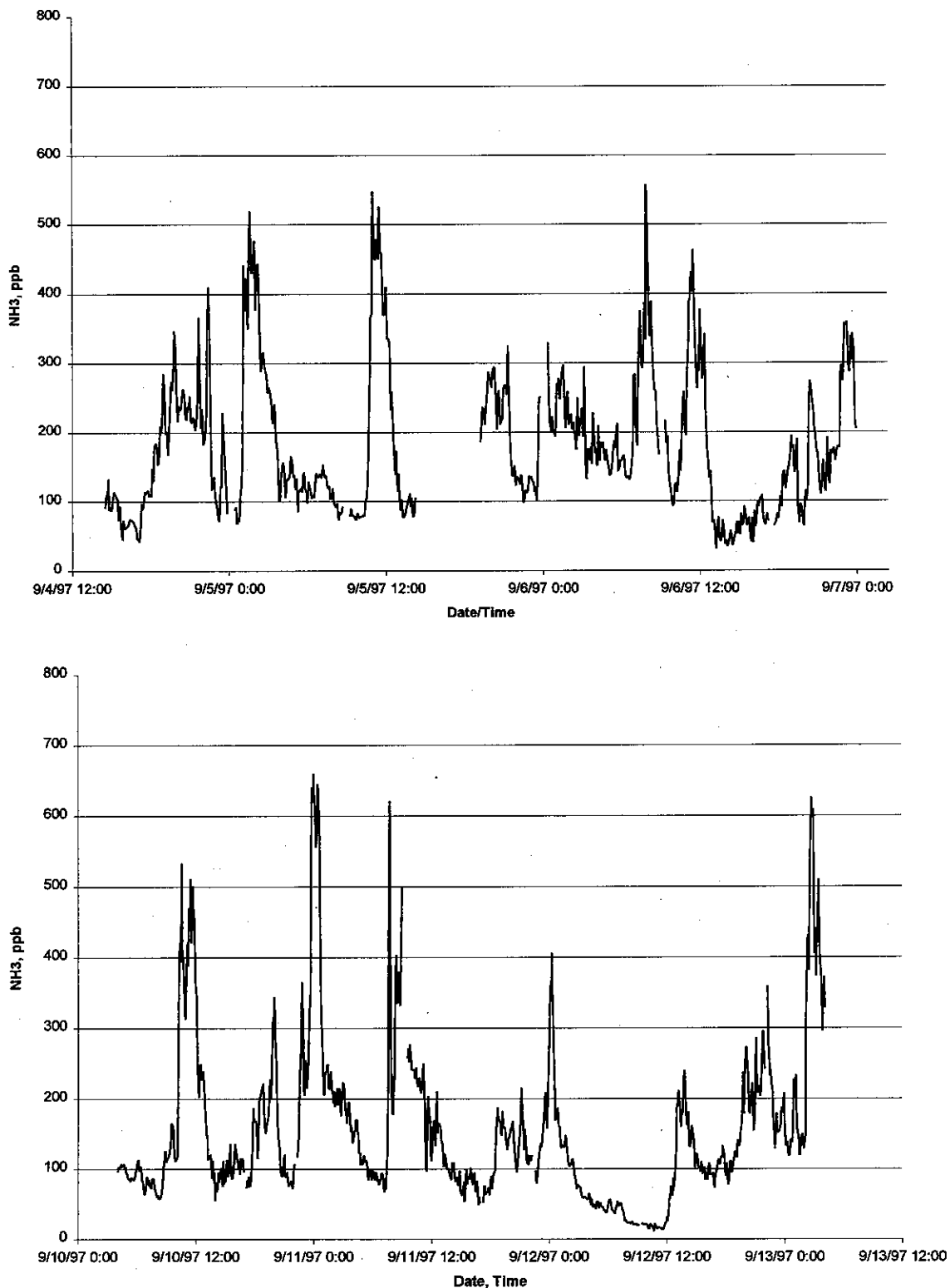
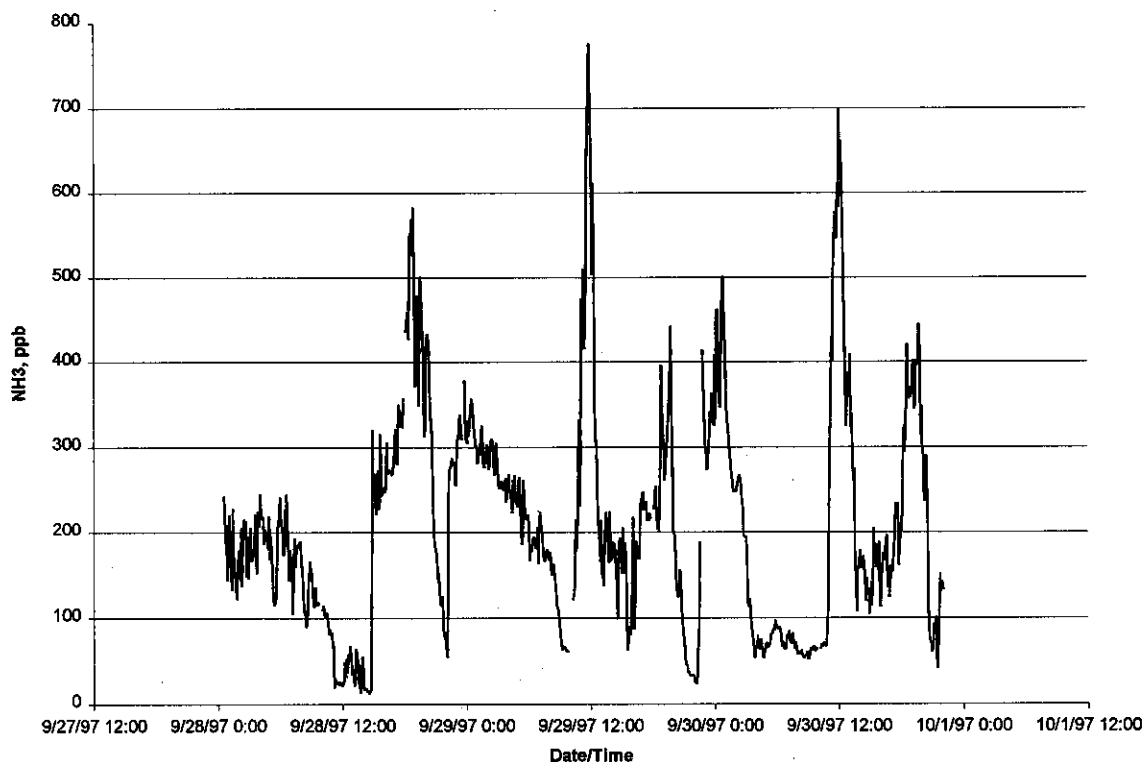
Figure 3-35. FTIR Measurements of Ammonia at Mira Loma.

Figure 3-35, continued.

3.2 Radiation Measurements

3.2.1 Non Wavelength Selective

Before deploying the Eppley PSP total radiation sensors, the Eppley TUVB UV radiation sensors, and the Eppley 8-28 total radiation sensors, groups of these sensors were operated together on the roof at CE-CERT. The primary purpose of the collocated measurements was to establish calibration factors for each instrument. Only one of the four UV radiometers, and one of the six total solar radiation (TSR) sensors, had current calibration factors. This procedure worked very well for the TSR sensors. All TSR sensors were very linear with respect to the certified sensor.

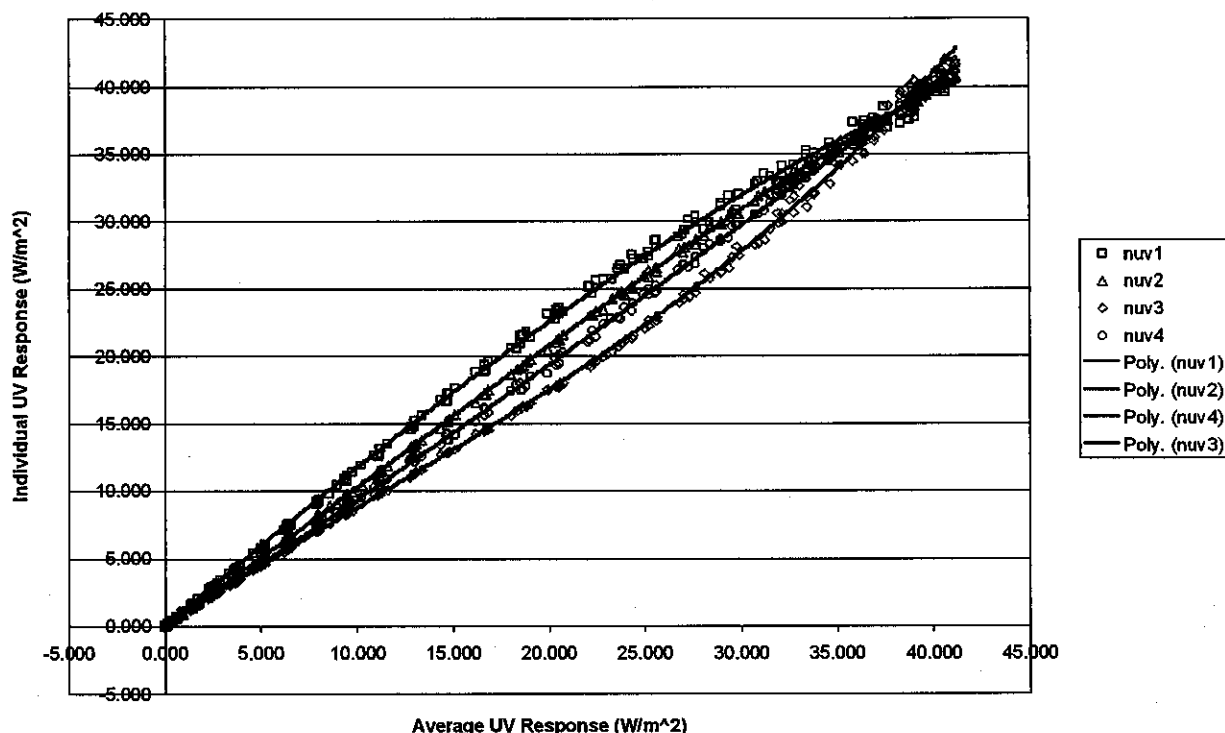
For both total solar radiation (TSR) and ultraviolet solar radiation (UVSR), data were collected continuously for the SCOS97-NARSTO measurement window at both sites. The diffuse total solar radiation (DIFSR) equipment did not operate until mid-August. The diffuse UV (DIFUV) measurements were done by manually screening a UV radiometer. All of the equipment at Mt. Wilson was moved on August 26 from on site at Mt. Wilson to another. This was done because the original site had several white buildings nearby and white rock was spread around the site. The site was moved because these white materials may bias the measurements due to reflection. The new site did not have any nearby features that would affect the radiometric measurements except trees to the west that might partially shade the monitors in the very late afternoon. Prior to moving the site, radiation shields were set up around the Eppley PSP and TUVB radiometers by ARB staff on July 21 in an effort to block reflections from white buildings without significantly

blocking view to the remainder of the sky. These shields consisted of short black cylinders and remained in place until the site was moved.

For each day at each site, data from the UV and total solar radiometers were plotted together versus time. The plots generally follow a smooth curve roughly proportional to cosine of the solar zenith angle. Periods that showed scattered noisy data for all sensors were marked suspect. These data are probably accurate, but represent variations due to variable cloud cover. They are not likely to be useful for data interpretation. Depending on the site and the season, some sensors appear to be affected by early morning or late afternoon shadows when the sun is low on the horizon. Data from the affected sensors were marked suspect when morning or evening shadows appeared evident. During the period when the radiation shield was in place at Mt. Wilson, the diurnal profile of radiation intensity does not follow a smooth cosine curve. There is a pronounced kink in the total solar radiation data between 11:00 and 13:00. The total solar radiation data from 11:00 and 13:00 at Mt. Wilson were flagged as suspect during this time period. The UV data may have been slightly affected but were not flagged.

In addition to flagging suspect data, the plots were reviewed and data flagged to indicate whether the sensor was in direct light, fully shaded, or partially shaded. During manual shading operations, the sensor shading intervals do not coincide with the data logger averaging intervals. Thus, the data logger averages will include partial shade and partial sun as the sensor is manually shaded or unshaded. Data points collected in full sunlight were flagged with "OK" and marked valid. Data collected in full shade were flagged with "F" and marked valid. Data collected partly in the shade were flagged with "P" and marked invalid.

Collocated sensor data were used to establish calibration factors for the UV radiometers. Three Eppley UV sensors were compared with a recently calibrated Eppley UV sensor on the roof at CE-CERT during June 1997. The four Eppley UV sensors were found to have response factors that ranged from 85% to 180% of the response from the calibrated UV sensor. It was also observed that the sensors were significantly non-linear with respect to each other. The response of each UV sensor was normalized with a simple multiplicative factor for that sensor. The factor was chosen so that the sensors agreed on average for a period of about one and a half hours on either side of solar noon. Figure 3-36 shows a scatterplot of each sensor response versus the average of all four sensors. This plot shows points for three complete days of data: May 30 and 31 and June 1, 1997. When we observed the non-linearities, we suspected that sensor position or level might be the source of the problem. We performed a series of experiments in which the sensors were carefully leveled, permuted throughout their spatial positions, and rotated about their axes in 90-degree increments. None of these variations affected the relationship between the sensor results. It is possible to apply a more complicated response correction that would linearize the responses of the various sensors. However, we do not know which sensor, if any, is responding linearly to the actual solar radiation intensity. Therefore, we applied the simple multiplicative factor described above.

Figure 3-36. Comparison of Four Eppley TUVR Sensors.

Collocated sensor data were used to establish calibration factors for the Eppley Model 8-48 total solar radiometers. Four Eppley model 8-48 TSR sensors and a second Eppley PSP sensor were compared with a recently calibrated Eppley model PSP on the roof at CE-CERT during August. Up to about 850 W/m^2 , the two Eppley PSP sensors were linear with respect to each other and had a slope of 1.00. But above this level, the response of the second sensor begins to fall off, becoming about 7% lower than the recently calibrated sensor at the peak intensity of 975 W/m^2 . The second PSP response tends to be lower than the calibrated sensor response during the morning and higher during the afternoon. No corrections were applied to the Eppley PSP sensors. The four Eppley model 8-48 total radiation sensors were nearly perfectly linear with respect to one another, but showed non-linearity with respect to the Eppley PSP sensors. Calibration factors were based on a linear fit of the Eppley 8-48 data to the recently calibrated Eppley PSP. The 8-48 sensors were about 10% higher at mid-scale and about 6% lower at full-scale than the PSP. Again, we used simple multiplicative corrections rather than attempting to linearize the results, because we do not know which sensor is in fact responding linearly to solar radiation.

The calibration factors used for data reduction are shown in Table 3-9.

Table 3-9. Sensor Calibration Factors.

Eppley Model	S/N	Measdev	Spectral Range	CE-CERT Site	Mt. Wilson Site	Factor mV/(w/m²)
PSP	25876F3	EPPS	0.285 – 2.8 μ m		WILS	0.00950
PSP	18971F3	EPPS	0.285 – 2.8 μ m	RICE		0.00960
PSP	30658F3	EPPS	0.285 – 2.8 μ m	RICE2		0.00925
8-48	1*	EPPLSR	0.285 – 2.8 μ m	RICE3	WILS	0.01028
8-48	2*	EPPLSR	0.285 – 2.8 μ m	RICE4	WILS2	0.01173
8-48	3*	EPPLSR	0.285 – 2.8 μ m	RICE		0.01100
8-48	4*	EPPLSR	0.285 – 2.8 μ m	RICE2		0.01010
TUVR	17692	EPPV	0.295 – 0.385 μ m	RICE3	WILS	(0.181 * 1.00)
TUVR	14920	EPPV	0.295 – 0.385 μ m	RICE4	WILS2	(0.181 * 1.80)
TUVR	13337	EPPV	0.295 – 0.385 μ m	RICE		(0.181 * 0.90)
TUVR	13338	EPPV	0.295 – 0.385 μ m	RICE2		(0.181 * 0.85)

* Serial numbers are: 26335, 26347, 26530, 27639, but not matched to sites.

The precision for the radiation data was set to 2%, 1% , and 0.5% of response for TUVR, 8-48, and PSP sensors, respectively. These values are based on manufacturer specifications for linearity. Those precision values are consistent with the scatter about the relationships between sensors. The manufacturer specifications for deviation from cosine law dependence range from 1% to 3% depending sensor up to about zenith angles of 70 degrees. However, significant deviations beyond these limits occur in our data with changes in zenith and azimuth angle. These range from a few percent to as much as 25%, depending on the sensor and the irradiance level chosen for normalization. Any data analysis that attempts to work with differences or ratios of irradiance levels will first require careful study of collocated data, and selection of normalization methods appropriate to the analysis at hand.

Summary of Results

Figure 3-37 and 3-38 show the radiometric measurements made at Mt. Wilson and CE-CERT, respectively, for the IOP periods of SCOS97-NARSTO. On August 22, the data indicate scattered clouds at both sites. The Riverside site also shows scattered clouds on September 5.

Figure 3-37. Total Solar Radiation (TSR), UV Solar (UVS), and Diffuse Solar Radiation (DIFSR) at Mt. Wilson for SCOS97-NARSTO IOP Periods.

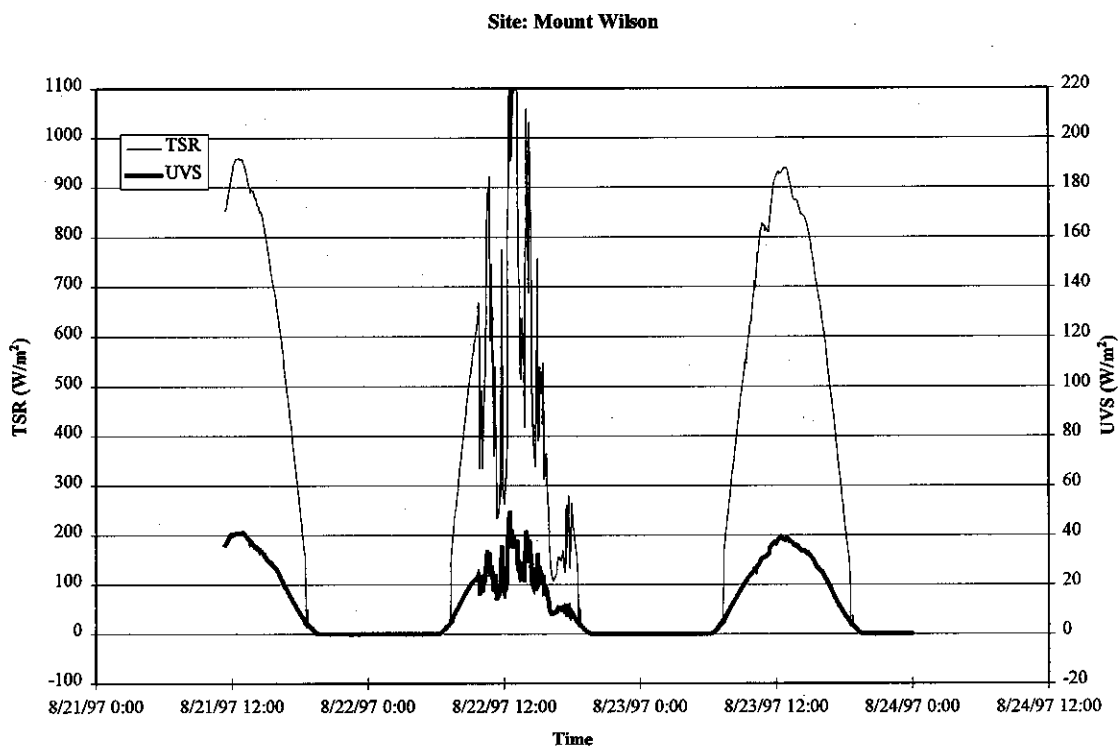
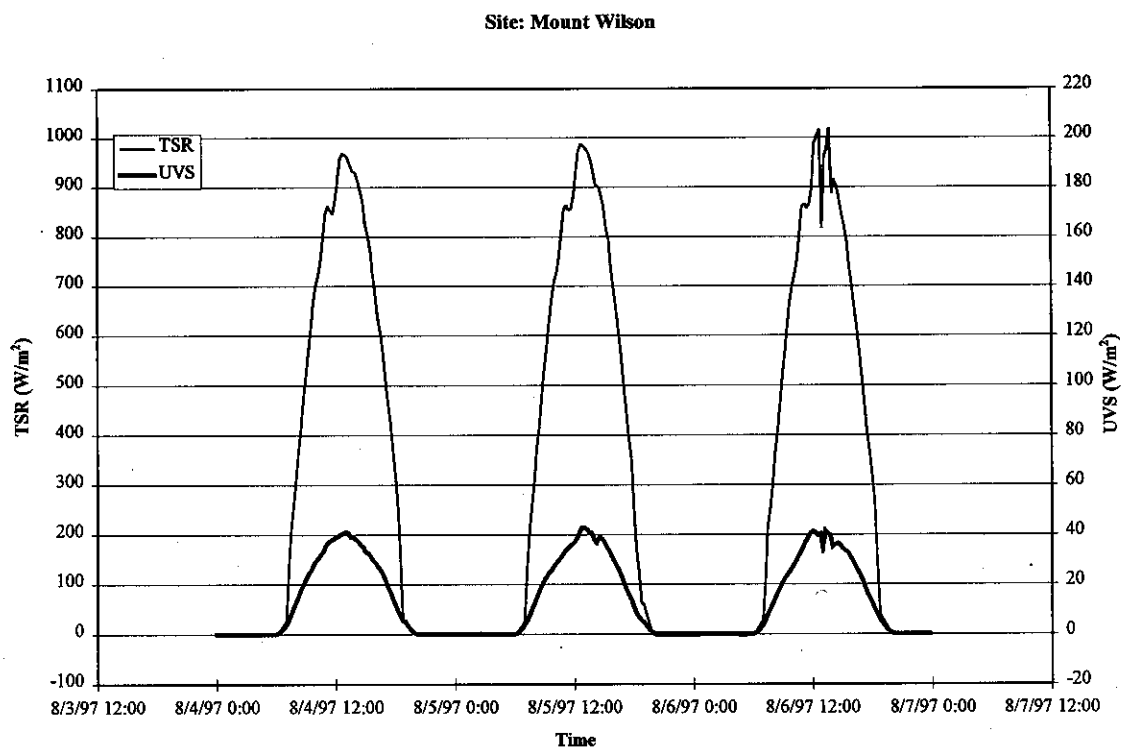


Figure 3-37, continued.

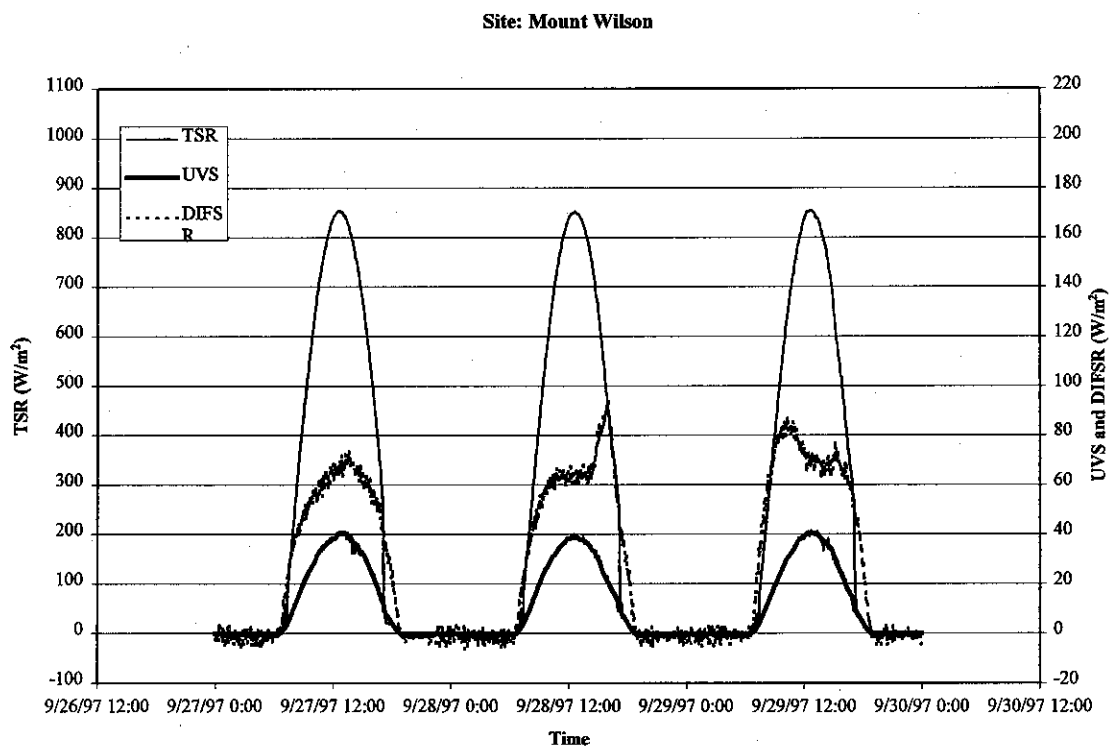
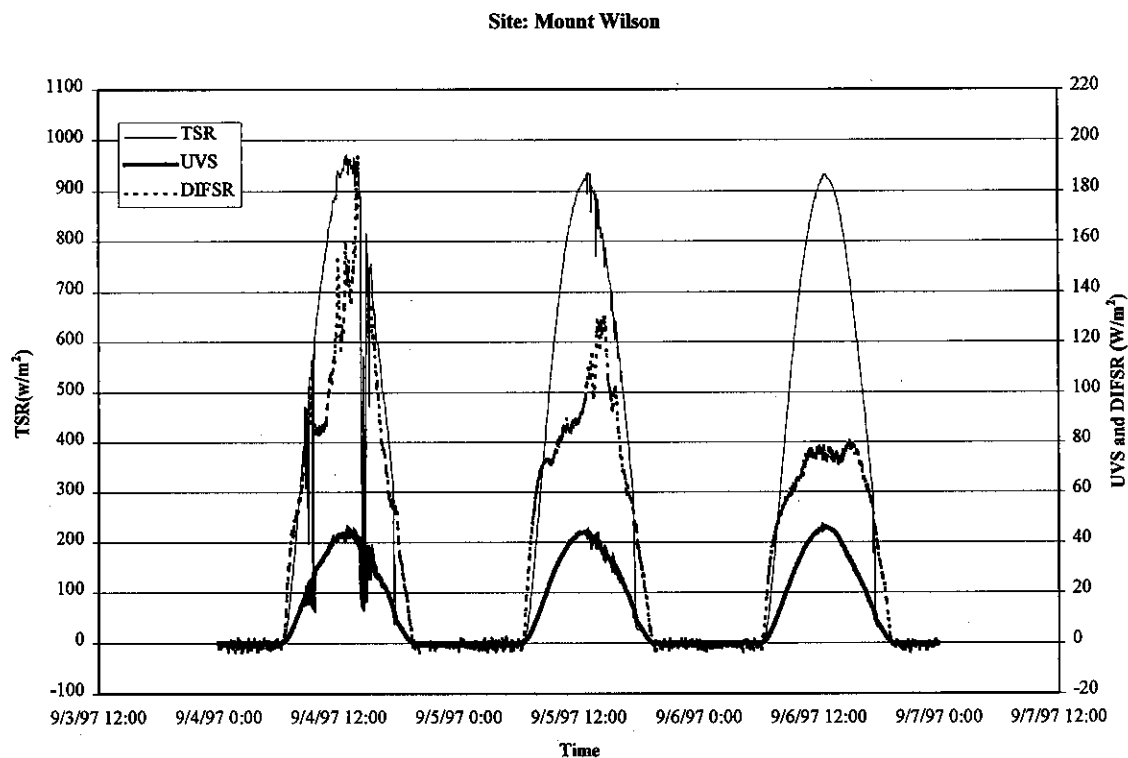


Figure 3-37, continued.

Site: Mount Wilson

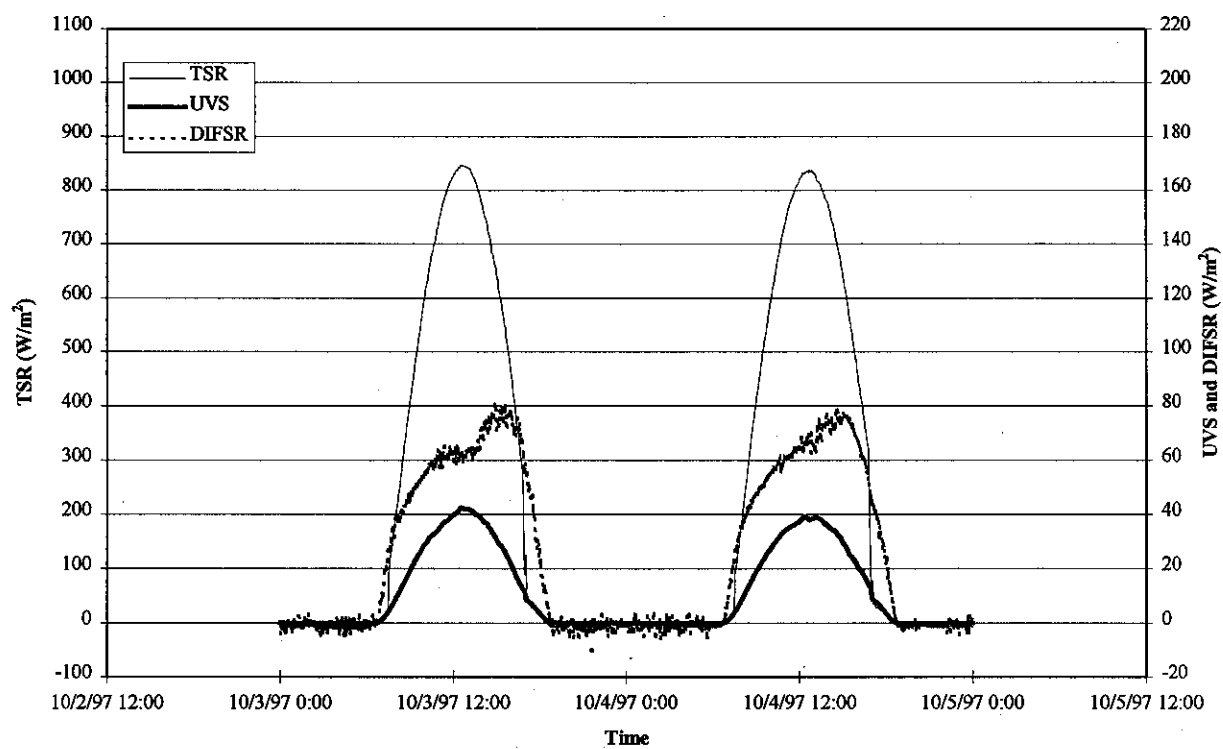


Figure 3-38. Total Solar Radiation (TSR), UV Solar (UVS), and Diffuse Solar Radiation (DIFSR) at CE-CERT in Riverside, CA, for SCOS97-NARSTO IOP Periods.

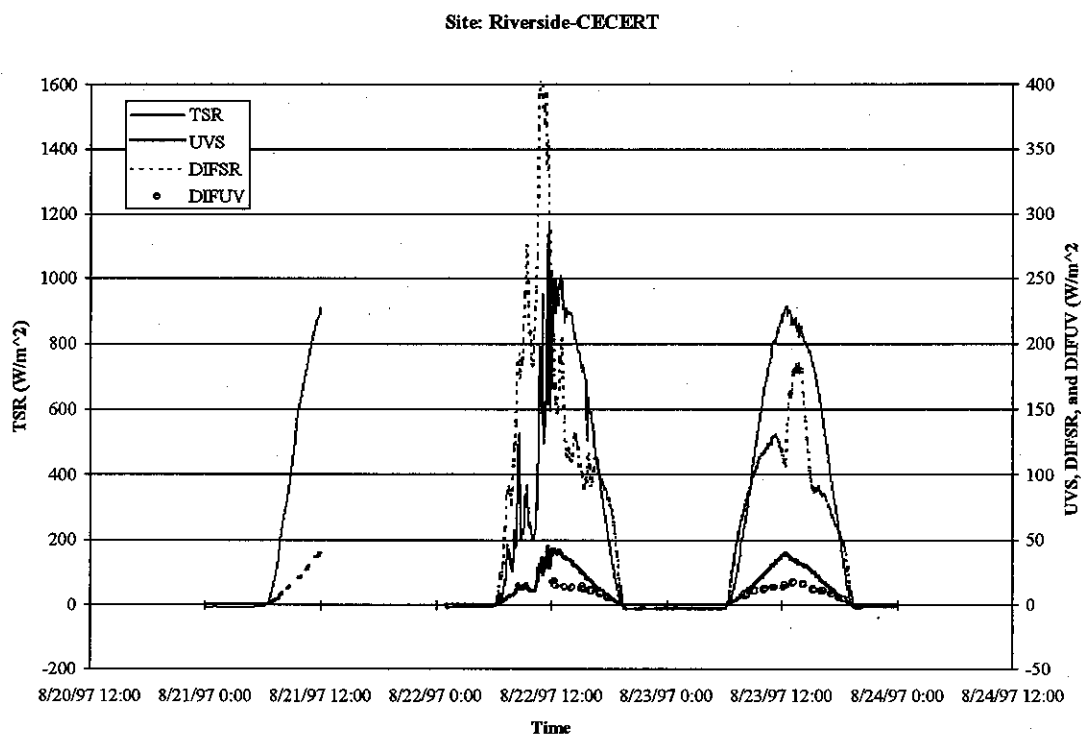
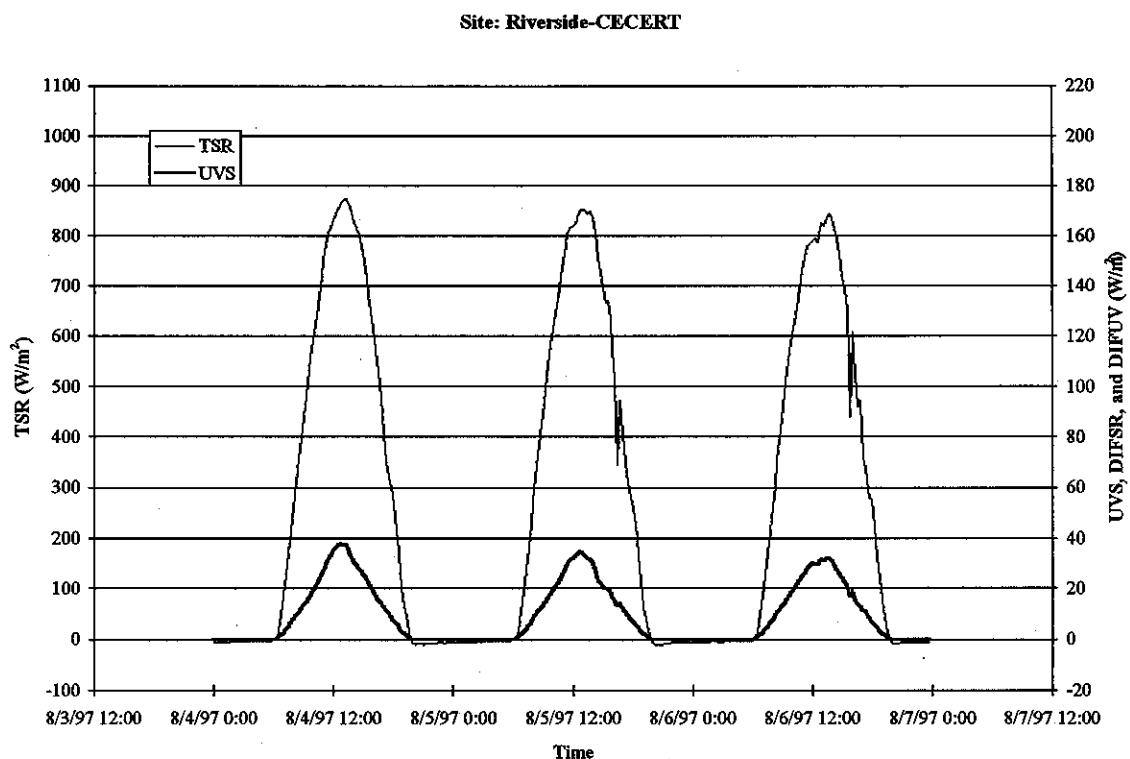
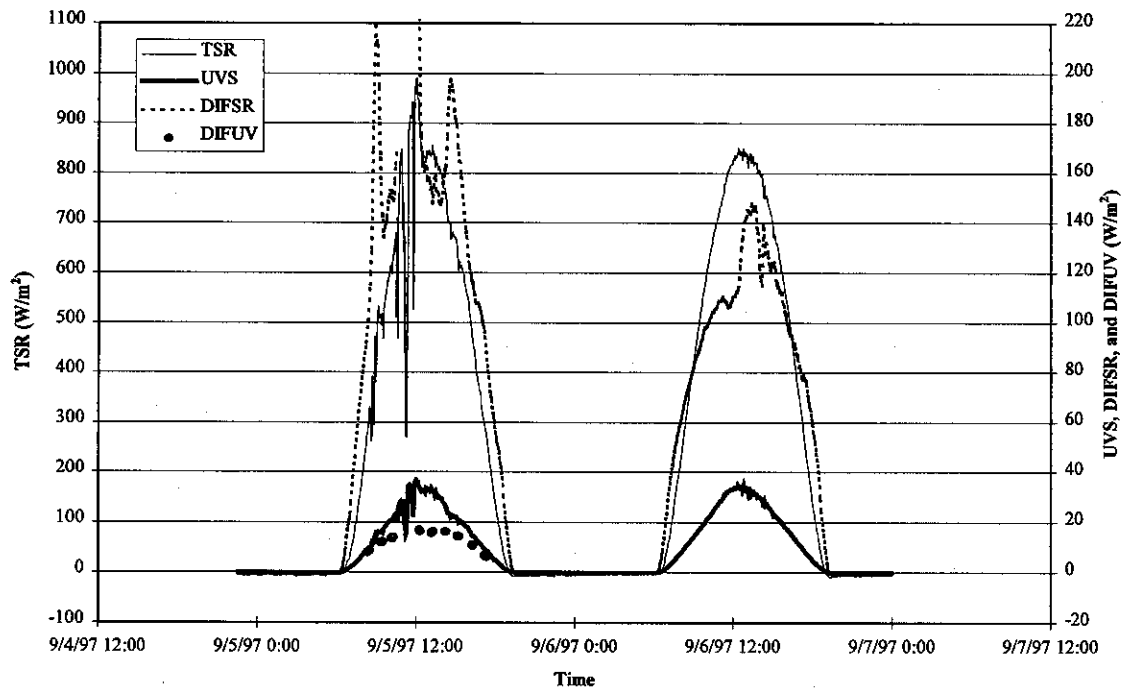


Figure 3-38, continued.

Site: Riverside-CECERT



Site: Riverside-CECERT

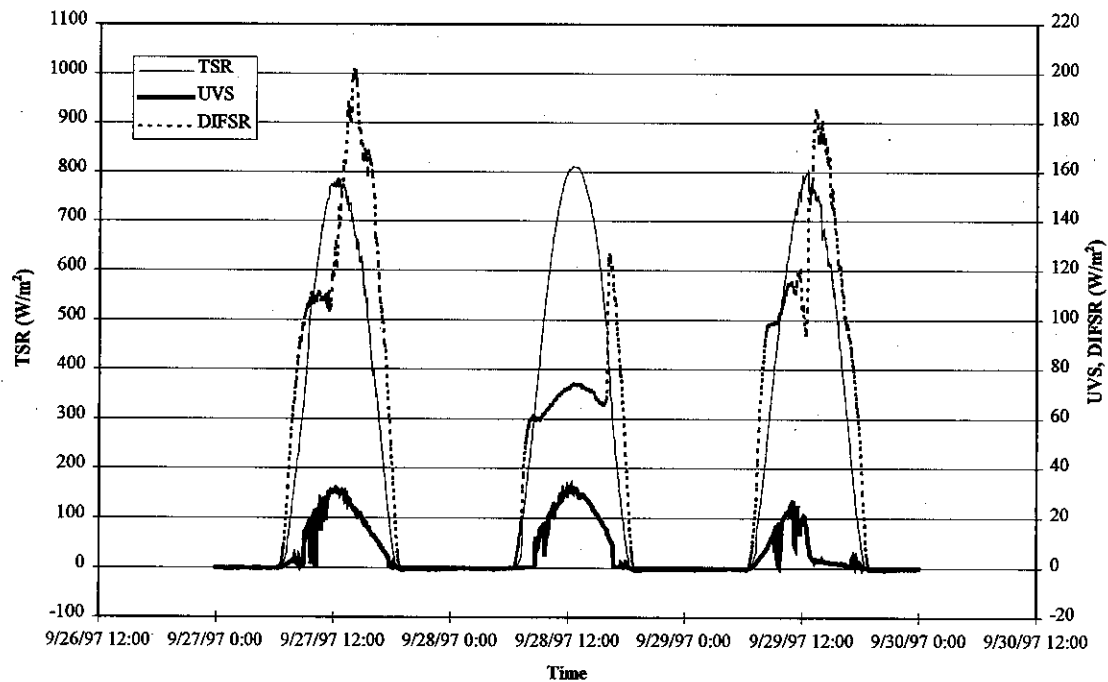
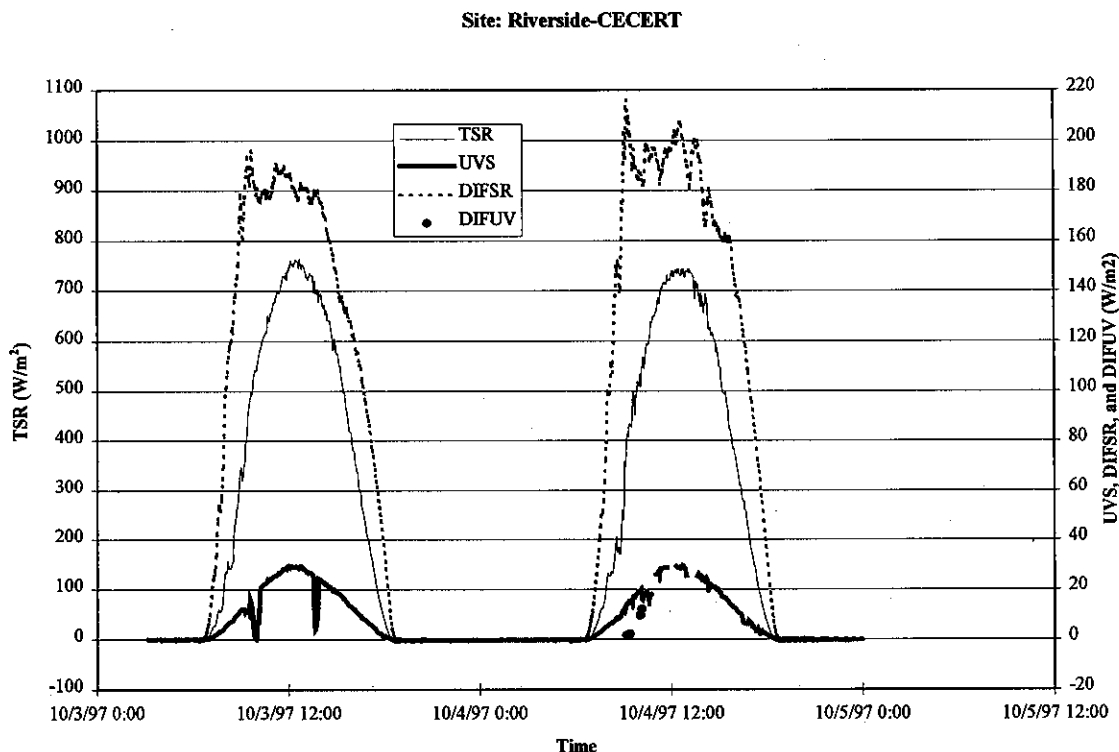


Figure 3-38, continued.

3.2.2 Wavelength Selective Instruments

The LICOR was the only wavelength-selective radiometer operated by CE-CERT. Measurements were taken during the two radiation intensives and as time permitted during the SCOS97-NARSTO IOP and Aerosol Intensive days.

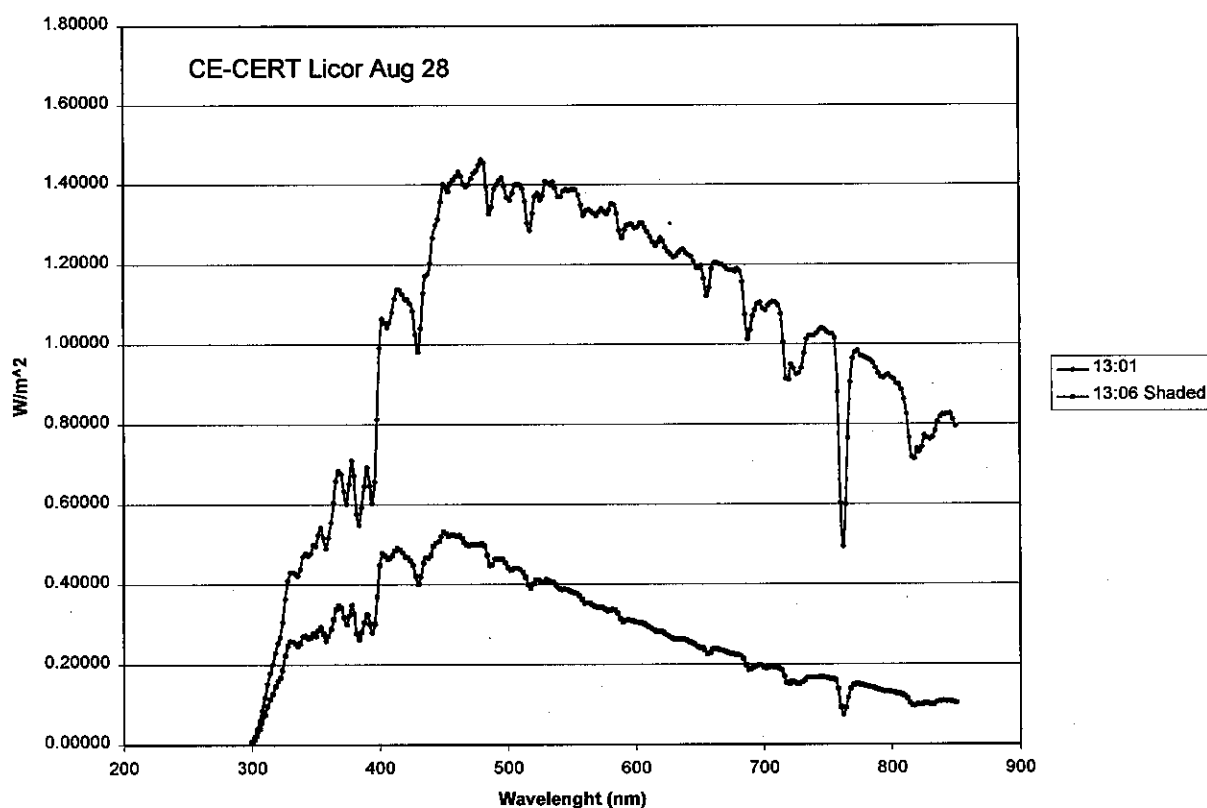
Summary of Data Validation for LICOR

Spectra were collected a pair at a time: one shaded and one unshaded within about five minutes of each other. Each pair was plotted together, one pair at a time. The plots were examined to verify that the shaded versus unshaded status for each spectrum was properly identified, to verify that each spectrum looked typical of normal daylight spectra, and to assure that dates and times for each spectra were correctly identified. Incorrect identifications such as reversal of shaded versus unshaded, or use of PST versus PDT times, were corrected. Most spectra were visually very similar. Spectra that looked atypical in their entirety were marked suspect. These were few and mainly attributable to clouds; all data points in such spectra were marked SUSC. A very few spectra had short sections of wavelength range that looked atypical. The cause for these anomalies could not be determined, but may have been caused by brief interferences such as passing clouds or shadows that occurred during the course of a spectral scan which took a couple of minutes to complete. In these cases, individual data points were marked SUS.

Summary of Results of LICOR

Figure 3-39 shows a typical plot of total and diffuse spectral data collected near noon on a clear day.

Figure 3-39. A Typical Shaded and Unshaded Solar Spectral Intensity Determined by the LICOR on August 28, 1997.



3.2.3 NO₂ Actinometry

Actinometry data were collected on various IOP days extending from June 29 through November 1. Staff from the CE-CERT Atmospheric Processes Lab operated the k_1 actinometer manually when they were available. Data, therefore, are available for only some of the IOP periods.

Summary of Data Validation

For each IOP day we reviewed diurnal plots of k_1 data. These typically follow a smooth arc, roughly proportional to the cosine of solar zenith angle. When irregular data were observed, we checked the raw NO, NO₂, and NO_x values, checked the keypunched data against the written logbooks for data transcription errors, checked the logbooks for problems noted, and checked the available continuous solar radiation data for evidence of clouds. Transcription errors were corrected, data having noted instrument problems were marked as invalid, initial dark values inconsistent with surrounding dark values were replaced with consistent ones. Data for times when the continuous radiation data indicated clouds were commented on, but remained marked as valid. Irregular data for which continuous radiation data indicated no clouds or for which continuous data were not available were marked as suspect.

The actinometer is operated on a high range to measure initial NO₂, but the amount of NO produced is relatively small. During the period from September 9 through October 4, the data were manually recorded from a front panel meter with very poor resolution. The resulting k_1 calculations during this period are very poor. Data from this period that showed a diurnal pattern

were marked suspect; and data that were extremely irregular were marked invalid. Precision was estimated at $\pm 10\%$ for the valid data, and as the larger of $\pm 10\%$ or 0.1 min^{-1} for the suspect data.

Summary of Results

Figure 3-40 summarizes the k_1 data obtained at the CE-CERT roof location of those IOP periods during which the actinometer was operated.

Figure 3-40. Values of k_1 Determined on the CE-CERT Roof for SCOS97-NARSTO IOP Periods.

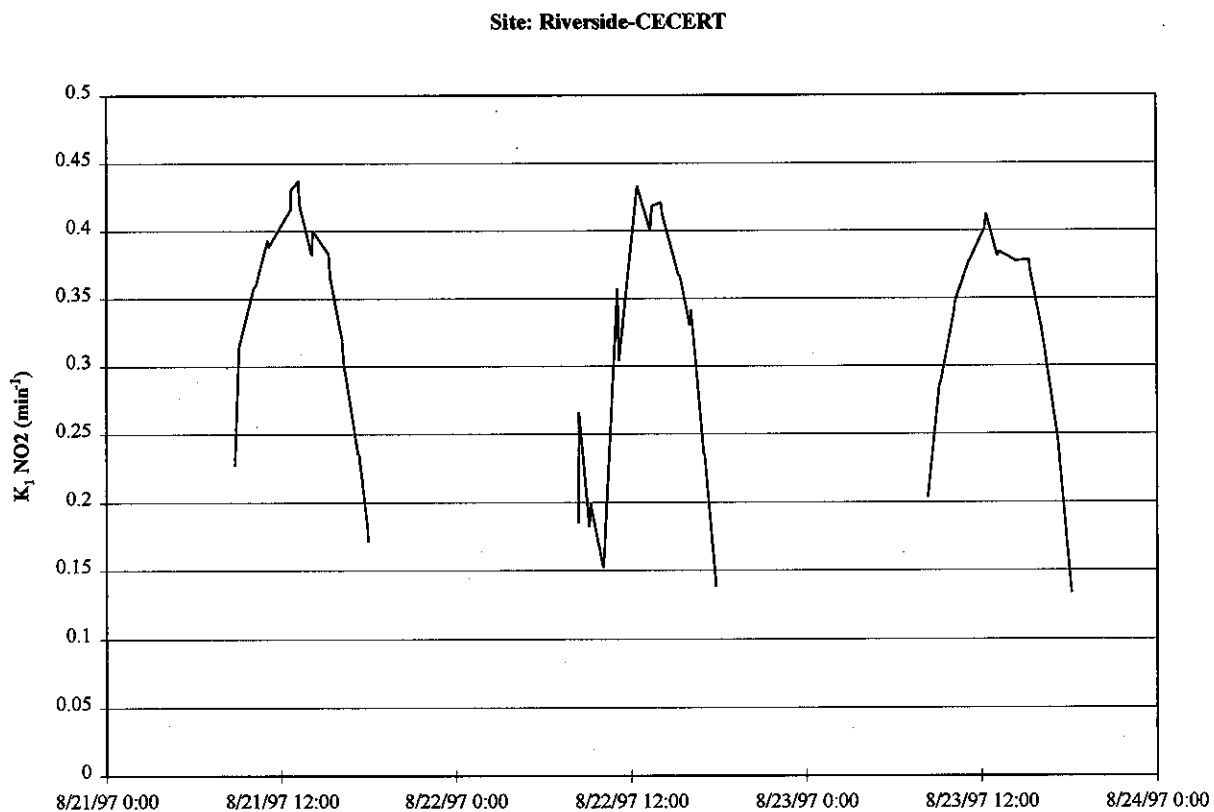
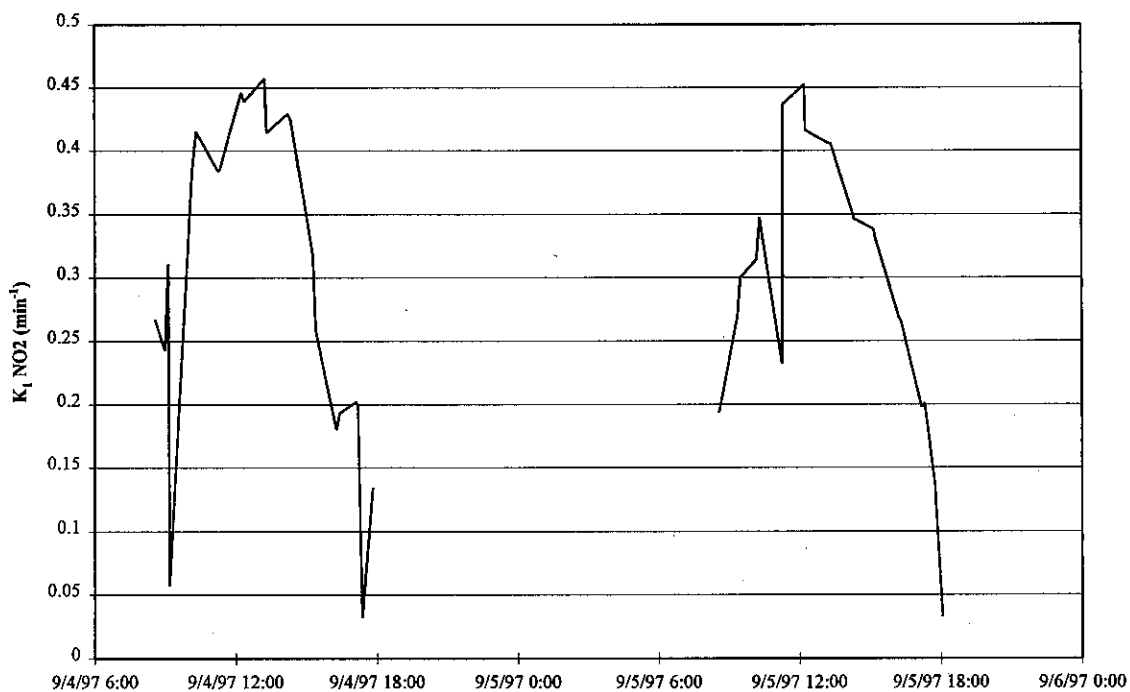
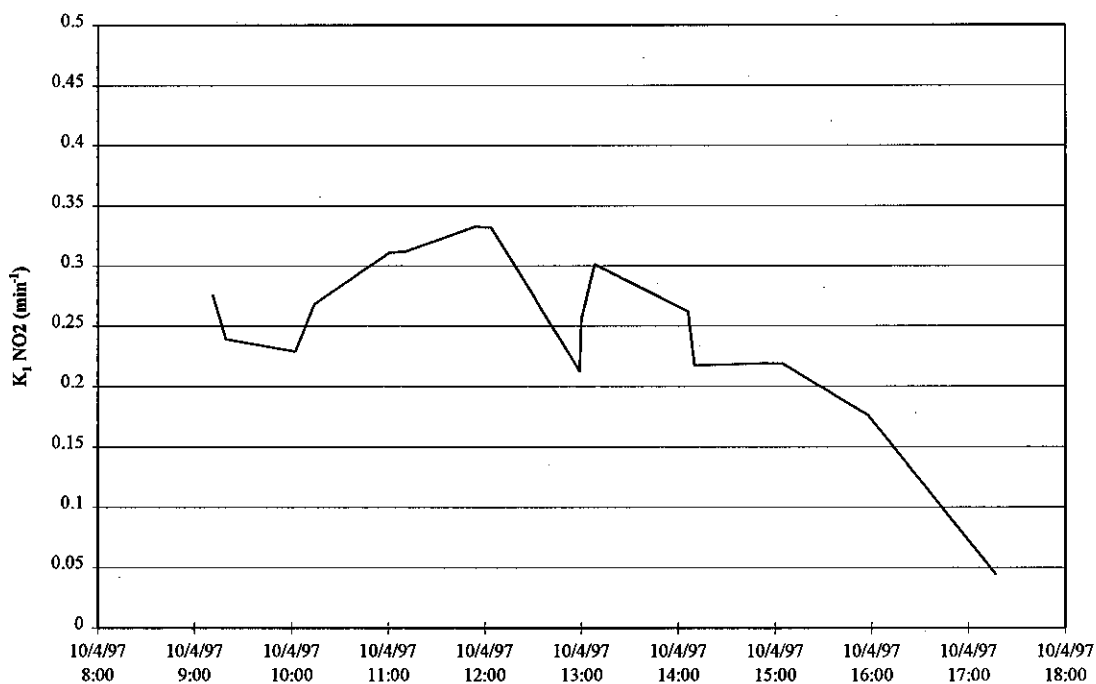


Figure 3-40, continued.**Site: Riverside-CECERT****Site: Riverside-CECERT**

3.2.4 UV Aethalometer (Black Carbon)

The instrument was operated continuously during the SCOS97-NARSTO measurement period except for a one-week period in August, when it broke and was sent back to the manufacturer for repairs.

Summary of Data Validation

All data were obtained from one UV aethalometer, but it was delivered in three different versions.

CEPRDmC1_RICE_Aethel_1_970804.csv contains analog data recorded by a data logger having time resolutions from 3 to 15 minutes at various times.

CEPRDmC1_RICE_Aethel_2_970804.csv contains digital data recorded by the aethalometer directly to daily disk files, having time resolutions from 5 minutes.

CEPRDmC1_RICE_Aethel_3_970804.zip contains the raw digital data files and accompanying digital summary/QC files recorded daily by the aethalometer directly to disk.

For files

CEPRDmC1_RICE_Aethel_1_970804.csv

CEPRDmC1_RICE_Aethel_2_970804.csv

Units are micrograms/m³, and all times are PDT.

In files

CEPRDmC1_RICE_Aethel_3_970804.zip the far right column is aerosol black carbon, the units are nanograms/m³ and all times are PST.

Neither

CEPRDmC1_RICE_Aethel_1_970804.csv

CEPRDmC1_RICE_Aethel_2_970804.csv

is complete. Both sets together provide more complete coverage than either set alone. They were not combined because there are overlapping time periods having different time resolutions.

The analog data were screened to remove noise spikes (single data points having zero or very high concentrations). Periods when the aethalometer appeared noisy or unusual were marked suspect in the CE-CERT QC code and suspect in the SCOS97-NARSTO QC code. The digital data included many fewer noise spikes and were generally smoother than the analog data. This may have been due to problems with the analog output or to screening built into the aethalometer recording software. We screened the digital data and identified periods when the data appeared noisy or suspicious. Suspect data were marked suspect in the CE-CERT QC code, but were marked valid in the SCOS97-NARSTO QC code. Although these periods were deemed suspicious enough to warrant closer examination, there was insufficient information to validate or invalidate the data. The data, therefore, should be considered valid.

The daily data files provide uncertainty information derived from lamp intensity fluctuations. These ranges from less than 1% up to a few percent from day to day depending on time and ambient concentration. In addition, flow rate uncertainties were estimated to be on the order of 2%. For the SCOS97-NARSTO database, we estimated precision a 3% of ambient concentration. This estimate is generally conservative, but may be exceeded from time to time. For more detail on a given day, consult the individual summary/QC data files for that day.

Summary of Results

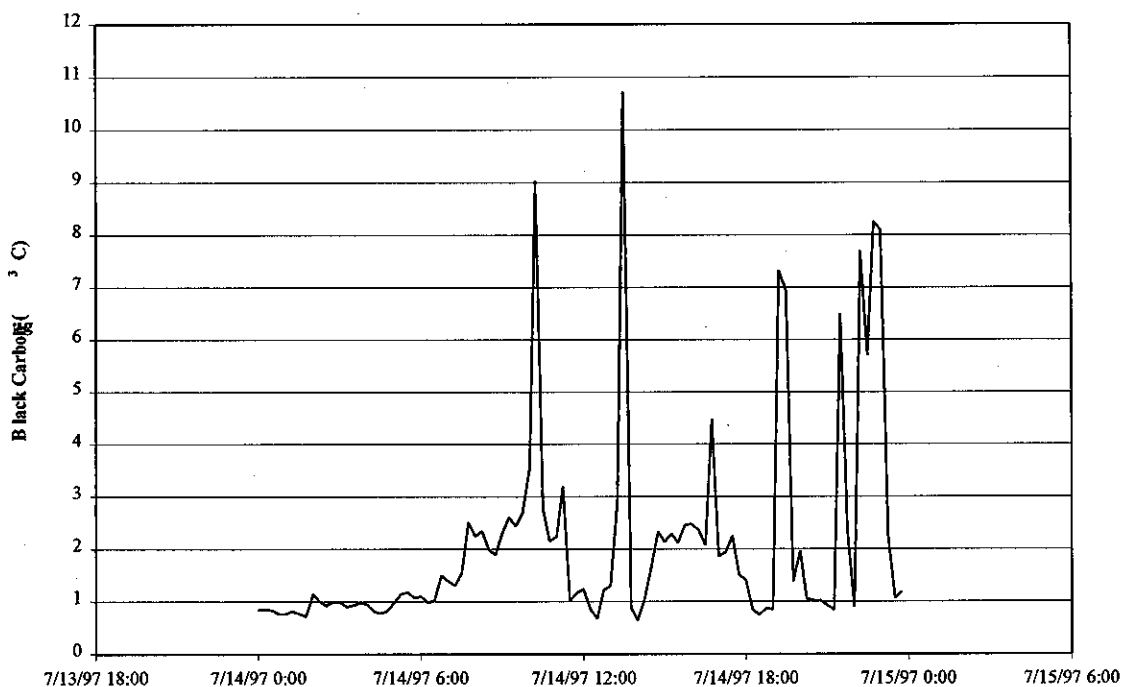
Figure 3-41 summarizes the absorption measurements made for the SCOS97-NARSTO IOP periods. The data are presented as units of black carbon. There was significant variability in the data, with peak concentrations generally in the morning. This would be indicative of local mobile sources. Diesel locomotives may also have caused some of the concentration spikes from train tracks approximately 200 meters to the east. These tracks generally pass only a few trains per day, but sometimes they park nearby and idle for long periods of time.

3.2.5 Light Scattering

An MRI model 1597 integrating nephelometer was operated at CE-CERT in Riverside. The instrument was housed in an air-conditioned trailer, with a 1 m sampling line to minimize temperature changes between outdoors and indoors. Freon 12 was used to calibrate the response. Zero and span checks were performed before, during or after IOPs. Data initially were recorded on a strip chart alone; after September 3, 1997, and until September 25, data also were recorded by the Portland State University research group using a data acquisition computer. The chart recorder had a wide dead band ($\pm 2\%$ of scale) and did not keep consistent time (± 1 hr/day). Hourly averages were manually determined from the chart only for IOP days; for other days the chart and instrument were not regularly maintained and the data were missing, uncertain with respect to time, and suspect with respect to instrument zero. After September 4, data were obtained from the PSU data system, also only for IOP days since routine zero/spans were only available for these periods would be suspect. Only valid data were submitted.

Figure 3-41. Concentration of Black Carbon on the CE-CERT Roof for the SCOS97-NARSTO IOP Periods.

Site: Riverside-CECERT



Site: Riverside-CECERT

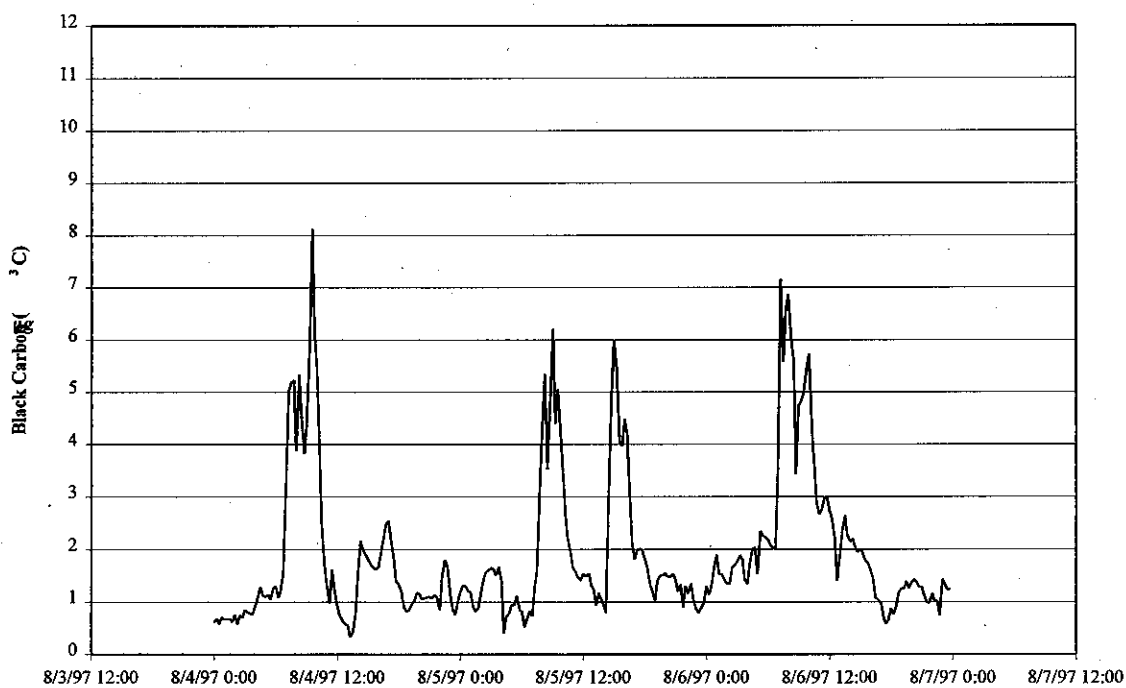
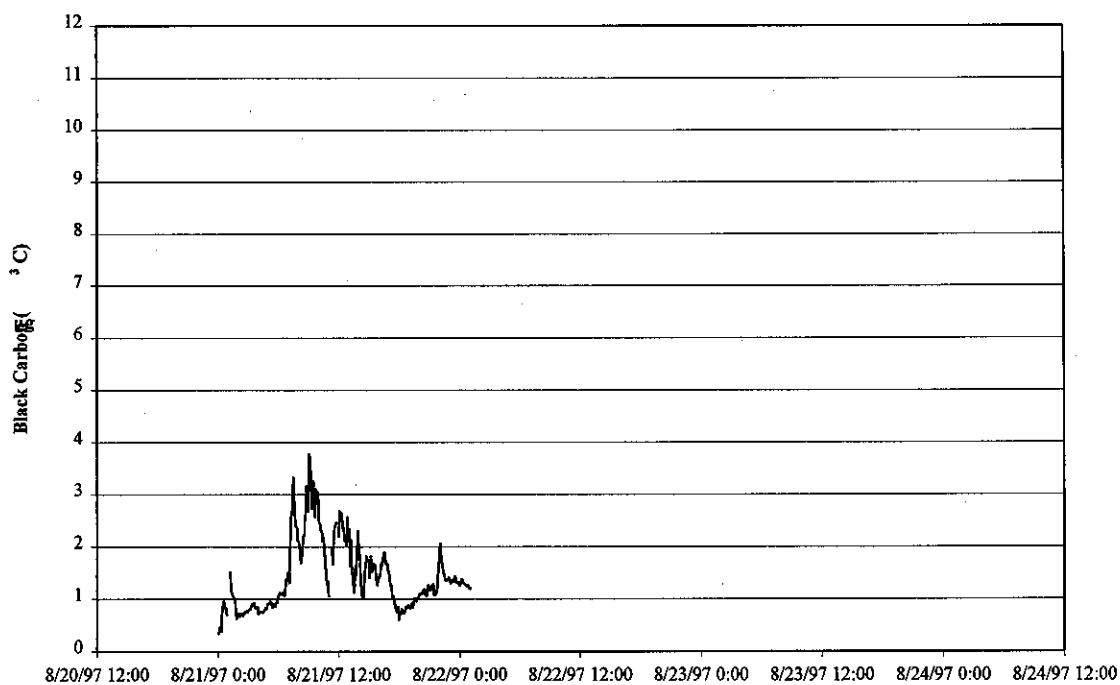


Figure 3-41, continued.

Site: Riverside-CECERT



Site: Riverside-CECERT

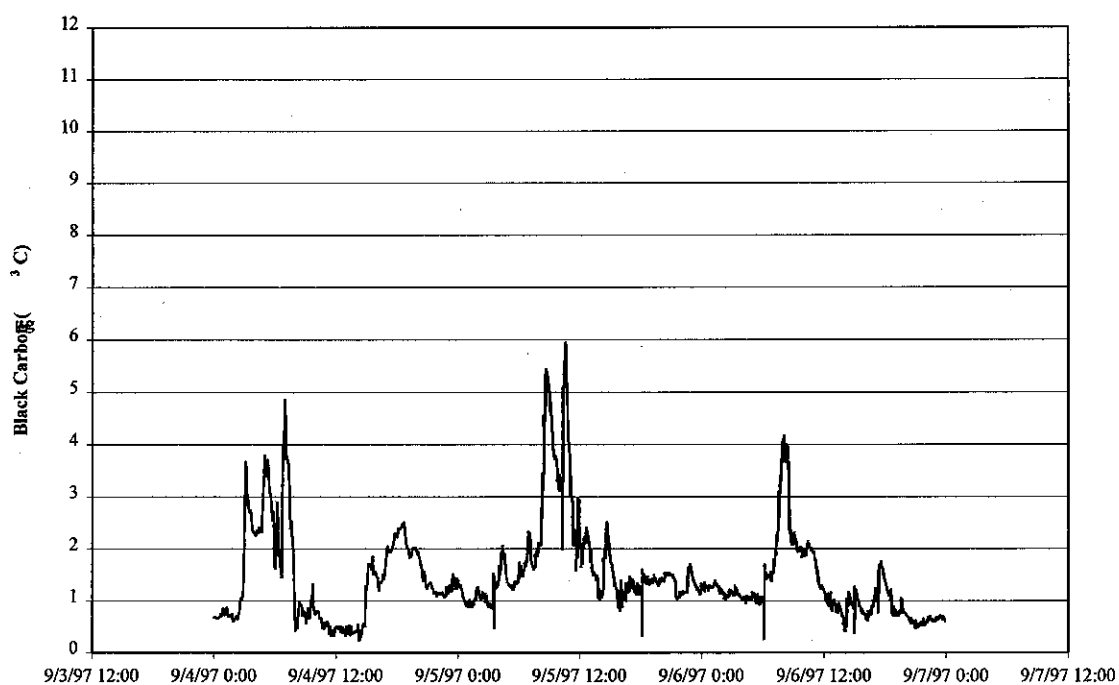
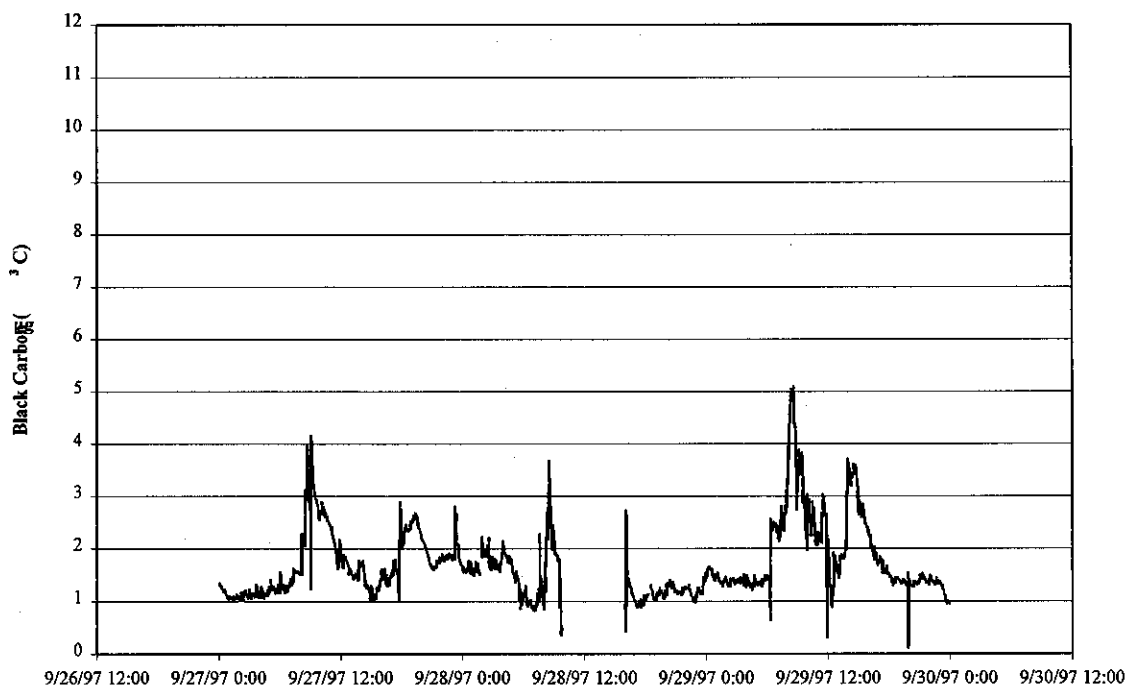
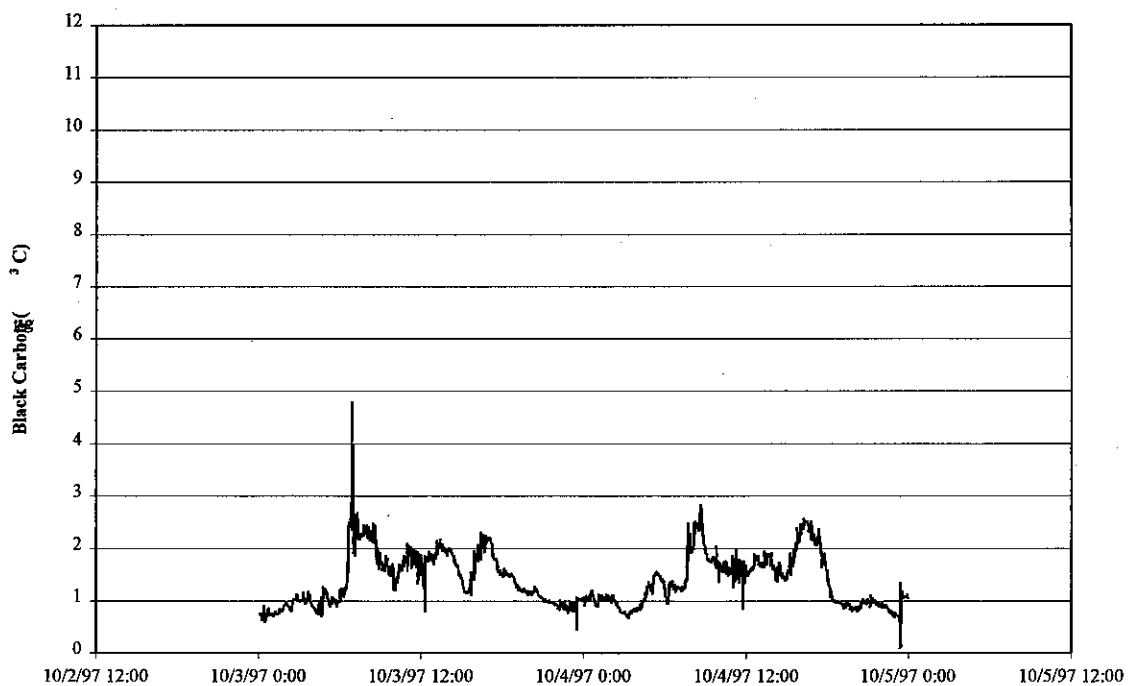


Figure 3-41, continued.

Site: Riverside-CECERT



Site: Riverside-CECERT



An NGN-2 integrating nephelometer was installed at the Mt. Wilson site. The instrument automatically measured its span at startup using Freon 134a and performed zero air checks approximately every 162 minutes. Analog data from the NGN-2 were recorded by the station data logger. Raw digital data and diagnostic information also were recorded by the NGN-2 to disk on a computer attached to the serial port of the NGN-2. The nephelometer was not operational until September 12, 1997. However, due to lamp problems, the September 28-29 and the October 3-4 intensives were missed. The only intensives for which we had data are the October 18 and the October 30-November 1 periods. Data from the data logger and the computer disk files agreed after correction for a scale factor of 2.0. Data for the archive were generated from the NGN-2 disk files because these had better time resolution (2 minutes). The span check applicable during this time period occurred at startup on October 17. Zero checks (Rayleigh scattering) occurred on schedule. They were nearly constant during both intensives. The single span check and a nominal average zero value were used to convert the data to particle scattering as follows:

$$\text{Bsp} = (\text{Total Response} - \text{Rayleigh Response}) * (71.46 - 10.02) / (105 - 39)$$

where

Freon 134a response = 105

Rayleigh Response = 39

Freon 134a Scattering = 71.46 MM⁻¹

Rayleigh Scattering = 10.02 MM⁻¹

Data look reasonable during the October 18 episode. However, during the October 30-November 1 intensive, ambient particle scattering often falls well below the Rayleigh scattering measured during zero air checks, indicating some problem with instrument operation. For this reason all of the data from the last intensive are marked suspect, and are given larger uncertainty.

A RAC paper tape sampler was also installed at Mt. Wilson. The instrument burned out several bulbs during the SCOS97-NARSTO monitoring period. Since communication through the phone line at the site was often problematic, this caused a significant amount of lost data. In addition, the instrument exhibited substantial drift. The RAC draws air through a paper filter tape for two hours then advances the filter tape to a new position for a new sample. The instrument continuously measures light intensity transmitted through the filter during the two-hour sample period. If light absorbing aerosol is being collected by the filter, then the output will be a saw-tooth pattern in which the transmitted light starts out high, gradually decreases during the sample period, and returns to its starting value when the filter tape is advanced. Data reduction entails establishing a baseline for the transmitted light intensity of a clean newly advanced filter; dividing sample light intensity by clean light intensity to obtain transmittance; calculating absorbance from transmittance; and finally dividing absorbance by sampled air volume to obtain COH, which is an indicator of absorbance per cubic meter of air.

Unfortunately, the instrumental record of transmitted light intensity at Mt. Wilson does not show a saw-tooth pattern. Instead the data record shows that the transmitted light intensity often drifted upward instead of downward during the two-hour sampling period, and that a filter advance often results in a drop in transmitted light rather than an increase to clean initial levels. The data show a pattern of step changes in the clean filter baseline caused by variability in clean filter tape transmittance, superimposed on a strong diurnal drift probably influenced by station temperature. The RAC sampler was not operated until the station at Mt. Wilson was moved to its second location on August 26, where station temperature was not controlled. Reducing this data would be a very labor-intensive effort requiring numerous assumptions and a good measure of creativity. The quality of the result would be poor. Instead, all of the raw transmitted light intensity data were marked suspect and submitted to the archive.

Summary of Results

Figure 3-42 shows the light scattering measurements obtained at CE-CERT during SCOS97-NARSTO IOP periods.

Figure 3-42. Coefficient of Light Scattering (bsp) at CE-CERT for the SCOS97-NARSTO IOP Periods.

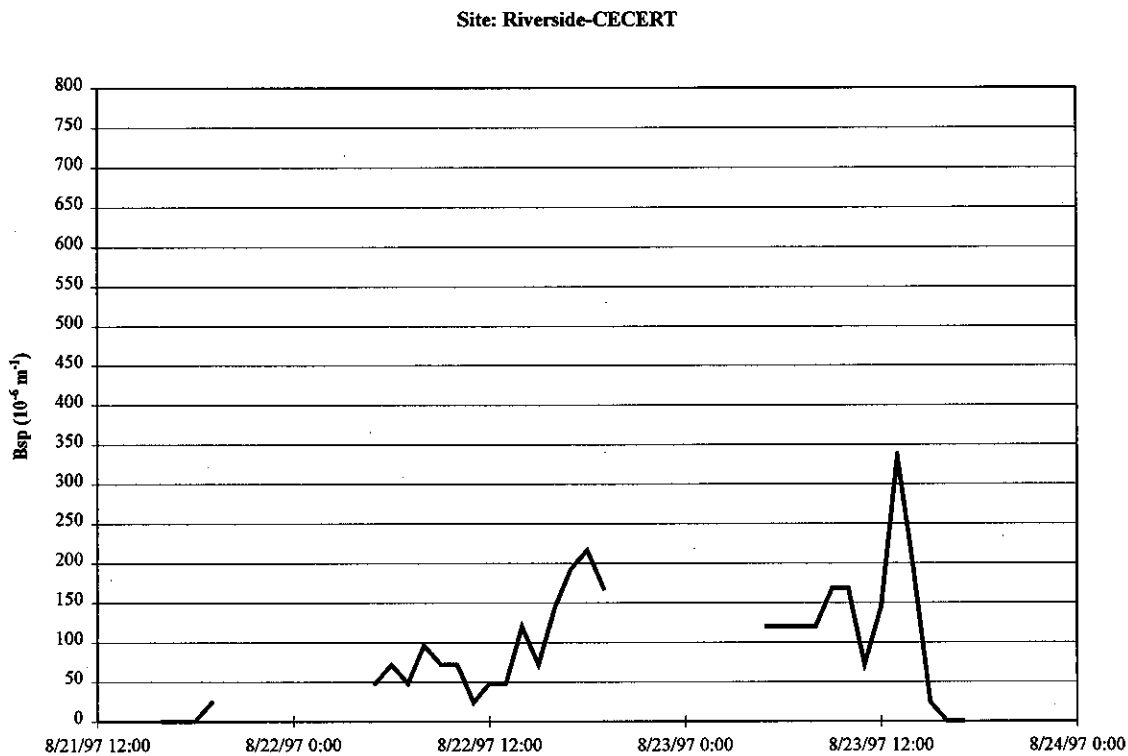
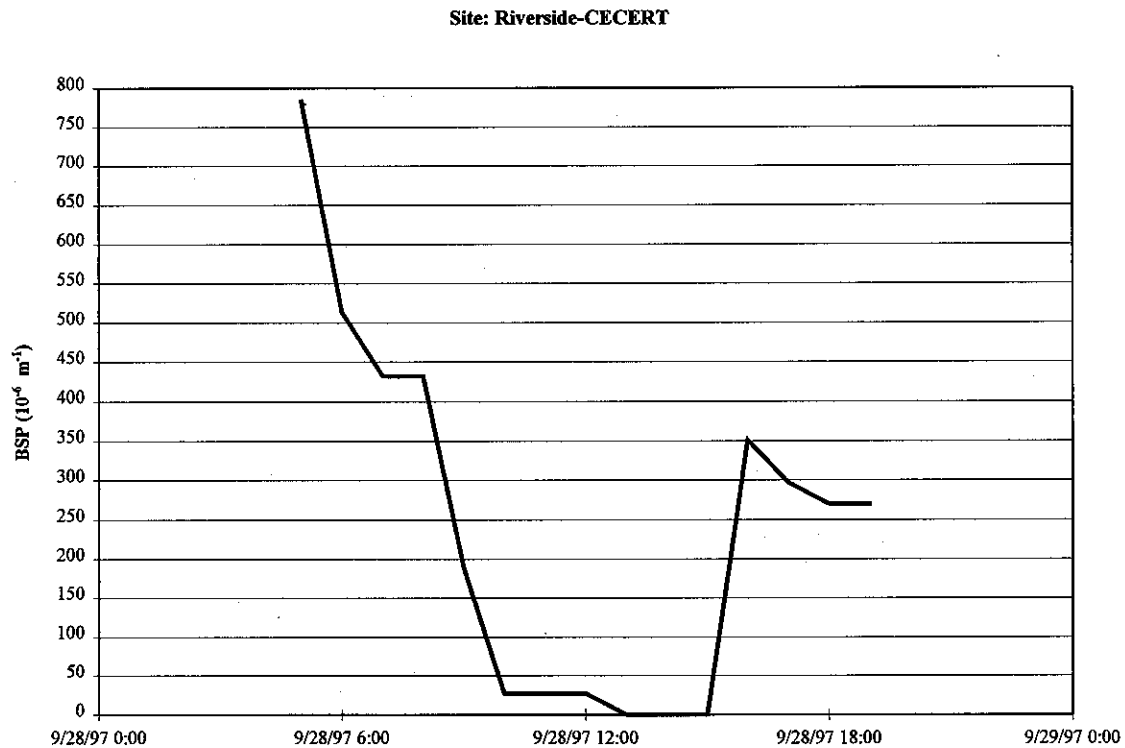
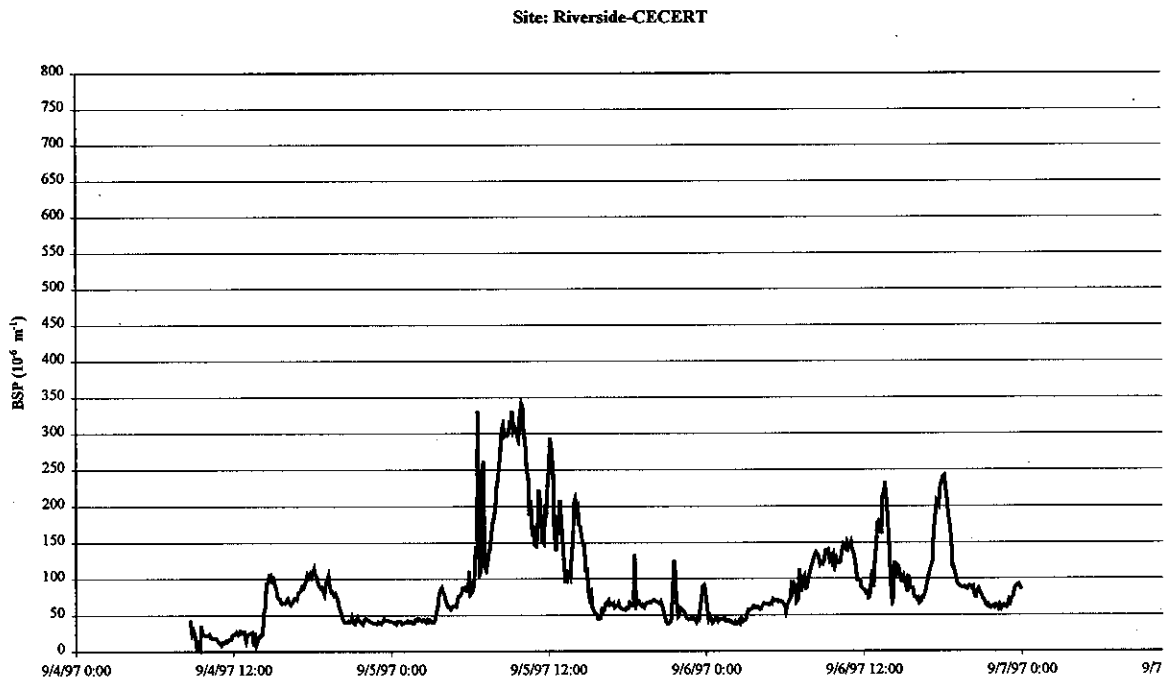


Figure 3-42, continued.



3.3 Other Support Activities

3.3.1 Ozone Monitoring

- San Nicolas Island

Two ozone analyzers were operated at San Nicolas Island to provide redundancy in case of instrument failure. NO_x , NO , and shelter temperature also were recorded at this site. The probes were located 3 m above the asphalt surface that surrounded the shelter that was approximately 10 m above sea level. We reviewed time series plots of all five parameters, scatter plots of ozone from analyzer 1 versus analyzer 2, station logs, and calibration data. Review showed that response for the backup ozone analyzer was low at the end of September and beginning of October due to a kinked sample line. The primary analyzer was not affected. Other than during this period, the two analyzers agreed with each other very closely, to within a precision of better than 2 ppb. Calibration checks were performed on July 29, 1997, and September 9, 1997. The slopes and intercepts from these calibrations were consistent with each other, and the average results were applied. Precision was set to the larger of 5 ppb or 5%. Shelter temperature at San Nicolas Island was not maintained. Ozone data having shelter temperatures not in the range between 20 and 30 °C were flagged as suspect. These limits were rarely exceeded, being occasionally low by 1 to 3 degrees. The ozone data collected during these times are still of good quality, but they were flagged for conformance with typical limits used in regulatory monitoring. Consideration could be given to making a temperature correction during these time periods. Given the low ozone levels, this is not worthwhile.

- ARCO Tower

The ozone analyzer at ARCO Tower was operated in a penthouse approximately 180 m above ground level. The probe was located approximately 15 cm from the louvered wall on the northwest side of the building. This placement was necessary so as not to interfere with the window washing lift. Because of the louvers, the probe was located in a moving air stream from the prevailing on-shore flow from the west in the daytime. The penthouse did not have temperature control, and the temperature was not monitored. The site was approved because the ARB felt its elevated location outweighed the poor environmental conditions. The analyzer at ARCO failed on August 23, 1997, and was replaced on August 25. There is one calibration prior to the replacement, August 13, and three calibrations were performed after the replacement: September 9, September 23, and October 22. The three calibrations after the replacement showed a trend a decreasing sensitivity and decreasing offset. The average of the first two calibrations was applied to the data after the analyzer replacement because it was felt that these two calibrations better represented performance at the times of IOPs.

After applying the slope and offset applicable to the data prior to the analyzer replacement, these data showed fairly stable behavior with nighttime ozone concentrations often falling below 5 ppb. The diurnal pattern is often double peaked, often having a broad peak extending from before noon to near midnight, superimposed on a sharp dip that occurs in the early evening. This may reflect depression by NO_x emissions during the evening rush hour, or perhaps changes in air mass as wind direction changes during the course of the afternoon and evening.

After applying the slope and offset applicable to data after the analyzer replacement, the ozone concentrations no longer dropped to low levels at night. Corrected ambient concentrations at night generally fell only into the range of 10 to 15 ppb, despite the corrected responses to zero air being near or below zero. When compared with the previous period, the baseline formed by ambient nighttime concentrations appears to have shifted up by 10 ppb. This behavior is suspicious, but plausible due to the elevated location; it is supported by three zero checks. The

behavior before the replacement looks more natural, but is supported by only one zero check. Because we do not know which period is accurate, we marked the entire data set suspect. This data can still be used to identify diurnal changes, but conclusions about absolute concentration levels should be drawn with caution.

- Mt. Wilson

The ozone analyzer was operated at Mt. Wilson from June 19, 1997, through November 13, 1997. The probe was located on a pole above the roof approximately 3 m above the ground. The site was moved on August 26, 1997, and the probe was placed above a nearby chain link fence, approximately 3 m above the ground. The elevation of both sites was approximately 1700 m msl. Before the move, the analyzer was operated in a station with temperature maintained between 20 and 25 °C. After the move, the analyzer was operated in an uncontrolled shelter, with temperatures ranging roughly from 5 to 35 °C. Calibrations were performed on September 15, September 30, and October 22, 1997. All three of these calibrations showed that the station analyzer front panel display was in close agreement with the transfer standard, but the results from the data acquisition system (DAS) were not. The calibration data showed that after the move, the DAS values were about 1.66 times the front panel display values, with correspondingly larger intercepts. We do not know why the DAS response was so high, but time series plots of the raw DAS data showed a very large increase in response when the site was relocated. This probably occurred as the result of a DAS problem introduced by the move. We do not have calibration prior to the move. Based on time series plots, however, the DAS was probably functioning normally at that time. For data after the move we applied an average calibration of the DAS response versus transfer standard ozone. For data before the move, we assumed that the DAS was accurately tracking the front panel display, and we applied the September 15 calibration of front panel response versus transfer standard ozone. Results for both periods were reported in ppbV. The transfer standard ozone concentrations were calculated by adjusting the transfer standard front panel readout using the cell pressure and temperature corrections. This was also done at San Nicolas Island and ARCO tower, but the corrections were minor. At Mt. Wilson and Tehachapi, these corrections amount to 14%. In view of the problems with the DAS and the lack of calibration data before the move, we set the uncertainty to 20 ppb. This is meant to approximate a 1-sigma uncertainty of 10% at the high end and a large uncertainty in offset at the low end. These data are useful of observing diurnal patterns, but absolute values should be interpreted with caution.

- Tehachapi

Surface ozone was monitored in Tehachapi, CA, to support the SCOS97-NARSTO ozone measurement network. The site was located on Jameson Road just south of where the road bends from east-west to north-south. The altitude is approximately 1,100 m. The site was located immediately north of the north road at a well operated by Calaveras Cement Company. The north-south section of Jameson Road was unpaved at the time of installation, but grading was being done for laying asphalt paving. The traffic density was approximately one car per minute during the middle of the day. The paving was completed between site visits occurring on July 31 and August 27. The area is largely open desert or agricultural with some light manufacturing. An air-conditioned trailer was used as a monitoring shelter. The station was equipped with a Dasibi model 1003AH ozone analyzer, an RM Young model AQ wind direction and velocity sensor, and a Qualimetrics temperature and RH probe mounted in a non-aspirated sun shield. A Campbell CR10 data logger was used to collect data. Shelter temperature was also recorded.

At installation and tear-down, multi-point calibrations were performed using a transfer standard. Site checks were performed every two to three weeks. During these site checks the instrument flow rate and sample and control frequencies were checked. A transfer standard was used for

zero and span checks before and after the inlet filter was renewed. During the site check, the data logger was downloaded to a laptop PC and the data copied to a floppy disk. The data logger also recorded site temperature to determine whether analyzers were operated within the temperature range required for EPA equivalency with the reference method. Per the CE-CERT SOP, instrument gain controls were not adjusted; calibration factors were applied to the data in post processing.

The first ozone calibration check visit occurred on August 25, 1997. At this time, the analyzer was found to be malfunctioning. This analyzer was replaced on August 27. Therefore, there are no calibration checks for the first analyzer, but the audit results discussed below verify that the calibration was accurate prior to the analyzer failure. The remainder of the checks were for the second analyzer. Since the elevation-corrected responses were within 5% of the transfer standard response, the calibration checks were not used to adjust the data. A single response factor of 1.1469 was applied to all data from both analyzers. The precision was calculated as the larger of 5 ppb or 5%.

An audit was performed on August 4 by the ARB. Using an altitude correction factor 1.1469, the site ozone was 4% less than "true" ozone. At the time of the audit, there was no CE-CERT representative to give the altitude correction factor. The auditor used the instrument read-out rather than the data logger's altitude-corrected data. Since the instrument appeared to be outside the $\pm 10\%$ of true criterion, the site was reaudited on September 25. The analyzer had been replaced on August 27. The result of this audit, after correction for the altitude factor, was that the site analyzer was 2% higher than "true" ozone. Both analyzers therefore passed the audit criterion.

Tehachapi data for ozone, temperature, RH, wind speed, and wind direction were plotted as time series and reviewed visually. Extended periods during which the analyzer response did not follow reasonable diurnal patterns were judged to be due to analyzer malfunction, and those periods were marked as invalid. Sharp spikes and short-term deviations from expected diurnal patterns were flagged as suspect.

In addition to the flagging based on review of time series plots, two other sets of flags were applied, one based on wind speed and one based on shelter temperature. Wind direction data from Tehachapi were flagged as suspect when the wind speed was below 1 meter per second. Ozone data from Tehachapi were flagged as suspect when the shelter temperature was lower than 15 or higher than 25 degrees °C. The air conditioner became inoperative during periods of high ambient temperature that caused the circuit breaker to trip. This problem was resolved on August 27 by replacing the circuit breaker with one of greater amperage. Later in the study, the shelter temperature became cold at night because the shelter was not equipped with a heater.

The Dasibi ozone analyzer can operate correctly over a large temperature range; the manual specifies 0-50 °C. However it is a photometric absorption measurement based on Beer's Law, and thus has a response that is directly proportional to cell pressure and inversely proportional to absolute temperature (i.e., directly proportional to air density in the cell). The instruments that we employed were not corrected for fluctuations in cell temperature and pressure. A temperature fluctuation of ± 5 °C results in a corresponding response fluctuation of less than $\pm 2\%$, which is negligible. We flagged data outside a ± 5 °C range because the response shift caused by temperature starts to become large enough that it should be compensated for. We chose 20 °C as the center of the range because the instrument was calibrated near this temperature and because this range encompasses the large majority of the data. The data flags beyond this temperature range do not indicate analyzer malfunction, but only serve as a warning that the inverse response to temperature should be considered before using this data.

The Quality Assurance Handbook for Air Pollution Measurement Systems, Vol. II (EPA, 1994) suggests that shelter temperature be held between 20 and 30 °C. It also suggests that the temperature should fluctuate no more than ± 2 degrees C, which therefore implies that the mean shelter temperature should be set to a value between 22 and 28 degrees C. Due to air conditioning failure and lack of a heater, we were not able to conform to these suggestions. Because this is a research program, and not compliance monitoring, failure to meet the EPA suggested conditions does not invalidate the data. We extended the temperature range from ± 2 degrees °C to ± 5 degrees C and used a center temperature of 20 °C. The effect of these modifications is to increase the uncertainty associated with temperature fluctuations from 0.7% to 1.7%.

The 11% of ozone data flagged as suspect is almost entirely due to shelter temperature exceeding the range 15 to 25 °C. The 27% of ozone data flagged as invalid consists primarily of the three-week period prior to August 27, during which the analyzer was malfunctioning. The 11% of wind direction data flagged as suspect is due to wind speeds near or below the threshold for proper operation of the wind vane. If the low wind speed periods are considered "calm," then the meteorological data capture is 100%.

Precision for ozone was estimated as the larger of 5 ppb or 5%. Precisions for the meteorological equipment was estimated as follows:

Relative humidity	(RH)	10%
Temperature	(TMP)	0.5 C
Wind direction, unit vector average	(WDV)	5 deg
Wind speed, scalar average	(WSA)	0.2 m/s
Sigma theta	(SGT)	-99

Summary of Results

Figures 3-43 through 3-46 summarize the ozone measured during IOP periods at San Nicolas Island, the penthouse of the ARCO Tower, Mt. Wilson, and Tehachapi, respectively. With the exception of the IOPs in late September, the San Nicolas Island ozone concentrations are between 20 and 50 ppb with maxima in the later afternoon. This is consistent with a background site. ARCO Tower ozone ranged from zero to over 150 ppb with maxima in the early afternoon. This is consistent with an urban source location.

At Tehachapi the ozone concentrations follow a typical diurnal profile, peaking at 80-100 ppb during the daytime and reaching a minimum of 0-40 ppb at night. This is behavior expected from a rural location that may be subject to some scavenging from local traffic.

Figure 3-43. Ozone Concentrations at San Nicolas Island during SCOS97-NARSTO IOP Periods.

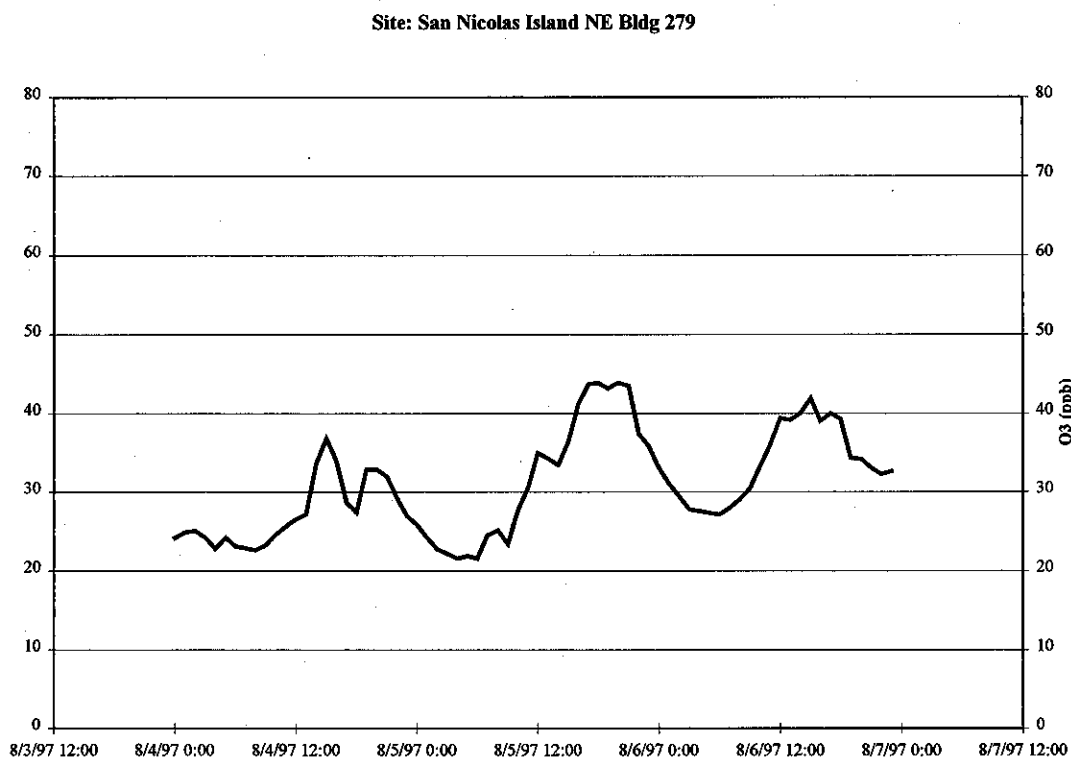


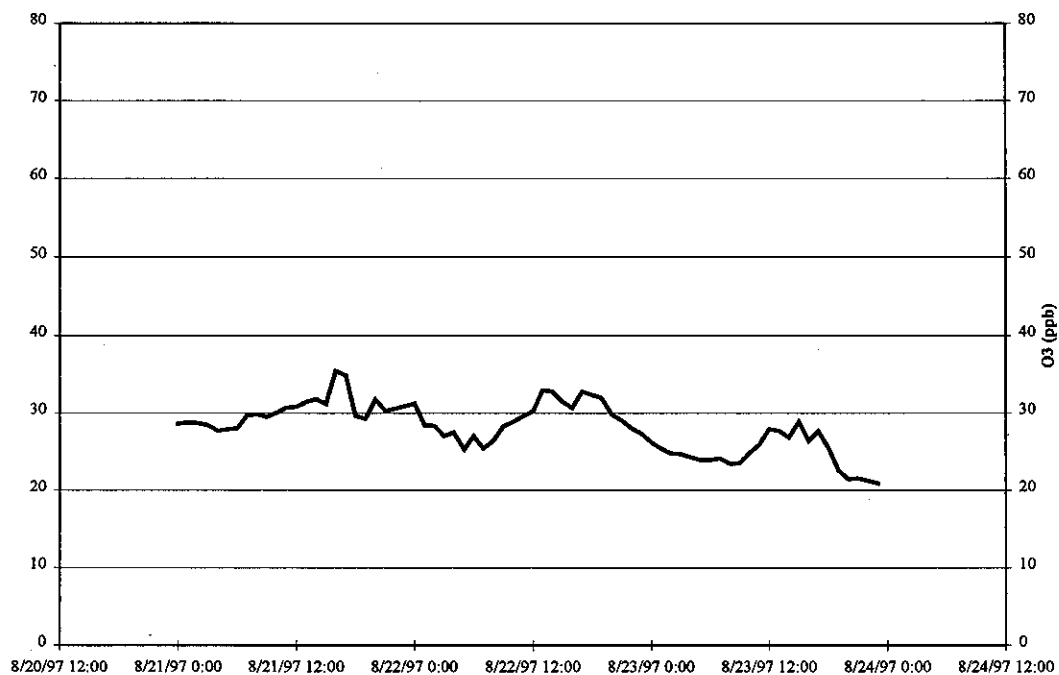
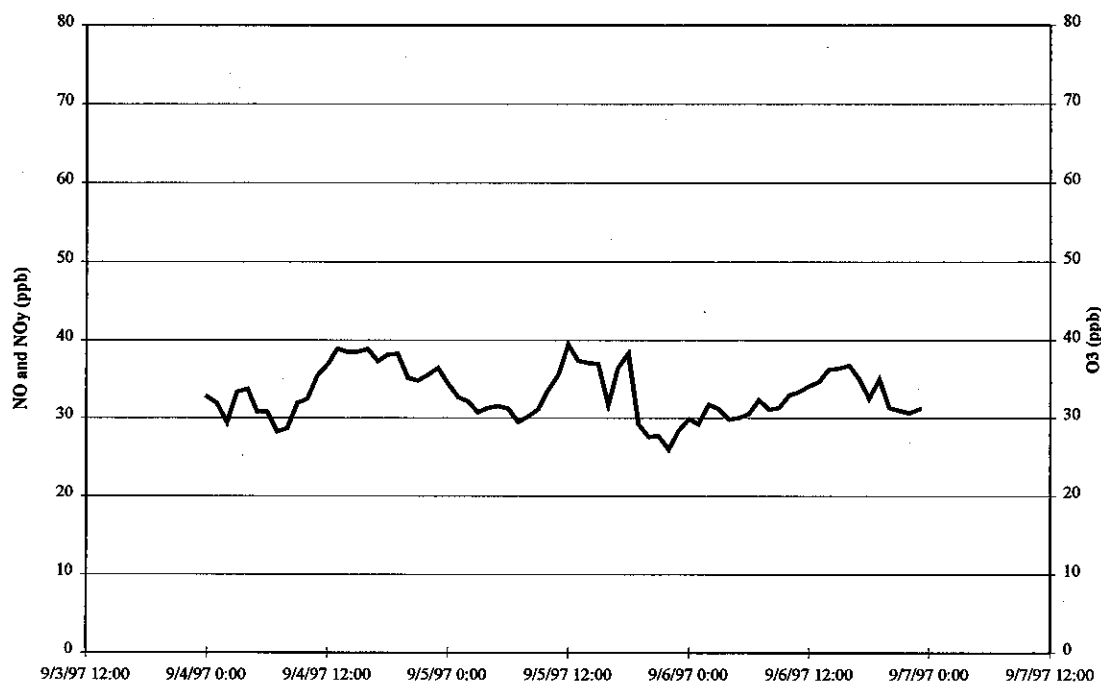
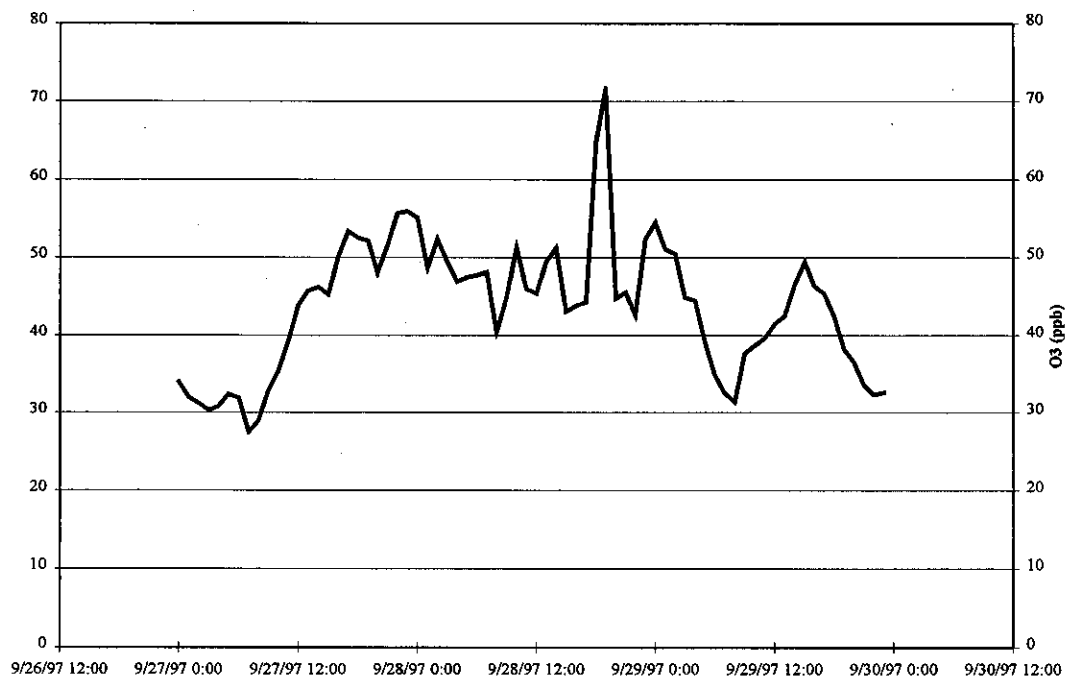
Figure 3-43, continued.**Site: San Nicolas Island NE Bldg 279****Site: San Nicolas Island NE Bldg 279**

Figure 3-43, continued.

Site: San Nicolas Island NE Bldg 279



Site: San Nicolas Island NE Bldg 279

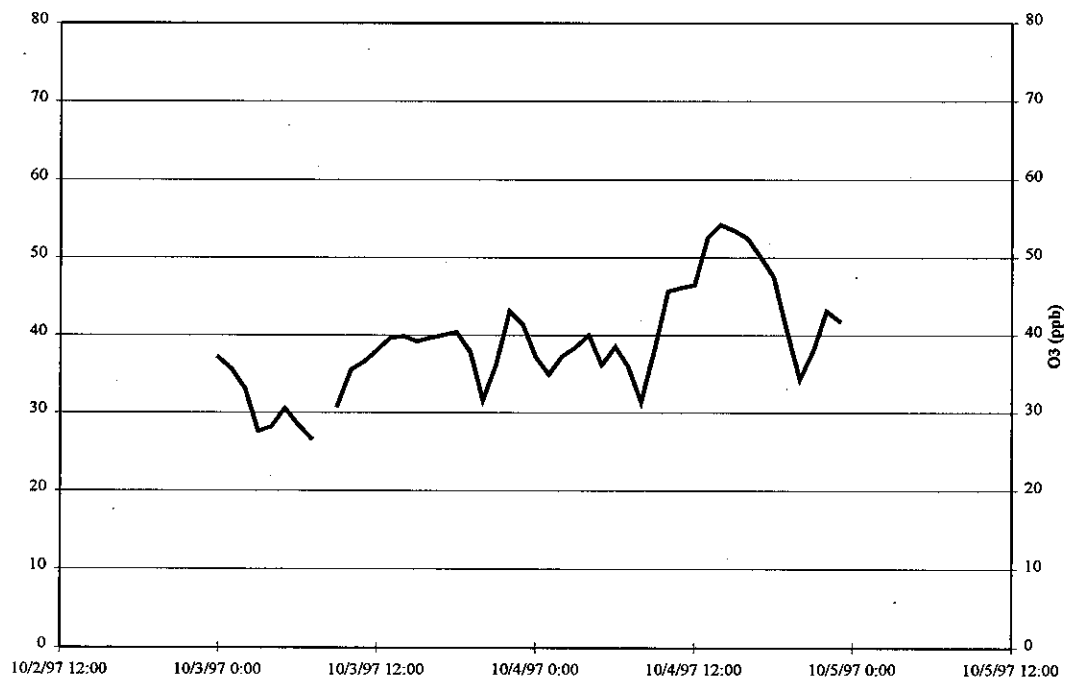


Figure 3-44. Ozone Concentrations at ARCO Tower Penthouse during SCOS97-NARSTO IOP Periods.

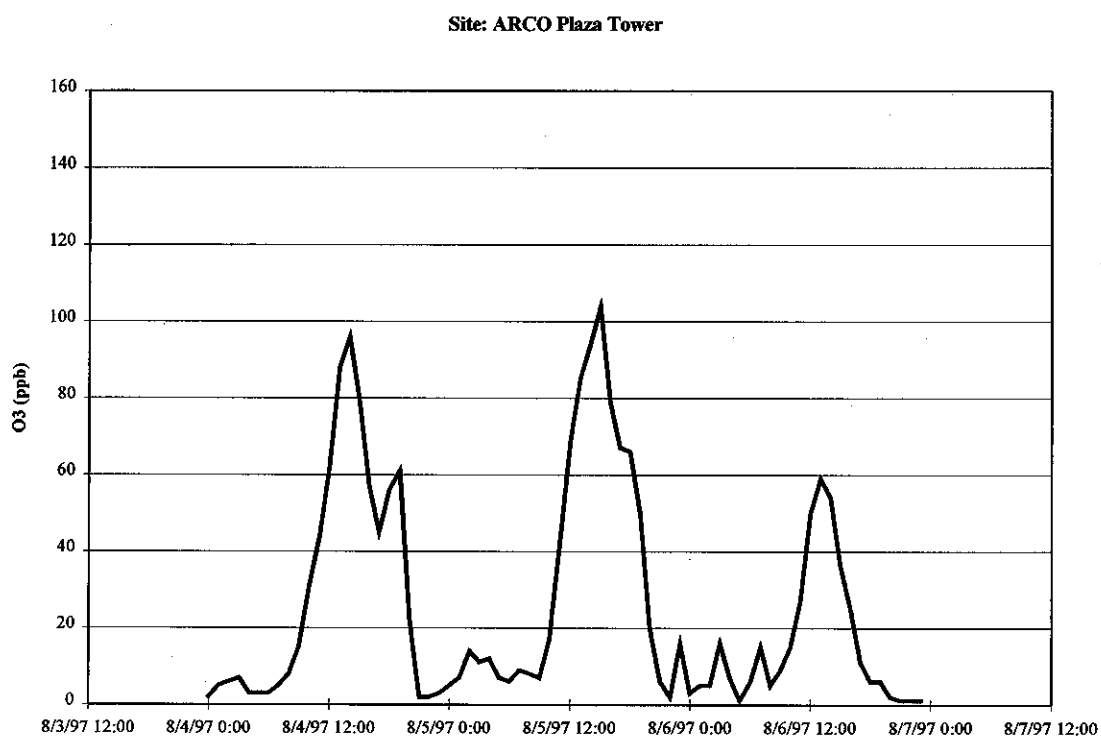
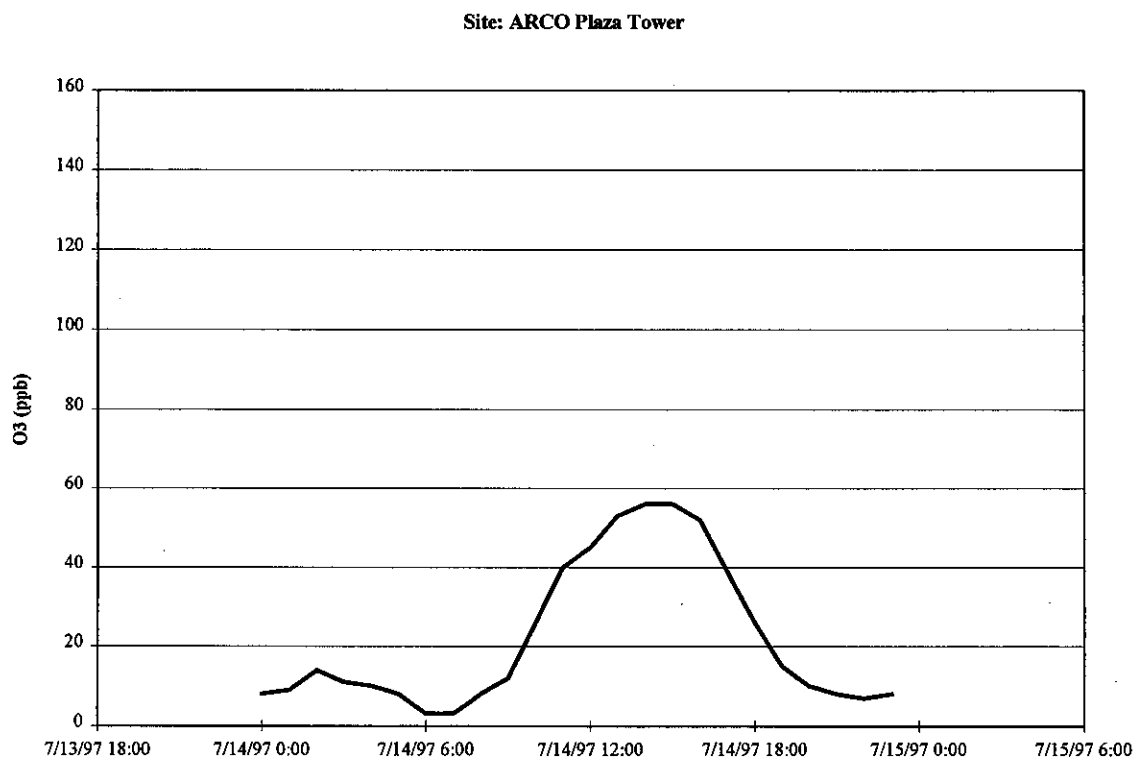
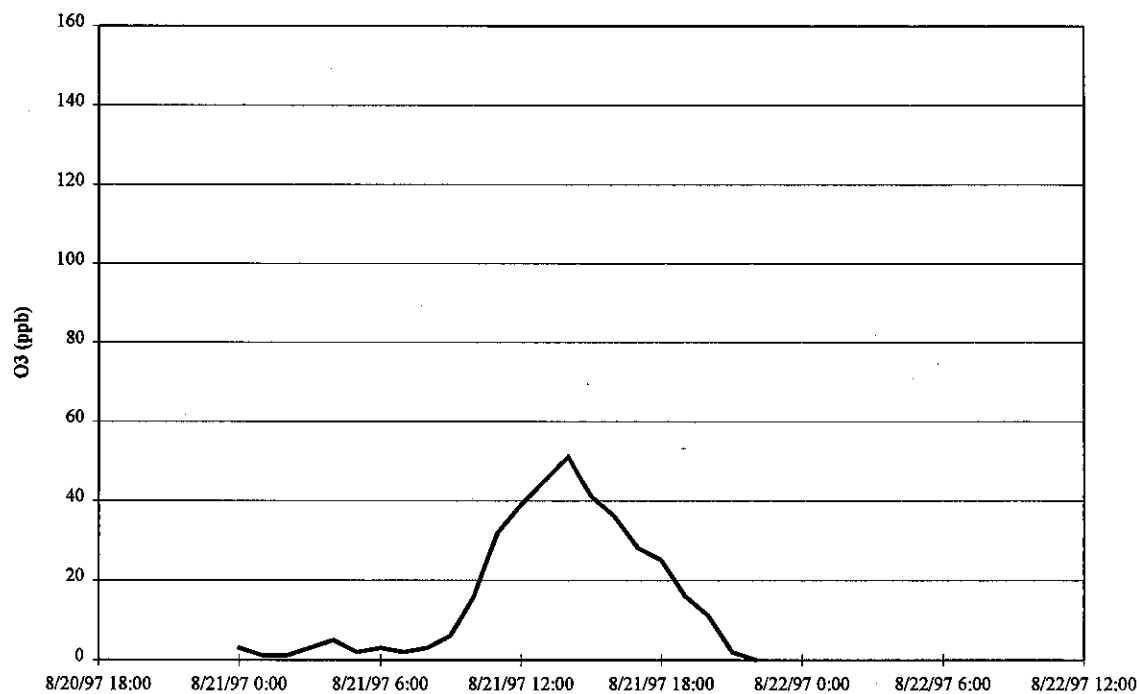


Figure 3-44, continued.

Site: ARCO Plaza Tower



Site: ARCO Plaza Tower

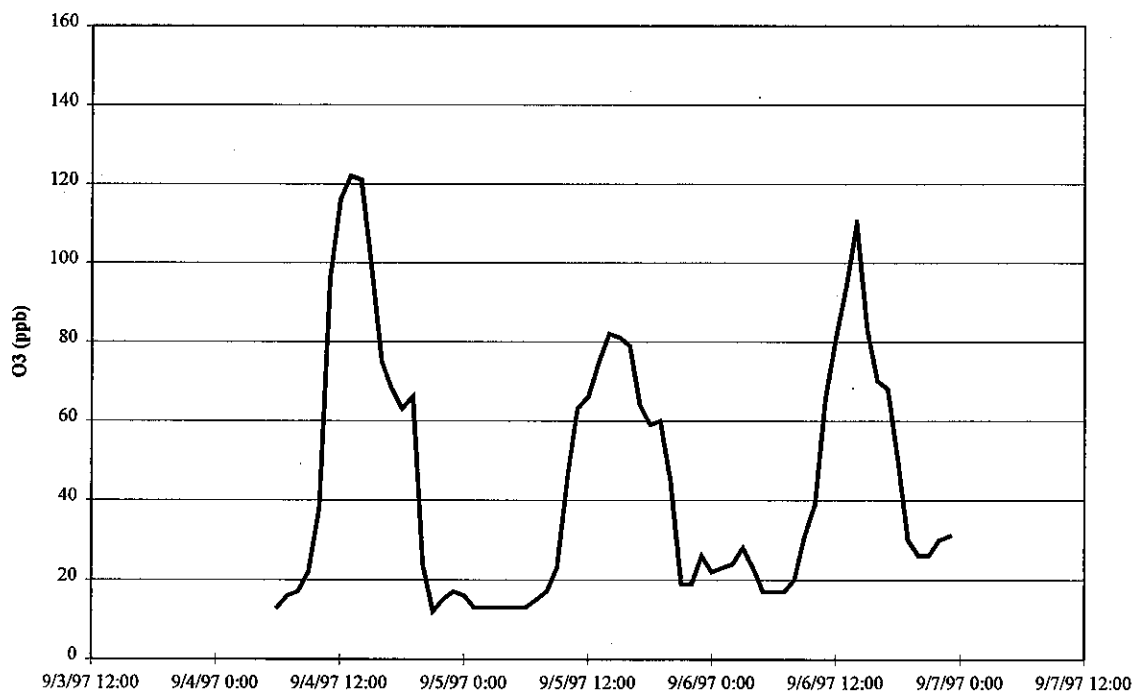
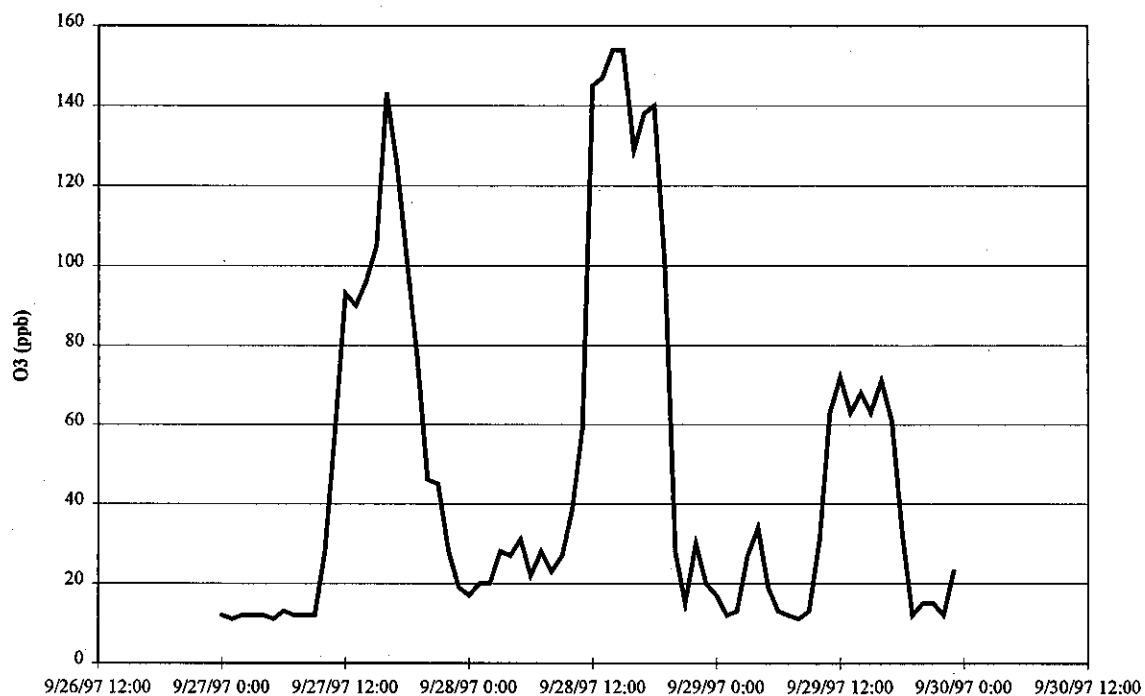


Figure 3-44, continued.

Site: ARCO Plaza Tower



Site: ARCO Plaza Tower

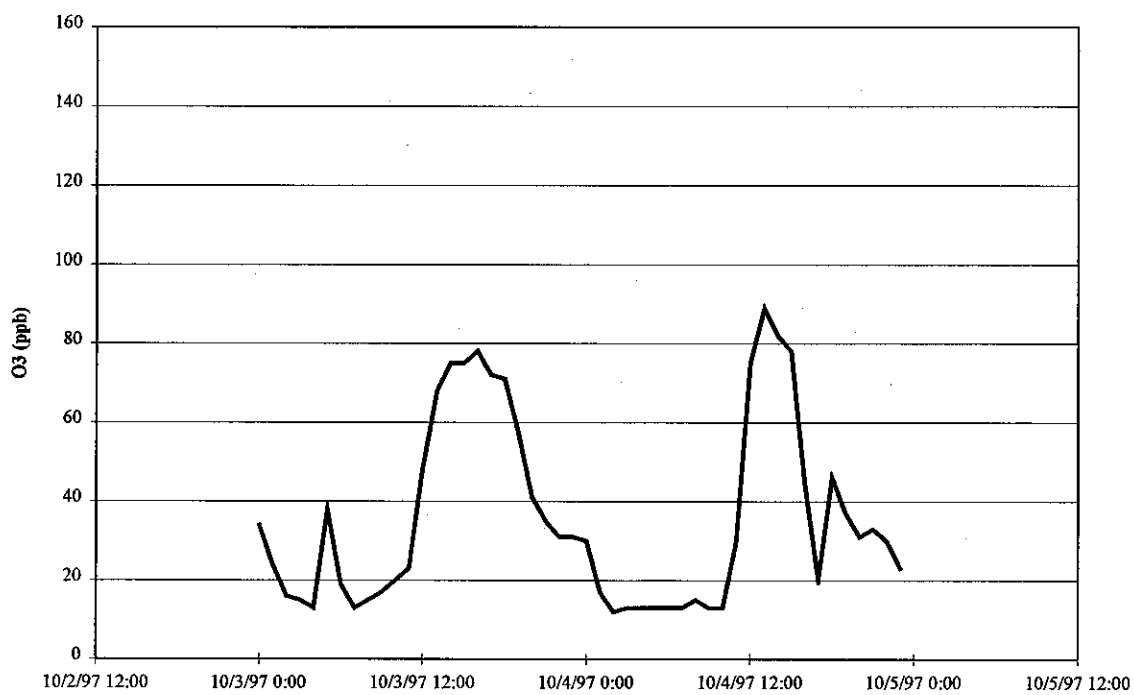


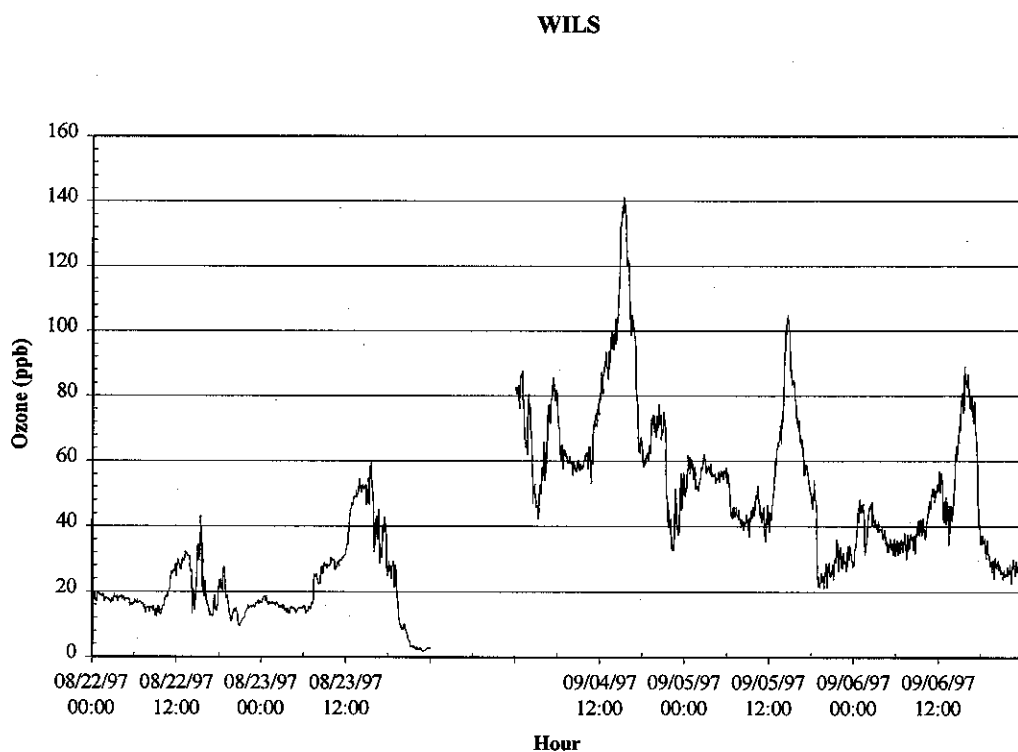
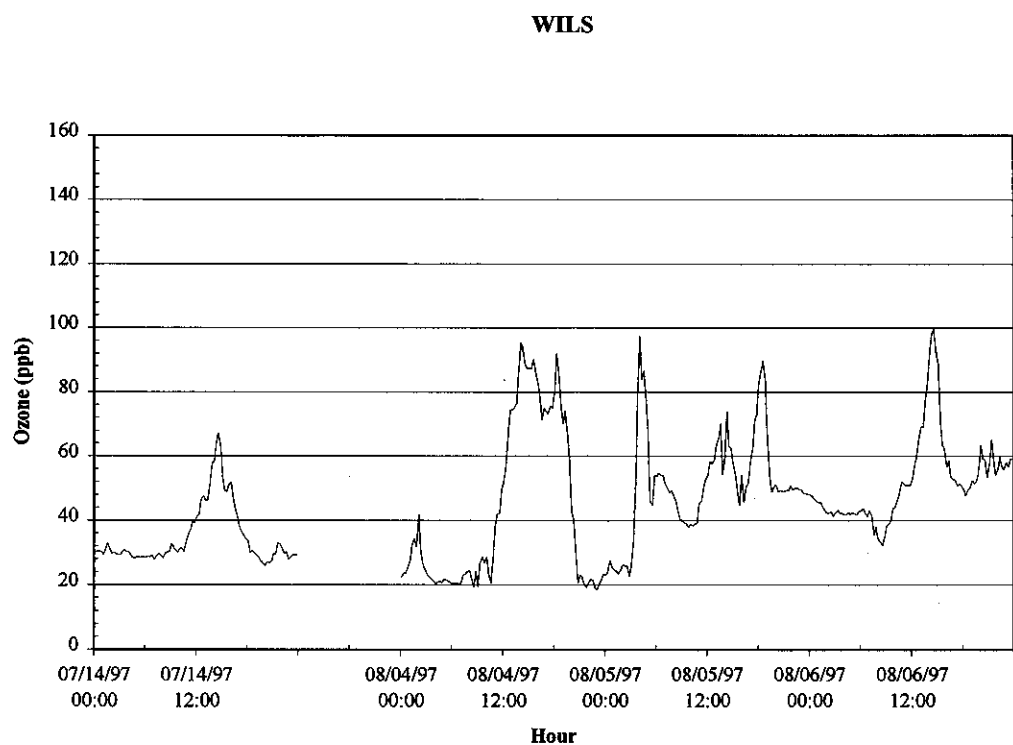
Figure 3-45. Ozone Concentrations at Mt. Wilson during SCOS97-NARSTO IOP Periods.

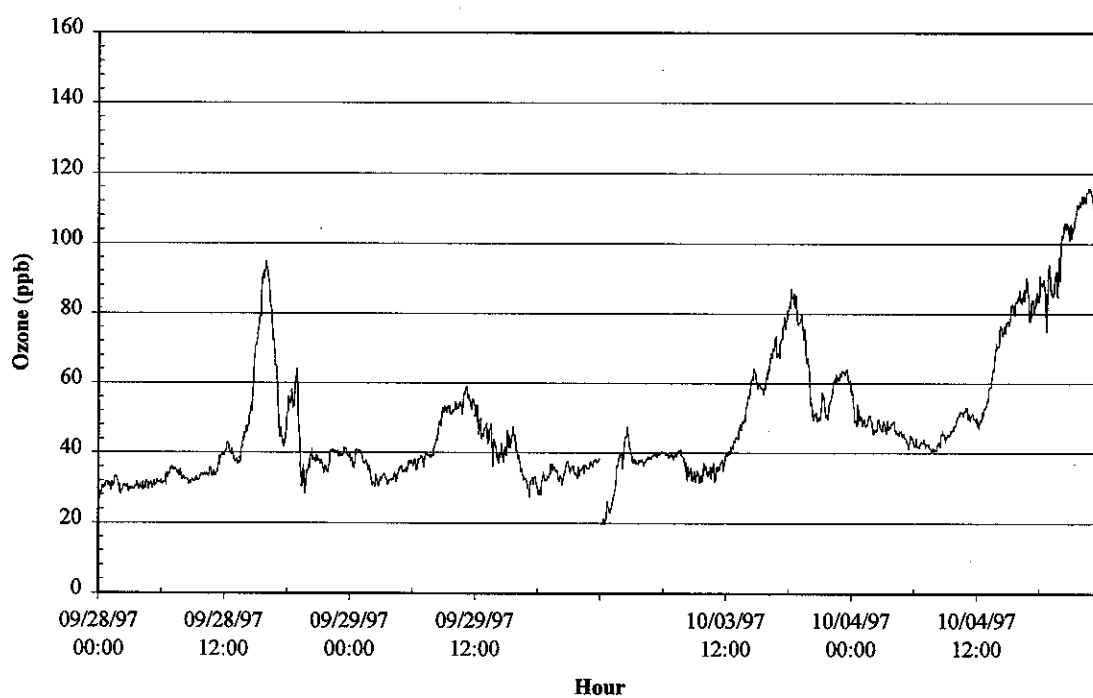
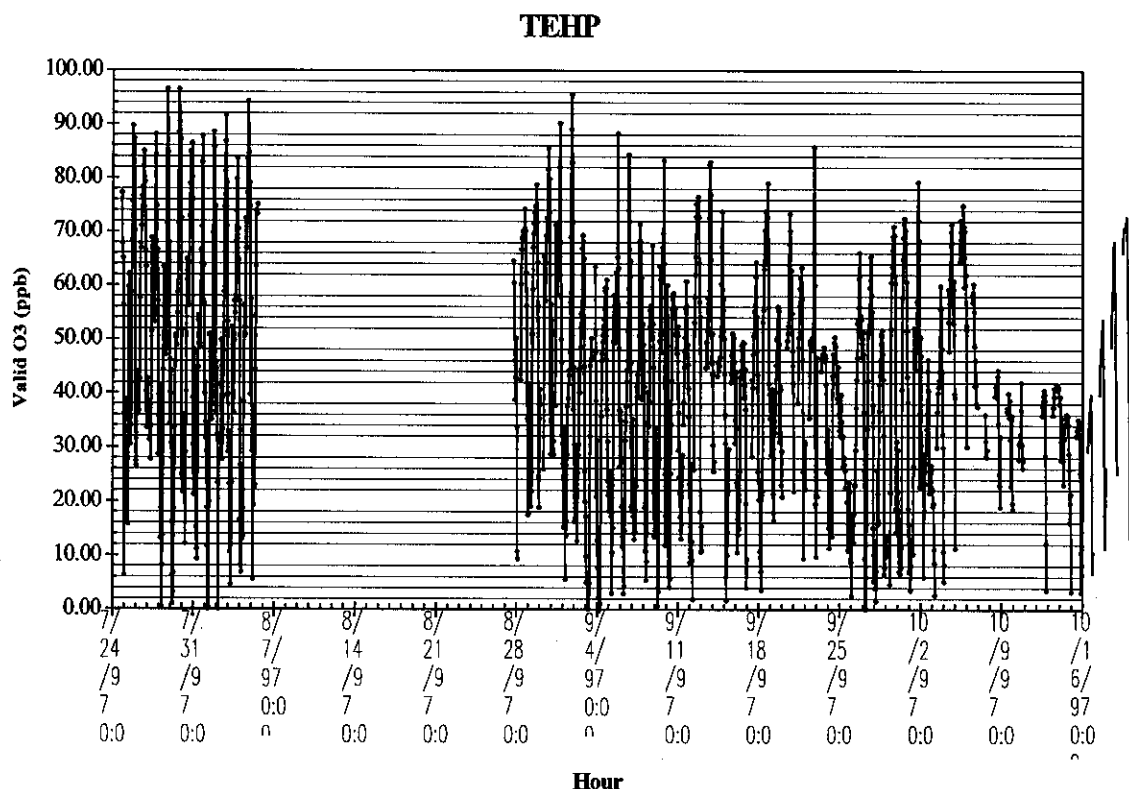
Figure 3-45, continued.**Mt. Wilson**

Figure 3-46. Ozone Concentrations at Tehachapi during SCOS97-NARSTO IOP Periods.



3.3.2 Meteorological Measurements at Mira Loma and Diamond Bar

Data were collected between August 29 and November 1, 1997 in Diamond Bar and September 10 to November 1, 1997, in Mira Loma. The data capture was 100%.

Summary of Operation and Validation

We reviewed time series plots of meteorological data for each day at each site. Periods when the sensors were down or offline were marked missing. When wind speed was below 0.5 m/s, wind direction was flagged as below threshold and marked suspect. When wind speed was below 1.0 m/s, wind direction was flagged as near threshold and marked suspect. Precisions were assigned based on manufacturer's specifications, and our experience, as follows: wind speed, 0.2 m/s; wind direction, 5 degrees; sigma theta, none assigned; temperature, 0.5 °C; relative humidity, 10% RH.

3.3.3 Quality Assurance Auditing

Aircraft Audits

- Ozone and NO_y

NO_y and ozone audits were performed by CE-CERT on the aircraft operated by UC Davis, the U.S. Navy, and Sonoma Technology, Inc. An offer was made to do the same for the aircraft operated by the San Diego APCD, but it was declined. We used a Columbia model 1700 calibrator to generate ozone and our Dasibi 1003AH transfer standard to quantify the concentration. Five-point calibration concentrations were conducted, and the results were plotted as a least squares fit. Relative to the CE-CERT determination, the slope of the STI aircraft was 8% low, the UCD aircraft 6% low, and the Navy aircraft within 1%. These calibrations were all performed near sea level, with temperature and pressure corrections made manually for the CE-CERT instrument. The NO_y calibrations are described in the next section.

- Broadband and UV Radiometers

The Caltech Pelican aircraft has Eppley PSP Total and UV radiometers of the same type used by CE-CERT at Mt. Wilson and Riverside. To determine the comparability of these instruments, a side-by-side test was performed at the El Monte airport on September 11, 1997. The radiometers on the aircraft were leveled by tilting the aircraft. The CE-CERT radiometers were then set next to the Pelicans and separately leveled. The analog outputs were recorded at ten-minute intervals from 1100 to 1500 hours PTD using a voltage meter.

Figures 3-47 and 3-48 plot the CE-CERT values versus the Pelicans for the total solar and UV radiometers, respectively. Since the data were collected over mid-day, the spread in values was small. For this reason the regression lines were forced through zero. The average ratio between the CE-CERT and Pelican's total radiometer was 1.00 ± 0.04 while the average ratio for the UV radiometers was 1.48 ± 0.06 . The reason for this discrepancy between the UV instruments is not known, and equivalent SCOS97-NARSTO monitoring data should be compared to determine whether a bias was also observed in these measurements.

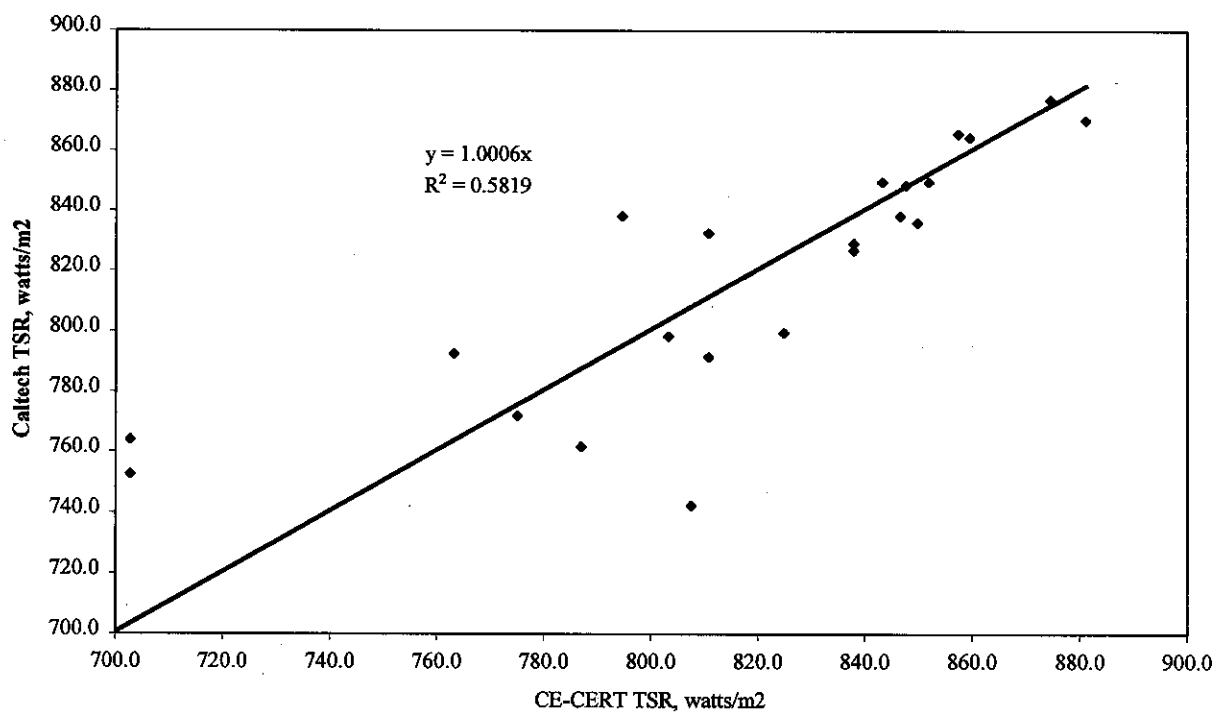
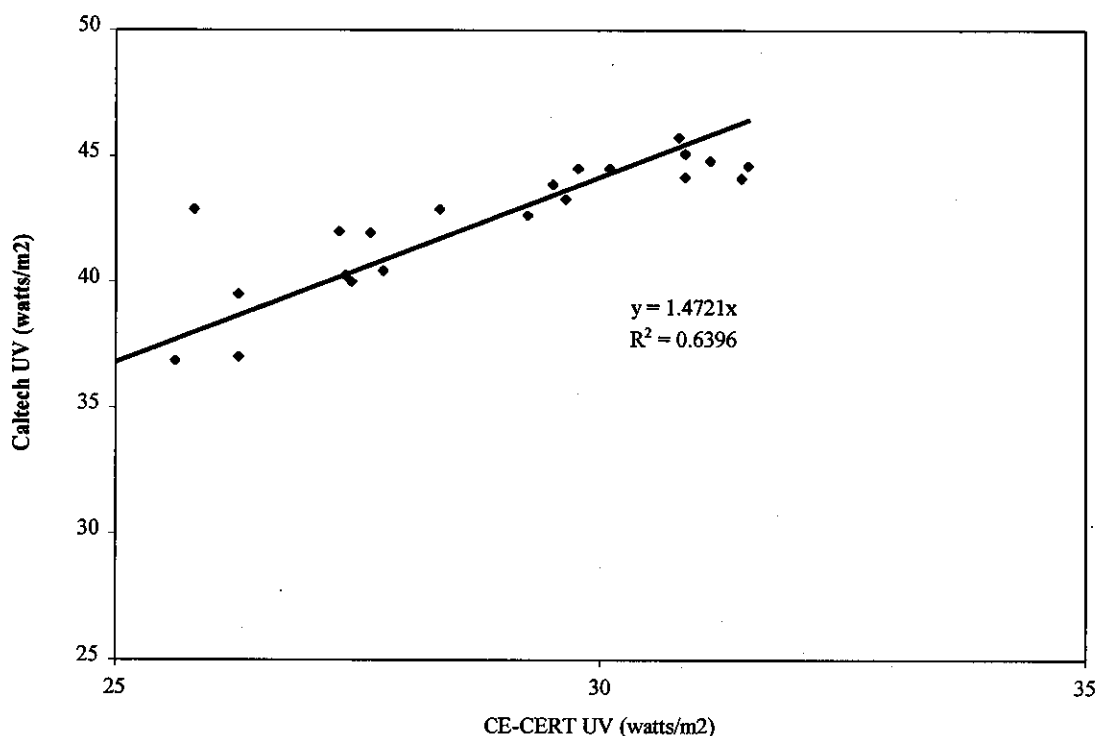
Figure 3-47. Comparison of CE-CERT and Pelican PSP Total Solar Radiometers.

Figure 3-48. Comparison of the CE-CERT and Pelican UV Radiometers.

3.3.4 NO_y Analyzer Audit Comparisons

To determine the comparability of the NO_y measurements conducted by various groups, a series of audit checks was performed between the groups where each site was checked by a group not involved with its normal operation. This was done after the SCOS97-NARSTO measurement period had ended. To do this, the auditor brought zero air, span gas, and a dilution calibrator to the site and challenged the site instrument with zero air and one or more NO concentrations within the normal ambient range. This was normally done with the operator of the site present. Concentrations were then read directly from the instrument and from the data system.

Table 3-10 summarizes the results obtained. Since CE-CERT was involved as either an auditor or auditee, the results were normalized to the concentrations calculated from CE-CERT calibrations. The instruments at Diamond Bar and Mira Loma were no longer working properly at the time of the audit and the logistics of performing an audit at San Nicolas Island were too difficult. The results show that the mean difference of NO_y was 6% lower than the CE-CERT value with a standard deviation of 6%. All of the values were within the $\pm 15\%$ recommended by the EPA as valid data. The CE-CERT certified NO calibration cylinder was then rechecked by the vendor, Scott-Marrin, Inc. The NO concentration was found to be 9.49 ppm. The certification value was 10.10, a difference that would make the CE-CERT audit concentrations 6% low.

NO span factors for data processing were originally calculated using the cylinder concentration of 10.10 ppm. Although the CE-CERT certified NO cylinder had dropped 6% in concentration according to the vendor, it was not determined when this drop had occurred. To calculate span

factors for final data processing of study monitoring data (not audit data), we used the mean cylinder determination, i.e. we reduced span factors by 3% from their original values.

Table 3-10. Summary of NO_y Comparisons.

Location	Instrument	Auditor	NO _y % Diff Rel to CE-CERT	NO _y -NA/NO Rel to CE-CERT	Comments
Alpine	Teco 42CY	CE-CERT	-8%	-8%	
Azusa	Teco 42CY, Dual Converter	SCAQMD	1%	3%	
Banning	Teco 42CY, Dual Converter	MAQMD	-3%	2%	
Barstow	Teco 42CY, Dual Converter	CE-CERT	-12%	-15%	
Cajon Pass NO _y	Teco 42C-External Converter	CE-CERT	-3%		NO _y audited by ARB also
Cajon Pass NO ₂	LPA-4	CE-CERT	-10%		NO ₂ audited by ARB also
Diamond Bar	Teco 42S- Dual Converter				Instrument Broke
Los Angeles-North Main	Teco 42C- Dual Converter	SCAQMD	NA		
Mira Loma	Teco 42CY, Dual Converter	SCAQMD			Instrument Broke
Mt Soledad	Teco 42CY, Dual Converter	SDAQMD	-8%	-8%	
San Nicolas Island	Teco 42S- Single Converter				Logistically too difficult
Simi Valley	Teco 42CY, Dual Converter	VCAQMD	-3%	-4%	
STI Aircraft (NO _y)		CE-CERT	0%	-3%	
STI Aircraft (NO ₂)		CE-CERT	-8%	-11%	
Riverside (SCAQMD gas)	Teco 42CY, Dual Converter	SCAQMD	-15%	-12%	
Riverside (CE-CERT gas)	Teco 42CY, Dual Converter	SCAQMD	-5%	-1%	
Twenty Nine Palms	Teco 42CY, Dual Converter	CE-CERT	5%	5%	
UCD Aircraft	Teco 42CY	CE-CERT	-11%	-11%	
Average			-6%	-5%	
Std Dev			6%	7%	

CE-CERT NO span gas originally certified at 10.10 ppm NO was found to be 9.49 ppm by the end of the study: 6% low.

3.3.5 PAN Audits

As an independent check for both the AVES and DGA PAN instruments, PAN was generated in a 100L Teflon bag at the CE-CERT laboratory, quantified with both a NO-NO_x analyzer and a PAN GC. The 100L bag was then transported to the Cajon or Calabasas sites operated by AVES or the Azusa site operated by DGA. During transport, the bag was shielded from light by placing it in a black polyethylene bag and maintained cool by placing it under the vehicle's air conditioner outlet while the air conditioner was set in the maximum cool position. This was done four times with an identical preparation each time. On October 17 the PAN concentration was measured at CE-CERT before and after transport and found to have dropped 10%, which is close to the analyzer's estimated precision of 5%. This indicates little loss of PAN despite eight hours in the bag. Table 3-11 summarizes the results obtained.

Table 3-11. Summary of PAN Audits.

Location	Date	PAN,ppb CE-CERT	NO _x , ppb CE-CERT	PAN, ppb AV, corr	NO ₂ , ppb AV, corr	PAN, ppb NO ₂ corr. CE-CERT NO _x	PAN, ppb DGA Azusa
Cajon Pass	30-Jul	26	42	4.7	13.0	29	NA
Cajon Pass	17-Oct	30	55	8.7	22.0	33	23
Calabasas	31-Jul	27	36	22.8	9.0	27	NA
Calabasas	16-Oct	52	65	19.6	34.0	31	26

The audits performed in July were only for the AVES sites, where Unisearch Associates Inc. LPA-4 instruments were used. The AVES instruments were calibrated only by using NO₂, which is measured by direct injection into the detector. Direct injection of known concentrations of PAN was not performed as part of the AVES calibration procedure. It is not clear how response to NO₂ determined in this manner would apply to the quantification of PAN, which is determined by separation through a chromatographic column prior to injection into the detector.

The PAN-containing bag was attached directly to the LPA-4 inlet line within the air monitoring shelter. Readings for both PAN and NO₂ were obtained. The values were recorded from the AVES data logger for the measurements made in July and directly from the LPA-4 printout for those made in October. In each case they were multiplied by factors supplied by AVES.

PAN measured by the LPA-4 at Cajon Pass was significantly lower than the PAN determined at CE-CERT for both the July and October audits, a factor of 5 in July and a factor of 4 in October. The relative standard deviation of the LPA-4 was approximately 10%. For Calabasas, the AVES PAN values were 15% lower than the CE-CERT concentration in July, but 69% lower in October. The relative standard deviation of multiple injections was approximately 5%. In October it is likely that the PAN determined by CE-CERT was too high, since it contained a large amount of NO₂ as determined by the LPA-4. Another way of determining PAN concentrations is to subtract the amount of NO₂ determined by the LPA-4 from the NO_x measured at CE-CERT. This assumes that only NO₂ and PAN are present and that the LPA-4 calibration is consistent with the NO_x analyzer. The results are shown in the second column from the right. This shows that all four bags contained a similar amount of PAN and the CE-CERT determination of October 16 is no longer an outlier. This similarity was expected, since all bags were prepared in exactly the same manner. Using this concentration, the Calabasas LPA-4 was 37% lower than the PAN in the bag, consistent with the results obtained in July.

On the DGN PAN audits, poor agreement was found the first time (52 ppb for CE-CERT GC, 26 ppb for DGA) and better agreement the second (30 ppb for CE-CERT GC and 23 ppb for DGA). As mentioned previously, it is likely that the CE-CERT GC analysis of the first sample was an outlier, due to a large amount of NO₂. Of the four bags prepared in an identical manner, this was the only one that differed by more than 10% by the CE-CERT GC analyses. As mentioned above, the PAN concentration determined by NO_x is corrected by the NO₂ determined by the LPA-4, the concentration would be 31 ppb, in good agreement with the DGA analysis.

The level of agreement between the CE-CERT and DGA PAN measurements are similar to other comparisons that have been reported (Blanchard et al., 1990; Krognes et al. 1996). We feel that the AVES instrument was not properly calibrated since PAN of known or estimated concentrations were not injected as part of the calibration procedure. Any agreement between this instrument's data and the PAN prepared by CE-CERT and measured by both CE-CERT and DGA analyzers is therefore fortuitous.

4.0 Conclusions

A data set of known precision and accuracy has been produced for a wide variety of aerometric measurements in support of the SCOS97-NARSTO study. The data set will be placed with other information collected during the study into a database that will form one of the most comprehensive data sets collected in the southern California area. The data will be used in air quality models to design ozone attainment strategies and to resolve intra-regional air pollution transport issues. The database will be available to the public after appropriate review and will provide a wealth of information that can be analyzed to provide insight into the many issues surrounding the ozone and particulate matter problem in the southern California area.

While many of the measurements were well-developed routine methods, several of the less commonly used instruments had generic problems that may limit the usefulness of data acquired from them. The Eppley broad band radiometers agree quite well during intercomparisons, but the same cannot be said of the UV instruments. These showed non-linear response that varied between instruments. Instruments would therefore give differing responses depending on the intensity of the sunlight. A single calibration factor is given by the manufacturer's calibration, but it is not clear whether this factor is result of curve fitting or the response at a particular light intensity. For the application of the data for airshed modeling, we felt that applying the factor at the peak intensity was most appropriate. Not only is this region not changing rapidly with time, but it is during the time of day when the light intensity has the greatest affect on photochemical production of ozone. With such a calibration, the instruments would have a more similar response during this part of the day.

The measurement of NO_y and nitric acid by a dual converter chemiluminescent analyzers showed peculiar artifacts. The use of externally-mounted NO_y converters on chemiluminescent NO analyzers is relatively new, and this study provided very useful information on their limitations in a high NO_x area such as southern California. The current Thermo Environmental converter (and possibly those from other manufacturers that are similar in design) appears to have two primary measurement artifacts, the magnitude of both apparently being dependent on the concentration of ambient pollutants. The first artifact is that they develop an artificial zero offset, most likely due to the capture and slow release of nitrogenous species (such as particulate nitrate or nitric acid). The second artifact is a changing efficiency of converting nitric acid to NO , although the converters showed nearly unit efficiency with NO_2 and n-propyl nitrate (a chemical that has been suggested as a surrogate for nitric acid to test converter efficiency). All of the instruments we operated had been checked out in the laboratory before installation in the field and found to have identical responses to both zero air and synthetically-generated nitric acid. None of these instruments, however, had been used to sample ambient air with high concentrations of various nitrogenous species since they were either new, last used in a background area, or used on smog chambers.

Despite these limitations, the NO_y measurements provided a more accurate measure of the concentration of nitrogenous species in the atmosphere. Indeed, the ratio of NO_y/HC may be more appropriate than NO_x/HC in describing the potential of polluted air to produce ozone.

Our approach for measuring nitric acid depended on the complete and immediate conversion of nitric acid to NO in the NO_y channel (that is accurate NO_y measurements) and complete removal of nitric acid in the other channel. While the former was questionable, we were successful in the latter by using a NaCl -impregnated denuder in combination with nylon filters (which were found by TDLAS measurements to rapidly drop in nitric acid removal efficiency as they sampled polluted air). The method also depended on both channels being perfectly matched with respect to response, since the nitric acid measurement was invariably the difference of two much larger numbers (typically an order of magnitude larger). Despite these limitations, we provided some

useful information of nitric acid concentrations in areas of southern California for which this measurement had not been previously made. Of particular interest is the occurrence of peak nitric acid in Banning and at other receptor areas late in the day, which may correspond to transport of a polluted air mass. In addition, the ratio of nitric acid to NO_y may be a useful indicator of the extent to which a polluted air mass has the potential to photochemically create more ozone.

The use of fabric denuders (Fitz and Tuazon, 1997), when coated with NaCl , again proved to be a reliable and accurate approach to measuring nitric acid, at least at the air encountered at the Azusa monitoring site, a location of high nitric acid that was collocated with a TDLAS. The denuder also proved to work well when coated with phosphoric acid in measuring ammonia at the Mira Loma site, a location of high ammonia that was collocated with a long-path FTIR with folded optics. While this denuder has been shown previously to be efficient and compare well with open path systems of several hundred meters (Coe et al., 1998) this was the first direct comparison with an open path point monitor.

5.0 Recommendations

It is difficult to accurately measure nitrogenous species in the atmosphere. To do so will require the development of more artifact-free converters for chemiluminescent analyzers or a different analytical approach. The elimination of all stainless steel surfaces in the converter may help pass nitrogenous species more quantitatively, as we have observed nitric acid to be efficiently removed by such steel surfaces. Such converters should be evaluated on ambient air by comparing with current converters.

While the TDLAS can provide accurate measurements of NO and NO_2 , it is too labor and capital intensive to be used on a routine basis. Alternative approaches should be evaluated in the laboratory and then tested on ambient air within the study area to determine whether the measurement contains artifacts and biases. This should be done well in advance of any major field study to provide a lead time to procure the instruments that will best meet the needs of the study.

The UV data obtained on the ground should be compared with those from the Pelican aircraft at the time it was flying near the ground site in order to confirm the bias observed during the intercomparison.

The use of the Unisearch Associates Inc LPA-4 Luminol-based instrument should be further evaluated. While the detection method does have interferences with PAN and ozone, it may be able to compensate for the PAN as the instrument makes this measurement chromatographically (and therefore free of interferences) and it may be possible to remove ozone with diffusion scrubbers.

With other methods of measuring nitrogenous species being developed, the need for performing another comprehensive comparison study such as that performed in southern California in 1986 is readily apparent, as no such study has been performed since.

If possible future air quality studies should evaluate developing methods well in advance so that appropriate planning and documentation can be effected.

6.0 Future Research Needs

The most important areas of future research relate to the measurement of nitrogen oxides. The routine measurement of NO_y , NO_2 , and nitric acid will be valuable inputs in evaluating photochemical airshed models and in applying them to determine cost-effective control strategies for ozone and particulate matter.

NO_y

The development of a NO_y analyzer can realistically proceed along two lines based on instruments that are currently available, using either a chemiluminescent or Luminol-based detection. Both of these instruments are reasonably priced, although the chemiluminescent instruments have been shown to require little maintenance whereas the limited use of the Luminol instruments indicates a higher level of maintenance is required. Each also has potential measurement artifacts. Given the well known durability of chemiluminescent analyzers, the development and extensive testing of converters that are more artifact-free is probably the most viable approach for this measurement. While converters that utilize heated gold converters with carbon monoxide added to the sample stream may be more appropriate than the molybdenum-based one that are now widely used, it is not likely that they will be readily accepted by the monitoring community due to the need of a support gas. Other alternatives, such as glass-line molybdenum converters, should be thoroughly evaluated. These evaluations should be first under the controlled conditions of smog chambers and a polluted ambient air. In both cases the NO_y components should be independently measured as accurately as possible using the best methods available. The ambient measurements need to be made over a period of at least a year to establish the response to different air pollutant mixtures and determine long term durability. High levels of quality control will be needed to evaluate the performance. These will include frequent zero and span checks and determining matrix effects by standard addition techniques.

NO_2

NO_2 is probably the most important species for which routine measurements are not currently made. While the Luminol-based instruments offer potential, their need of support chemicals will most likely limit their acceptability, as will their potential for high maintenance. Selective scrubbing of nitrogenous species followed by chemiluminescent detection may offer a reasonable alternative as will selective reduction to NO . While such methods have been used in the past, but have not been adequately pursued, most likely by lack of a regulatory drive. Such methods need to be re-evaluated and, if appropriate, thoroughly tested, again using smog chambers for the initial tests and polluted ambient air. The TDLAS would be the appropriate reference for these type of evaluations.

Nitric Acid

The routine accurate measurement of nitric acid is also critical, especially in southern California, in modeling the atmospheric chemistry and determining the potential for particulate formation. The dual converter chemiluminescent approach should be modified so that both channels are identical in every way except for nitric acid. This can be done using a NaCl -coated diffusion denuder to selectively remove the nitric acid rather than a nylon filter that also removes particulate nitrate (and tends to become overloaded). The method should be tested more thoroughly under the controlled conditions of a smog chamber in which a TDLAS can be used as a reference. Comprehensive ambient evaluations are also needed as with the NO_y evaluations. A quality control step that needs to be added is the response to air which has had the nitric acid selectively removed to determine if both channels are perfectly matched with respect to zero and converter efficiency.

The dual denuder chemiluminescent approach to measuring nitric acid has the inherent analytical limitation of obtaining the value by subtracting one larger number from another. A direct nitric approach is needed that will allow measurements to be routinely made in real-time and that also does not require high capital costs or maintenance. This need will become more important as NO_y levels decline as more stringent NO_x controls are implemented.

7.0 References

- Anlauf, K.G.; Wiebe, H.A.; Tuazon, E.C.; Winer, A.M.; Mackay, G.I.; Schiff, H.I.; Ellestad, T.G.; and Knapp, K.T (1991) Intercomparison of atmospheric nitric acid measurements at elevated concentrations. *Atmos. Environ.* **25A**, 393-399.
- Blanchard, P.; Shepson, P.B.; So, K.W.; Schiff, H.I.; Bottenheim, J.W.; Gallant, A.J.; Drummond, J.W.; and Wong, P (1990). A comparison of calibration and measurement techniques for gas chromatographic determination of atmospheric peroxyacetyl nitrate (PAN). *Atmos. Environ.* **24A**, 2839-2846.
- Carter, W.P.L.; Luo, D.; and Malkina, I.L. (1997). Environmental Chamber Studies for Development of an Updated Photochemical Mechanism for VOC Reactivity Assessment. Final Report to California Air Resources Board Contract 92-345, Coordinating Research Council Project M-9, and National Renewable Energy Laboratory Contract ZE-2-12252-07. November 26.
- Carter, W.P.L. (1998). Updated Maximum Incremental Reactivity Scale for Regulatory Applications. Preliminary Report to California Air Resources Board Contract No- 95-308. August 6.
- Coe, D.L.; Chinkin, L.R.; Loomis, C.; Wilkinson, J.; Zwicker, J.; Fitz, D.R.; Pankratz, D.; and Ringler, E. (1998). Technical Support Study 15: Evaluation and Improvement of Methods for Determining Ammonia Emissions in the San Joaquin Valley. Sonoma Technology Inc. Final Report STI-95310-1759. Prepared for the California Air Resources Board.
- Federal Register (1975) Vol. 40, No. 33, pp 7052-7060.
- Fitz, D.R., and Tuazon, E.C. (1997). Evaluation of a Sampling Methodology for Acidic Species. Final Report, California Air Resources Board Contract 94-338.
- Fujita, E.M.; Green, M.C.; Keislar, R.E.; Koracin, D.R.; Moosmüller, H.; and Watson, J.O. (1996) 1997 Southern California Ozone Study (SCOS97): Field Study Plan. Prepared for California Air Resources Board Contract 93-326.
- Grosjean, E.; Grosjean, D.; Fraser, M.P.; and Cass, G.R. (1996) Air Quality Model Evaluation for Organics. 3. Peroxyacetyl Nitrate and Peroxypropionyl Nitrate in Los Angeles Air. *Environ. Sci. Technol.*, **30**:2704-2714.
- Hartsell, B. (1997) Private communication.
- Hering, S.V.; Lawson, D.R.; and 38 other authors (1988). The Nitric Acid Shootout: Field Comparison of Measurement Methods *Atmos. Environ.* **22**:1519-1539.

Holdren, M.W., and Spicer, C.W. (1984) Field Compatible Calibration Procedure for Peroxyacetyl Nitrate. *Environ. Sci. Technol.* **18**:113-116.

Krognes, T.; Danalatos, D.; Glavas, S.; Collin, P.; Toupance, G.; Hollander, J.C.T.; Schmitt, R.; Qyola, P.; Romero, R.; Ciccioli, P.; Dipalo, V.; Cecinato, A.; Patier, R.F.; Bomboi, M.T.; Rudolph, J.; Muller, K.P.; Schrimpf, W.; Libert, Y.; and Geiss, H. (1996) Interlaboratory calibration of peroxyacetyl nitrate liquid standards. *Atmos. Environ* **30**:991-996.

Mackay, G.I., and Schiff, H.I. (1987) Methods Comparison Measurements during the Carbonaceous Methods Comparison Study. Glendora, CA, August 1986: Tunable Diode Laser Absorption Spectrometer Measurements of HCHO, H₂O₂, and HNO₃. Final Report to California Air Resources Board, Contract No A5-189-32. October 21.

Spicer, C.W.; Howes, J.E. Jr.; Bishop, T.A.; Arnold, L.H.; and Stevens, R.K. (1982) Nitric Acid Measurement Methods: an Intercomparison. *Atmos. Environ.* **16**:1487-1509.

Tuazon, E., and Fitz, D.R. (1998). Comparison of Methods for Measuring Nitric Acid in Southern California. Submitted to *Atmos. Env.*

Tuazon, E.C.; Blanchard, C.L.; Hering, S.V.; Lucas, D.; and Mackay, G.I. (1995) A Review of Nitric Acid Measurements by Tunable Diode Laser Absorption Spectrometry (TDLAS). Final Report to California Air Resources Board Contract 93-300.

U.S. Environmental Protection Agency (1984). Quality Assurance Handbook for Air Pollution Monitoring Systems: Volume II, Ambient Air Specific Methods. EPA-600/4-77-027a, Environmental Monitoring Systems Laboratory, Research Triangle Park, NC. December.

Vecera, Z., and Dasgupta, P.K. (1991) Measurement of Ambient Nitrous Acid and a Reliable Calibration Source for Gaseous Nitrous Acid. *Environ. Sci. Technol.* **25**:255-260.

White, J.U. (1976) Very Long Optical Paths in Air. *J. Opt Soc. Am.* **66**:411-416.

Winer, A.M.; Peters, J.W.; Smith, J.P.; and Pitts, J.N. Jr- (1974) Response of Commercial Chemiluminescent NO-NO₂ Analyzers to Other Nitrogen-containing Compounds *Environ. Sci. Technol.* **8**:1118-1121.

Zafonte, L.; Rieger, P.L.; and Holmes, J.R. (1977) Nitrogen dioxide photolysis in the Los Angeles Atmosphere. *Environ. Sci. Technol.* **11**:483-487.